APPLICATION OF THE MICROWAVE DISCHARGE TO CHEMICAL PROCESSING

by

R.M. SAMBROOK

A Thesis

Submitted for the degree of

Doctor of Philosophy

Loughborough University of Technology

Supervisor: Dr. B.W. Brooks

Department of Chemical Engineering. November, 1970.

Summary

A study has been made of the parameters affecting chemical reactions in a microwave discharge. Emphasis was placed upon investigating the possibility of promoting selective reactions and their application to chemical processing.

An attempt was made to produce hydrazine in an ammonia discharge. Flow rates, pressures and power inputs in the reactor were varied. Hydrazine was not detected under the experimental conditions investigated. Hydrogen and nitrogen were found in a constant mole ratio of 3:1. The formation of NH radicals in the microwave discharge of ammonia was postulated.

The reactions of gaseous benzene in the microwave discharge have been studied. Acetylene, 1,3-butadiene and diphenyl were the major products. The presence of nickel in the benzene discharge promoted the conversion of benzene to diphenyl. In discharges of mixtures of benzene and carbon dioxide, the benzene molecule was protected by the carbon dioxide. In mixtures of benzene and ammonia, the discharge products were almost entirely amino-substituted derivatives of azobenzene.

The cyclohexane discharge yielded propylene and butene-1 as the major products. The presence of nickel in the discharge promoted the reaction to propylene whilst hindering the formation of butene-1. This effect was also found in discharges of mixtures of cyclohexane and carbon dioxide.

In conclusion several systems have been studied in the microwave discharge. Evidence was found of the ability to promote certain reactions by influencing the discharge characteristics. A potentially important process, i.e. the production of derivatives of azobenzene, was noted.

ACKNOWLEDGEMENTS

The author wishes to thank the following: Professor D.C. Freshwater for his interest and encouragement; Dr. B.W. Brooks for supervising this research; Miss M.H. Neal for typing the thesis; the technical staff; the Science Research Council for their financial support.

Contents

Section			Page
1	Introduction		1
2	The Physical Nature of Electric Discharges		2
	2.1.	The d.c. Glow Discharge	2
	2.1.1.	Breakdown Conditions for the d.c. Glow Discharge	2
	2.1.2.	The Regions of the d.c. Glow Discharge	8
	2.1.3.	The Positive Column	10
	2.2.	The Electric Arc	14
	2.3.	A.C. Discharges	14
	2.3.1.	Radio-Frequency and Microwave Discharges	17
	2.3.2.	Pulsed Microwave Discharges	20
3	Collision Theory		22
	3.1.	Elastic Collisions	23
	3.1.1.	Mean Free Path	23
	3.1.2.	Collision Cross-Section	25
	3.2.	Inelastic Collisions	27
	3.2.1.	Excitation	27
	3.2.2.	Ionization	30
4	Basic Discharge Reactions		33
	4.1.	Ionization by Electron Impact	33
	4.2.	Atom Transfer	34
	4.3.	Ion-Molecule Reactions	34
	4.4.	Charge Transfer Reactions	35
	4.5.	Electron-Ion Recombination Reactions	36
	4.6.	Excitation of Ions	36
	4.7.	Free Radical Reactions	36
5	Some Examples of Systems Previously Studied		40
	5.1.	Inorganic Gases in the Electric Discharge	41
	5.1.1.	The Hydrogen Discharge	42
	5.1.2.	The Nitrogen Discharge	43
	5.1.3.	Polyatomic Gases	44
	5.1.4.	Mixtures of Gases	45
	5.2.	Organic Vapours in the Electric Discharge	46
	5.2.1.	The Methane Discharge	46

		Page
5.2.2.	The Production of O-containing Compounds	48
5.2.3.	The Formation of Hydrogen Cyanide	50
5.2.4.	Polymer Production in the Discharge	50
5.2.5.	Methanol	31
5.2.6.	Saturated C_6 Hydrocarbons	52
5.2.7.	Benzene	53
6	The Choice, Operation and Testing of the Microwave Equipment	57
6.1.	Choice of Electrical System	57
6.2.	Description of Microwave Equipment	58
6.3.	Preliminary Testing	65
7	Reactor Design	67
7.1.	Types of Reactors	67
7.1.1.	Steady-State Plug Flow Reactor	67
7.1.2.	Steady-State CFSTR Reactor	69
7.2.	Residence Time	70
7.3.	Limitations Imposed by the Cavity Design	71
7.4.	Selectivity and Preservation Problems	74
7.5.	Type of Reactor Used in the Present Work	75
8	Choice of Systems for Investigation	78
8.1.	Scouting Experiments	79
8.1.1.	The Methanol Discharge	79
8.1.2.	The n-Hexane and Cyclohexane Discharges	79
8.1.3.	The Benzene Discharge	81
8.2.	Conclusions	83
9	The Application of the Microwave Discharge to the Production of Hydrazine from Ammonia	85
9.1.	Investigations of the Ammonia Discharge from the Literature	87
9.1.1.	Basic Decomposition Processes	87
9.1.2.	Investigations of the Parameters Affecting the Yield of Hydrazine	93
9.1.3.	Commercial Systems for Production of Hydrazine from Ammonia	95
9.2.	Analytical Techniques for the Determination of Hydrazine	97
9.3.	Experimental Details	100

		Page
9.3.1.	Simple Flow System	100
9.3.2.	Investigation by On-line G.L.C. Analysis	103
9.3.3.	Investigation by Analysis of the Condensed Products	108
9.4.	Temperature Profile in the Ammonia Discharge	112
9.5.	Experimental Results : Ammonia Studies	113
9.5.1.	Discussion of Results : Ammonia Studies	113
9.5.2.	Interpretation of Results : Ammonia Studies	115
10	Some Reactions of Benzene in the Microwave Discharge	127
10.1.	Experimental Details : Benzene Studies	127
10.2.	Experimental Results : Benzene Studies	129
10.3.	Discussion of Results : Benzene Studies	131
10.3.1.	Benzene Alone : the Low Boilers	131
10.3.2.	Benzene Alone : the High Boilers	131
10.3.3.	Benzene and Nickel Wire : the Low Boilers	133
10.3.4.	Benzene and Nickel Wire : the High Boilers	133
10.4.	Visual Observation of the Discharge	134
10.5.	Interpretation of Results : the Low Boilers	134
10.5.1.	Interpretation of Results : the High Boilers	137
10.6.	Reaction Profiles of the Volatile Products	140
10.7.	Hydrogen Balance	140
10.8.	Benzene and Carbon Dioxide	141
10.8.1.	Discussion of Results	141
10.8.2.	Interpretation of Results	142
10.9.	Benzene and Ammonia	144
10.9.1.	Discussion of Results	144
10.9.2.	Interpretation of Results	145
10.10.	General Observations : Benzene Studies	149
10.10.1.	Energy Yields	149
10.10.2.	Conclusions	150
11	Some Reactions of Cyclohexane in the Microwave Discharge	184
11.1.	Experimental Details : Cyclohexane Studies	184
11.2.	Experimental Results : Cyclohexane Studies	184
11.3.	Discussion of Results : Cyclohexane Studies	186
11.3.1.	Cyclohexane Alone	186
11.3.2.	Cyclohexane with Nickel Present	187
11.4.	Hydrogen Balance	188
11.5.	Visual Observations	189

			Page
	11.6.	Interpretation of Results : Cyclohexane Studies	189
	11.6.1.	Mass Spectrometry and Radiolysis Data from the Literature	189
	11.6.2.	Interpretation of the Microwave Discharge Results	191
	11.7.	Cyclohexane and Carbon Dioxide	197
	11.7.1.	Discussion of Results : Cyclohexane to Carbon Dioxide, 2:1	197
	11.7.2.	Cyclohexane and Carbon Dioxide; 1:1 and Carbon Dioxide in Excess	198
	11.8.	Interpretation of Results	198
	11.9.	Conclusions : Cyclohexane Studies	200
12	Comparison of the Benzene and Cyclohexane Discharges		214
	12.1.	General Conclusion	214
	12.2.	Proposals for Further Work	215
Appendix A		Reaction Profiles : Complex Reactions	217
Appendix B		Temperature Profiles of the Benzene and Cyclohexane Discharges	219
Bibliography			221

INTRODUCTION

1. Introduction

For a number of years the electric discharge has been acknowledged as a ready source of highly excited atoms and molecules. Interest has been mainly concerned with atomic and sub-atomic phenomena rather than the development of commercially viable processes. In fact the production of ozone is still the only widely used commercial process developed from electric discharge work. However, evidence is now available to show that the electric discharge can compete with conventional methods in the manufacture of specialised chemicals. This is essentially because discharge reactions are usually fast one-stage processes compared with the multi-stage processes of normal chemical techniques. This applies not only to organic but also to inorganic synthetic chemistry.

With the prospect of cheaper electricity from nuclear power, the electric discharge method will be much more competitive commercially in the near future. It is this view that has stimulated new interest in discharge phenomena.

THE PHYSICAL NATURE

OF ELECTRIC DISCHARGES

2. The Physical Nature of Electric Discharges

Electric discharges can take place over a very wide range of gas pressures and carry currents ranging from 10^{-12} to 10^{+6} amps. They may be steady-state processes or transients of very short duration. The characteristics of a particular discharge depend greatly on the electrical parameters such as applied voltage, frequency, electrode material etc.

2.1. The d.c. Glow Discharge

A typical voltage-current plot of a low pressure d.c. flow discharge is shown in Fig. 1. In the initial portion of the voltage-current curve, A - D, the current is very low and thus the concentration of excited atoms and ions is so low that the deactivation processes resulting in the emission of light are not visible in the electrode gap. Hence the region is called the dark discharge region. Chemically the region is not of great interest as the energies involved are small.

The transition into the visible discharge region, F - I, is shown by a sharp increase in the current and a voltage drop. The discharge is also self-sustaining. If the gas pressure is under about 25 mm Hg the discharge is called a glow discharge. At higher pressures the discharge appears striated and is called a silent discharge. If in this region curved electroded are used, a non-homogeneous field is set up near the electrode surfaces and the discharge plasma concentrates in this region forming a corona discharge.

2.1.1. Breakdown Conditions for the d.c. Glow Discharge

The transition to the glow discharge occurs when the applied voltage is sufficient to ionize the gas. Townsend[1] investigated

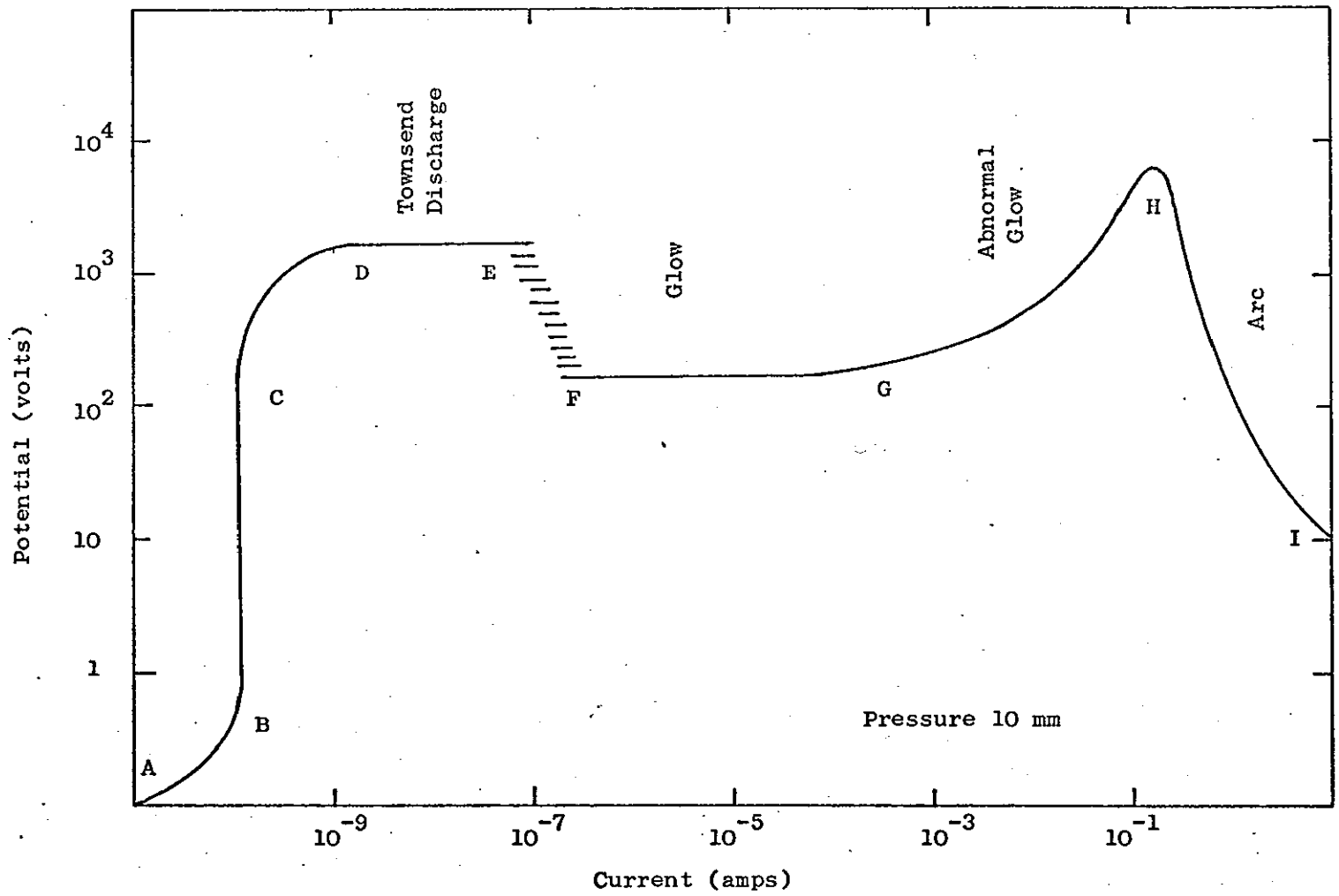

Figure 1 A Typical Voltage-current Plot of the Low Pressure d.c. Flow Discharge

the point of breakdown fully. The ionization was assumed to be entirely due to the electrons and thus the electron energy, which is determined by the field strength, was the controlling factor in breakdown. Townsend introduced an ionization coefficient, α, which he defined as the number of ionizing collisions made on average by an electron in travelling one centimetre in the direction of the electric field. The ionization coefficient is therefore related to the electron collision cross-section of the gas molecules and also to the mean energy gained by an electron between collisions. The mean energy gained is given by

$$\text{mean energy per electron} = E\, e\lambda$$

where E = field strength, volts/cm.

λ = mean free path of the electron, cm.

e = electronic charge

The number of collisions of any kind the electron undergoes is dependent on the pressure and therefore, from the definition, α is also proportional to the pressure.

Hence

$$\alpha = p\, f\, (E\, e\lambda) \text{ at constant temperature}$$

where f is some unknown function.

Also,

$$\lambda \propto \left(\frac{1}{p}\right) \text{ at constant temperature}$$

thus,

$$\alpha = p\, F\, \left(\frac{Ee}{p}\right)$$

where F is a number function to f, or

$$\frac{\alpha}{p} = \phi\, \left(\frac{E}{p}\right)$$

where, again ϕ is a function similar to F, f.

Experiments have shown the last relationship to hold over a wide range of E and p. Townsend[1] derived an approximation for ϕ

and found,

$$\frac{\alpha}{p} = Ae^{-B/Ep}$$

in which A and B are constants depending on the gas used.

To allow for the secondary emission of electrons by electrode processes, Townsend[1] introduced a second ionization coefficient, γ. The value of γ depends on the nature of the gas and the electrode material. Values of the order of 10^{-2} are common. Generally γ is taken as representing all the secondary electron producing processes such as the photoelectric emission at the cathode.

Using these ionization coefficients Townsend[2] defined a criterion for the point of breakdown of the gas where,

$$\gamma . e^{\alpha d} = \gamma + 1 \qquad d \text{ being the electrode spacing}$$

as $\gamma \leqslant 1$

$$\gamma . e^{\alpha d} = 1$$

This is sometimes called the Townsend criterion. Experiments have largely justified the criterion but it does however refer to a steady-state condition which is difficult to attain experimentally.

Paschen[1] considered only the gas pressure and electrode spacing in developing an expression for the breakdown voltage, V_B. He proposed,

$$V_B = f\,(pd) \text{ at constant temperature}$$

To avoid the restriction of constant temperature the equation was modified to,

$$V_B = f^1\,(nd)$$

n being the gas concentration which defines the mean free path whatever the gas temperature. The functions f and f^1 based on

α have been derived in several forms but with a limited validity. The most important finding, however, of Paschen's law is the minimum found in plots of V_B against pd. This minimum has a unique value for any combination of gas and electrode material. The minimum in the curve corresponds to the minimum potential at which breakdown is possible. This is usually of the order of several hundred volts at pressures of about 1 mm Hg. The minimum is present because at $pd < (pd)_{min.}$ the number of collisions by an electron crossing the electrode gap is less and thus the probability of ionization per collision is higher as the electron energies are higher. For $pd > (pd)_{min.}$ the reverse holds. Examples are shown in Fig. 2.

The so-called Paschen curves are greatly changed by the addition of small amounts of a different gas to the system. A well-known case is the addition of argon to neon. The neon breakdown voltage is greatly reduced due to the metastable neon atoms causing ionization of the argon by the Penning effect.

The application of a voltage greater than the breakdown voltage causes the production of a number of primary electrons which produce secondary electrons leading to an electron avalanche. A time lag exists between the application of the required voltage and the breakdown of the gas. The time lag is usually considered in two parts; one is the time which elapses until a primary electron appears which initiates breakdown, the statistical time lag. This is dependent on the number of primary electrons produced per second from the cathode or in the gap. The other component is the time taken for breakdown to develope following the appearance of the successful electron, the formatative time lag. This depends on the transit

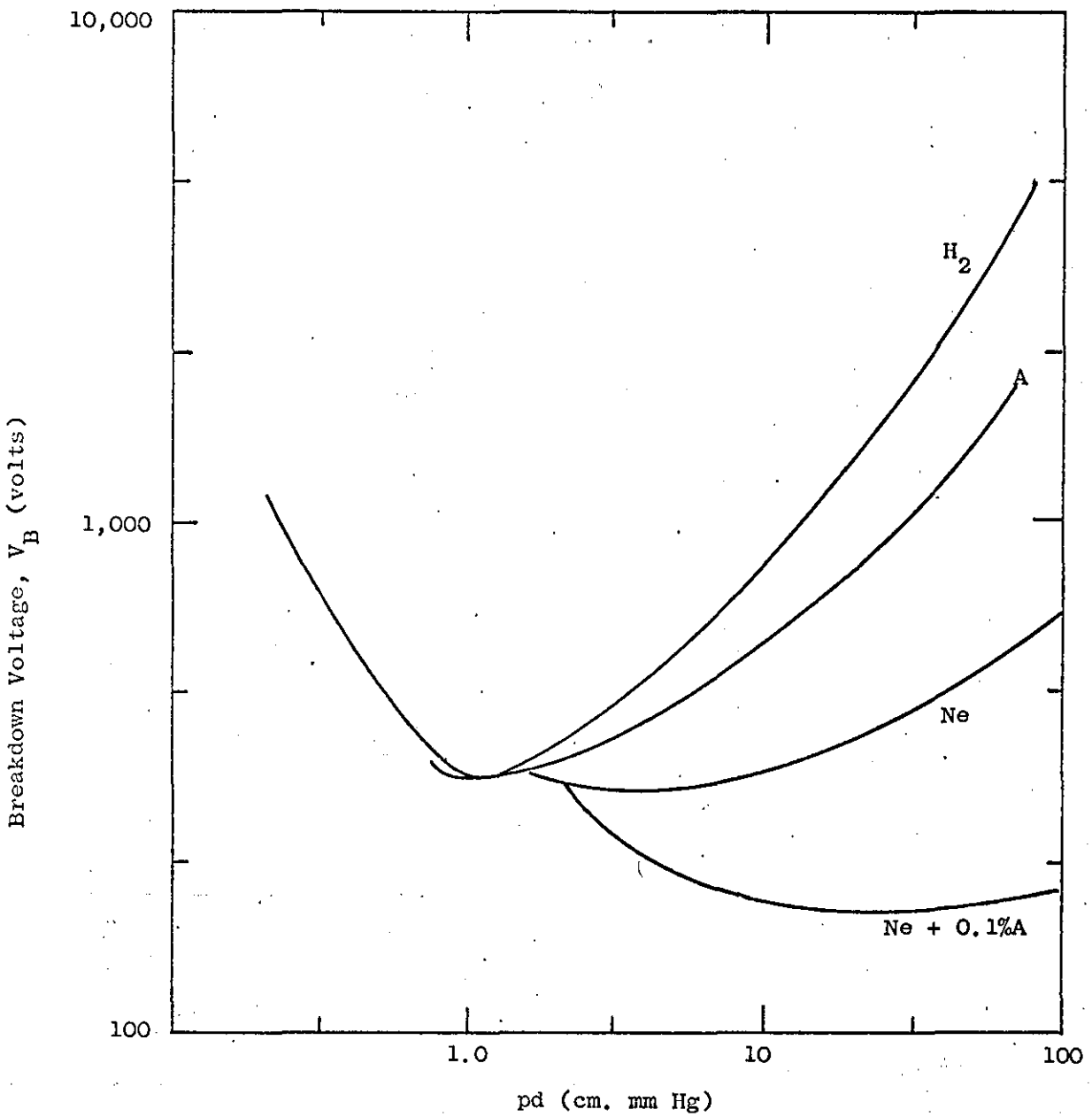

Figure 2 Paschen Curves of Various Gases, for Uniform Field.

time of a positive ion from the anode to the cathode. Both components of the total time lag depend on the excess voltage applied above the breakdown voltage. As the applied voltage decreases to the breakdown voltage, the time lag increases.

At values of pd above the minimum found from the Paschen curves, the breakdown voltage increases almost linearly with pd. Consequently, the field strength at breakdown depends only on p, e.g. 33 kV/cm for breakdown in dry air at atmospheric pressure. It is only at very high pressures that Paschen's law is not followed[3].

Experiments by Meek[3] have shown the space charge to be of greater importance as the pressure increases. If the space charge becomes large enough, the increased field causes auxiliary ionization. This results in streamers in the discharge. Also at high pressures the breakdown voltage depends little on the electrode material.

2.1.2. The Regions of the d.c. Glow Discharge

Varying conditions exist in the different regions of the discharge, and these are determined by the voltage, electric field, and charge density, see Fig. 3. The voltage across the cathode region of length dc, from the cathode to the anode end of the dark space is known as the cathode fall; usually of the order of several hundreds of volts. A relationship exists between the cathode fall and the breakdown voltage for a specified system of electrodes and gases. The cathode fall is independent of the discharge current or pressure and is a function of cathode material and the gas only. It also constitutes the major part of the total voltage drop. The length, dc, of the region however, does depend on pressure, and

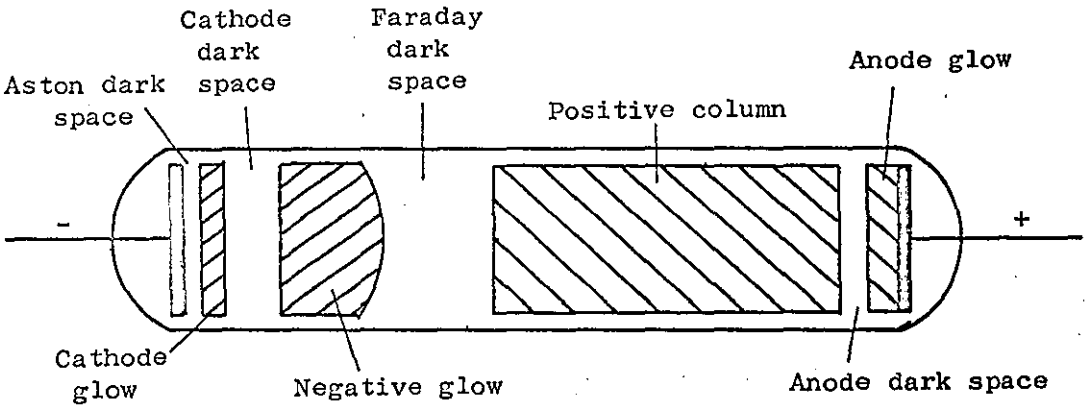

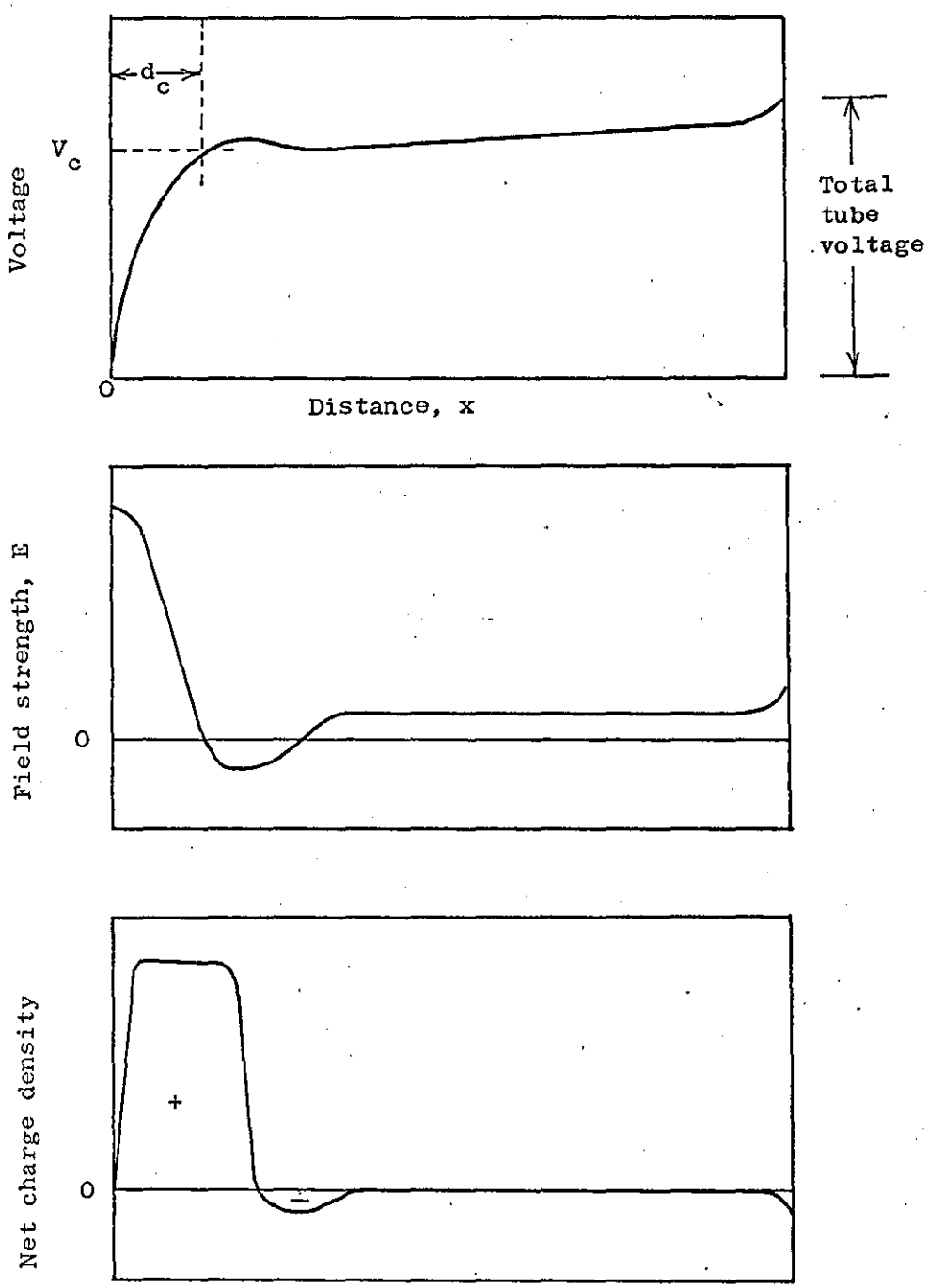

Figure 3 Regions of the Glow Discharge at Low Pressure

decreases proportionately with increasing pressure.

The anode fall is approximately equal to the ionization potential of the gas and occupies a region a few millimeters from the anode. The voltage drop across this region is found from the product of the field strength and the length of the positive column.

The current density has been shown to vary with the square of the gas pressure and is a constant for a specific gas - electrode system.

The positive column and the cathode fall regions are the places of chemical reaction. However, the greater volume of the positive column means the overall reaction rate is controlled by the positive column even though the highest rate of reaction per unit volume is found in the cathode fall region.

2.1.3. The Positive Column

Von Engel and Steenbeck[4] have derived a theory which presents a qualitative view of how the electric field strength and electron temperature vary with the pressure and reactor dimensions. In a stable discharge the electrons lost by diffusion to the walls are replaced by ionization of neutral gas particles. The ionization rate is determined by the field strength. Von Engel and Steenbeck postulated that under steady-state conditions the radial electron distribution at any point along the positive column is described by a Bessel function,

$$n = n_o J_o(r/\Lambda)$$

where

$$\frac{1}{\Lambda} = \frac{2.405}{R} = \sqrt{\frac{\nu_i}{D_A}}$$

r = discharge radius

n_o = electron density at the centre of the tube.

R = the tube radius.

ν_i = ionization frequency.

and D_A = ambipolar diffusion coefficient.

The equation defines the conditions for maintaining the electron density profile with constant n. The diffusion length, Λ, gives a measure of the distance an average electron will travel in a volume before it produces one new charged particle.

At pressures of less than 10 mm Hg the electron mean free path is large enough for the electrons to gain appreciable energy between collisions. The result of elastic collisions is to randomize the electrons and this gives the electrons an effective temperature much higher than that of the gas. Electron temperatures of up to 50,000°K are not unusual for pressures of less than 1 mm Hg. The lower the pressure, the less is the rest of the gas affected by the discharge and at very low pressures the gas temperature is not much above the ambient.

The electron energy necessary to maintain the ionization rate has been shown to be solely a function of $p\Lambda$ or pR for a particular gas. Examples of electron energies are given in Fig. 4a. However, it should be noted that the theory that predicts the dependence on $p\Lambda$ or pR does assume a Maxwellian distribution of electron energies and also does not take into account electron-ion recombination in the gas, electron attachment, or ionization in stages. A unique curve of E/p versus R/p is obtained for a particular gas. Curves for hydrogen, nitrogen, and air are shown in Fig. 4b.

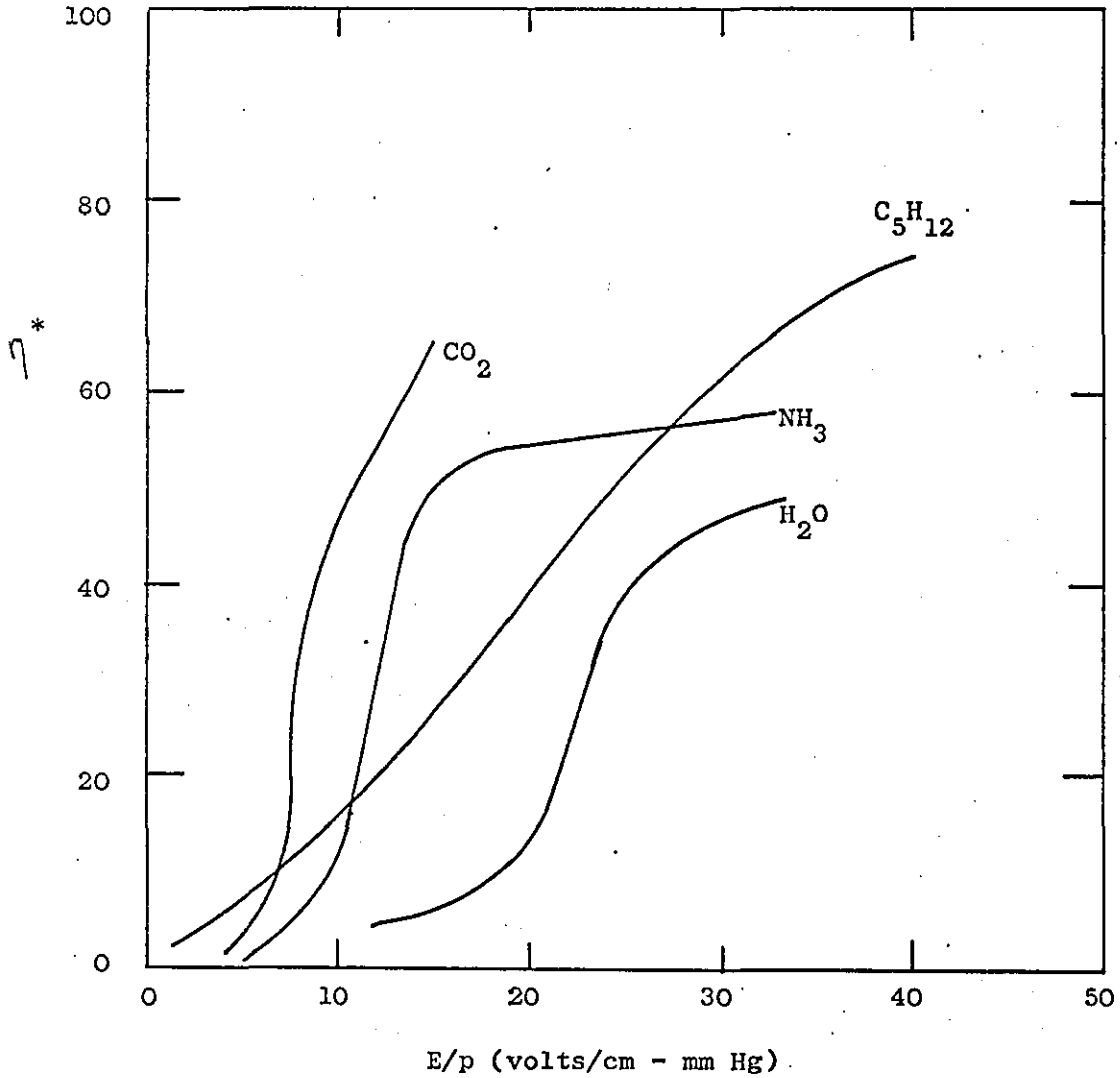

Figure 4a Indication of the Variation of Electron Energy for Various Gases

η^* is related to the Townsend energy factor η by a dimensionless factor, F, which is usually close to unity. By assuming a particular gas temperature, the mean electron energy can be calculated from,

$$\text{mean electron energy} = \eta \frac{3}{2} kT$$

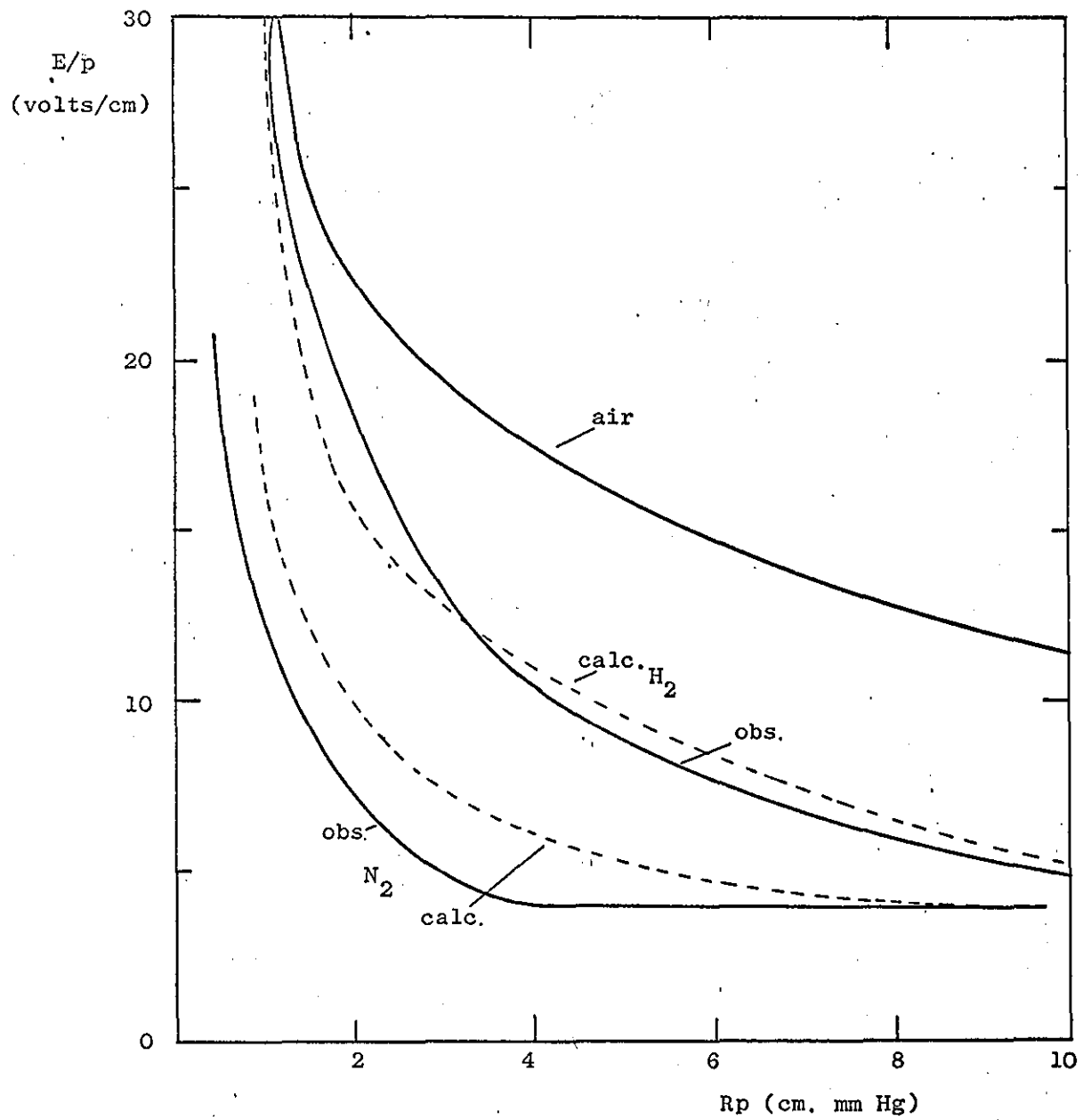

Figure 4b Examples of Curves of E/p Versus Rp for Various Gases.

2.2. The Electric Arc

The electric arc discharge is sustained mainly by the thermionic emission of electrons from the cathode, in contrast to the glow discharge. The most characteristic feature of an arc is the low value of the cathode fall, usually about ten volts. The current density in the gas and at the electrode surfaces is also very much higher than in a glow discharge. Current densities of up to hundreds of amps per sq. cm. in the gas phase and up to millions of amps per sq. cm. at the electrode are not unusual. The gas also attains high temperatures, 5,000 to 50,000^{o}K at high pressures. At low pressures the gas temperature may be little above ambient.

The electric field strength varies considerably with the current at a fixed pressure, see Fig. 5. This is indicated by an increase in gas temperature with increasing current flow. The current density j is proportional to the product of the electron density n and the field strength, i.e.

$$j \propto n E \qquad E \propto j/n$$

With increasing current, j increases resulting in a rise in the gas temperature. However, n increases exponentially with increasing gas temperature, resulting in a decreasing field strength.

2.3. A.C. Discharges

The characteristics of an a.c. discharge depend very much on the frequency of the discharge. At low frequencies, $\lesssim$ 100 c/s, the discharge is similar to the corresponding d.c. discharge. Breakdown takes place at the beginning of each half-cycle of current. Because of the low frequency the ionization in the discharge path has sufficient time to reach a low level before

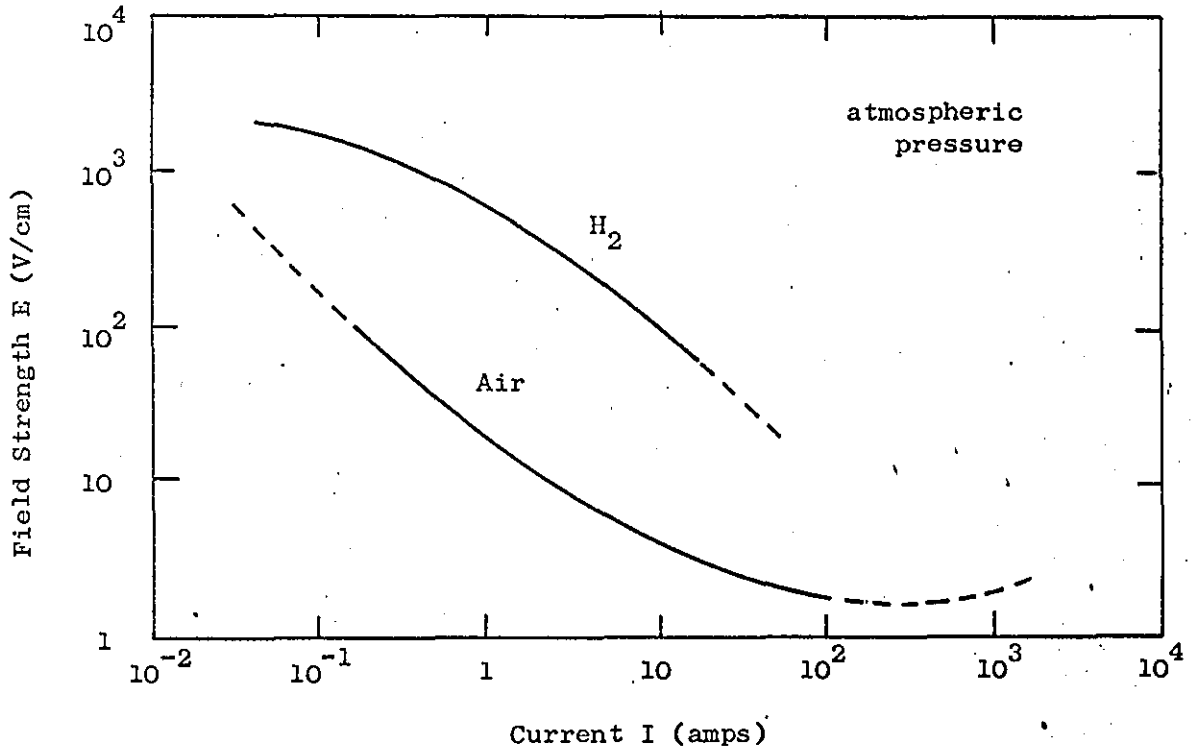

Figure 5a The Electric Field Strength E in a Positive Arc Column Versus Current

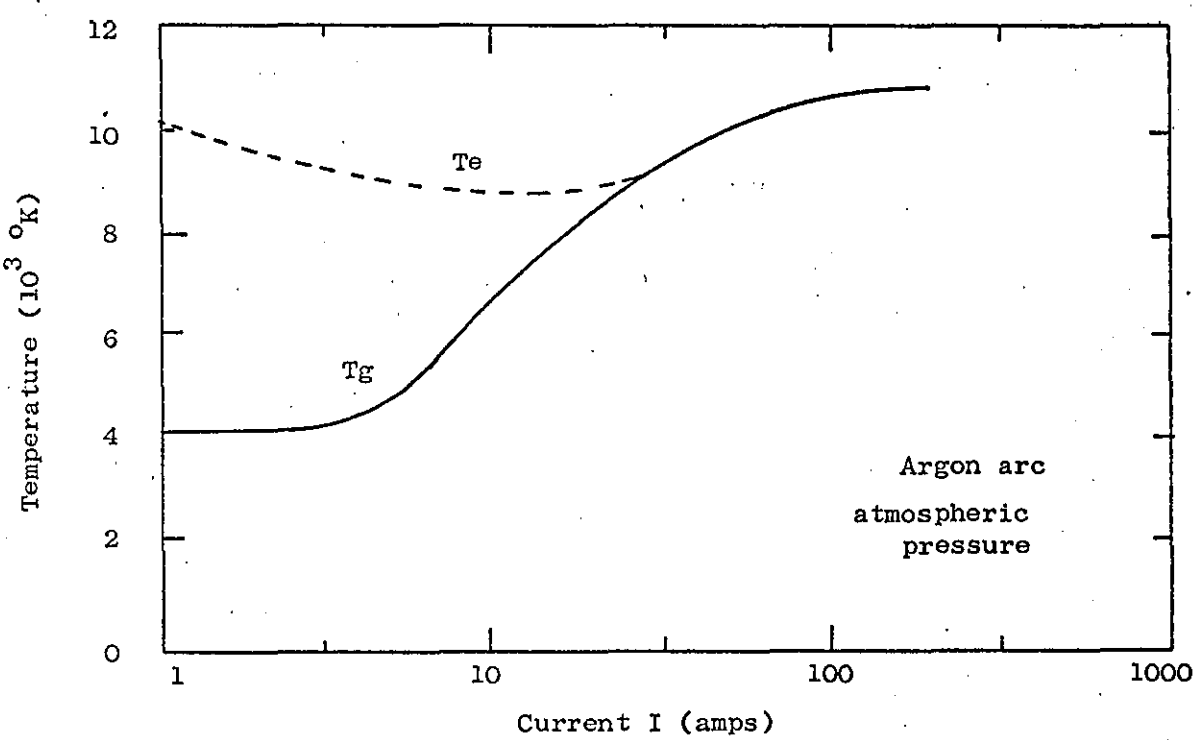

Figure 5b Variation of Electron and Gas Temperature with Discharge Current

the voltage builds up in the reverse direction. Essentially this means the discharge is extinguished at each point of zero current. Further breakdown depends on the voltage applied after the zero current point. The voltage however depends on the current and thus there is a variable component, the restriking voltage, which is dependent on the number of ionized species left in the discharge path from the previous discharge cycle. The stability of the low frequency a.c. discharge depends greatly on the overall electrical circuit. A capacitor - resistance network is more likely to give a stable discharge than a purely resistive circuit. The electrode material also displays a great influence on the stability of the discharge due to differences in "recovery" time. For instance carbon electrodes give a more stable discharge than, say, copper due to their longer "recovery" time. If the electrodes are of differing materials the breakdown in each half-cycle will be different.

As the frequency is increased the discharge cannot adjust to the rapid changes in current flow and so the discharge conditions tend to a mean i.e. with increasing current the discharge conditions are appropriate to a smaller current than actually flows, and vice-versa.

At frequencies of $>$ few kc/s the degree of ionization in the gas is nearly constant. This means that breakdown is not required at the beginning of each half-cycle. Hence the discharge is much more stable. At these frequencies there is often little difference between an arc and a glow discharge.

As the frequency is still further increased to the Mc/s region, the discharge current is independent of electrode

processes as the electron amplitude is less than the discharge length unless at very low pressure. Consequently, it is the diffusion theory of breakdown which is applied. The electrons are produced entirely in the gas phase. The current may use electrodes or may be an electrodeless arrangement as in the ring or toroidal discharges. Though these types of discharge are better known in high temperature plasma experiments, a stable discharge can be maintained at low power.

2.3.1. Radio-Frequency and Microwave Discharges

The more recent forms of the electrodeless discharge involve the use of a microwave or radio-frequency power source. Again the electron production takes place entirely in the gas phase. At radio-frequencies the power is transferred to the gas phase by either an inductive or a capacative coupling. At microwave frequencies efficient power transference is achieved by using a resonant cavity or by passing the discharge tube directly through a section of wave guide. The power gain from the field can be calculated from the equation,

$$P = e \mu E^2 = \frac{e^2 . E^2}{m . \nu_m} \left(\frac{\nu_m^2}{\nu_m^2 + w^2} \right)$$

where μ is the electron mobility.

ν_m the momentum transfer collision frequency which is equal to $\frac{}{\nu_c (1-\cos\theta)}$ for the elastic scattering of low energy electrons.

The electric field required to maintain a high frequency discharge is usually much less than that required for breakdown, and is always less than for a corresponding d.c. discharge due to the absence of the cathode fall. The conditions for the breakdown of the gas and for sustaining the discharge are approximately defined by the diffusion theory. This assumes the

major loss of electrons is due to the diffusion of electrons to the walls of the discharge tube. For a cylinder of radius r, length d, the general equation from the diffusion theory reduces to,

$$\frac{1}{\Lambda^2} = \frac{\pi^2}{d} + \left(\frac{2.405}{r}^2\right)$$

Romig[5], experimenting with a flow system in a helium r.f discharge, found the active discharge was decreased and a higher electric field was needed to maintain a steady-state discharge in comparison with a static helium r.f. discharge system. The above equation was modified to account for this,

$$\frac{1}{\Lambda^2} = \left(\frac{2.405}{R}^2\right) + \left(\frac{\pi}{2L}^2\right)$$

where R is the discharge radius,

and L is the discharge half-length.

The radial electron density distribution is a Bessel function; the axial distribution is shown in Fig. 6. An increase in the linear flow rate, for a tube of fixed geometry, was found to decrease the value of Λ and move the maximum electron concentration downstream.

The main consequence of the diffusion theory is that both the maintaining electric field and the breakdown voltage vary with pressure. A plot of the product $E_{eff}\Lambda$ (E_{eff} is the field strength corrected for frequency) against $p\Lambda$ gives a curve analogous to the Paschen curves for d.c. breakdown when plotted in similar parameters. Various other parameters can be used, such as,

$$E_{eff}\Lambda \ , \ \Lambda p \ , \ pf \ , \ E_{eff/p}$$

Brown and co-workers[6,7] have found good agreement between

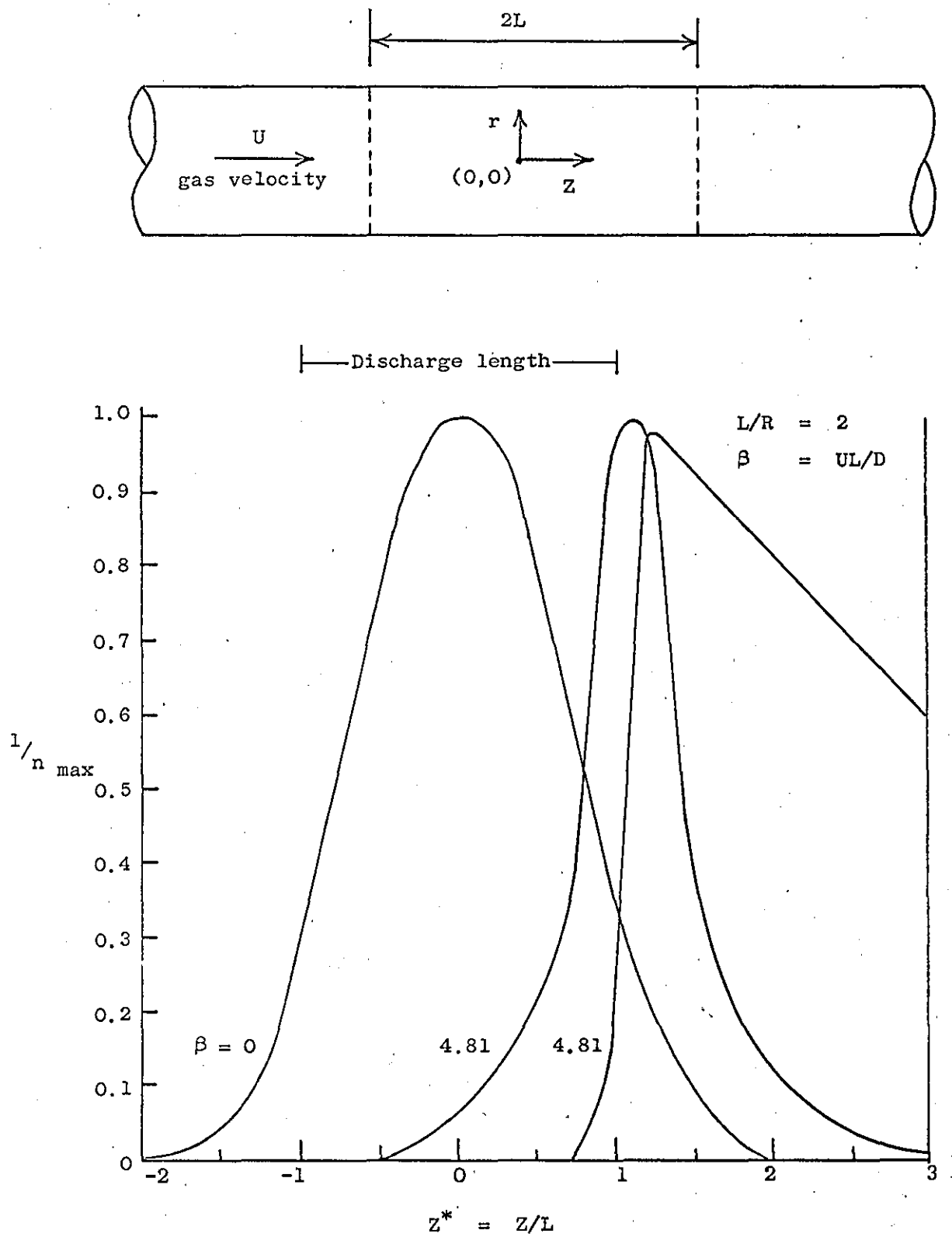

Figure 6 Electron-density Distribution in a Flow System

experiment and theory from measurements of breakdown fields in microwave cavities. The breakdown potential curves show a minimum at about 10 mm Hg. for microwave frequencies in dimensions of a few centimeters. The lower the frequency the lower the pressure at which the microwave breakdown occurs for a given vessel.

2.3.2. Pulsed Microwave Discharges

The simple diffusion theory assumes the approach to breakdown proceeds gradually. However, discharges can be obtained by high frequency pulses. This means that the electron density must grow so rapidly that a stable state is reached during the lifetime of the pulse. Thus the total time lag, the statistical time lag plus the formatative time lag, before breakdown occurs must be less than the length of the pulse. As found for d.c. discharges, the total time lag decreases when the applied voltage is increased. It would seem therefore that the shorter the pulse, the greater the breakdown voltage. Experiments by several workers,[8,9,10] using gases at pressures up to one atmosphere, with pulses of microwave field (f 3,000 Mc/s) of up to a few μ sec. confirmed the theoretical predictions. For instance, in discharges in the rare gases where the formatative time lag is long, the breakdown voltage was five times greater than in a continuous microwave field. The concept of the breakdown condition being when the electron production balances the electron loss by diffusion does not apply. The breakdown condition has in fact been shown to be determined by the field necessary to build up a certain critical number of ion-pairs within the pulse. Since the energy gained per mean free path is

COLLISION THEORY

$$\Delta \in = \frac{e}{2m} \cdot \frac{1}{\nu^2+w^2} \cdot E_0^2$$

the number of ion pairs produced by an electron in time, t, should depend on $E_0^2.t$ and hence, given constant irradiation of the gap to reduce the statistical time lag to negligible proportions, breakdown should occur at constant values of $E_0^2.t$. This has been experimentally confirmed in neon[11].

However, the breakdown field in polyatomic gases does not vary with the length of the pulse and is about the same as the continuous breakdown field. This may be due to the very short formatative time lag found for polyatomic gases. Again the concept of the electron gain balancing the electron loss for breakdown does not appear to hold. Instead, the idea that a few favourable collisions lead immediately to instability and breakdown. This is feasible at microwave frequencies when oscillating electrons, sweeping repeatedly through a small volume of gas, give a concentration of excited atoms which are subsequently ionized by further collisions. It should be noted that at microwave frequencies, $\sim 3 \times 10^9$ c/s, electrons make about twenty oscillations during the half-life of an excited state and thus the two-stage process is feasible. The experiments of Prowse and Lane[12] lend some support to this theory of two-stage ionization but they are not conclusive.

3. Collision Theory

Three types of collisions by electrons have to be considered i.e., elastic, inelastic and superelastic collisions. In an elastic collision the electrons simply bounce off the atom or molecule losing some kinetic energy but there is no change in the internal energy levels of the atom or molecule. If the collision is inelastic, a change in the internal state of the atom or molecule occurs with a consequent loss of the kinetic energy of the electron. The change may involve excitation of the atom or molecule to one of its characteristic states, or there may be single or multiple ionization. Generally, in excitation the atom returns to its ground state very quickly and radiates energy. However, some states may exist for times of the order of milliseconds before radiating away the energy acquired in the collision. These are called metastable states and sometimes play an important role in gas discharge phenomena. A type of collision which is inelastic and involves radiation at the time of the collision and sometimes electron capture, is called radiative.

Collisions between excited atoms or between an excited atom and one in the ground state, can result in the potential energy of the excited atom being released as kinetic energy of the resultant particles; if ionization of one of the atoms occurs, much of the available surplus energy is carried away by the ejected electron. Such collisions are termed superelastic. One process of special interest in discharges is the ionization of one kind of atom by an impact with the metastable state of another kind, i.e. the Penning effect. Common molecular gases, having an ionization potential of approximately 15 electron

volts are easily ionized by metastable atoms of the rare gases ($V_{metastable}$ 16-20 volts).

3.1. Elastic Collisions

The kinetic theory of gases indicates something of the detailed processes involving individual particles of the gas. Its application is necessary to comprehend the behaviour of gas discharges where collisional processes are all important.

The pressure, p, of a gas arises from the collisions of the gas particles with the walls of its container and can be expressed as,

$$p = \frac{nmC^2}{3}$$

where n = number density or concentration of particles.

m = mass of each particle.

C = root mean square velocity of the particles.

Using the perfect gas law equation, it follows,

$$nmC^2 V = 3RT$$

from which the mean energy of a particle is,

$$\tfrac{1}{2}mC^2 = \frac{3}{2}\frac{RT}{nV}$$

substituting k = R/nV, Boltzmann's constant mean kinetic energy per particle = 3/2 kT.

At room temperature, the mean energy per particle is about 0.04 eV.

Several concepts based on kinetic theory principles can be put forward to explain the behaviour of gas discharges by collisional processes.

3.1.1. Mean Free Path

The mean free path, λ, of the particles of a gas is the average distance which any one travels between collisions. For

a mixture of gases, the mean free path of a particle of type 1 between collisions with any other type of component particle is:

$$\lambda_1 = \frac{1}{\pi \sum_r n_r d_{1r}^2 \sqrt{(1+\frac{m_1}{m_r})}}$$

where $d_{ir} = \frac{1}{2}(d_1 + d_r)$, d is the diameter of the particle and m_r = mass of an r-type particle.

For r = 1, the equation reduces to,

$$\lambda = \frac{1}{2(n\pi d)^2}$$

In a gas discharge, the gas often consists of a single type of neutral particle with a very small proportion of ions and electrons. Assuming that ions behave exactly as neutral molecules in elastic collisions and electron - electron collisions are negligible, then the equation gives the mean free path of an electron as,

$$\lambda_e = \frac{1}{\pi n d^2}$$

since the mass and diameter of an electron may be ignored when compared with another particle.

Obviously the expressions will only give approximate values as gas particles are not elastic spheres of fixed diameter. However, the expressions may be used to define an effective cross-section for any type of collision. Where a particle may undergo different types of collisions, for example elastic or inelastic, different values of λ can always be defined as the average distances between successive collisions of each type, even although the path is not then "free".

Perhaps the important result is that λ varies inversely as density or, at constant temperature, as pressure, though this does not always apply to electrons.

3.1.2. Collision Cross-Section

The probability P of a particle making a collision in unit distance of its path is simply the reciprocal of its mean free path, λ. For collision by an electron the probability P is,

$$P = \frac{nq}{4}$$

where $q = \frac{\pi d^2}{4}$ i.e. the cross-section of the particle.
The probability P depends by definition on the concentration n. For this reason values of P are usually quoted for a gas pressure of 1 mm Hg and temperature 0°C, at which $n = 3.56 \times 10^{16}$ cm^{-3}. This value is known as the efficiency of the process considered, the term most commonly applied to excitation or ionization of gas particles by electrons.

A cross-section can be calculated for any type of collision. For example q_i for ionization, q_x for excitation or q_e for elastic collisions. The actual value of a cross-section is not a constant for a particular type of collision; it depends very much on the relative kinetic energy of the particles before they collide. It is therefore usual to express cross-sections, or collision probabilities as functions of energy, see Fig. 7.

The kinetic energy of relative motion of two particles of masses m_1 and m_2 can be shown to be,

$$\epsilon_r = \tfrac{1}{2} \cdot \frac{m_1 m_2}{m_1 + m_2} \cdot v_r^2$$

where v_r is the relative velocity.

If $m_1 \ll m_2$,

$$\epsilon_r = \tfrac{1}{2} \cdot m_1 v_r^2$$

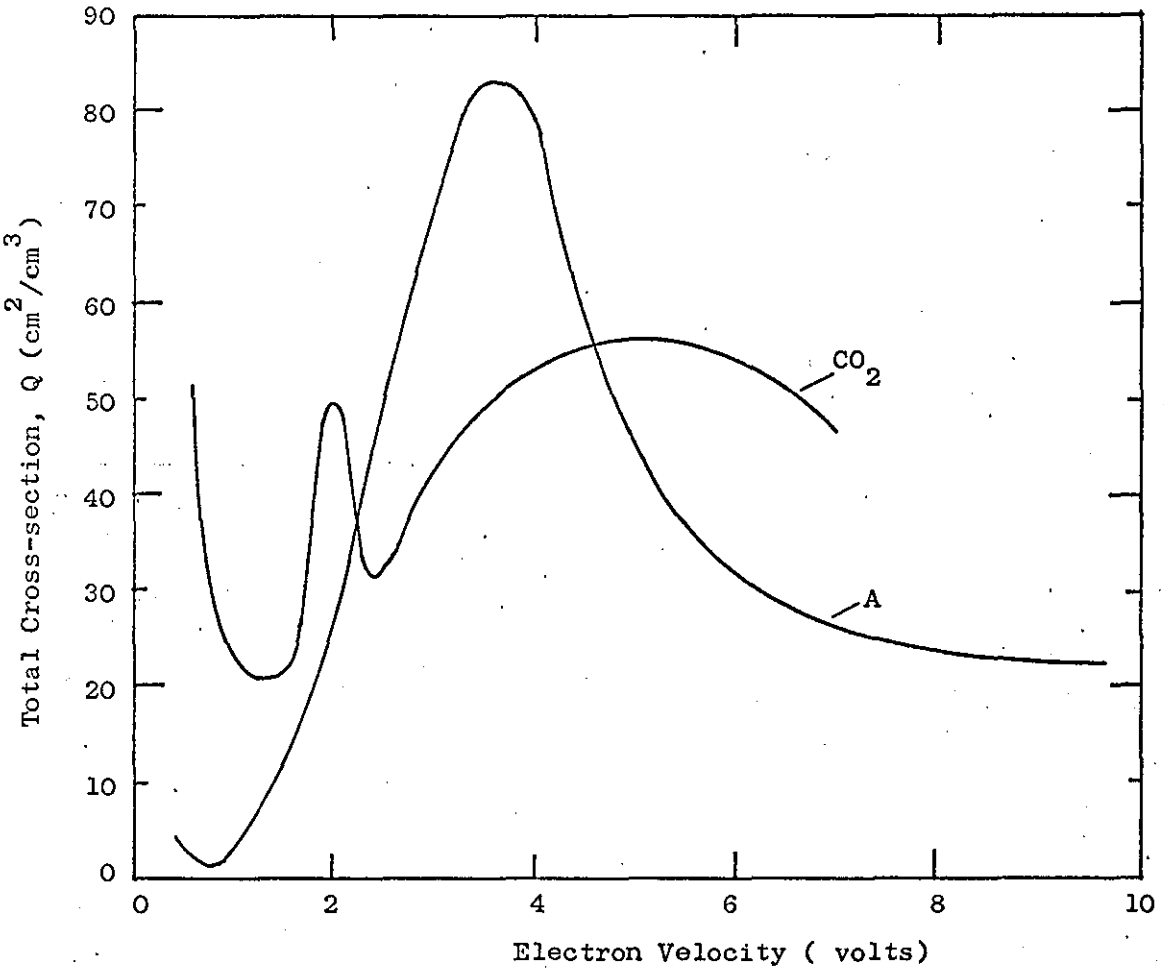

Figure 7a Total Cross-sections for Elastic Collision by electrons, at 1 mm Hg and 0°C

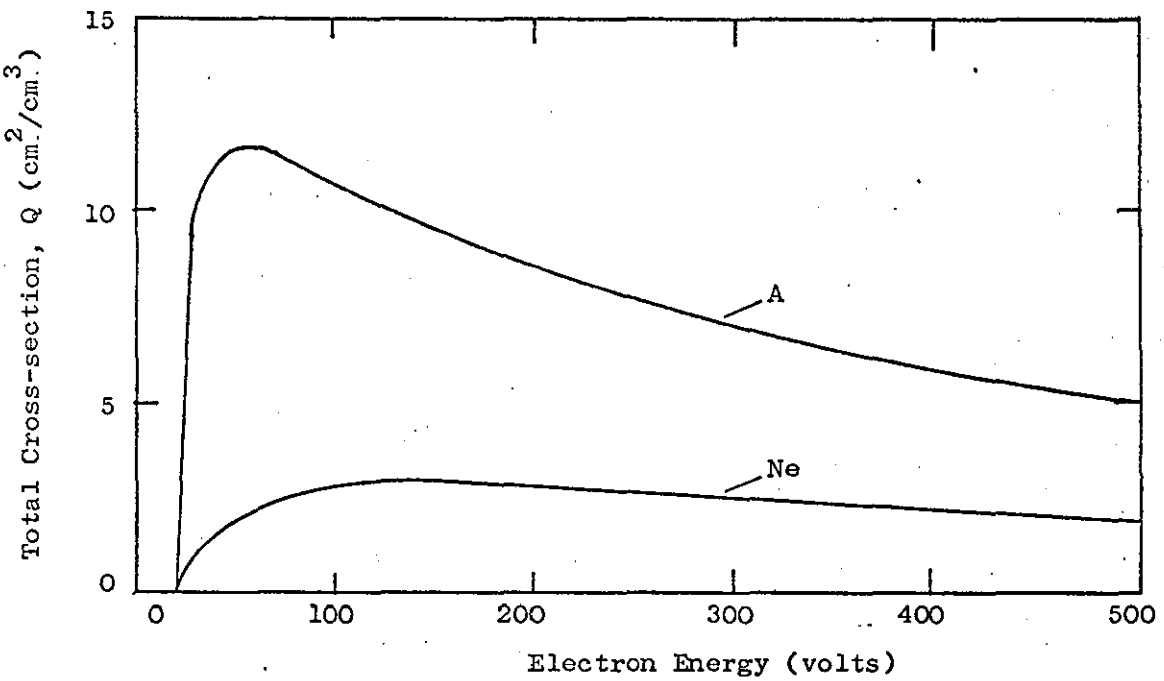

Figure 7b Total Cross-sections for Ionization by Electrons, at 1 mm Hg and 0°C

For an electron and a gas particle, v_r is approximately the velocity of the electron, since the heavier particles are very much slower. Therefore, the kinetic energy of relative motion is essentially that of the electron.

3.2. Inelastic Collisions

In an inelastic collision some of the kinetic energy of the impinging particle is converted into potential energy. This energy may be sufficient to excite or ionize an atom. In discharges the electron-molecule collisions are of great significance.

3.2.1. Excitation

Excitation can occur when the energy of the colliding electron exceeds the excitation potential of the atom for a particular state. Quantum conditions must apply and thus, linear and angular momentum must be conserved in the collision. Therefore, the change in angular momentum, p, in the collision must balance the change in the angular momentum of the atom in its initial and final state, i.e.

$$\Delta p = \frac{h}{2\pi} \cdot \Delta J$$

where ΔJ is the change in the principal quantum number. If the exciting electrons have exactly the energy necessary to excite the atom to a particular state, they must hit at precisely the right angle to satisfy the above condition. The electron after the collision would also be stationary. Obviously the probability of this is extremely small. The probability of excitation, P_x, increases at higher electron energies when the electron itself can carry away the excess energy in a direction which helps to satisfy the angular momentum condition. Usually

the excitation efficiency, h_x, is used, where

$$h_x = P_x / P_c$$

where P_c is the collision probability. Typical examples of h_x are shown in Fig. 8.

In atoms having two valency electrons, singlet - singlet transitions show a broad maximum with the maximum probability or cross-section, lying at energies several times the threshold level for excitation. Singlet-triplet transitions can also occur. In cases where the atoms have weak spin-orbit coupling, the change in spin in the transition is accomplished by the impinging electron replacing one atomic electron. This happens only in a narrow band of energies; the maximum probability occurring at just above the threshold level, see Fig. 9.

The angular distribution of the scattered electrons after excitation is very similar to that resulting from elastic collisions. However, when the electron loses a large fraction of energy the similarity of the elastic and inelastic scattering curves is reduced. This is also true for energy losses by ionization.

In certain circumstances it is possible for more than one valency electron in the atom to be excited to a higher level. The total energy of the doubly excited atom may be greater than the ionization potential of the normal atom. Both electrons can then revert to the ground state and emit a single quantum of energy, or one electron falls back to the ground state and the other electron is ejected from the atom with the excess energy. This process is called auto-ionization.

Excitation and ionization can also be produced by the impact of positive ions or neutral atoms. The cross-section for these

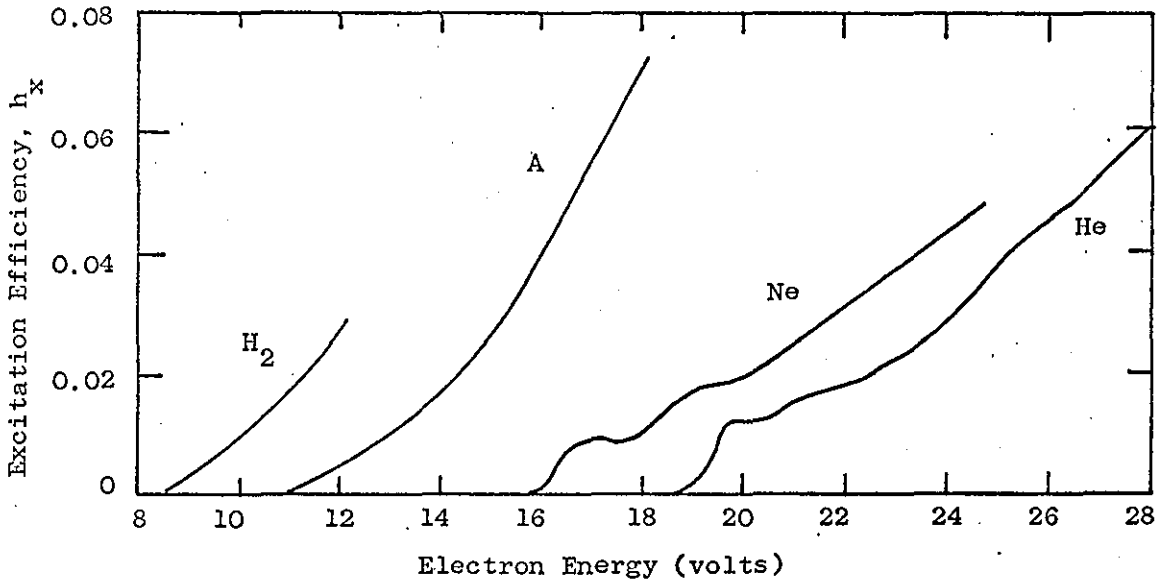

Figure 8 Efficiency of Excitation for Electrons in Helium, Neon, Argon, and Hydrogen

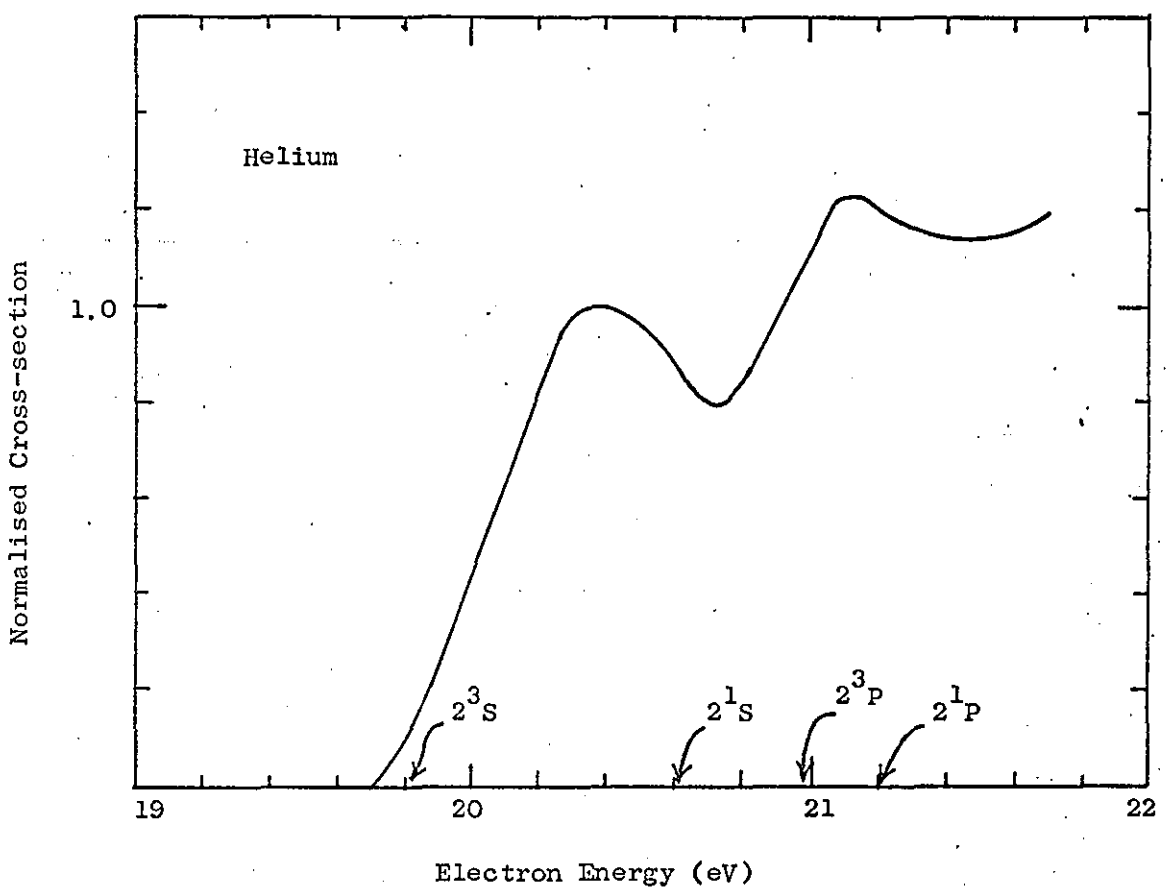

Figure 9 The Electron Impact Excitation Function for Helium Near the Threshold

processes are much smaller than for electron impact except for high energies, of the order of 200eV and above, when the relative velocity becomes comparable with that of electrons. Momentum must be conserved and thus the threshold energy is no longer simply the required energy of the electron transition. Experimental values for the threshold energies are not easily obtained.

3.2.2. Ionization

Ionization can occur when the energy of the electrons exceeds the ionization potential of the neutral atom. The usual quantum conditions are not applicable because the electron is ejected from the atom. The probability of ionization per collision, P_i, rises rapidly as the energy of the electrons increases. The parameter, h_i, the ionization efficiency,

$$h_i = P_i / P_c \qquad \text{where } P_c \text{ is the collision probability}$$

is usually used to express the dependence of the ionization on the electron energy. Typical examples of h_i are shown in Fig.10

The excess energy required to ionize an atom in an excited state is lower than that associated with the ionization of an atom in its ground state. The ionization cross-section of an excited atom is also larger due to the outer electron being in an orbit of greater radius.

If a gas is sufficiently hot, the random energy of an atom may occasionally be sufficient to ionize another upon collision. This process is called thermal ionization and is important in high pressure arc discharges. The process need not occur in a single collision. Cumulative ionization is possible, where several successive collisions give sufficient energy, through

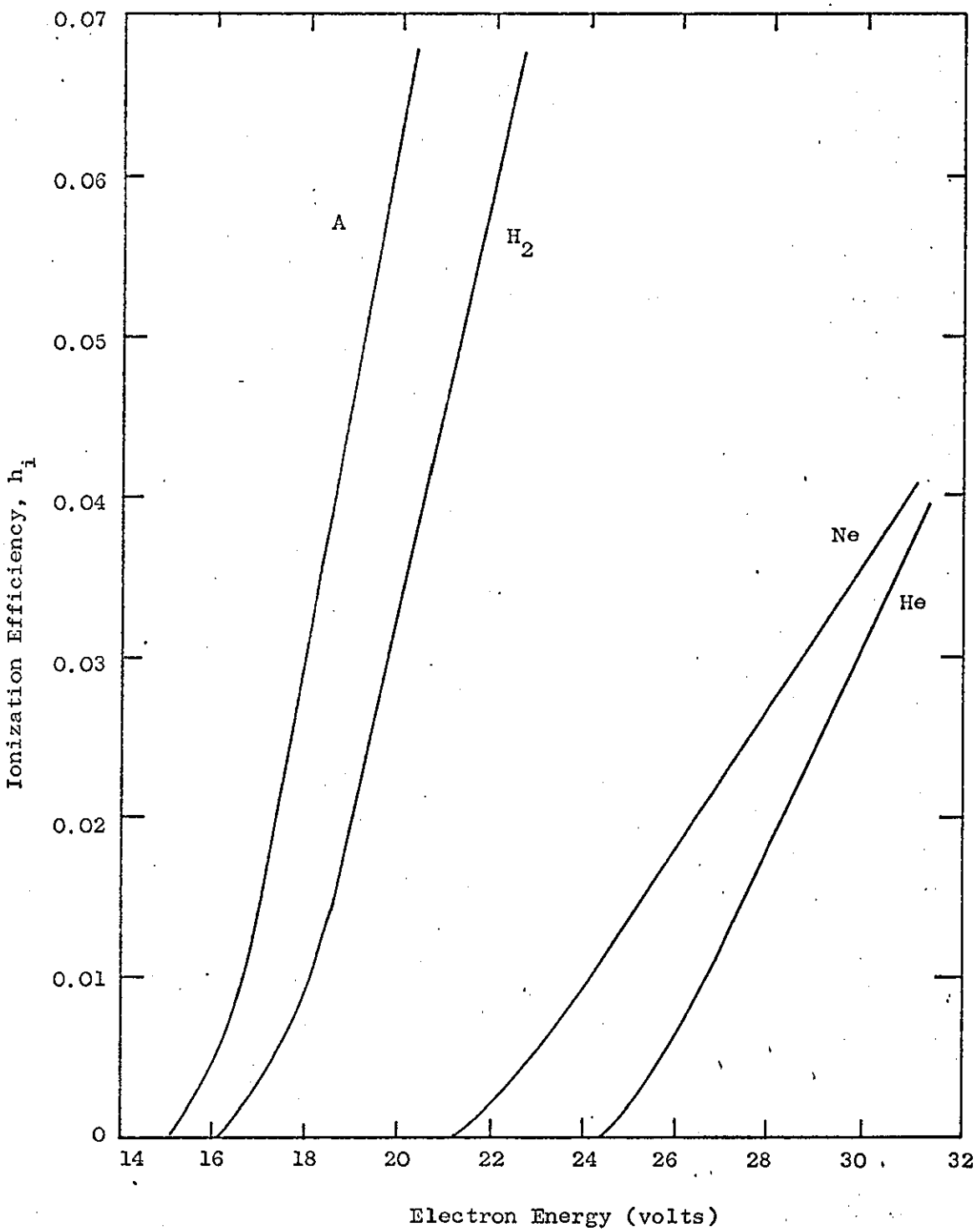

Figure 10 Efficiency of Ionization for Electrons in Various Gases

various stages of excitation finally to ionize an atom. Cumulative ionization can occur with any kind of ionizing collisions, and can be important at high pressure and temperature, when collisions are frequent enough to give a high probability that an excited atom will suffer a collision during its lifetime. The possibility also remains that the excited atom may deactivate on collision.

It should be noted that the discussions on excitation and ionization above relate to experiments carried out at low pressures, usually $\lesssim$ 1mm Hg. Their application to systems at higher pressures and energies requires caution. However, sufficient evidence is available to show the general trends can be applied to higher pressures and higher energy regions.

BASIC DISCHARGE REACTIONS

4. Basic Discharge Reactions

The discharge consists of various excited species, electrons, radicals, ions and neutral gas molecules. Each of these may be subjected to collisions from one another, resulting in deactivation or reaction to give new excited or ionized species. The various reactions can be conveniently sub-divided as follows:

4.1. Ionization by Electron Impact

Electron capture can occur at low energies when a particle is subject to an electron collision resulting in the formation of a negative ion. This ion may then dissociate to give a negative ion and a free radical

$$AB + e \longrightarrow AB^{-} \begin{cases} \swarrow A + B^{-} \\ \searrow A^{-} + B \end{cases}$$

Electron capture occurs at energies in the region of 5-7 eV and thus is likely to occur frequently in the discharge. Higher electron energies may cause the molecule to fragment spontaneously into ions.

$$AB + e \begin{cases} \nearrow A^{+} + B^{-} + e \\ \searrow B^{+} + A^{-} + e \end{cases}$$

This decomposition usually occurs at energies from 10-15 eV. At even higher electron energies, the impinging electron may cause the ejection of a valency electron giving a positively charged molecule which may then fragment to a positive ion and a free radical. The ionization reactions are particularly applicable to the low frequency a.c. or the d.c. glow discharge.

Two other low energy processes are the attachment of electrons to neutral atoms or molecules without subsequent fragmentation of the negative ions. Radiative attachment is

represented by,

$$e + AB \longrightarrow (AB^-)^* \longrightarrow AB^- + h$$

In three body attachment, stabilization is effected by collision with a third body, such as another particle or the vessel wall, e.g.

$$e + AB \longrightarrow (AB^-)^*$$

$$(AB^-)^* + AB \longrightarrow AB^- + (AB)^*$$

4.2. Atom Transfer

This type of reaction involves the abstraction by a positively charged particle of a simple atom, usually hydrogen, from a neutral gas molecule. These reactions can be an important source of free radicals in the discharge e.g.

$$N_2^+ + H_2 \longrightarrow N_2H^+ + H \qquad \text{ref.(13)}$$

$$CH_4 + C_3H_6 \longrightarrow CH_5^+ + C_3H_5 \qquad \text{ref.(14)}$$

$$O^+ + CO_2 \longrightarrow O_2^+ + CO \qquad \text{ref.(15)}$$

If the reactants are the same species then the reaction is called a symmetrical transfer reaction, e.g.

$$H_2^+ + H \longrightarrow H_3^+ + H \qquad \text{ref.(13)}$$

$$NH_3^+ + NH_3 \longrightarrow NH_4^+ + NH_2 \qquad \text{ref.(16)}$$

$$CH_4^+ + CH_4 \longrightarrow CH_5^+ + CH_3 \qquad \text{ref.(17)}$$

4.3. Ion-molecule Reactions

Ion-molecule reactions can greatly influence the chemical properties of the discharge. The reactions often lead to more than one set of products. The importance of these reactions increases with increasing pressure.

$$CH_3^+ + CH_4 \longrightarrow C_2H_5^+ + H_2 \qquad \text{ref.(13)}$$

$$C_2H_2^+ + C_2H_2 \longrightarrow \begin{cases} C_4H_2^+ + H_2 \\ C_4H_3^+ + H \end{cases} \qquad \text{ref.(18)}$$

$$CH_4^+ + O_2 \longrightarrow CH_3O^+ + OH \qquad \text{ref.(19)}$$

Positive ion transfer reactions can occur, usually in discharges of simple molecules and lead to the formation of free radicals, e.g.

$$O_2^+ + H_2 \longrightarrow O + H_2O^+ \qquad \text{ref.(20)}$$

$$C_2H_6^+ + H_2O \longrightarrow C_2H_5 + H_3O^+ \qquad \text{ref.(17)}$$

An important reaction found in hydrocarbon discharges is the hydrogen abstraction reaction, e.g.

$$C_2H_5^+ + C_3H_8 \longrightarrow C_2H_6 + C_3H_7^+ \qquad \text{ref.(21)}$$

$$C_2H_4^+ + C_3H_8 \longrightarrow C_2H_8 + C_3H_7^+ \qquad \text{ref.(21)}$$

4.4. Charge Transfer Reactions

These reactions are very rapid and also an important secondary source of free radicals. They are particularly important in simple gases and especially those gases containing small amounts of a different gas. A classic example of this is the ionization of argon by the small admixture of neon to the discharge. Other examples are,

$$O_2^+ + N \longrightarrow NO^+ + O \qquad \text{ref.(22)}$$

$$C_2H_2^+ + C_2H_4 \longrightarrow C_2H_4^+ + C_2H_2 \qquad \text{ref.(23)}$$

4.5. Electron - Ion Recombination Reactions

These are important in that they generate other excited species in the discharge, e.g.

$$N_2^+ + e \longrightarrow N + N \qquad \text{ref.(22)}$$

$$NO^+ + e \longrightarrow N + O \qquad \text{ref.(21)}$$

At higher pressures in the discharge the ion-molecule reactions assume a greater importance. At atmospheric pressure ion-ion reactions become significant.

4.6. Excitation of Ions

If an ion undergoes further electron impact, the ion is excited to a higher state. These excited ionic species can then react with neutral gas molecules to give more complex ionic species as well as free radicals.

$$(C_2H_6^+)^* + C_2H_6 \longrightarrow C_2H_7^+ + C_2H_5 \qquad \text{ref.(21)}$$

$$(N_2^+)^* + N_2 \longrightarrow N_3^+ + N \qquad \text{ref.(24)}$$

If the ionic concentration were sufficiently high the type of reaction above could be of great significance to chemical synthesis in the discharge.

4.7. Free Radical Reactions

Many of the products from the ionized or excited species in the discharge are free radicals. These species play an important role in the reactions leading to chemical synthesis. As the free radicals are very reactive their reactions are very fast even though they may enter into multi-stage processes.

Free radicals can undergo several types of reactions. One of the most common is the combination of two free radicals to

give a stable molecule, e.g.

$$CH_3^{\cdot} + CH_3^{\cdot} \longrightarrow C_2H_6 \qquad \text{ref.(25)}$$

$$C_2H_5^{\cdot} + C_2H_5^{\cdot} \longrightarrow C_4H_{10} \qquad \text{ref.(26)}$$

$$CH_3^{\cdot} + H^{\cdot} \longrightarrow CH_4 \qquad \text{ref.(25)}$$

It is an energetically favourable reaction as the heat of formation of the new bond is liberated, and so it frequently proceeds with little or no energy of activation. However removal of the liberated energy by a third body or surface is sometimes required to prevent rapid dissociation of the newly formed molecule. When polyatomic radicals recombine, the life of the collision complex is so much greater than for atoms that deactivation normally occurs during the life of the complex. Lifetimes of about 10^{-5} secs. are typical for hydrocarbon radicals at approximately 1 mm Hg.

One of the more important reactions for chemical synthesis is the aromatic substitution by a free radical e.g.,

$$NH_2^{\cdot} + \phi H \longrightarrow \phi NH_2 + H^{\cdot} \qquad \text{ref.(27)}$$

$$OH^{\cdot} + \phi H \longrightarrow \phi OH + H^{\cdot} \qquad \text{ref.(27)}$$

$$C_2H_5^{\cdot} + \phi H \longrightarrow \phi C_2H_5 + H^{\cdot} \qquad \text{ref.(27)}$$

Hydrogen abstraction reactions can lead to chain reactions of the type,

$$R^{\cdot} + R^1Y \longrightarrow RY + R^{1\cdot}$$

as R^1 is capable of performing a further abstractions e.g.,

$$C_6H_5^{\cdot} + H_2O \longrightarrow C_6H_6 + OH^{\cdot} \qquad \text{ref.(26)}$$

Disproportionation reactions to give molecular products are also possible,

$$2C_2H_5^{\cdot} \longrightarrow C_2H_4 + C_2H_6 \qquad \text{ref.(26)}$$

usually as an alternative to combination of two radicals. The tendency for a free radical to decompose into a smaller radical increases with increase in chain length. The free methyl radical is stable up to 1000°C. The free ethyl radical is not so stable, and radicals higher than ethyl readily decompose into methyl or ethyl radicals and an olefin e.g.

$$CH_3 - CH_2 - \dot{C}H_2 \longrightarrow \dot{C}H_3 + CH_2 = CH_2 \quad \text{ref.(25)}$$

Oxygen containing radicals are also particularly prone to fragmentations, e.g.

$$R^{1}\cdot + RCHO \longrightarrow R^{1}H + \dot{R}CO \quad \text{ref.(25)}$$

$$\dot{R}CO \longrightarrow \dot{R} + CO$$

Because radicals are electrically neutral, the relative strengths of the bonds approximate to their activation energies. Thermochemical studies ~~have given~~ gave the bond dissociation energy which is the energy required to break specific bonds for the formation of free radicals, and thus indicates broadly the path of radical reactions. Examples are given in Table 1 for the common gases. Bond dissociation energies vary very much with structure.

Free radicals play an important role in chemical synthesis in an electrical discharge. However, the variety of interactions possible between free radicals, radicals and neutral molecules, radicals and ions tend to give a broad range of products from the discharge, i.e. a loss in specificity.

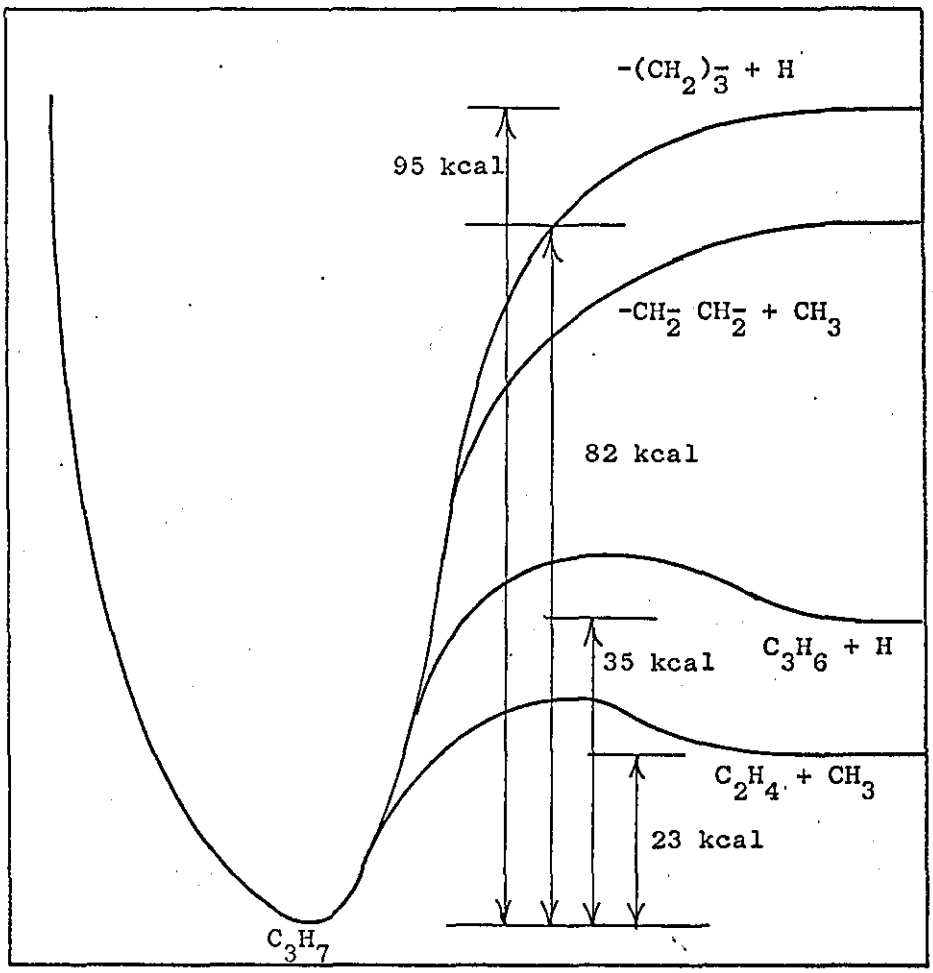

Figure 11 Different Modes of Dissociation of a Propyl Radical Depending on the Energy Input

Bond	D (kcal/mole)	D (eV/molecule)
H - H	104	4.52
N - N	170	7.37
O - O	117	5.08
NH_2 - H	97	4.2
C_6H_5 - H	102	4.41

Table 1 Bond Dissociation Energies at 25°C

SOME EXAMPLES OF SYSTEMS

PREVIOUSLY STUDIED

5. Some Examples of Systems Previously Studied

The electric discharge in its various forms has long been of interest in chemical synthesis. Because of the highly excited species produced in a discharge, many chemical systems that are unreactive under ordinary conditions undergo chemical reaction. It is these normally unattainable reactions which are of considerable interest, particularly in the search for direct routes to larger organic molecules such as aniline, phenol, etc. from reactions in benzene vapour. The production of hydrazine from ammonia has received fresh interest with the increasing demand for hydrazine for water treatment and in the production of heterocyclics. The investigations published in the literature have varied from attempts to determine the processes involved in a simple discharge such as the hydrogen discharge, to purely chemical studies of more complicated molecules such as benzene, toluene, subjected to a discharge. Empirical relationships have been presented in an attempt to correlate yields of products with the physical parameters of electric field strength, pressure, residence time, flow rate, etc.

Basically, the energy necessary for the production of chemically active species is supplied to the gas primarily by electron collisions. Dissociation of the gas into free radicals is often the result of complex interactions between electrons, ions and molecules. In the ordinary low pressure discharge, dissociation is almost entirely due to electron - molecule collisions. Collisions between atoms and molecules become important only in the high pressure discharges where gas temperatures reach values of the order of 10^5 ^{o}K.

5.1. Inorganic Gases in the Electric Discharge

The chemical systems studied and the types of the discharge reported in the literature cover a wide field. One of the earlier applications of the electric discharge was the production of ozone from oxygen or air, i.e. the Siemens ozonizer. A great deal of work has since been carried out on the system though it is mostly covered by patents. As such the information available from the general literature is mainly concerned with reactor design with little reference to the fundamental processes involved. The essential reactions have been postulated as follows[28,29]

$$O_2 + e \longrightarrow O_2^+ + e$$

$$O_2 + e \longrightarrow O_2^* + e$$

the excited oxygen molecule then dissociating to give two oxygen atoms,

$$O_2^* \longrightarrow O^\cdot + O^*$$

which then undergo reaction with neutral molecules of oxygen to give ozone,

$$O^\cdot + O_2 + W \longrightarrow O_3 + W$$

Reaction between excited oxygen atoms can occur in the gas phase to give excited ozone molecules which can either decompose or deactivate on the vessel walls.

$$O_2 + O^* \longrightarrow O_3^*$$

$$W + O_3^* \longrightarrow O_3 + W$$

The ozone is susceptible to decomposition by two routes,

$$O_3 + O^\cdot \longrightarrow 2O_2$$

$$O_3 + e \longrightarrow O_2 + O^\cdot + e$$

The ozone yield can be increased by cooling the vessel walls so the ozone liquefies and runs out from the discharge zone. By increasing the amount of solid surface, the yield of ozone is increased[30]. As the power of the discharge is increased, the conversion passes through a maximum[31]. Increasing the flow rate increases the energy yield but decreases the percentage conversion[32].

The demand for ozone is usually for a diluted form, it being easier to store and use. Ozone is widely used for water purification in Europe and the demand for ozone is expected to grow in future years. The ozone is effective not only in the elimination of bacterial and virus activity but also removes taste, odour, and colour from polluted water. The ozonizer is usually operated at atmospheric pressure and low power input conditions. Normal operating energy yields are 45 - 50 g/Kwhr.

5.1.1. <u>The Hydrogen Discharge</u>

The hydrogen discharge has been extensively studied[33-35]. Rate constants for the production of hydrogen atoms have been calculated and are of the order of 10^{-9} cc/molecule sec. for the reaction[36],

$$H_2 + e \longrightarrow H^{\cdot} + H^{\cdot} + e$$

The hydrogen atom production can be supplemented by fast electron-ion recombination at the wall, and the ion-molecule reaction.

$$H_2^+ + H_2 \longrightarrow H_3^+ + H^{\cdot}$$

Atoms are lost from the discharge by diffusion to the walls and subsequent recombination,

$$H^{\cdot} + H^{\cdot} + W \longrightarrow H_2 + W$$

The rate of recombination of the hydrogen atoms is influenced by the nature of the surface of the wall. Small admixtures of other gases also have a marked effect on the recombination rate of hydrogen atoms[37,38]. For instance, the presence of 0.1% water in the discharge enables an atom concentration of up to 10% to be built up. Whether this increase is solely owing to a reduction in wall activity or to a change in the production processes in the discharge is not yet clear. The breakdown field in a microwave discharge in hydrogen is lowered by about 30% in the presence of small amounts of water[37].

5.1.2. The Nitrogen Discharge

The presence of water vapour also has a strong influence on the nitrogen atom concentration in a nitrogen discharge. In dry nitrogen, in both d.c. and microwave discharges, the conversion to nitrogen atoms is approximately 1%[39,40]. In the presence of water vapour or oxygen however, conversions to nitrogen atoms have varied from 4% up to complete dissociation of the nitrogen[41-4 No satisfactory interpretation has yet been reported to explain the marked effect on the discharge characteristics of traces of water vapour. A similar increase in the atom concentration has been reported in a wet oxygen discharge in comparison with a dry oxygen discharge[44,45].

The nitrogen discharge has stimulated great interest because of the so-called "nitrogen afterglow". The existence of long lived vibrationally excited ground-state molecules have been suggested as the cause of the afterglow. The main ion produced in the discharge is N_2^+ at a potential of 15.7 eV[46]. Atom production proceeds via the dissociation of excited states. The rate constant for the dissociation has been calculated to be

in the order of 10^{-11} ccs/molecule sec. Vibrational excitation occurs at very low electron energies.

Young et al[47], with a microwave discharge, found that the degree of dissociation of the nitrogen was largely determined by the amount of impurities present. Other experiments have indicated that sufficiently pure nitrogen might not dissociate. This may also apply to very pure hydrogen. Young et al[47] also showed that the addition of nitric oxide and to a lesser extent oxygen after the discharge but before the afterglow produced a large increase in the degree of dissociation of nitrogen. The nitrogen atom concentration was also dependent on the linear flow rate of the nitrogen input. The addition of sulphur hexafluoride greatly extended the length of the afterglow and increased the intensity[47,48].

5.1.3. Polyatomic Gases

The experiments on the diatomic gases indicate that the discharge characteristics can be altered dramatically by the presence of impurities. The nature of the surface of the discharge tube has also a great influence on the concentration of atoms in the discharge. The effects are also found in discharges of polyatomic gases such as carbon dioxide, ammonia etc. but are less marked.

Semiokhin[49] studied the dissociation of carbon dioxide in a silent discharge in a circulating flow system. The degree of dissociation, α, was investigated as a function of the gas pressure, over the range 100 - 700 mm Hg, the power input to the discharge and the wall temperature. The maximum value for the degree of dissociation was found at a pressure of 300 mm Hg at a power input of about 50 watts when α = 34%. The proposed

dissociation reaction was,

$$CO_2 \underset{k_1}{\overset{k_o}{\rightleftharpoons}} CO + \tfrac{1}{2}O_2$$

k_o increased with increasing pressure from 0.005 to 0.013 over the pressure range 100 - 700 mm Hg. k_1 increased from 0.023 to 0.047 units over the same range; units of k_o, k_1 not given. k_o was calculated as the amount of carbon dioxide that dissociated per unit of electrical energy at high velocities of gas flow i.e. when U/V 0, where U/V is the energy per unit of gas flow. The wall temperature had little influence on the rates of reaction. The dissociation of the carbon dioxide was influenced by the presence of other gases[50]. Helium was found to decrease the degree of dissociation; argon had a negligible effect; and nitrogen increased the dissociation of carbon dioxide, over the range 4 - 60% content in the carbon dioxide feed. The addition of CO and O decreased the dissociation in agreement with the Le Chateliers principle. α was independent of power over the range 30 - 100 watts but increased greatly over the range 30 - 100 watts.

In the presence of 3 - 25% of water, Wilde et al[51], found the carbon dioxide decomposed to give up to 9% of carbon monoxide in a high frequency electric arc.

5.1.4. Mixtures of Gases

The reaction between nitrogen and oxygen in the electric discharge yields various nitrogen oxides depending on the conditions employed. Nitric oxide appears to be the primary product of the reaction[4,52] McCarthy[53] similarly found in a microwave discharge of 2,450 Mc/s, the primary reaction was to nitric oxide though some nitrogen dioxide was also formed. Yields of up to 13% nitric oxide were obtained.

Strutt[54] reported finding N_2O_3 in the quenched product of the discharge according to the mechanism,

$$2NO + N^{\cdot} \longrightarrow NO_2 + N_2$$

$$NO_2 + NO \longrightarrow N_2O_3$$

Several workers have shown that the addition of water vapour leads to the production of nitric acid but the yields were not commercially valuable[4].

Other inorganic systems have been studied including the production of hydrazine from ammonia, discussed fully on page 87 Chlorine has been produced in good yield by the oxidation of hydrogen chloride in a microwave discharge[55]. Various phosphorous compounds such as disilanylphosphine[56], diphosphorous tetrachloride[57] have been synthesized; sulphur trioxide has been prepared from sulphur dioxide[58]; various haloboron compounds and halosulphur compounds have also been made[59,60]. Of these, the two processes of major interest have been the production of ozone and of hydrazine.

5.2. Organic Vapours in the Electric Discharge

The application of the electric discharge to organic synthetic chemistry perhaps offers more opportunity to promote a commercial process than in the inorganic systems. The greater part of work so far reported has mainly concerned the production of acetylene from various hydrocarbons. However, recent work has shown much larger molecules can be synthesized under selective discharge conditions.

5.2.1. The Methane Discharge

Numerous patents have been filed on the manufacture of acetylene in an electric discharge. H'in and Eremin[61]

investigated the effect of the reactor dimensions, and the use of a spray absorbent on the synthesis of acetylene in an electric arc in methane. ~~The effect of~~ Preheating the gas increased the total conversion. The injection of a spray of water, under predetermined optimum conditions, increased the total conversion from 0.43 to 0.78% of which 0.32% to 54% was to acetylene. The ratio of the acetylene conversion to the total conversion was independent of the energy input and was unaffected by preheating or cooling of the input stream.

Popovici[62], in a high frequency discharge in methane, found not only acetylene but also ethylacetylene, cyclopentadiene, indene and formaldehyde which came from small amounts of air in the methane. The discharge also gave a $(CH)_n$ type polymer. The formation of this polymer was postulated as being due to $(CH)^+$ ions migrating to the cathode where they were neutralized to give CH radicals which polymerised to $(CH)_n$.

Badareu[63] obtained similar results from a d.c. glow discharge in methane between aluminium electrodes. The yield of acetylene was very sensitive to flow rate and passed through a sharp maximum as the flow was increased. The yield of acetylene varied up to 25% from the reaction.

$$2CH_4 \longrightarrow C_2H_2 + 3H_2$$

Increasing the length of the positive column increased the yield of acetylene considerably. Carbon was not formed, probably because of the large concentration of hydrogen atoms present. Ultra-violet spectra showed the presence of CH, CH^+, acetylene and possibly benzene. A polymer of the $(CH)_n$ type was found in the neighbourhood of the electrodes.

Tsentsiper et al[64] studied the conversion of not only

methane but also hydrocarbons such as ethane, propane, ethylene and propylene in a static system. The predominant reaction process from all these hydrocarbons was the production of acetylene and to a slight extent ethylene; pressure range 10 - 150 mm Hg, current 50 - 6,000 mA. The presence of hydrogen or argon lowered the conversion to acetylene. This reduction in yield increased with dilution and was more marked for hydrogen than argon. However, the transition from an arc discharge to a glow discharge occurred on dilution of the original hydrocarbon. The differences in acetylene yields could thus be attributed, partially or wholly, to this transition and not to the chemical effect of the presence of hydrogen or argon.

5.2.2. The Production of O-containing Compounds in the Discharge

Formaldehyde has been prepared by the slow oxidation of methane in electric discharges. Badareu, Popovici and Albu[65] studied the effect of a spark discharge on a flowing methane/air mixture at atmospheric pressure. Formaldehyde was produced and the yield depended on the linear flow rate, on the mole ratio of methane to air and on the electrode distance. The maximum yield obtained was 25.7 g. HCHO/cu metre of methane.

Thornton and Sergio[66] investigated the production of formaldehyde in a methane and water high frequency discharge between axial electrodes. A mixture of methane and water was sprayed into the discharge zone; pressure 80 mm Hg and a power input of 30 watts. The presence of the water spray increased their yield of formaldehyde from 0.38 g/Kwh to 1.5 g/Kwh at a water flow of 30 - 56 g/min. In the presence of 37.5% air the formaldehyde yield increased from 0.86 to 2.31 g/Kwh at a water flow of 30 - 60 g/min. The production of carbon monoxide was

also greater with air present. Although yields were still low, the improvement in yields justified the spray absorbent technique. The spray has the effect of reducing the residence time of the product without reducing the conversion per pass.

In the presence of ozone, produced in situ from oxygen in a Seimens ozonizer at 8-11.65 kV, methane is converted to formaldehyde, acids and peroxides[67]. The rate of conversion of the oxygen to ozone was higher than that of the required products. The conditions of the discharge were thus set to achieve predominance of the reaction,

$$CH_3OO\cdot \longrightarrow HCHO + OH$$

which was obtained by a high oxygen concentration in the initial gas mixture. In all cases conversions were higher at higher voltages. Dilution with argon enabled the influence of the partial pressures of the components to be investigated. The conversion into formaldehyde increased linearly with the methane concentration. Hence it was concluded the slow oxidation of methane was determined by the partial pressure of methane in the reaction mixture. This indicated a similarity in mechanism of this oxidation reaction to that at high temperatures (400 - 815°C)[68]. A change in the vessel material from quartz to rasotherm glass altered the product ratios, the perioxides being favoured. This clearly showed the importance of the nature of the wall surface on the dissociation reactions.

Mixtures of carbon dioxide and methane or carbon monoxide and methane were subjected to a silent discharge at 700 mm Hg with a discharge current of 18 mA[69]. The carbon dioxide and methane mixture gave a 17% yield of O-containing compounds of which 60 - 70% were carbonyl compounds. The yield of

O-containing compounds was reduced to 5% when the carbon dioxide was replaced by carbon monoxide. On lowering the applied voltage, from 3.0 kV to 0.5 kV above the breakdown voltage, the total conversion increased. Increasing the residence time and/or the percentage of carbon dioxide in the mixture increased the conversion.

5.2.3. The Formation of Hydrogen Cyanide in the Discharge

Miyazaki[70], using a 100 Mc/s discharge at atmospheric pressure, found hydrogen cyanide was produced from a mixture of methane, nitrogen and/or ammonia. The rate of conversion to hydrogen cyanide was retarded by the hydrogen produced from the decomposition of the methane. Packing the discharge tube with glass fibres promoted the rate of formation of hydrogen cyanide. An increase in discharge frequency to 250 Mc/s increased the yield of hydrogen cyanide to 80%. With ammonia present, the reaction to give hydrogen cyanide was postulated as proceeding via the interaction of NH and CH radicals.

Many more organic discharge processes have been reported e.g. alkyl chloride from the chlorination of alcohols[71,72]; phosgene from the decomposition of chlorinated hydrocarbons[73]; ammino-acid synthesis from carbon, oxygen and hydrogen etc.[74,75]. All of which indicate the wide field of application of the electric discharge to organic chemistry.

5.2.4. Polymer Production in the Discharge

One of the latest developments of interest is the production of thin layers of polymer on surfaces by an electric discharge. Potential applications include the plating of metals and other surfaces to increase their resistance to corrosion and abrasion. Applications are also possible in the electronics industry where

thin layer plating techniques are essential. Compounds which normally polymerize in the bulk phase give the best films, e.g. methyl methacrylate. The films are usually uniform and have a high electrical resistance. Films can be prepared from the vapour of practically any organic material although there is a wide variation in the rate of film lay-down. Hay[76] has investigated the polymerisation of organic vapours on electrode surfaces and on moving substrates. A 1 Mc/s high-voltage supply was imposed on the gap between insulated electrodes with a mixture of monomer vapour and nitrogen in the gap at a total pressure of 1 atmosphere. Monomers included vinyl compounds such as styrene, acrylonitrile, 1-octene, acrylic acid mono-allylamine and tri-allylamine and non-vinyl compounds such as benzene, toluene and benzotrifluoride. Yields of polymer were increased in many cases by the inclusion of a halogen compound with the monomer. Reaction mechanisms are complex and can not be satisfactorily explained.

Systems considered to be of particular interest to the present work included the production of ethylene glycol from methanol, the kinetics of the dissociation of cyclohexane in comparison with benzene or with linear hexane and polymer formation in benzene discharges.

5.2.5. Methanol

Only scanty information on the reactions of methanol in an electric discharge can be found in the literature. Takahishi[77] studied the decomposition of methanol in a high frequency discharge in a closed system. The influence of additions of hydrogen and methane to the discharge were also

studied. CO, H, CH_4, HCHO and H_2O were obtained as the main products in amounts varying with the quantity of hydrogen and methane added to the system. The reactions,

$$CH_3OH \longrightarrow CH_3^{\cdot} + OH^{\cdot}$$

and $$CH_3OH \longrightarrow 2H^{\cdot} + HCHO$$

were proposed as the primary dissociation of methanol.

Kokurin and Gruzdera[78] found that methanol in an electric arc gave mainly carbon monoxide and water. The decomposition process was similar to that in an electrodeless discharge in a quartz tube at 6 Mc/s, in the stationary vapour[79]. Identification of bands of lines in the emmision spectrum due to CH, OH, CO, H_2, H, C was made.

Anaud has investigated the vapour-phase chlorination of methanol in a silent discharge[72].

5.2.6 Saturated C_6 Hydrocarbons

Coates[80] has made a detailed study of the microwave induced dissociation of n-hexane. Using a flow system at 1 mm Hg, 25 individual components were detected. Apart from this one investigation little other information exists in the literature.

Cyclohexane is also only scantily reported in the literature. Arnold[81] investigated the dissociation of cyclohexane in d.c. discharges at 50 c/s and 535 c/s. The major reaction products were C_2, C_3 and C_4 hydrocarbons.

Inoue[82] studied the slow oxidation of cyclohexane in a silent discharge. Cyclohexanol and cyclohexanone were obtained as the main products.

5.2.7. Benzene

Stille et al[83] investigated the reaction of benzene in an r.f. glow discharge. The phenyl radical was detected from the emission spectra. A complex mixture of products was obtained including poly (phenylenes), diphenyl, fulvene, acetylene, allene and methylacetylene.

Kraajveld and Waterman[84] subjected benzene vapour to a gas discharge at 2,400V, 50 mA, and at a pressure of 2 mm Hg. The linear flow rate of the benzene vapour influenced the yield of diphenyl. Decreasing the linear flow rate increased both the total conversion of the benzene and the percentage yield of diphenyl. Under optimum conditions the yield of diphenyl constituted 30% of the benzene converted.

The influence of varying vapour pressures in the formation of diphenyl in a flow discharge through benzene vapour has been studied[85]. At lower vapour pressures (5 mm Hg) the benzene was nearly completely destroyed, and band spectra of C_2, CH and benzene were observed. At higher vapour pressures (10 - 20 mm Hg) the discharge behaviour was entirely different, and a continuous band spectrum was observed from 2,600 A to 5,400 A. Under the latter conditions diphenyl was obtained.

Schuler et al[86] analysed by gas-liquid chromatography the products from a d.c. flow discharge in benzene. Diphenyl, toluene, ethylbenzene, phenylacetylene, and naphthalene were identified. Of the benzene converted 50% was a polymeric material which was benzene soluble and had a molecular weight of 708. A polymeric material was also detected when the saturated vapours of benzene and toluene were subjected to a high frequency discharge[87]. Yellow-brown

solids were deposited on the walls of the discharge tube and were found to be partially soluble in benzene.

Vastola and Wightman[88] investigated the reactions of benzene in a microwave discharge, with a maximum power input of 85W at 2450 Mc/s and pressures below 1 mm Hg in a static system. No gaseous products were detected though a yellowish hydrocarbon film was found on the surface of the reactor vessel. Infra-red analysis indicated that the film was unsaturated but contained no aromatic bonding. The films also exhibited high concentrations of free spins. This suggested the CH radical was probably responsible for the polymer film.

Streitweiser and Ward also investigated the decomposition of benzene in a microwave discharge[89]. However, the benzene was admixed with helium before entering the discharge zone. Some tar and carbonaceous material was formed and also some low boilers, of which hydrogen, methane and acetylene were identified by gas chromatography. However, they found negligible proportions ($< 0.005\%$) of polyaryls.

Ranney and O'Connor investigated the reactors of benzene vapour in a corona discharge. Excitation of benzene vapour in a 15 kV corona discharge reactor at atmospheric pressure and 45°C gave an 8.5% conversion to identifiable products. Diphenyl, O-m-p terphenyls, phenyl cycloalkenes, fulvene, 1, 3, and 1, 4 - cyclohexadienes, cyclohexene and acetylene were quantitatively determined. The polymeric material was a yellow solid, largely soluble in benzene, with a major fraction having average molecular weight of 4000. Lower molecular weight fractions of about 300 were isolated as

yellow, tacky resins. Infra-red and nuclear magnetic resonance spectra indicated only mono-substituted phenyl groups pendent to the main chain with no evidence for polymer build-up by way of consecutive phenyl linkages and random hydrogenation. A phenyl or benzyl substituted five numbered ring containing one double bond was indicated as the average repeating unit.

Kawahata[91] studied the vapour phase decomposition of aromatic and hydroaromatic hydrocarbons by an electrical corona discharge of 10 kc/s in hydrogen. Hydrogen containing a certain concentration of organic vapour was preheated and fed into the discharge zone. The reactor temperature was 300°C and the pressure 70 - 760 mm Hg. Condensed products included m-cresol, α-methylnaphthalene, tetrahydronaphthalene, decahydronaphthalene and dihydrophenanthrene. Formation of solid films on the reactor wall was also observed.

A study has been made of the conversion of benzene to a polymeric substance in a radio-frequency discharge[92]. A 3.69 M Hz generator coupled capacitively to a pyrex flow reactor, pressures 1 - 20 mm Hg. Depending on conditions employed, the polymerisation resulted in either a complete conversion to a solid polymer or a low conversion to a liquid polymer. Infra-red spectra showed the polymers to be structurally similar. Infra-red and nuclear magnetic resonance data suggested a basic polymeric structure similar to that of polystyrene. The difference between the solid and liquid polymers was postulated as being one of crosslinking.

There is also evidence from the literature that the addition of another gas to the benzene discharge can result in

reactions with the phenyl radicals. Sugino and Inoue[93] investigated the reactions of benzene and dry air in a Siemens ozonizer. A voltage of 15 kV was used at a discharge current of 1.25 mA. Up to 10% of benzene was present in the gas mixture, at a total flow rate of 0.12 - 0.30 litres/hour. Phenol was obtained in a yield of 25 - 30% of the reacted benzene. An unidentified solid was also found. The overall conversion efficiency was 0.9 - 3.3%.

The production of aromatic amines from benzene in an electric discharge has been patented[94]. Benzene vapour was used in a 2.1 ratio with ammonia gas, and the resulting mixture at 90°C passed through a silent electric discharge at atmospheric pressure. Aniline was produced in approximately 5.5% yield based on the total input.

Sugino and Inoue[95] investigated the reactions of benzene and ammonia in a Berthelot tube. The electrical parameters were set at 13 kV, 2.5 mA, 50 c/s. A flow rate of 42 litre/hour at 730 mm Hg and 30°C was maintained. Approximately 0.2% of the benzene reacted, the yield of aniline being about 30% of the reacted benzene. Small amounts of m-phenylenediamine and other unidentified amines and hydrocarbons were also found.

Prilezhaeva and Naether[27] studied the chemical reactions of benzene with other gases in a high frequency electrodeless discharge by means of absorption, emission and fluorescence spectrocopy. They found evidence for the following equilibrium reactions,

$$\phi H + NH_3 \longrightarrow \phi NH_2 + H_2$$

$$\phi H + CH_4 \longrightarrow \phi CH_3 + H_2$$

$$\phi H + CO \longrightarrow \phi CHO$$

THE CHOICE, OPERATION AND PRELIMINARY TESTING OF THE MICROWAVE EQUIPMENT

6.1. Choice of Electrical System

The advantages and disadvantages of the electric arc, the d.c. glow discharge, and the microwave discharge were examined carefully before a choice was made of which system to use.

The main drawbacks of the electric arc are:

1) The presence of electrodes constitutes a major contamination problem, especially in a high intensity arc.

2) Most of the energy supplied to the system essentially raises the gas temperature which may vary from 5,000 - 50,000°K. The efficiency of chemical activation based on the energy input is thus low.

3) As the electric arc is sustained by thermal processes, only reactions with favourable high temperature thermodynamics or kinetics are of possible interest.

Apart from the chemical aspects, the electric arc needs a costly high current power supply. Electrode cooling may be an added complication. Thus economically and chemically the electric arc is limited in its application.

The d.c. glow discharge also has the problem of possible contamination from electrodes. However, evidence is available to show that the d.c. glow discharge is capable of producing appreciable numbers of free radicals. However, the discharge is not very stable above 30 mm Hg. and the characteristics of the discharge may alter. Commercially therefore the d.c. glow discharge, though electrically simple, is costly to operate because of the low pressures involved.

The advent of commercial microwave systems in industry, e.g. in drying processes, has greatly facilitated the acquisition of microwave equipment. However, the high cost of microwave power

relative to d.c. power is a disadvantage.

McCarthy[53] has shown the microwave discharge to be more efficient in producing free radicals per energy unit than the d.c. glow discharge. The microwave discharge once initiated at low pressure will persist as a glow discharge at pressures up to atmospheric pressure. McCarthy found that pulsing of the microwaves though increasing the breakdown voltage, doubled the yield of free radicals compared with a continuous microwave power discharge.

One of the most important advantages over the d.c. glow discharge is the absence of electrodes in the microwave discharge. However, if a metal catalyst was needed it may be inserted in the microwave discharge without markedly altering the characteristics of the discharge.

Another electrodeless system, the radio-frequency discharge, was also considered. However the difficulty of obtaining efficient power transference to the reactor led to its rejection in favour of the microwave discharge.

In conclusion the possibility of increased chemical activity in the microwave compared with the d.c. glow discharge or electric arc discharge prompted the choice of the microwave system.

6.2. Description of the Microwave Equipment

Basically the system consists of a microwave power generator and power supply, linked to a cavity resonator by a coupling and matching system of wave guides, see Fig. 12. Unused power is dissipated in a water load. A power monitoring device is also incorporated. A gas flow tube may be placed axially in the cavity.

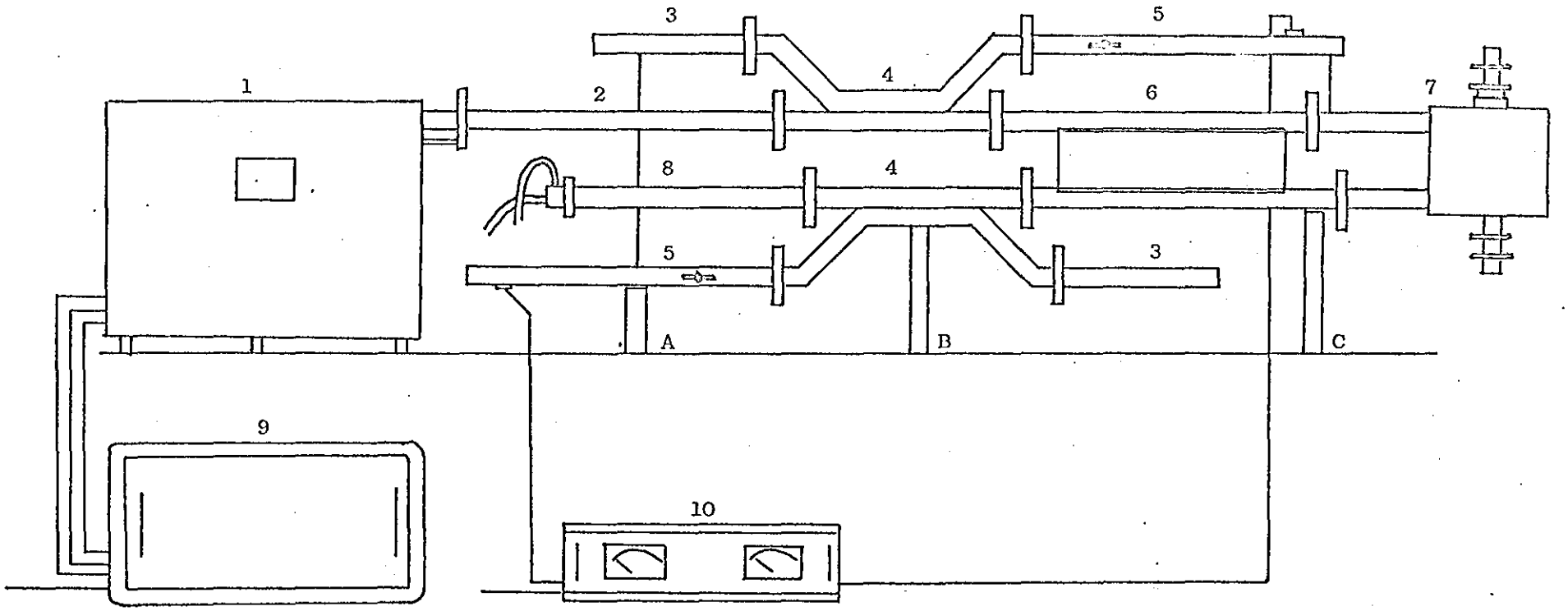

1. R.F. Power Generator
2. 2" Wave Guide
3. Loads
4. 40 dB Coupler
5. Calibrated Thermistor Mounts.
6. 3 dB Coupler
7. Cavity Resonator
8. Water Load
9. Magnetron Power Unit
10. Thermistor Power Monitor

A,B,C, Supports

Figure 12 General Layout of the Plasmex 4 Plasma Excitation Equipment

The source of the microwave power is a magnetron, the Mullard JP2 - 2.5A, operating in the band 2.35 to 2.55 GHz. The mean power level can be adjusted from 0.8 kw to 2.5 kw. The magnetron power supply unit has a current regulated output, the level of which is adjusted by the magnetron current control. The system is protected from accidental damage by a safety interlock circuit.

The wave guide system is constructed of wave guide 10. The H_{10} configuration is used for the microwave transmission. Wave guide theory uses the concept of a field of force characterized by electric and magnetic vectors instead of the usual concepts of current and voltage. A consequence of this theory is that there are two basic types of waves which can be propagated. The first is called a transverse magnetic or E wave. This has its magnetic vector in a plane normal to the direction of propagation, but has a component of electric force in the direction of propagation. The second, having an entirely transverse electric force and an axial component of magnetic force, is called a transverse electric or H wave. Various forms of E and H waves are possible with characteristics dependent on the values given to the boundary conditions usually referred to as the parameters m and n. These parameters can have integral values only, and these are limited for given dimensions and a given impressed frequency by the inequality.

$$\frac{W}{\gamma} > \left[\left(\frac{m\pi}{a} \right)^2 + \left(\frac{n\pi}{b} \right)^2 \right]^{\frac{1}{2}}$$

where W = $2\pi f$, where f is the frequency

γ = velocity of light in the medium

a = width of the wave guide

b = height of the wave guide

The values of the subscripts m, n determine the number of half-sinusoids in the distribution of field intensity along the sides, a and b, of the wave guide respectively. The type H_{10} is of special interest since it has the simplest configuration of all hollow tube waves. The electric field has only one component, which is parallel to the side of length b, and has a half-sinusoidal amplitude distribution along the side a, see Fig.13. The propagation constant and critical frequency are dependent only upon the dimension a, the critical wavelength being given by the simple expression, $\lambda_o = 2a$. The critical frequency determines the boundary between the transmission and attenuation regions. Above this frequency the attenuation is zero; below it the wave suffers rapid exponential attenuation.

The matching of the wave guide to the cavity resonator is achieved by using a 3dB directional coupler which prevents deterioration of the match presented to the magnetron when the cavity itself is out of tune. The 3dB coupler divides the power between two energising inputs to the resonator. Like phase reflections from these inputs passing back into the 3dB coupler recombine, diverting energy from the magnetron and dissipating it in the water load.

The cavity resonator is of a cylindrical design supporting the H_{112} mode and has axial access for reactor tubes up to one inch diameter. The axial length of the cavity equals the wavelength of the microwaves. The H_{112} mode of operation determines the positions of maximum electric field strength in the cavity, see Fig. 14. The resonant frequency of the cavity resonator has to be tuned to the frequency of oscillation of the magnetron. This is effected by rotation of one of the access

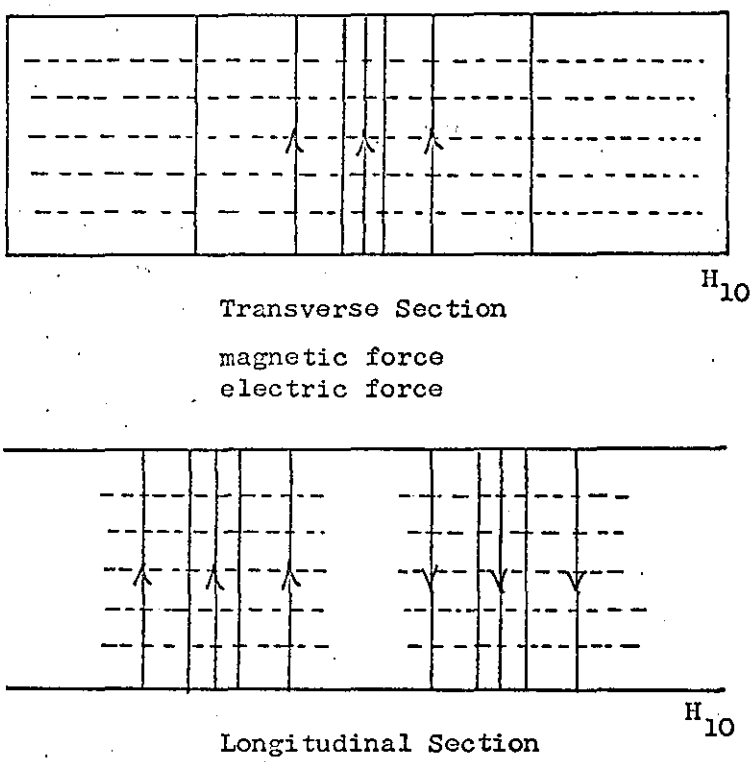

Figure 13 Lines of Force of Waves in a Rectangular Guide : the H_{10} Mode

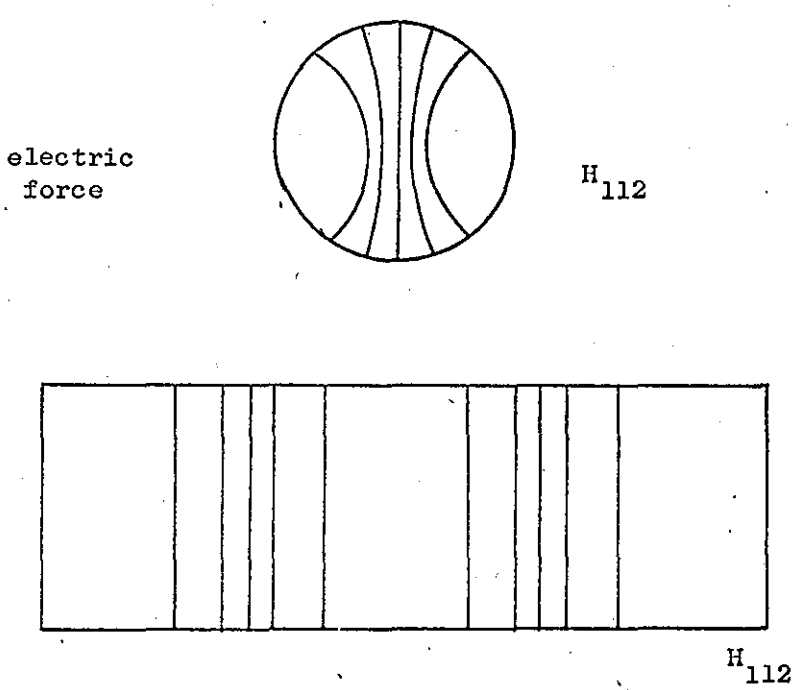

Figure 14 The H_{112} Mode of Oscillation in a Cylindrical Cavity Resonator

tube assemblies situated at one end of the cavity. The control is operated as a screw driven piston. The correct tuning-point is indicated by a sharp dip in the reading of the reflected power meter and a stable incident power reading. Adjustment is made for a minimum reflected power reading. In some cases a short delay occurs before a discharge is struck. Conversely a discharge may start immediately, in which case the tuning is very broad and occupies most of the piston travel. The strongest discharge coincides with a minimum reflected power reading.

The cavity resonator is coupled to the rest of the wave guide system by two feed wave guides between which is situated the 3dB directional coupling element described previously. The two identical feeds into the cavity are spaced to suit the relative phases of the power in the wave guides. Under normal tuning conditions power reflections of equal amplitude and phase from the cavity are dissipated in the water load. However an undesirable phase relationship is possible when an empty cavity was partially off tune. This gave a spurious reflected power dip and a rise in the incident power reading. At such times, to ensure longer magnetron life, full power was avoided.

Inefficient power transfer to the cavity can occur if the matching of the cavity to its feed wave guides is incorrect. This matching is achieved by the use of the probe feeds penetrating through the irises into the cavity, see Fig. 15. During operation changes in the matching may be required owing to the varying nature of the gas and the dimensions of the gas flow tube. This is made apparent by an excessively low proportion of absorbed power. The degree of penetration of the

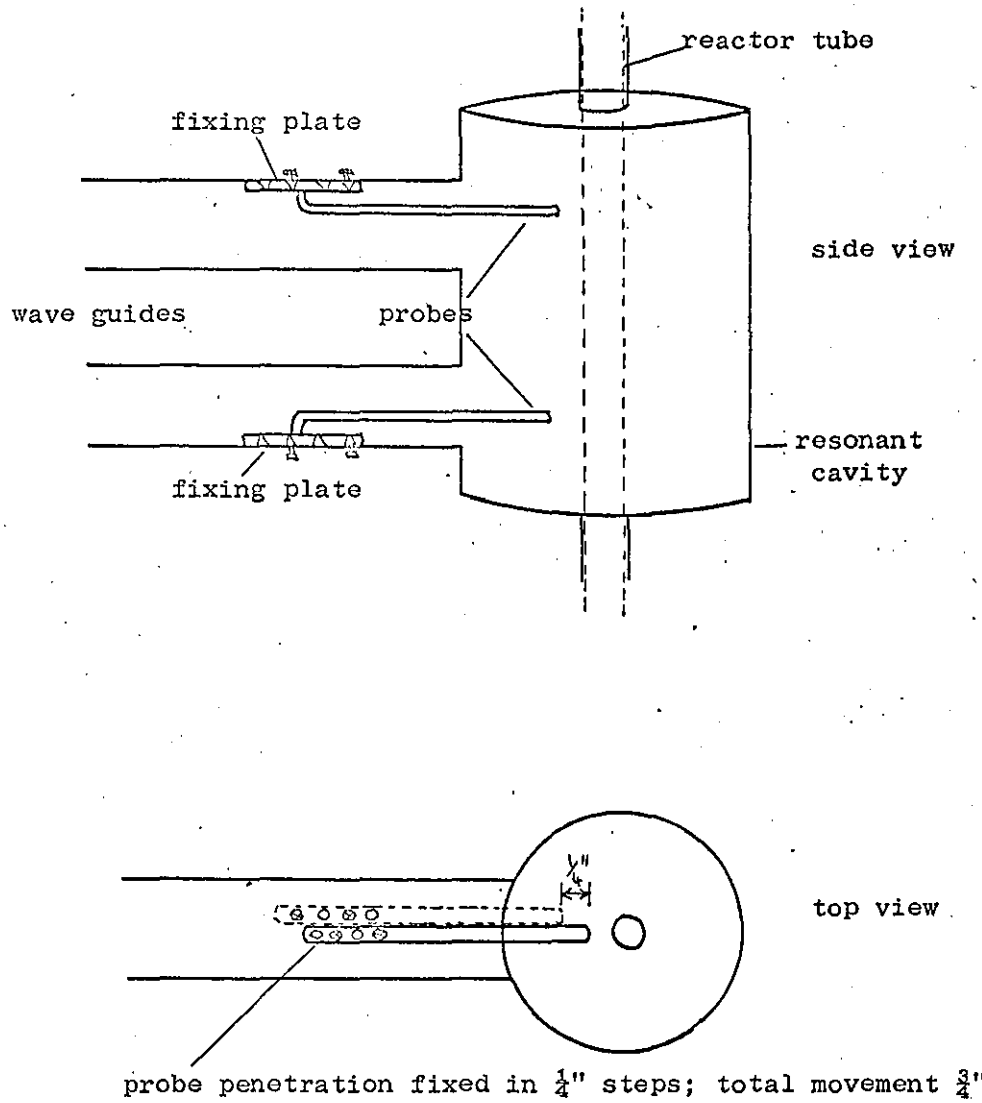

Figure 15 Matching of the Cavity to the Wave Guides by Probe Feeds

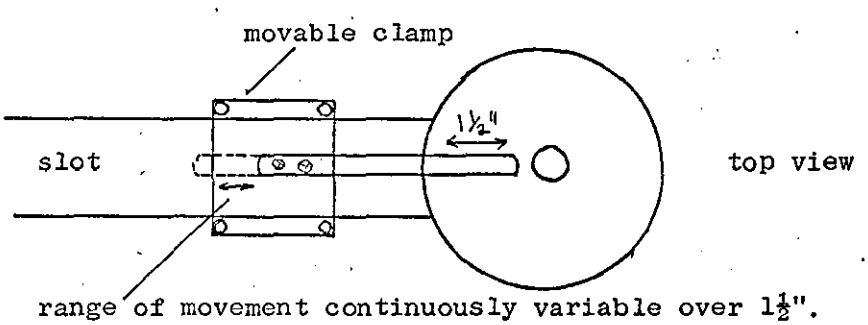

Figure 16 Probe Movement Modified, in the Present Work, to Provide Finer Tuning of the Cavity

probes is adjustable in quarter inch steps.

The movement of the probes was later modified to provide a continuously variable adjustment, see Fig. 16. However it was found that the possible advantages of the finer adjustment were minimal in obtaining better matching over the range of gas pressures and flow rates used. Especially when compared with the difficulties of aligning the new system correctly and retuning to a particular tuning point after movement.

Under certain conditions, arcing occurred in the tuning assembly of the cavity. This was usually due to a bad earth on the shorting plate and was cured by cleaning of the earthing contacts.

6.3. Preliminary Testing

The microwave generator and the associated wave guides were a prototype design supplied by Microwave Instruments Limited, designated the Plasmex 4 system. Predelivery testing of the equipment had been very scanty, usually amounting to sustaining a discharge in air at 1 mm Hg pressure for a duration of thirty seconds. Hence a rigorous preliminary examination was undertaken.

Samples of the vapour of several organic liquids were subjected to the microwave field, at varying pressures, see Table 2. This provided a quick survey of the performance potential of the apparatus. A major problem arose early in the experimentation from the melting of the pyrex reactor tubes. Even when externally cooled, the lifetime of the tube was less than thirty seconds. Also discharges were difficult to obtain at pressures greater than 10⁻³mm Hg in a static system.

The adoption of silica as the reactor tube material transformed the performance of the equipment. Discharges were

easily obtained, on minimum input power, up to pressures of 120 mm Hg, see Table 2. The lifetime of the silica tube was also much greater than that of the pyrex tube. The difference in the performance between the silica and pyrex tubes was attributed partly to the lower dielectric constant of the silica which meant the silica was more transparent to the microwaves.

The power absorption, whether in a static or flow system, in the discharge was, not unexpectedly, found to vary with pressure; the higher the pressure, the higher the power absorption. However the power absorption at a fixed pressure varied with the sample of vapour used.

Table 2. A Comparison of the Performance of Silica and Pyrex Reactor Tubes

sample vapour	reactor pressure	discharge maintained	
		pyrex tube	silica tube
nitrobenzene	3-5	yes	yes
ethanol	40-45	no	yes
methanol	90-100	no	yes
acetone	180-200	no	with difficulty
diethyl ether	350-370	no	no

microwave input power 0.78 Kw

REACTOR DESIGN

7. Reactor Design

7.1. Types of Reactors

There are two types of idealised reactors applicable to flow systems:

(1) The plug-flow, tubular flow reactor in which the residence time is constant for all components but with varying composition along the flow path.

(2) The backmix or CFSTR reactor, the contents of which are uniform in composition but with varying residence times.

7.1.1. 1) Steady-state Plug Flow Reactor

As the composition varies along a flow path, a mass balance for a particular reaction component must be made for a differential element of volume dV. For component A we can state,

input A = output A + reacted A

from Fig. 17 in a volume dV,

input A, moles/time = F_A

output A, moles/time = $F_A + dF_A$

reacted A, moles/time = $(-r_A)dV$

hence,

$$F_A = (F_A + dF_A) + (-r_A)dV$$

now

$$dF_A = d\,F_{AO}(1-X_A) = -F_{AO}dX_A$$

substituting,

$$F_{AO}dX_A = (-r_A)dV$$

This equation defines the state of component A in a section of the reactor of volume dV. Integration of the expression

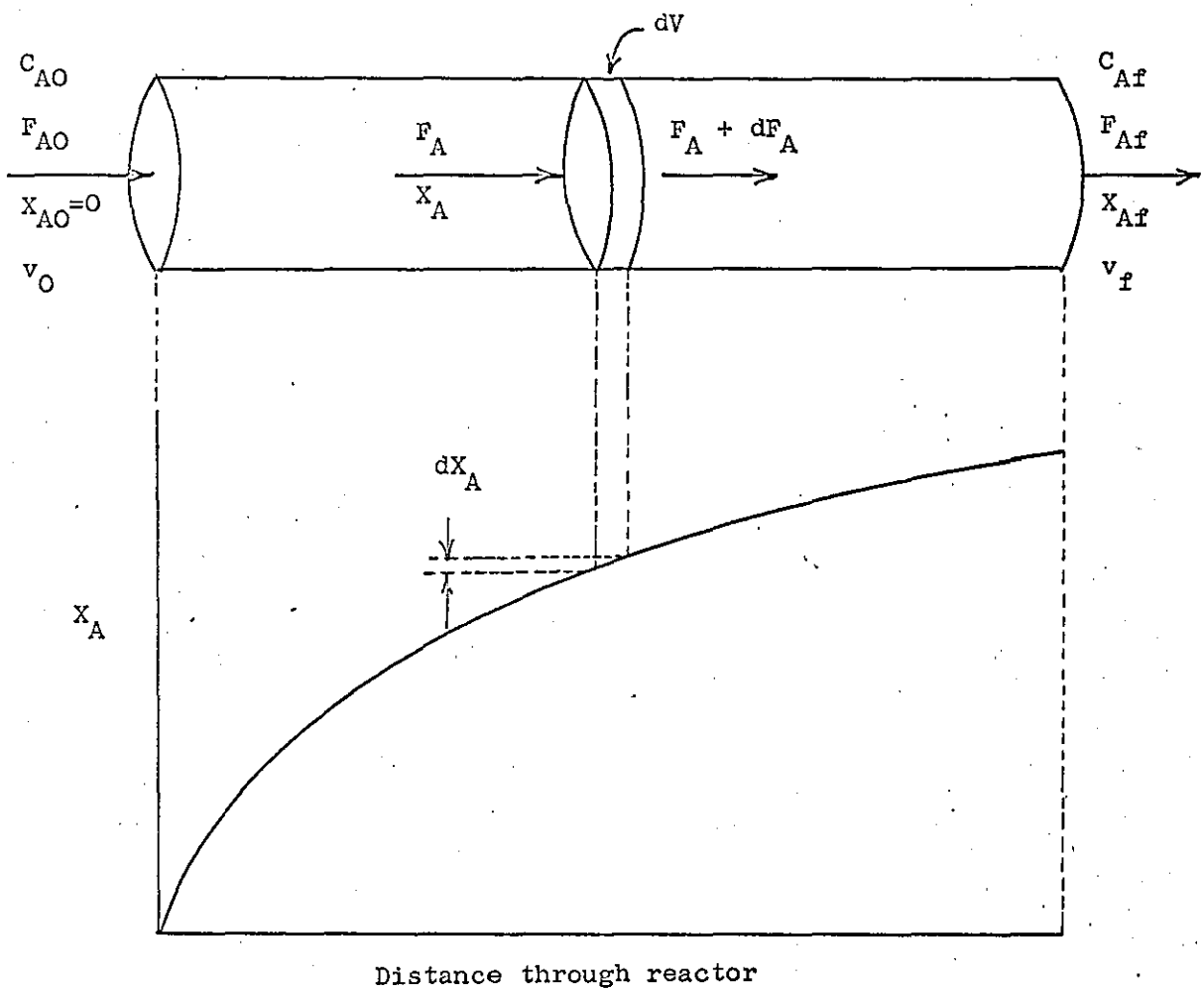

Figure 17 Variables for a Plug Flow Reactor

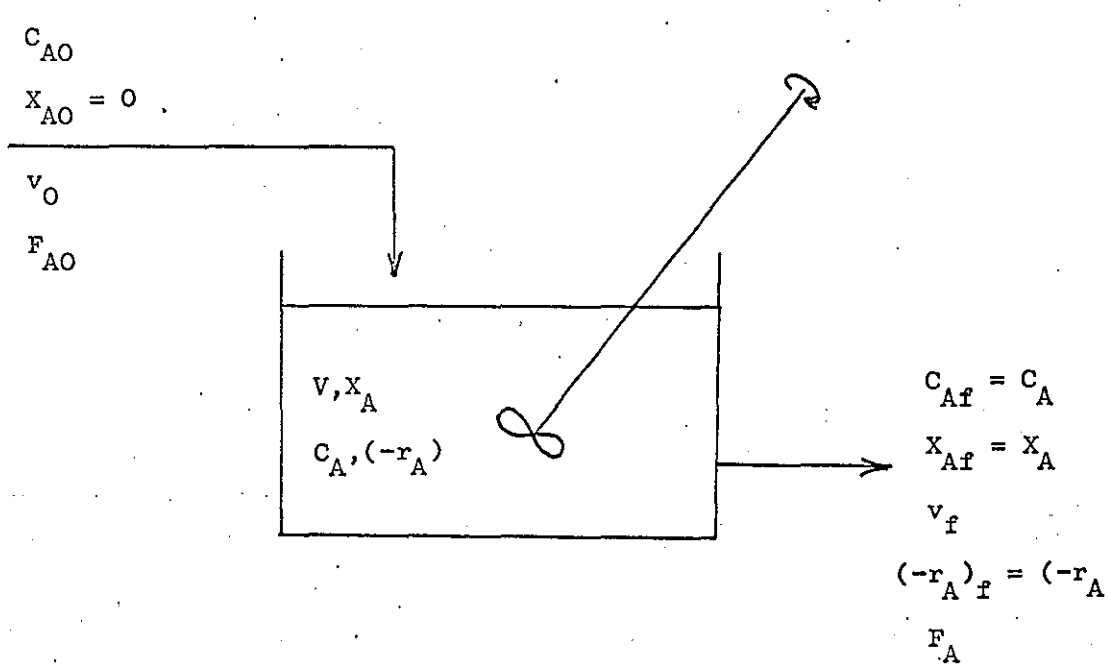

Figure 18 Variables for a Backmix Flow Reactor

gives the state of A in the reactor as a whole. F_{AO} can be regarded as constant, though r_A will be dependent on the concentration of the component stream. Regrouping of the terms in the expression gives,

$$\int_0^V dV/F_{AO} = \int_0^{X_{Af}} \frac{dX_A}{-r_A}$$

$$\frac{V}{F_{AO}} = \int_0^{X_{Af}} \frac{dX_A}{-r_A}$$

this may be expressed as a function of space time,

$$\tau = C_{AO} \int_0^{X_{Af}} \frac{dX_A}{-r_A}$$

The rate constants of any reaction may be obtained by plotting $-1/r_A$ versus X_A and evaluating the area under this curve between the appropriate limits.

7.1.2. 2) Steady-state CFSTR Reactor

As the composition is uniform we may consider the reactor as a whole. Again with reference to a component A,

input A = output A + reacted A

from Fig. 18 in the reactor as a whole,

input A, moles/time = F_{AO}

output A, moles/time = $F_A = F_{AO}(1-X_A)$

reacted A, moles/time = $(-r_A).V$

hence,

$$F_{AO} = F_A + (-r_A).V$$

$$= F_{AO}(1-X_A) + (-r_A).V$$

$$F_{AO}.X = (-r_A).V$$

on rearranging,

$$\frac{V}{F_{AO}} = \frac{V}{v_0 . C_{AO}} = \frac{X_A}{-r_A}$$

or,

$$= \frac{V}{v_0} \quad \frac{C_{AO} X_A}{-r_A}$$

The design equation for the reactor shows that knowing any three of the four terms X_A, $-r_A$, V, F_{AO} gives the fourth term directly. Thus in kinetic experiments, each run at a given τ will give a corresponding value for the rate of reaction directly.

7.2. Residence Time

In the CFSTR reactor the residence time of the species is variable. This means that in a system where the product is less stable in the discharge zone than the reactants, the yield of product will vary depending on the amount of backmixing. Thus if a constant yield of product is required under set conditions the CFSTR reactor should be avoided.

In the plug flow reactor the residence time for each element of fluid is a constant. The equation is complicated by the varying density along a flow path though this may be allowed for. The expression,

$$t = N_{AO} \int_0^{X_{Af}} \frac{dX_A}{(-r_A)V}$$

is obtained for a particular component A.

In the discharge systems under investigation in the present work the reactions observed are usually of the type,

$$A \longrightarrow R \longrightarrow S$$

or

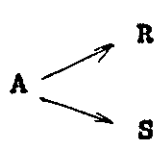

Concentration - time curves can be calculated from theory for these reactions for different values of the rate constants. Each curve is unique for a particular value of rate constant. These may be compared with experimental results. However, many of the curves are of a similar shape which leads to difficulties in selecting the correct mechanisms of reaction by experiment, especially if the kinetic data are somewhat scattered.

7.3. Limitations Imposed by the Cavity Design

In the present work the geometry and working mode of the resonant cavity severely limits the shape and dimensions of the reactor vessel. The H_{112} mode of the resonant cavity dictates the presence of two points of intense electric field, separated by a half wavelength, in the axis of the cavity. A discharge can be struck at either of these two points see Fig. 14.

The simplest reactor is a tube placed in the vertical axis of the resonant cavity. The diameter of the tube determines the linear flow rate in the reactor. The value of the linear flow rate greatly influences the nature and yield of the products of many discharge reactions. It follows therefore that the diameter of the tube is important. The geometry of the cavity however restricts the outer diameter of the reactor tube to 25 mm. Moreover a reactor tube of 12 mm and below in diameter was found to create difficulties in timing the cavity for efficient power transference to the gas.

Experiments were made to determine the influence of the reactor tube diameter on the ease of breakdown and maintenance of a discharge. The results were difficult to correlate owing to the necessity to retune the cavity for each tube. Broadly no

difference in the reactor performance was found between reactor tubes of outer diameters 16 - 25 mm, under static conditions.

Whereas the inlet and outlet diameters are restricted, inside the cavity the diameter of the tube could be increased up to 30 mm axially, and up to 100 mm if displaced to one side of the cavity. This displacement is necessary to avoid contact with the metal coupling probes in the cavity, see Fig. 19. As basic microwave theory dictates that the discharge will only occur at one point in the cavity, the reactor in Fig. 19 could be simplified, see Fig. 20. Experiments at low pressure, $\angle$ 5mm Hg, showed no benefit in power absorption or in the ease of breakdown of the gas when compared with the simple tube reactor. The design would almost certainly increase the average residence time of the chemical species in the discharge. This may be an advantage in certain chemical reactions. If so there exists the danger of the gas stream bypassing the extra reactor volume. This problem may be solved simply by placing baffles in the appropriate places, see Fig. 19.

The nature of the walls of the discharge tube has been shown to be of great importance in free radical reactions. In the microwave discharge, silica is the only suitable tube material. Techniques of coating the wall with various films, for example of phosphoric acid, to reduce the "activity" of the wall are not feasible as they are not transparent to microwaves. Possibly pure hydrocarbons in the C_{10} to C_{14} range could be used.

The temperature of the walls may be controlled over the range -120°C to +200°C with the use of a reactor tube in the form of a condenser. A cooled reactor tube is described fully on page 110. The temperature control may be achieved with a

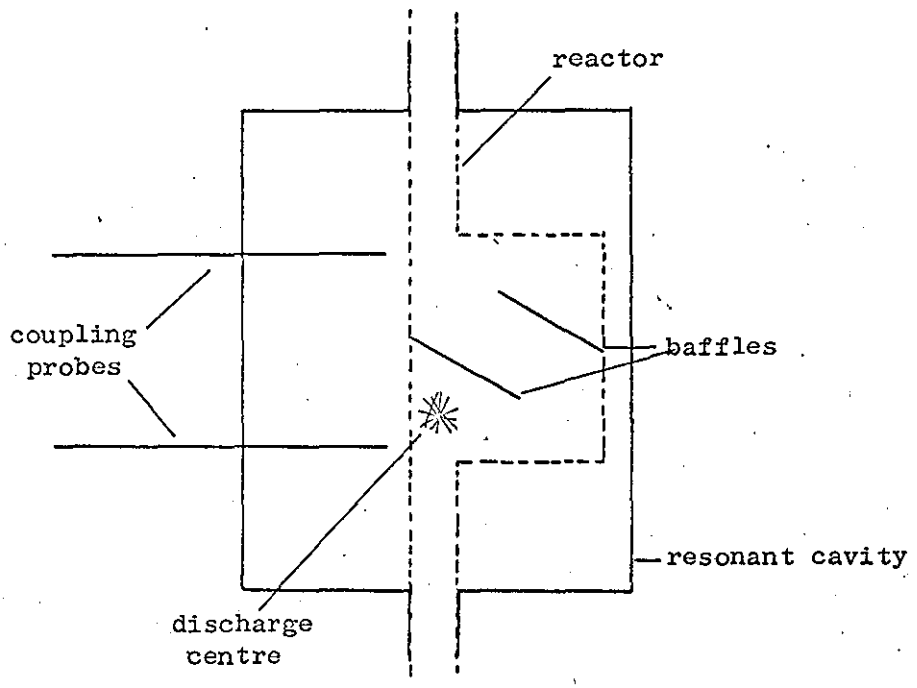

Figure 19 Suggested Reactor Design for Increased Backmixing

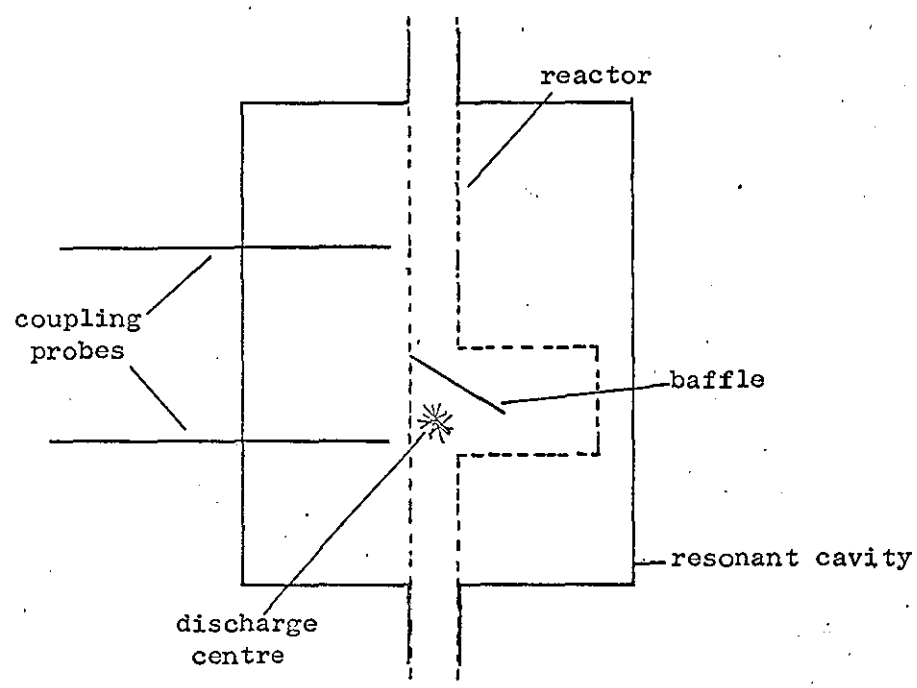

Figure 20 Variation of Design for Increased Backmixing

suitable choice of coolant which must be transparent to microwaves. Experiments with the cooled reactor tube were dissappointing but this was partly due to the sensitivity of the resonant cavity to small changes in the reactor design. The reactor tube may of course operate efficiently if a different working mode was adapted for microwave power transference

7.4. Selectivity and Preservation Problems

One of the advantages of the microwave system is the absence of electrodes. However to improve the selectivity of a chemical reaction or perhaps to help remove an active species, usually hydrogen atoms, from the discharge a metal catalyst is sometimes necessary. Fortunately it was found that in the present work a metal catalyst may be placed in the reactor tube without altering the physical characteristics of the microwave discharge. It is perhaps the choice of whether a metal catalyst is needed that is the advantage over the d.c. discharge rather than the absence of electrodes.

One of the major problems in discharge chemistry is that the products are frequently less stable in the discharge than the reactants. Thus, any technique that reduces the residence time of the unstable products in the discharge is of great importance. Increasing the linear flow rate and/or using a catalyst to limit the product decomposition, have their limitations commercially owing to the cost of providing high pumping rates and/or the removal of dead catalyst from the reactor.

Recently the spray absorbent technique has come to the fore. Research into the production of hydrazine from ammonia has shown that by spraying an absorbent into the discharge zone, to

remove the hydrazine as it is formed, greatly increases the yield of hydrazine[99]. Ethylene glycol has been used as an absorbent. This method is akin to reducing the residence time of the products in the discharge. The cost of separating the product from the absorbent should not be forgotten in assessing the economic value of a process using the spray absorbent technique. Unfortunately we have found the application of this technique to the microwave discharge to be very limited. This is because the temperature of the discharge is usually sufficient to vapourize the absorbent which causes a very rapid rise in pressure in the discharge zone leading to the extinguishing of the discharge.

A technique which may be of great importance to microwave discharge chemistry is the pulsing of the microwave radiation. McCarthy[53] has shown that by simply pulsing the microwaves he obtained double the yield of free radicals compared with a continuous wave, for a number of discharge systems. The pulsing of the microwave power effectively changes the residence time of the excited species in the discharge. The extra cost of providing facilities should be easily offset by the increased chemical activity in the discharge.

7.5. Type of Reactor Used in the Present Work

The reactor tube used in the majority of our experiments was a simple split-diameter tube as shown in Fig.21. The cavity was tuned to obtain a discharge in the wide part of the tube thus ensuring a constant distance from the discharge centre to the cold trap. The reactor type is almost certainly a hybrid of the plug flow and CFSTR idealised reactors. The thermal eddies and turbulence in the discharge zone must cause

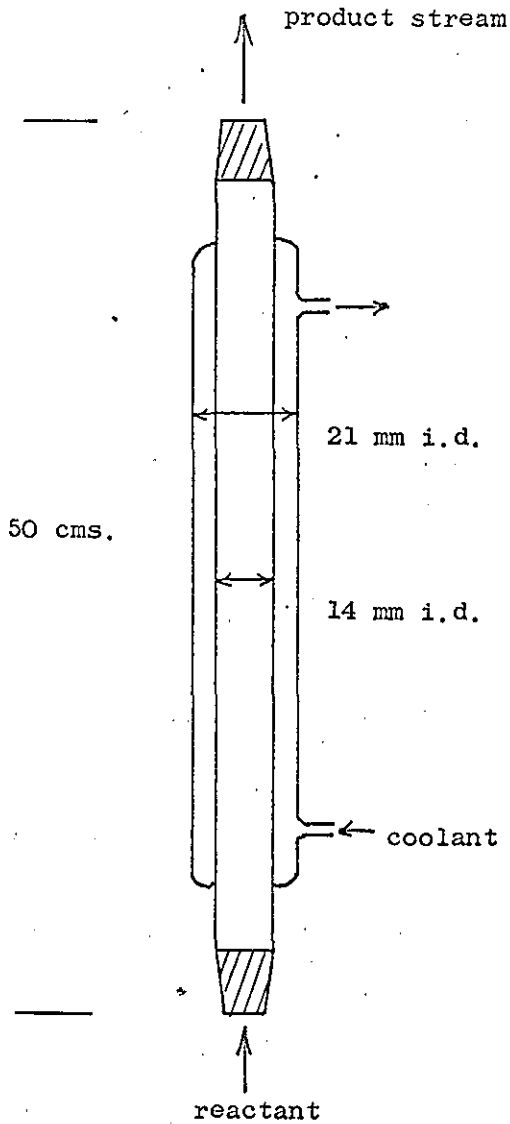

Figure 21a Cooled Silica Reactor Tube

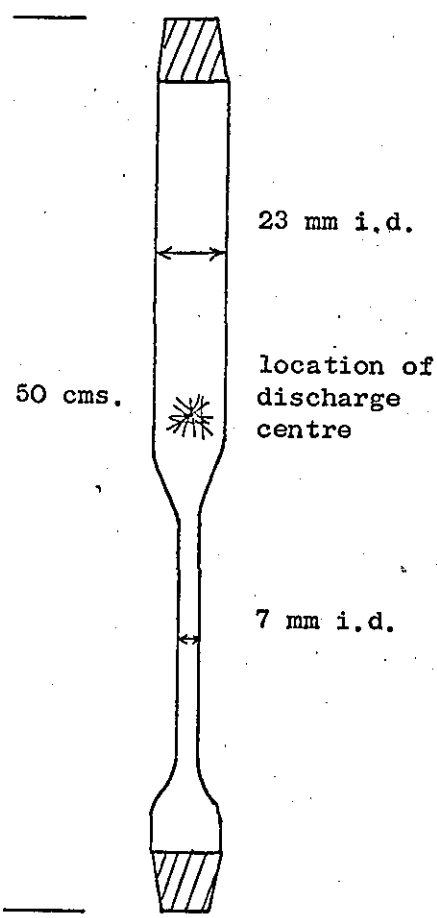

Figure 21b Split-diameter Reactor Tube

mixing of the gas stream.

Several special reactors such as the silica condenser were used in the ammonia work. Again they were considered hybrids of the plug flow and CFSTR idealised reactors.

CHOICE OF SYSTEMS

FOR INVESTIGATION

8. Choice of Systems for Investigation

Methanol, n-hexane, cyclohexane, benzene and ammonia were considered as suitable for investigation in the microwave discharge. From the literature enough evidence had been reported to indicate any one of these compounds should provide sufficient data to establish the performance potential of the microwave discharge from a research and an economic point of view. Each compound named above offered scope for detailed study.

Methanol is a simple molecule and the number of possible products is limited. The methanol discharge could thus be investigated without the need for complicated analytical techniques. The possibility of producing ethylene glycol in commercial yields was noted.

The saturated C_6 hydrocarbons, n-hexane and cyclohexane were chosen not only to judge the performance of the microwave equipment but in the hope of eventually comparing the kinetics of breakdown and subsequent reactions of a linear hydrocarbon and with a ring system. Products of commercial interest were thought to be unlikely.

The benzene discharge appeared to be a promising system from the data reported in the literature. A comparison with other discharge systems could be made and also with discharges initiated by similar microwave equipment. Commercially the system could prove profitable if compounds such as aniline, diphenyl etc. could be produced in high enough yields.

One of the chemical processes especially suitable for investigation was the production of hydrazine from the dissociation of ammonia. An efficient, cheap method for producing hydrazine would be of great commercial interest and value. Again the performance of microwave discharge could be

compared with the numerous investigations of the ammonia discharge reported in the literature.

8.1. Scouting Experiments

8.1.1. The Methanol Discharge

Flow rates of 0.04 to 0.15 moles/min. over a range of pressures, 15 - 40 mm Hg were tried. The methanol gave a deep blue discharge. The formation of tar and carbonaceous material was not observed under the conditions of the experiment. Analysis of the condensed sample stream was made on a Perkin Elmer dual flame ionization chromatograph with a check analysis on a Pye 104 single flame ionization chromatograph. Evidence of two low boiling products in very low yield was found. Higher boiling products such as ethylene glycol were not found.

8.1.2. The N-hexane and Cyclohexane Discharges

N-hexane gave a very bright blue discharge. Several runs at flow rates 0.01 to 0.10 moles/min. over the pressure range 10 - 20 mm Hg were made. The formation of an amber film on the sides of the discharge tube was noted. Unfortunately the gas-liquid chromatographic analysis showed the n-hexane to be impure. Qualitatively the existence of four new low boiling components was found. The presence of nickel wire in the discharge reduced the total conversion and also the number of low boiling products to three. The formation of two high boilers was noted. A pale reddish glow was seen near the nickel wire and was probably due to the emission spectrum of the hydrogen atom recombinations.

Several runs were also carried out with cyclohexane in which the flow rates were varied over the range 0.01 to 0.1 moles/min.

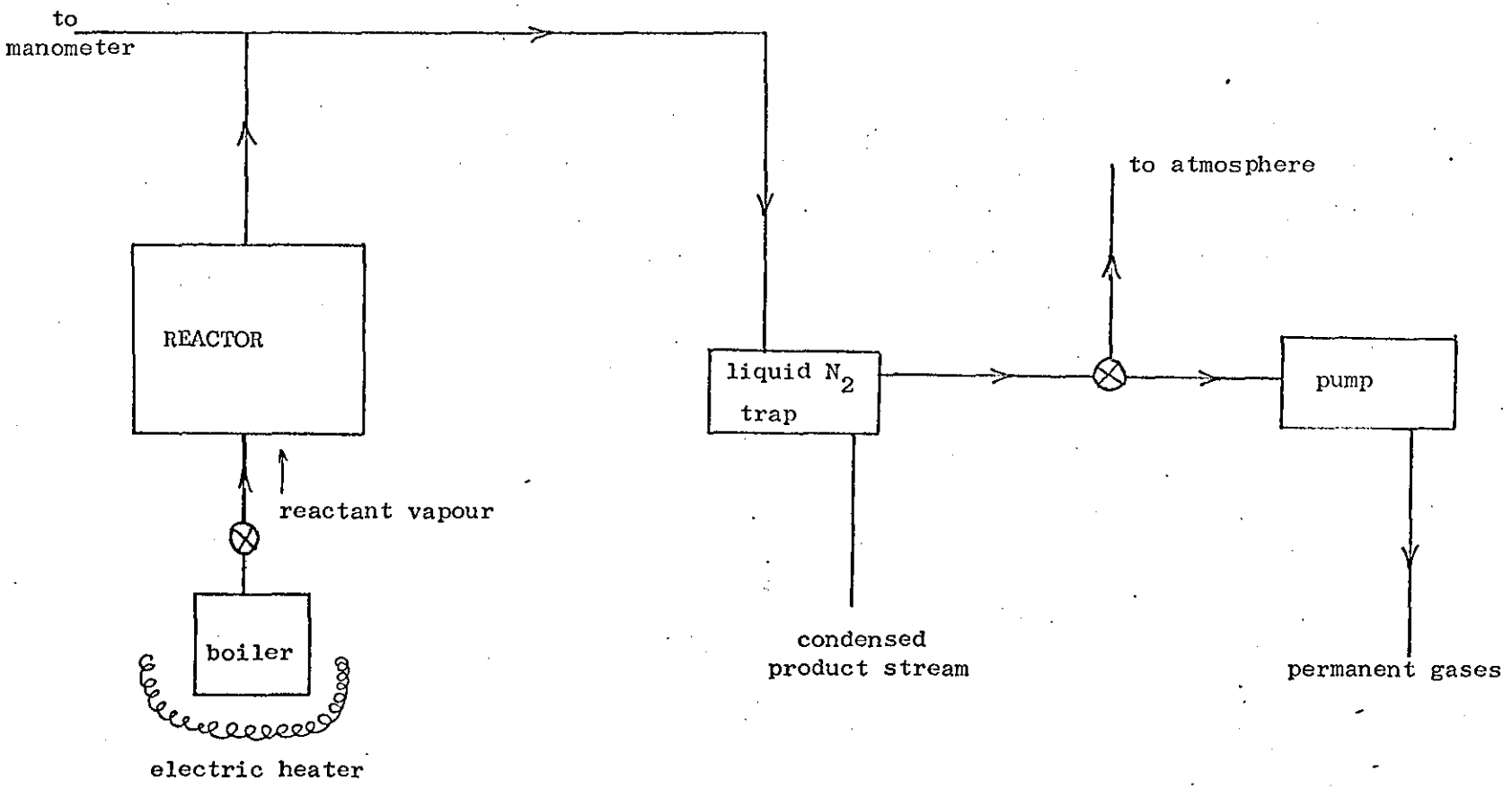

Figure 22 Experimental Layout for Scouting Experiments

over the pressure range 10 - 60 mm Hg. The discharge was usually a red-orange colour though this may have been due to the noticeable deposits of carbon and an amber solid on the silica surface of the reactor tube. Four low boiling components and one high boiling component were found by analysis of the condensed sample stream. The presence of nickel wire in the discharge reduced the carbon and amber solid formation to negligible proportions. The conversion to other gaseous products was also lowered.

8.1.3. The Benzene Discharge

Under the experimental conditions used, flow rates of 0.01 to 0.1 moles/min. and pressures ranging from 10 to 25 mm Hg, the benzene at first gave a pale blue discharge. However, the discharge changed quickly to a red glow consequent with the formation of carbon and an amber solid on the walls of the discharge tube. There was an interesting formation of products in the reactor tube, see Fig. 24. The wall above the discharge was covered by carbon deposits, whilst round the discharge zone itself the walls were covered by an amber solid only. This amber solid was also found along the length of the delivery tubes to the cold trap.

Analysis of the condensed product stream showed the presence of three low boilers and one high boiler. The conversion to the low boilers increased as the energy input increased. The presence of nickel wire in the discharge zone reduced the carbon formation and a pale yellow solid was deposited on the walls. The pale blue colour of the benzene discharge remained throughout the experiment. The nickel wire also reduced the low boilers to two and the one high boiler remained.

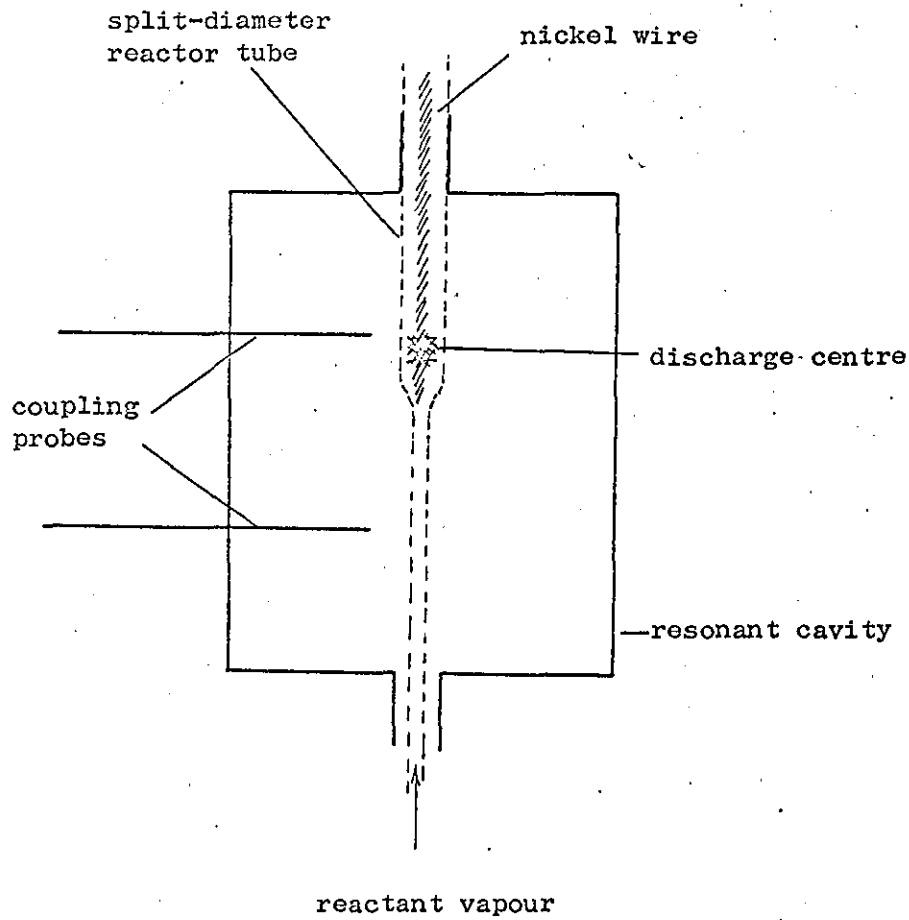

Figure 23 Location of the Nickel in the Discharge Tube

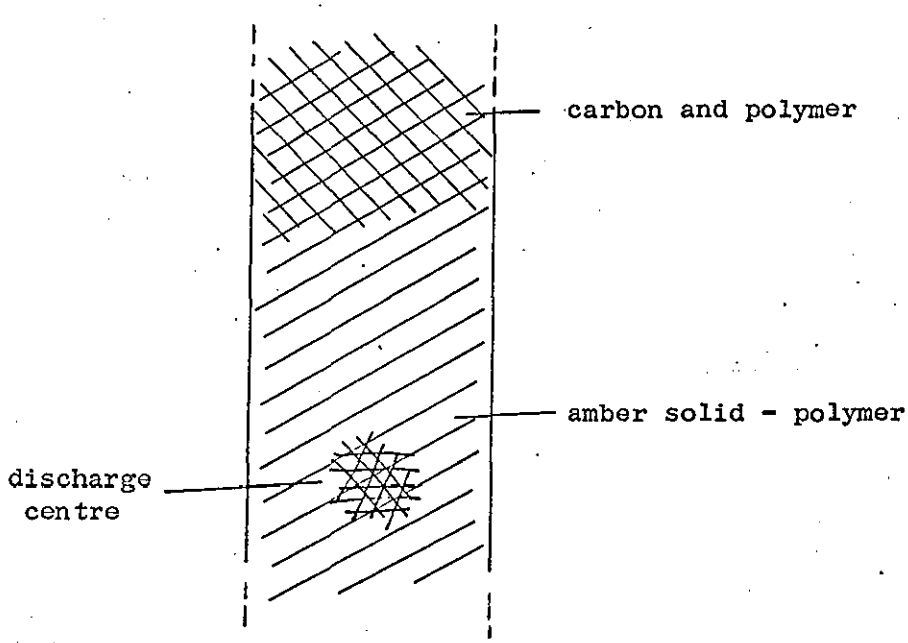

Figure 24 Formation of Carbon and Polymer from Benzene in the Discharge Tube

Mixtures of ammonia and benzene in mole ratios ranging from 2:1 to 5:1 were passed through the discharge. Benzene flow rates were varied from 0.03 to 0.08 moles/min. over a pressure range 10 - 25 mm Hg. The colour of the discharge varied from bright blue to almost white depending on the percentage of ammonia present. In all cases the decomposition of the benzene to polymers, carbon and other products was less than for the pure benzene or benzene and nickel systems. A most interesting feature of the benzene-ammonia discharge was the discovery of a purple solid in the cold trap. The colour of the solid indicated a structure containing an azo group, i.e. the benzene and ammonia had interacted in the discharge. The purple solid was partially soluble in benzene but completely soluble in acetone. Aniline was possibly detected as a minor product.

Discharges in benzene mixed with carbon dioxide, mole ratios from 2:1 to 4:1 respectively, were also obtained. Decomposition to tar and carbonaceous matter was very slight. No other products were detected.

8.2. Conclusions

The microwave discharge in methanol offered little of interest. Decomposition was slight and products of commercial interest such as ethylene glycol were not detected. Hence no further work on methanol was proposed.

The n-hexane discharge, though several gaseous products were found, presented difficulties in that the n-hexane contained a high percentage of impurities. The cost of obtaining pure n-hexane was prohibitive to the present work and therefore further investigation was precluded.

The cyclohexane system was more promising. Pure cyclohexane could be obtained cheaply and there was a sufficient number of new products to be able to investigate the performance of the microwave discharge. The marked effect of the presence of nickel wire in the discharge indicated the possibilities of modifying the discharge to improve selectivity etc.

The discharge in benzene vapour proved to be the most interesting of the systems tried. The yields of discharge products were modified considerably by the inclusion of nickel wire in the discharge, or by admixing ammonia or carbon dioxide. A solid, possibly a derivative of azo-benzene structure, was obtained from the benzene and ammonia discharge. This indicated perhaps that some interaction of phenyl radicals and amino or imino radicals occurred in the discharge.

It was therefore proposed that the benzene discharge be investigated further. The cyclohexane discharge was also suggested as suitable for further investigation if only to compare the breakdown of a saturated with an unsaturated ring system. The methanol and n-hexane systems were excluded for the reasons discussed previously. The ammonia discharge was also to be investigated further, not only because of the great commercial interest but also to judge the performance of the microwave discharge in the dissociation of small molecules.

THE APPLICATION OF THE MICROWAVE DISCHARGE TO THE PRODUCTION OF HYDRAZINE FROM AMMONIA

9. The Application of the Microwave Discharge to the Production of Hydrazine from Ammonia

Early methods for the preparation of hydrazine salts, from which the hydrate was produced, depended chiefly on the reduction of compounds containing a nitrogen to nitrogen linkage. Only later was the decomposition and/or oxidation of ammonia and its derivatives utilized in the preparation of hydrazine. Of these, only the Raschig synthesis, which involves the partial "oxidation" of ammonia by hypochlorite, has been the only preparative method to be developed commercially. However the synthesis as developed by Raschig in 1907, though simple in its appearance, still represents a very expensive chemical process. It is for this reason hydrazine particularly, and its salts, are not widely used industrially.

Hydrazine has an interesting and useful chemistry. Hydrazine is used not only as the free base and its common inorganic compounds, but also as an intermediate for the production of other useful classes of inorganic and organic compounds. With the availability of cheap hydrazine, either in the form of the hydrate or other salts, such applications could be considerably extended.

One of the main uses of hydrazine is as an organic intermediate in the manufacture of heterocyclic compounds. Hydrazine is also used as an intermediate in the preparation of phenylhydrazines which are used in the manufacture of azo-compounds. Hydrazoic acid and its derivatives are prepared from hydrazine. The reducing properties of hydrazine have been applied to several specific cases of water treatment.

Perhaps the best known use of hydrazine is as a rocket fuel. When used with powerful oxidising agents such as hydrogen peroxide,

oxygen, and fuming nitric acid it is an excellent fuel. However the reaction with oxygen has recently assumed an even greater importance with the development of the hydrazine - air fuel cell. This has proved to be very efficient. The production of cheap hydrazine would offer great potential in this respect.

Considerable interest has also been shown in the use of hydrazine derivatives in the plastics field. The products formed either by reaction with aldehydes or ketones, are said to be clear, resistant to hydrolysis and capable of being moulded, drawn and spun into fibres. Hydrazine and derivatives have also been shown to be useful as solder fluxes, antioxidants, in the metallization of glass and plastics, photographic chemicals, insecticides and fungicides, therapeutic compounds, and rubber softeners and plasticizers.

It is apparent that hydrazine if available at a competitive cost, would find widespread application in both inorganic and organic syntheses. It is upon this cost reduction basis that a great deal of research has been carried out in recent years. The research has either involved:

a) an attempt to produce hydrazine by the direct combination of hydrogen and nitrogen.

or

b) the synthesis from ammonia either by dehydrogenation or by some cheaper and more efficient oxidative method.

Research with the electrical discharge has involved both the above processes. However the synthesis from ammonia has found preference.

9.1. Investigations of the Ammonia Discharge from the Literature

The decomposition of ammonia in the electrical discharge has been studied fairly extensively but with few consistent results. Yields of hydrazine reported for various discharge systems have ranged from 0 - 50% based on the ammonia input[96-102,118-121]. A number of correlations have been put forward for the yield of hydrazine and electrical discharge parameters such as discharge current, field strength etc., The basic mechanism of the decomposition of the ammonia has been likened to that found in the photolysis of ammonia. However confusion still exists as to the mechanism and products of the primary dissociation reaction of ammonia.

9.1.1. Basic Decomposition Processes

Attempts have been made to identify spectroscopically the excited species first formed. Herzberg and Ramsay[103], studying discharges in streaming ammonia, found an extremely complicated multi-line spectrum, called the α - bands, in the region 4,200 - 8,300 A. The α - bands were also observed when ammonia was irradiated with ultra-violet light. The α - bands were suspected to be due to vibrational transitions of the NH_2 radical, though they may also be a transition between two excited states of ammonia. Photochemical studies suggest,

$$NH_3 + h\gamma \longrightarrow \dot{NH_2} + \dot{H}$$

Ammonia, decomposed in a flash photolysis experiment at 10 mm Hg[104], showed approximately fifty absorption lines in the region 5,700 - 6,900 A coinciding with the emission spectrum discussed above and no doubt due to the same species. The structure of the spectra, both emission and absorption, showed a poorly resolved fine structure, without obvious regularity and

was not compatible with molecules containing more than one nitrogen atom. Also the fact that the α - bands occurred in the absorption spectrum suggested very strongly the lower state of the molecule involved was the ground state. This immediately eliminated NH and NH_3 as carriers since their absorption spectrum was well known. It was concluded that the α - bands were due to the free NH_2 radical. The complicated structure of the spectrum was accounted for by the fact that NH_2, in its excited state, was a quasi-linear molecule i.e. it has a slightly bent structure in which, with increasing amplitude of the bending vibration, a transition of the rotational levels from those of a nearly symmetric top to those of a linear molecule took place.

Dressler and Ramsay[105] have analysed the transition $^2A_1 - {}^2B_1$ both for NH_2 and ND_2. In the ground state, $\tilde{X}\ {}^2B_1$, the molecule is strongly bent as in the ground state of H_2O while in the excited state, $\tilde{A}\ {}^2A_1$, it is nearly linear, as mentioned above. The two states arose from a single $^2\Pi_u$ state of the linear molecule because of a strong vibronic (Renner-Teller) interaction.

Recently Okabe and Lenzi[106] have studied the photodissociation process of ammonia in the vacuum ultraviolet. They found evidence for the existence of both NH_2 and NH radicals at varying wavelengths of incident radiation.

at wavelength	$>$	2,000 Å	NH_2 only
1600 to		2,000 Å	both radicals detected
	$<$	1,600 Å	NH only

For incident light of below 1200 A Okabe and Lenzi found the ionization process,

$$NH_3 \longrightarrow NH_3^+ + e$$

Stukel and Wedge[107] experimented with flashing ammonia at pressures of 0.1 to 0.8 mm Hg. with vacuum ultraviolet. Their results were basically in agreement with other workers[108,109] The NH species was found $\lesssim$ 1 μ sec. after the flash and so was concluded to be a primary species.

The formation of the free radicals NH_2 and NH arising from the decomposition of ammonia by an electrical discharge, photolysis, etc. has thus been shown to depend on the energy supplied to the system. Low energy conditions are favoured for the formation of NH_2. Higher energy promoted the formation of the NH radicals. The energy of formation of NH_2 is given as 3.8 eV. From the wavelength of radiation at which NH is first observed the energy required for the formation of NH is approximately 8.0 eV.

The experiments of Hanes and Bair[110], with a pulsed r.f. discharge in pure ammonia, indicated that NH_2 was the primary product and that NH was relatively unimportant. The primary process was assumed to be essentially the same as in the photolysis of ammonia

$$NH_3 + \text{energy} \longrightarrow (NH_3)^* \longrightarrow \dot{NH_2} + \dot{H} \qquad (1)$$

The rate of decomposition was independent of total pressure under the conditions of their experiments i.e. pressure 0.4 - 0.8 mm Hg, static discharge system. Confirmation of the primary dissociation of ammonia into NH_2, was supplied by Dyne[111] who, using a 5 kW r.f. oscillator, observed α ~ bands in absorption due to NH_2 radicals. The discharge was pale mauve at approximately 10 mm Hg.

The NH_2 radicals once formed can then undergo a number of reactions of which

$$\dot{NH_2} + \dot{NH_2} \longrightarrow N_2H_4 \qquad (2)$$

is the major process. The reaction between NH_2 and NH_3 has been shown to be energetically unfavourable[112]. However, the back-reaction with hydrogen atoms,

$$NH_2^{\cdot} + H^{\cdot} \longrightarrow NH_3 \qquad (3)$$

can occur but is pressure dependent.

The hydrazine formed by reaction (2) is very susceptible to attack, particularly by H atoms. The mechanism of the reaction of hydrogen atoms with hydrazine as given by Wiig and Kistiakowsky[113] is as follows,

$$H^{\cdot} + N_2H_4 \longrightarrow H_2 + N_2H_3^{\cdot} \qquad (5)$$

$$N_2H_3^{\cdot} + N_2H_3^{\cdot} \longrightarrow 2NH_3 + N_2 \qquad (6)$$

The investigations of Dixon[114] agreed with the above scheme. However the observed decomposition of one mole of hydrazine led to more than one mole of permanent gas and less than one mole of ammonia, indicating that a side reaction destroyed some N_2H_3. Dixon[114] proposed the following reaction,

$$H^{\cdot} + N_2H_3^{\cdot} \longrightarrow 2H_2 + N_2 \qquad (7)$$

This reaction would increase in rate as the hydrogen atom concentration increased, thus decreasing the ammonia yield but increasing the yield of permanent gas above that expected, in accordance with the experimental results. The experiments were performed at pressures $<$ 1 mm Hg. Dixon also found that the hydrogen atom concentration had to be ten times in excess of the hydrazine concentration in order to obtain total decomposition of the hydrazine. It was suggested that the majority of the hydrogen atoms were being removed by recombination on the walls of the containing vessel, under the experimental conditions, before reaction with the hydrazine molecules occurred.

The attack of hydrogen atoms on hydrazine also gave a faint green-yellow luminescence in the spectral region 5,200 - 5,700 A i.e. in the α - bands region. Ghosh and Bair[115] attributed the luminescence to the reaction

$$N_2H_4 + H^{\cdot} \longrightarrow NH_3 + NH_2^{\cdot}\,(^2A_1)^* \qquad (8)$$

Estimates of the emission quantium yield showed that reaction (8) was a relatively minor process.

Schiavello and Volpi[116] studied the reaction of hydrazine with deuterium atoms and found 95% of the ammonia formed as the final product was undeuterated. Hence the major reaction process was the hydrogen abstraction reaction,

$$N_2H_4 + H^{\cdot} \longrightarrow N_2H_3^{\cdot} + H_2 \qquad (5)$$

i.e. in agreement with the findings of Dixon and other workers. However the results obtained from the experiments on the attack of hydrogen atoms on hydrazine must be viewed with caution. Not only were the pressures involved low, < 1 mm Hg in most cases, but only hydrazine was present as the initial reactant, a case far removed from studying the decomposition of ammonia where hydrazine is only a minor product. Bearing in mind the discussions above, a general reaction scheme can be predicted for the decomposition of ammonia in an electrical discharge or by photolysis etc. The importance of the individual reactions depends on the physical characteristics of the decomposition, e.g. ammonia flow rate, pressure, energy input, etc.

$$NH_3 + \text{energy} \longrightarrow (NH_3)^* \longrightarrow NH_2^{\cdot} + H^{\cdot} \qquad (1)$$

$$NH_2^{\cdot} + NH_2^{\cdot} \longrightarrow N_2H_4 \qquad (2)$$

side-reaction,

$$NH_2^{\cdot} + H^{\cdot} \longrightarrow NH_3 \qquad (3)$$

$$H^{\cdot} + H^{\cdot} + M \longrightarrow H_2 \qquad (4)$$

$$N_2H_4 + H^{\cdot} \longrightarrow H_2 + N_2H_3^{\cdot} \qquad (5)$$

$$N_2H_3^{\cdot} + N_2H_3^{\cdot} \longrightarrow 2NH_3 + N_2 \qquad (6)$$

$$N_2H_3^{\cdot} + H^{\cdot} \longrightarrow 2H_2 + N_2 \qquad (7)$$

$$N_2H_4 + H^{\cdot} \longrightarrow NH_3 + NH_2^{\cdot} \qquad (8)$$

Again it should be noted that the above reactions are consistent with results obtained at pressures of $\angle$ 10 mm Hg, low energy inputs and flow rates of $0 - 10^{-3}$ moles NH_3/min. The ammonia may be excited to numerous states from which the dissociation to amino radicals and hydrogen atoms is possible, or deactivation by collision or energy loss by radiation may take place.

Higher energies and pressures appear to favour the formation of the NH radical in the primary dissociation of ammonia. Little research has been carried out as to the processes by which NH is used up, though Diesen[117], in shock wave experiments, has found evidence for the reaction,

$$\ddot{NH}^{\cdot\cdot} + \ddot{NH}^{\cdot\cdot} \longrightarrow N_2\ddot{H}_2^{*} \longrightarrow N_2 + H_2$$

The following reaction sequence indicates the possible processes,

$$NH_3 + \text{energy} \longrightarrow (NH_3)^{*} \longrightarrow \ddot{NH}^{\cdot\cdot} + 2H^{\cdot} \qquad (1)$$

$$\ddot{NH}^{\cdot\cdot} + \ddot{NH}^{\cdot\cdot} \longrightarrow N_2\ddot{H}_2^{*} \longrightarrow N_2 + H_2 \qquad (2)$$

$$\ddot{NH}^{\cdot\cdot} + H^{\cdot} \longrightarrow NH_2^{\cdot} \qquad (3)$$

$$\ddot{NH}^{\cdot\cdot} + NH_2^{\cdot} \longrightarrow N_2H_3^{\cdot} \qquad (4)$$

$$N_2H_3^{\cdot} + N_2H_3^{\cdot} \longrightarrow 2NH_3 + N_2 \qquad (5)$$

$$NH_2^{\cdot} + NH_2^{\cdot} \longrightarrow N_2H_4 \qquad (6)$$

$$NH_2^{\cdot} + H^{\cdot} \longrightarrow NH_3 \qquad (7)$$

$$H^{\cdot} + H^{\cdot} + M \longrightarrow H_2 \qquad (8)$$

The importance of individual reactions will depend greatly on the physical and geometrical characteristics of the discharge reactor.

In conclusion basic research has shown that NH_2, the amino radical, is the species formed by the primary dissociation of ammonia at low excitation energies and low pressures. The NH radical is formed either by the primary dissociation or ammonia or by a secondary reaction between excited NH_2 radicals, at higher excitation energies and higher ammonia pressures.

9.1.2. Investigations of the Parameters Affecting the Yield of Hydrazine

Many workers have taken a less basic approach to the subject of the decomposition of ammonia and have concentrated more on increasing the yield of hydrazine and determining the parameters affecting the yield. Empirical relationships have been postulated to explain their results, for instance in relating discharge current to pressure, field strength to pressure, residence time to yield, etc. An investigation of Devins and Burton[118] into the decomposition of ammonia in a d.c. electric discharge in the pressure range 0.6 - 11 mm Hg showed hydrazine, nitrogen and hydrogen were produced. Nitrogen was in fact produced uniformly throughout the discharge whilst hydrazine was produced significantly only in the positive column. The hydrazine yield was limited by a back reaction with atomic hydrogen. Catalysis of hydrogen atom removal, using platinum black films, increased the hydrazine yield. This phenomena was confirmed by other workers[119,120].

Miyazaki[121], using a silent discharge system, found the rate of decomposition of the ammonia was suppressed by the hydrogen atoms produced by the decomposition. Hydrazine was not

observed over the pressure range 5 - 15 mm Hg.

Ouchi[122] made observations of the effect of varying the characteristics of the discharge itself. Intermittent discharges gave a hydrazine yield approximately twice that from a 50 c/s discharge. Electrical yields from rectangular waves and impulse waves were found to vary inversely with the product of electric power times the residence time of ammonia in the discharge.

McDonald and Gunning[123] investigated the mercury - 6 ($^3P_1$) - photosensitized decomposition of ammonia at room temperature under both flow and static conditions. Nitrogen and hydrogen were produced in the static experiments whilst hydrazine was an additional product in the flow experiments. The quantum yield of ammonia decomposition in the flow experiments did not depend on the flow rate but increased in an exponential manner from a value of 0.09 at 650 mm Hg towards unity at low pressures as the reaction pressure was decreased. The percentage of the decomposed ammonia which was recovered as hydrazine increased from zero at low flow rate to 95% at high flow rates. At a fixed flow rate, the hydrazine to nitrogen ratio increased as the ammonia pressure was increased, from zero to a maximum value which was pressure independent at higher pressures. Also the hydrazine to nitrogen ratio increased as the incident intensity of 2537 A radiation was decreased. When ethylene was added to the mixture, the hydrazine to nitrogen ratio was markedly increased; probably due to the rapid reaction of the H atoms with the carbon-carbon double hand. However, when platinum wire was introduced into the irradiated zone, the reaction was found to be unchanged. This last result is in direct conflict with the results of other workers[118-120]. Pressures varied up to 650 mm H

and linear flow rates from 20 - 1600 cms/sec. Further experiments by McDonald and Gunning[124] showed that the rate of decomposition of ammonia was independent of the linear flow rate but depended upon the ammonia pressure in the reaction zone. The fraction of ammonia decomposed which was recovered as hydrazine while independent of ammonia pressure, increased markedly with increasing linear flow rate from zero in the static system to 0.84 at a linear flow rate of 1750 cm/sec. They also found that the energy yield of the ammonia decomposed under flow conditions was consistently higher by a factor of approximately two than for static conditions at the same pressures.

Two important conclusions can be drawn from these investigations,

a) as hydrazine is more susceptible to decomposition in the discharge than ammonia itself, it follows that the residence time of hydrazine in the discharge must be as low as possible.

b) as hydrazine is also lost by the reaction with hydrogen atoms produced in the discharge, any catalyst or technique that aids the recombination of the hydrogen atoms must increase the yield of hydrazine.

9.1.3. Commercial Systems for Production of Hydrazine from Ammonia

One of the more successful attempts at hydrazine production has been patented by Manion and Davies[125]. The process involves preheating of the ammonia to 350 - 400°C, and passing the ammonia through a glass discharge tube at flows of 9,000 - 30,000 cms/min. and pressures of 5-50 mm Hg. The discharge tube

contained a number of inert non-conductive projections extending outwards from the inner walls of the tube between the electrodes in the area of the electrical discharge. They found that the combination of maximum surface and minimum residence time in the discharge region resulted in a substantial increase in the yield of hydrazine. Yields of hydrazine ranged from 20 g/Kwh to 36 g/Kwh at approximately 40 mm Hg, and a linear flow rate 9,000 cms/sec. The extended surfaces were, presenting a large area of surface in the active region of the glow discharge, effective as a catalyst in bringing about the recombination of hydrogen atoms. The back reaction of hydrogen and hydrazine has been shown to seriously reduce the possible yield of hydrazine. However the manufacture of hydrazine by the proposed apparatus would be very expensive due to the need for very high capacity pumping and a separation/purification system to deal with a product stream containing approximately 0.1 - 0.2% by weight of hydrazine.

Recently work has been carried out using an absorbent to remove the hydrazine from the discharge zone. The technique is equivalent to reducing the residence time of the hydrazine in the discharge and hence, as discussed above, must increase the yield of hydrazine. Thornton and Spedding[99] used ethylene glycol as the absorbent, and so far have obtained yields of up to 10 g/Kwh in a d.c. discharge. However the separation and purification of the hydrazine could still prove costly.

Thornton[99] experimented further with a d.c. pulsed discharge with a variable on-period. Pulses of duration in the range 10^{-4} - 10^{-5} sec. were used. The pulsing of the power had the effect of decreasing the residence time of the excited

species in the reactor. This led to a considerable increase in the yield of hydrazine. As the on-period was shortened the yield rose and became independent of the power intensity. The best yield obtained so far was about 15 g/Kwh.

Devins and Burton[126], found that hydrazine formed in yields up to about 30 g/Kwh from a d.c. discharge in a stream of ammonia for a short period in the pressure range 3 - 10 mm Hg. Maximum yield was obtained by preheating the reaction vessel to about 200°C and by utilizing a Pt catalyst inside the glow chamber. The reactor was designed so the ammonia flowed transversely through the positive column which resulted in a residence time of not more than 10 milliseconds.

9.2. Analytical Techniques for the Determination of Hydrazine

Before commencing the investigation into the decomposition of ammonia in the microwave discharge, a method for determining hydrazine in the presence of ammonia was required. However it has been found that the combination of an acidimetric with an oxidimetric method affords a procedure for determining both total base and hydrazine. For example, a hydrazine solution after titration with standard acid can be titrated, using the iodate method. The difference in the two titres gives a measure of the amount of other basic components that are present. Accuracy of this procedure has been proved by the work of Penneman and Andrieth[127]. However with the concentration of ammonia envisaged, the above method would be inconvenient with a very large titration for ammonia.

Andrews[128] showed that in the presence of a high concentration of hydrochloric acid (3-9 M), iodate is reduced ultimately to iodine monochloride.

$$IO_3^- + 6H^+ + Cl^- + 4e \longrightarrow ICl + 3H_2O$$

The iodine monochloride forms a complex ion with the chloride ion,

$$ICl + Cl^- \longrightarrow ICl_2^-$$

In the initial stages of the reaction free iodine is liberated; as more titrant is added, the oxidation proceeds to iodine monochloride, and the dark colour of the solution gradually disappears. Hydrazine reacts with potassium iodate under the above Andrews conditions, thus:-

$$IO_3^- + H_2H_4 + 2H^+ + Cl^- \longrightarrow ICl + N_2 + 3H_2O$$

Hence we have a specific titration, which utilizes the reducing power of hydrazine, in the presence of ammonia. The detection of the end-point is by the disappearance of the iodine colour from a few mls of carbon tetrachloride added to the sample solution. The extraction end-point is very sharp. Starch cannot be used as the characteristic blue colour of the starch-iodine complex is not formed at high acid concentration. Modifications have been proposed to the above titration but show no specific advantage over the basic method[129].

A standard solution of iodate is prepared from dissolving 5.350 g in 1 litre. The solution is 0.1 N only for the reaction

$$IO_3^- + 6H^+ + Cl^- + 4e \longrightarrow ICl + 3H_2O$$

The procedure is quite simple. To a glass-stoppered flask containing the solution of the sample is added 20% more than an equal volume of concentrated hydrochloric acid (12 N) and 5 mls of carbon tetrachloride. Standard iodate solution is then added until the aqueous layer begins to change from a dark brown colour to a light yellow. At this point the iodate is

added dropwise and the solution shaken vigorously after the addition of each drop. When the iodine colour is completely discharged from the solvent layer, the end-point has been reached. The final normality of the acid should be between 3 and 5. The simplicity of the method provides a very convenient way of analysing for hydrazine.

A colourimetric method, using the dye-p - dimethylamino-benzaldehyde, has been suggested and proved accurate by Pesez and Petit[130]. The compound reacts with hydrazine to yield an azine that rearranges in the presence of strong acid to give a quinoid structure with an intense red orange colour.

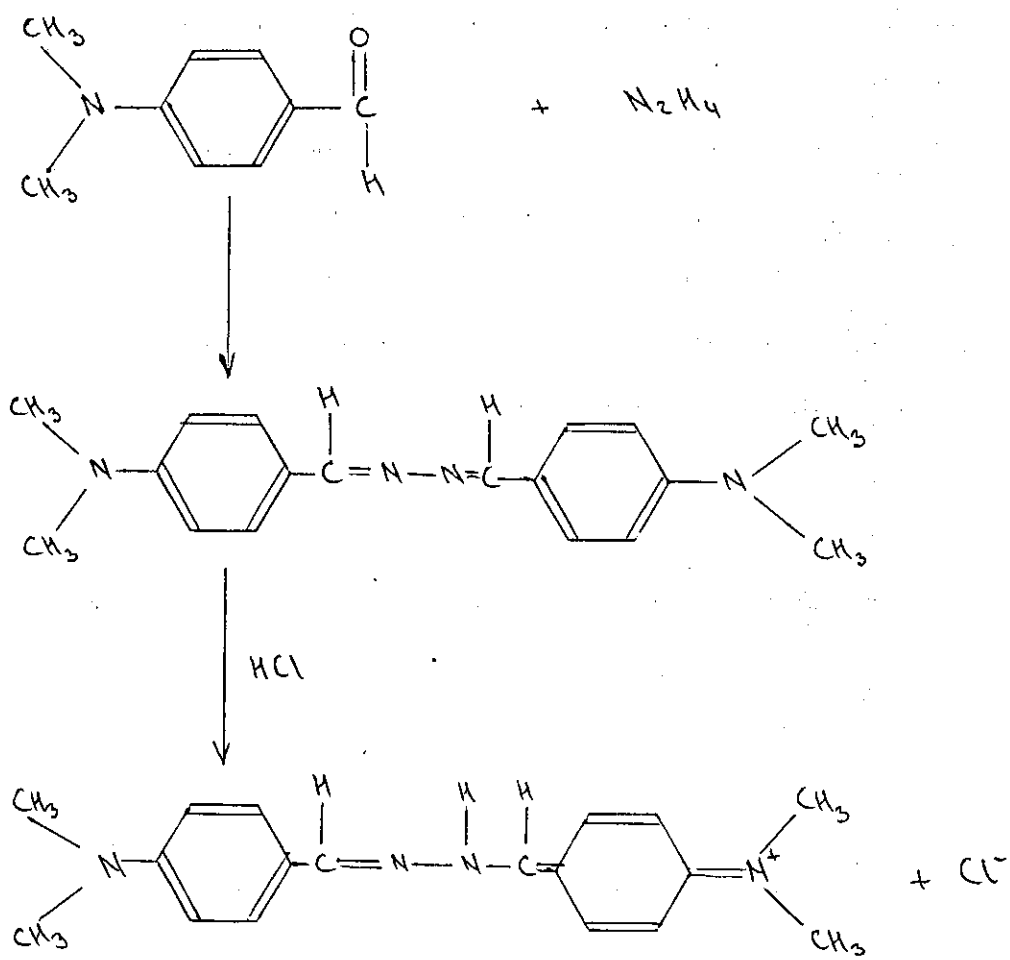

The absorption maximum is at 4,500 A, and the intensity of the absorption was found to be linear with concentration in the range 0.08 to 0.8 μ g per ml. The colour was found to reach a maximum intensity after 15 mins and is stable.

9.3. Experimental Details

9.3.1. Simple Flow System

Preliminary testing of the microwave system had shown it was possible to maintain a discharge under flow conditions and fairly high pressures. The heating effect of the microwaves precluded experiments under static conditions. For a flow system, the main requirements for investigating the performance of the ammonia discharge were,

a) a measurement of the flow rate, pressure and temperature of the ammonia gas.

b) a collection system for the hydrazine.

c) an absorption system for the waste ammonia.

The ammonia gas was of greater than 99.9% purity, obtained from I.C.I. Limited, and was used without further treatment.

At first the ammonia effluent was absorbed in a series of absorption traps containing strong hydrochloric acid solution. The exhaust gases from the reactor were initially cooled by a "cold finger" placed across the gas flow. Preliminary experiments also involved the addition of the colour reagent p-dimethylaminobenzoldehyde in strong hydrochloric acid to the first absorption trap to give an immediate indication of the presence of hydrazine.

A straight silica tube, internal diameter 22 mm, was used as the discharge reactor. The system was flushed with nitrogen.

Ammonia was introduced and a discharge obtained easily on the minimum input power available, approximately 0.8 kw. Absorption of power was ~ 20%. However the pressure and flow rate of ammonia were impossible to measure owing to a pulsing phenomena which resulted from the absorption of the waste ammonia gas in the traps. Estimated pressure was $> 40 < 100$ mm Hg. The pulsing was diminished, however, by packing the traps with Raschig rings and also bubblers, grade 0, were fitted to the delivery tubes. Several runs were carried out, flow rates 0.1 - 0.3 moles NH_3/min and reactor pressures 130 - 200 mm Hg, without hydrazine being detected. However certain conclusions could be drawn;

a) flow rate and pressures were now measurable.

b) the absorption capacity of the traps was too low.

c) the major problem developed in obtaining a good vacuum was due mainly to the number of large quickfit joints and taps in the system.

To obtain the required absorption capacity for the ammonia, a 5' Q.V.F. packed column was introduced into the system, see Fig. 25. A good vacuum was still obtained. The hydrazine was to be absorbed in two small traps before the Q.V.F. column. However, the small traps again were the limiting factor becoming rapidly saturated with ammonia. Several runs were made, flow rates 0.2 - 0.4 moles NH_3/min and reactor pressures 40 - 400 mm Hg. No hydrazine was detected.

A proposal to absorb the exhaust gases completely in the Q.V.F. column was abandoned. The dilution effect of the five litres of hydrochloric acid in the tower was too great for an accurate hydrazine analysis.

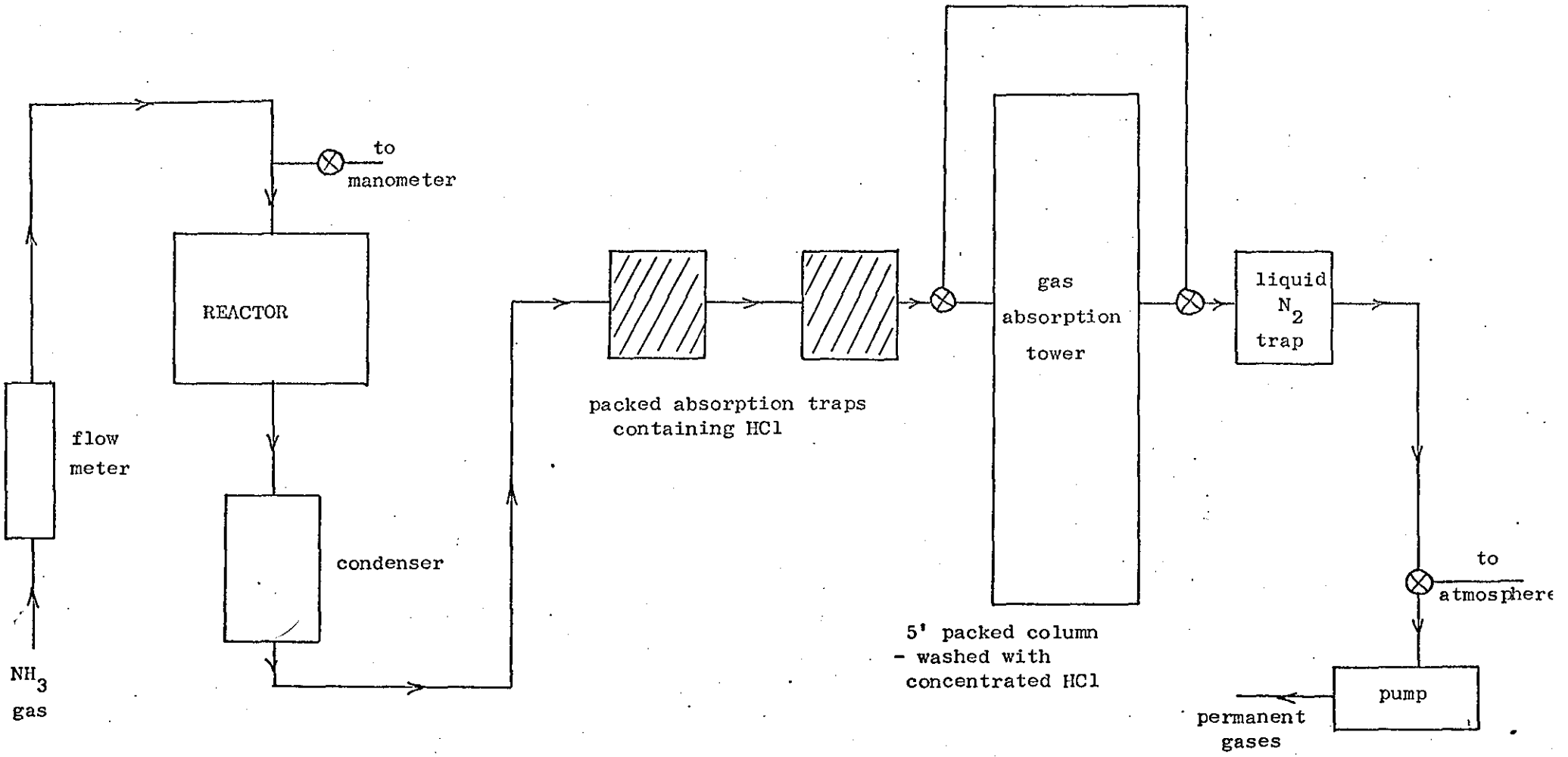

Figure 25 Simple Flow System for the Absorption of the Ammonia Discharge Products

9.3.2. Investigation by On-line G.L.C. Analysis

The acquisition of a gas chromatograph unit facilitated on-line analysis of the reactor exhaust gases. The basic unit consisted of a Pye Model 34, 104 series gas-liquid chromatograph. This has an isothermal oven and a kathomometer detector. A 5' glass column packed with polyethylene glycol 1000 on Chromosorb W was chosen. Nitrogen and argon were available as carrier gases though helium would provide a much higher sensitivity to hydrazine. The use of helium as a carrier gas was restricted due to its high cost. The preparation of standard moles to peak area curves for nitrogen, hydrogen and ammonia could be accomplished without difficulty. The problem lay in quantifying the hydrazine analyses. Hydrazine hydrate was chosen to prepare a calibration curve for hydrazine. Small amounts of hydrazine hydrate (0 - 1 µl) were injected. Hydrazine was easily detectable. Injections were made of mixtures of hydrazine hydrate and ammonia solution. The ammonia and/or water had no effect on the size or shape of the hydrazine peak.

To make quantitative measurements on the products from the reactor we needed to know

a) the pressure of the gaseous mixture.

b) the volume of the sample loop.

c) the temperature of the gaseous mixture.

A sample valve was supplied with the chromatograph. This was made of Teflon and was suitable for sampling under vacuum. Various sample loops, ½ ml - 25 mls could be fitted. The valve was fitted into the flow system as close to the discharge as possible. Several runs were made but no hydrazine was detected.

The gas sample obtained was also thought to have been due to diffusion which of course would lead to false product ratios.

The best way of obtaining a representative product sample was to allow the full flow of the discharge exit stream through the sample valve. Unfortunately the small bore of the teflon valve so restricted the ammonia flow in the system that the pressure quickly built up to the point where the discharge was extinguished. A system using two 4-way taps in series was devised and constructed. The volume of the sample loop was 63.5 ccs.

The above operations could be carried out quickly and hence repeated sampling was possible with small time intervals. Several runs were carried out using nitrogen or argon as the carrier gas. The flow rates ranged from 0.1 to 0.5 moles/min and the pressures from 40 - 400 mm Hg. Hydrazine was not definitely detected from the chromatograph.

There were three possible reasons for hydrazine not being detected.

a) the operating conditions of the chromatograph were such that any hydrazine decomposed on the column. This was unlikely as samples of hydrazine hydrate survived under similar operating conditions.

b) the hydrazine was condensing out in the delivery tubes before reaching the chromatograph.

c) any hydrazine formed in the discharge spontaneously decomposed under the conditions prevailing in the discharge.

To exclude the possibility of the hydrazine condensing before the G.L.C. the whole of the sampling loop and associated pipework was bound with asbestos and electrical heating wire. The temperature of the sample loop could be varied up to approximately 100^{o}C by the use of a variac. Runs were carried out at flow rates of 0.1 to 0.5 moles NH_3/min and pressures of 40 - 400 mm Hg. Helium was used as the carrier gas. Hydrazine was not detected.

In view of the failure to obtain even traces of hydrazine it was decided to analyse the reactor effluent to see if any nitrogen or hydrogen was formed in the discharge. The operating conditions of the G.L.C. were suitably altered to

separate the permanent gases from the ammonia. Using a modified sample loop, the percentage decomposition of the ammonia was determined by sampling the whole of the discharge product stream. The ammonia flow rate was varied, the pressure being kept approximately constant, see table 4. The ratio of the permanent gases, hydrogen to nitrogen, was found to be 3:1, under the experimental conditions used. This indicated the complete dissociation of the ammonia, the hydrazine and any excited species into hydrogen and nitrogen. This prompted the determination of the hydrogen to nitrogen ratio over a much wider range of experimental conditions.

A cylindrical reactor tube, internal diameter 22 mm, was used in the experiments to detect hydrogen and/or nitrogen from the microwave discharge in ammonia. The sample loop for the G.L.C. was placed after the liquid nitrogen trap and thus only permanent gases were detected. The operating conditions of the G.L.C. were such that hydrogen and nitrogen were easily separated, see Fig. 30. A molecular sieve type 5A column was used with helium as a carrier gas. A series of runs were carried out, varying the ammonia flow rate and pressure. Hydrogen and nitrogen were both detected and the mole ratios calculated, see Tables 5a, b, c.

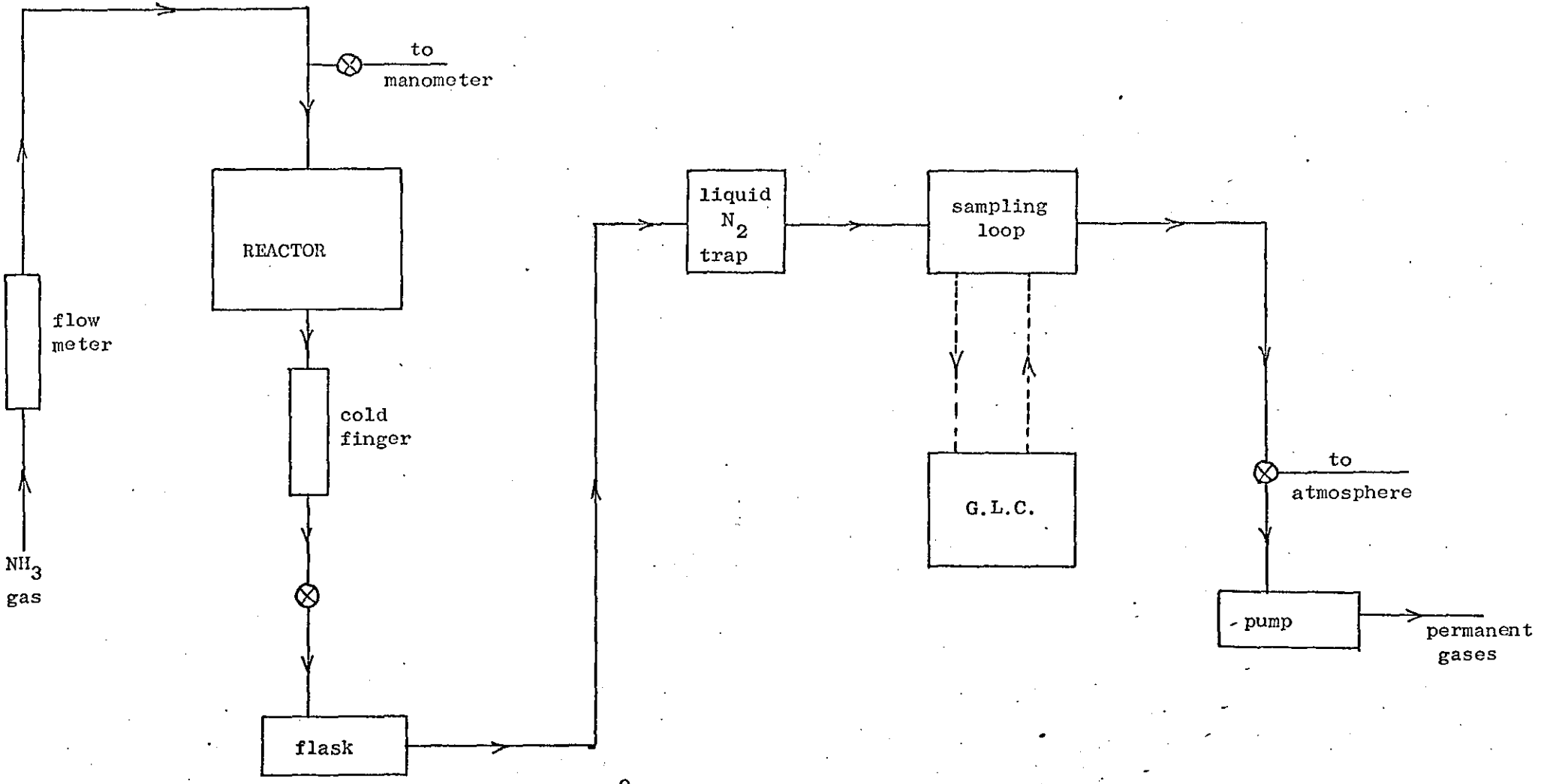

Figure 26 Flow System for On-line Analysis of the Permanent

9.3.3. Investigation by Analysis of the Condensed Products

Apart from the on-line sampling of the discharge stream for analysis on the G.L.C., numerous experiments were carried out in which the reactor gases were condensed in a cold trap for later analysis. At first the coolant cardice/acetone, was chosen such that only any hydrazine would condense at the temperature of the cold trap, i.e. the production and separation of the hydrazine from the ammonia could be conveniently carried out in the one apparatus. A large coil condenser with a flask attached were placed downstream of the discharge see Fig. 27 in a cold trap at -40°C. Several experimental runs were made at reactor pressures between 100 - 160 mm Hg, and a flow rate of 0.2 to 0.4 moles NH_3/min. At the end of a run the flask and condenser were washed with dilute hydrochloric acid and the washings tested for the presence of hydrazine, with the colour reagent p-dimethylamino-benzaldehyde. Hydrazine was not detected.

It was though possible that any hydrazine formed may still be carried through the cold trap by the flow of ammonia vapour. This problem was circumvented by using a lower temperature, -100°C, and freezing out the ammonia as well. Liquid nitrogen was used in the cold trap. Many experiments were carried out over a range of reactor pressures from 100 to 400 mm Hg and between flow rates of 0.2 to 0.5 moles NH_3/min. The potassium iodate titration was used in the analysis for hydrazine. However hydrazine was not found.

The possibility of any hydrazine formed in the discharge decomposing before reaching the cold trap prompted a proposal for further post-discharge cooling. A "cold finger" was placed

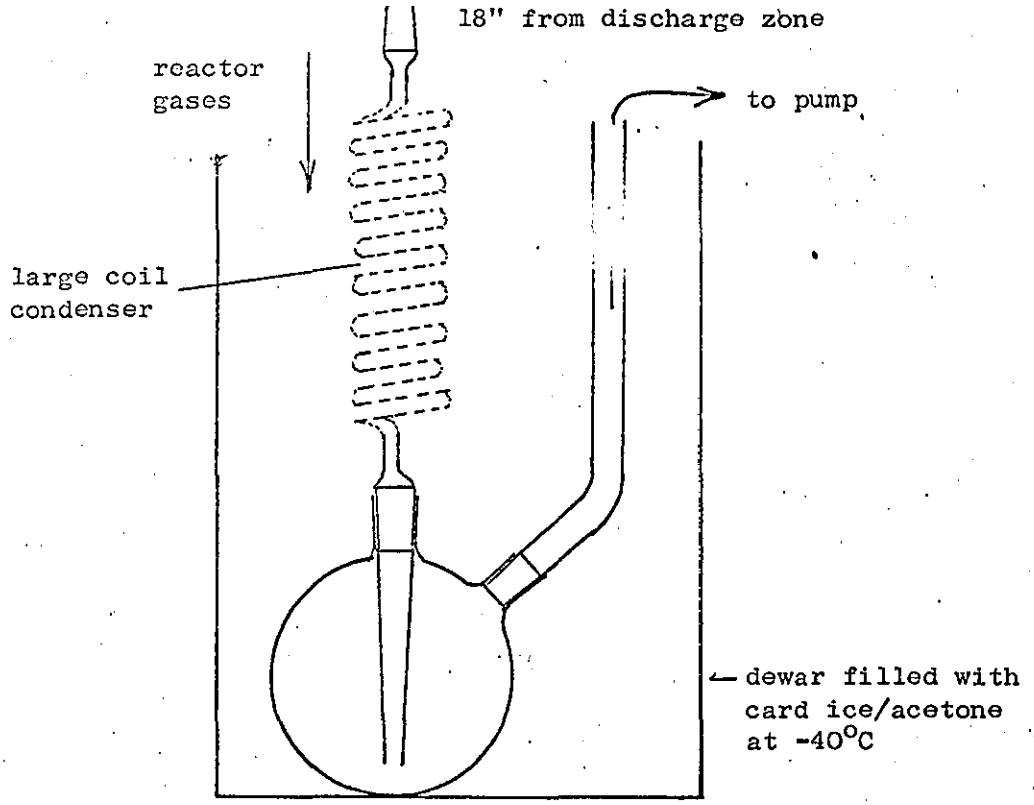

Figure 27 Large Coil Condenser Arrangement for Trapping Hydrazi

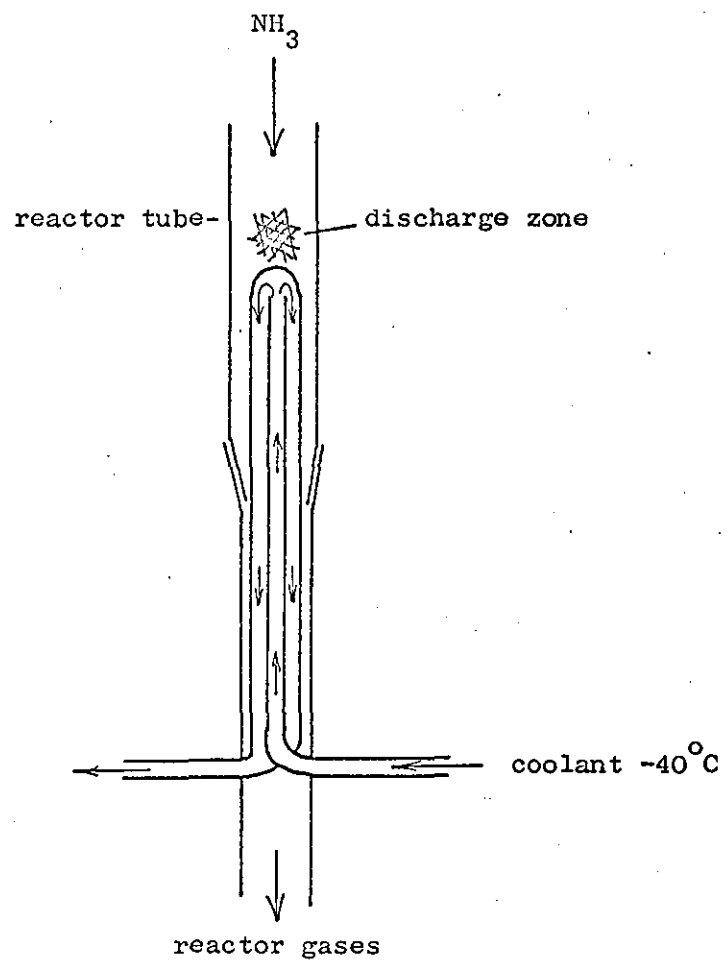

Figure 28 "Cold Finger" Arrangement used for Post-discharge Cooling

immediately downstream of the discharge zone, see Fig. 28. A jacketed coil condenser was connected to the "cold finger" and thence to a flask immersed in coolant at -100°C. A peri-staltic pump was used to pump coolant, methylcyclohexane cooled by liquid nitrogen, at 40°C round the "cold finger" and condenser. With this post-discharge cooling, experiments were made over flow rates ranging from 0.02 to 0.2 moles NH_3/min, and reactor pressures from 30 to 200 mm Hg. The analysis of the resulting condensates showed no evidence for the presence of hydrazine.

It has been reported in the literature that hydrazine decomposed rapidly on hot silica surfaces[132]. Obviously the longer the residence time of the hydrazine in the reactor tube the greater the chance of decomposition on the silica surface. Unfortunately a further reduction in the residence time was beyond the pumping capacity of the equipment. It was therefore proposed to cool the silica surface by using a silica condenser as the reactor, see Fig. 21a. The "cold finger" and coil condenser previously described were kept in the system, see Fig. 29. Methylcyclohexane, cooled by liquid nitrogen to -40°C, was pumped round all three cooling devices. The cavity was re-tuned. A discharge in ammonia was obtained at both points of high field strength in the cavity, theoretically impossible, see section resulting in a large absorption of power. Further testing showed that at pressures of $>$ 50 mm Hg only a single discharge was present. At pressures $>$ 100 mm Hg arcing occurred in the cavity. A change of coolant to a transformer oil, Diala B (Shell), did not solve the above problems. Moreover the tuning of the cavity was found to be greatly upset,

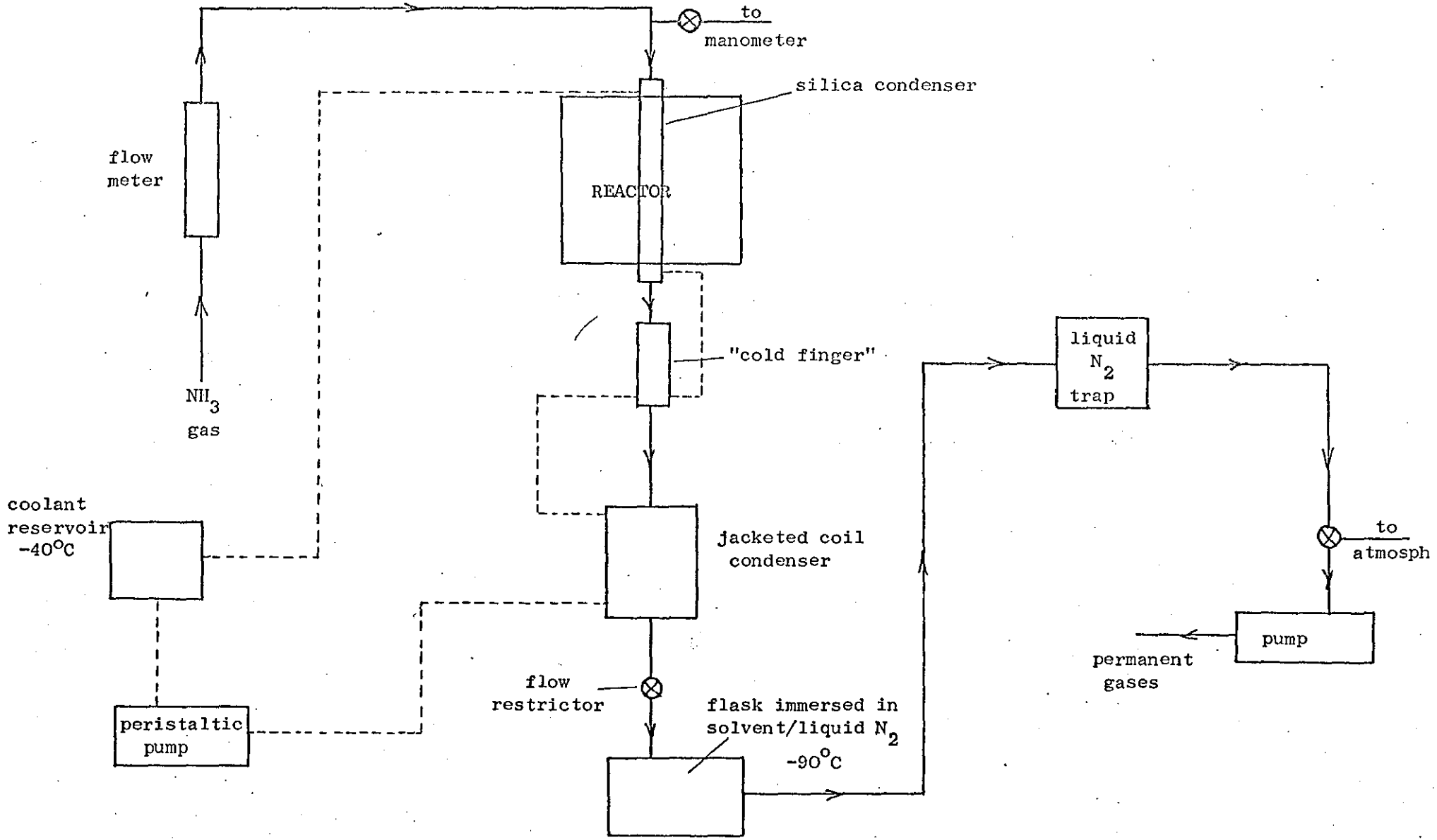

Figure 29 Flow System for the Cooling and Trapping of the Ammonia Discharge Products

and on-tune conditions were difficult to obtain.

A problem of moisture condensation on the outer surface of the silica condenser, resulting in an increase in power absorption, was solved by blowing dry nitrogen continuously through the cavity.

A condenser similar to the original but with larger internal diameters, 18 mm and 23 mm respectively, was made. This was in view of the difficulties experienced with reactor tubes of diameters 14 mm and less in previous experiments, see section 7.3. On testing, normal tuning conditions were present in the cavity and a single discharge was obtained. However prolonged testing of the silica condenser showed changes in the cavity tuning occurred as the coolant warmed up during a run. In view of the difficulties with the cavity tuning, the cooling of the reactor tube was abandoned. Possibly the only solution would be a change in the cavity itself. Either a change in the mode of power transference or a complete removal of the resonant cavity and use, for example, a tapered wedge arrangement.

9.4. Temperature Profile in the Ammonia Discharge

As mentioned in the introduction the formation of free radicals is promoted by a low gas temperature and a high electron temperature in the discharge. Fig. 32 shows the temperature gradient existing through the ammonia discharge under the stated conditions. A bare Ni-Cr/Al-Ni thermocouple, connected to a bridge circuit was used for the temperature measurement. Maximum temperatures of approximately 1000^{o}C were found for the operating conditions of 40 mm Hg pressure, 0.04 moles/min. The temperature fell away rapidly to approximately 600^{o}C five centimetres downstream of the discharge. Higher

pressures, e.g. 60 mm Hg, 0.05 moles/min raised the maximum recorded temperature to around 1100°C. It should be noted that the thermocouple was open to bombardment by excited species and recombination of atoms on the surface of the thermocouple. The temperatures recorded were therefore higher than the actual temperature in the discharge. However the low gas temperatures found were condusive to the production of free radicals.

9.5. Experimental Results : Ammonia Studies

The ammonia flow rates were estimated as being accurate to within ±5%. The reactor pressure was measured on a mercury manometer to within ±2%. The microwave power monitors operated at an overall accuracy of ±15% but with a reproducibility of 95%.

The conditions for analysis of the permanent gases on the G.L.C. were as follows,

Pye 104, Model 34, gas chromatography unit

helium carrier gas, 50 mls/min

bridge current, 240 mA

oven temperature, 20°C

molecular sieve column Type 5A, 5' long, ¼ i.d. 60 - 80 mesh.

Based on the component peak areas obtained from the chromatograph estimates were made of the hydrogen and nitrogen content to within an overall accuracy of ±5% but with a reproducibility of greater than 98%.

All data tabulated was obtained with minimum power output from the microwave generator, i.e. 0.78 Kw.

9.5.1. Discussion of Results : Ammonia Studies

The variation of the power absorption in the reactor with varying ammonia flow rates and pressures is indicated in Figs. 33

and 34. At a constant flow rate an increase in pressure increases the power absorption. Again at a constant pressure, an increase in the flow rate leads to a decrease in the power absorption. It follows that there are certain flow rates and pressures for which the efficiency of power transference to the discharge is an optimum. These conditions may not necessarily be the best for the desired chemical reactions to take place.

The power intensity in the discharge is difficult to define owing to the nature of the discharge. The discharge centre probably occupies no more than 1 cc. but the discharge zone can, under certain conditions, occupy the entire length of the reactor tube, a volume of up to 60 ccs. At maximum power input from the microwave generator, an electric field of 5,000 volts/cm. is present at the centre of the discharge. However, it should be noted that the efficiency of the power transference is greatly affected by the tuning of the cavity. For instance, a change in the reactor pressure of say 20 mm Hg necessitates the retuning of the resonant cavity to maintain efficient power transfer.

Table 3 indicates the wide range of experimental conditions used in the attempts to produce hydrazine.

Fig. 35 shows the variation of the mole percentage decomposition of the ammonia with the mole flow rate of ammonia. The actual percentage varies from 6.7% at flow rate of 0.015 moles NH_3/min to 0.08% at 0.3 moles NH_3/min. The ammonia decomposed to the permanent gases; a hydrogen to nitrogen ratio of 3:1 was found. The plot of percentage decomposition against flow rate shows an exponential decrease in decomposition from low to high flow rates of ammonia. This is consistent with the

view that the longer the residence time in the discharge the greater the likelihood of electron collisions with neutral ammonia molecules to give excited species. However this raises the problem that as hydrazine is more susceptible to dissociation than the ammonia in the discharge, the residence time should be as short as possible. This means in fact high linear flow rates to reduce the residence time which however leads to a decrease in the percentage decomposition of the starting material, i.e. ammonia.

Tables 5ab and c represent the ammonia pressures and flow rates used in the determination of the hydrogen to nitrogen ratios. From the analysis of the permanent gases produced from the decomposition of ammonia in the discharge, it was found that the mole ratio of hydrogen to nitrogen was consistently 3:1, the ammonia decomposed through transient species to give hydrogen and nitrogen. If hydrazine was formed at all under the conditions of the experiments it spontaneously decomposed to other excited species which finally gave hydrogen and nitrogen.

9.5.2. Interpretation of Results : Ammonia Studies

Hydrazine has not so far been prepared in a microwave discharge[131] though d.c. discharges have met with some success[125,126]. The temperature of the discharge centre was less than 1000°C and this should not in itself prevent formation or cause the decomposition of hydrazine or its precursors. The complete absence of hydrazine, even under analytical conditions capable of detecting less than one part per million of hydrazine, suggests the necessary precursor, i.e. the NH_2 radical was not formed in sufficient numbers in

the discharge to give hydrazine. The production of the permanent gases in the discharge must therefore have arisen from the dissociation of ammonia to NH radicals. If this assumption is correct and NH is the free radical formed rather than NH_2, this would prohibit any possibility of the formation of hydrazine.

The colour of the discharge tends to support the existence of NH radicals in the discharge, see Fig.31. At low pressures the colour of the discharge is pale mauve, which would indicate the presence of NH rather than NH_2[132]. At higher pressures collisional deactivation of the excited ammonia molecules is important and thus the concentration of free radicals is low. The yellow colour of the discharge would thus be the normal emission spectrum of ammonia in a discharge[132].

NH radicals have not been found in equivalent d.c. or low frequency discharges. This raises the point of whether the microwave discharge induces higher levels of excitation in the gas molecules in the discharge to give a different distribution of free radicals or other transient species compared with other discharge systems.

9.5.3. Conclusions : Ammonia Studies

In conclusion the decomposition of ammonia in a microwave discharge has been investigated. Evidence of hydrazine formation was not found. The only products were the permanent gases, hydrogen and nitrogen, in a mole ratio of 3:1. There exists the possibility that the microwave discharge excites the molecules to higher energy levels than does the equivalent d.c. discharge, see section 10.5. Further work on the system is needed to confirm the presence of NH or NH_2 in the discharge,

by spectroscopic means. If NH_2 radicals are found, hydrazine may possibly be found by increasing the linear flow rate of ammonia and using reactor pressures in the 20 - 50 mm Hg region. The silica tube reactor may need coating to reduce the possibility of hydrazine decomposition on the hot silica surface[133]. Means of reducing the residence time of the excited species and hydrazine in the discharge by pulsing of the microwaves and/or by a spray absorbent, should be examined, see section 7.4. The effect of the presence of a metal catalyst, such as nickel or platinum, in the discharge should also be investigated.

EXPERIMENTAL DATA : AMMONIA STUDIES

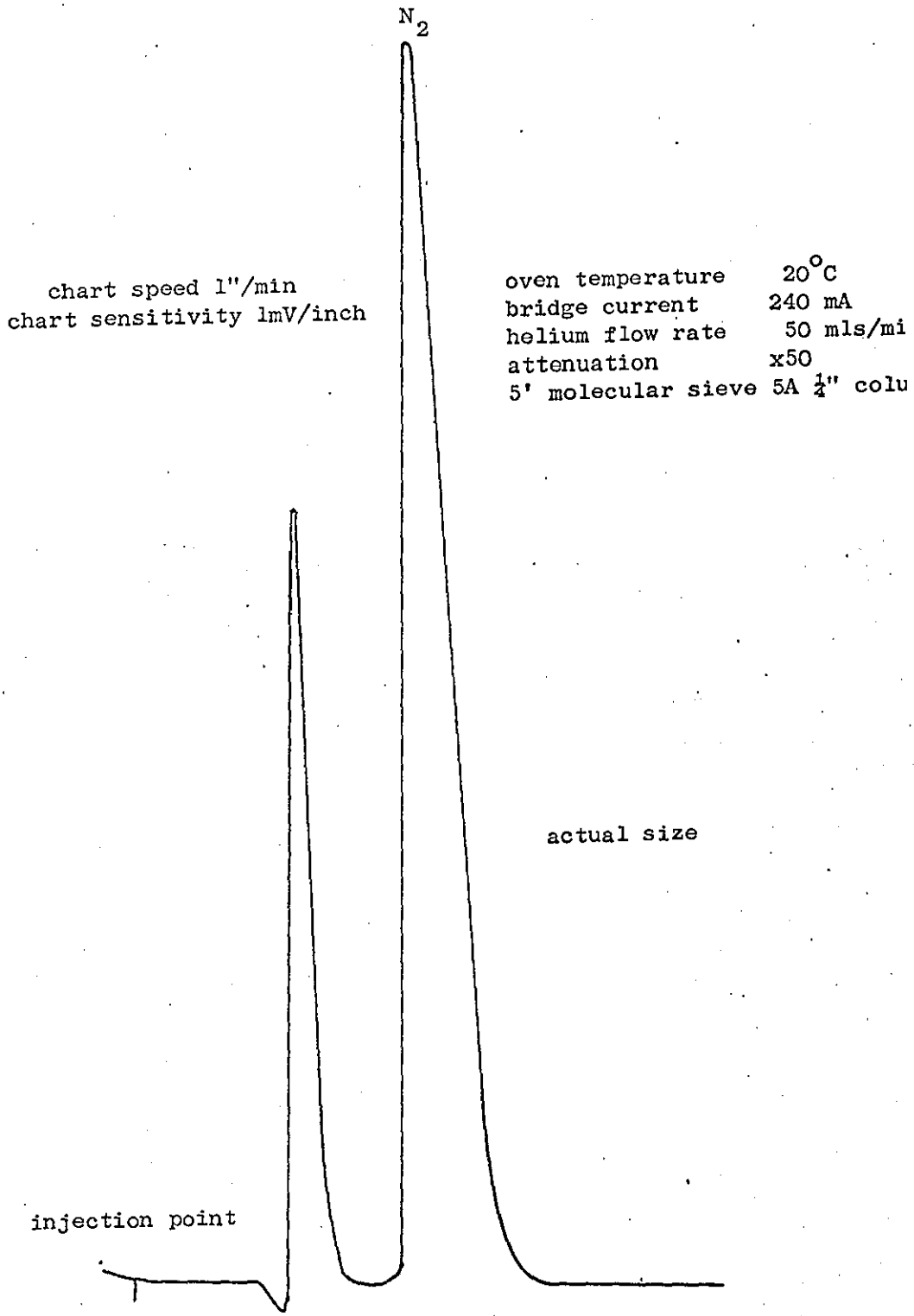

Figure 30 Example of the Separation of the Permanent Gases.

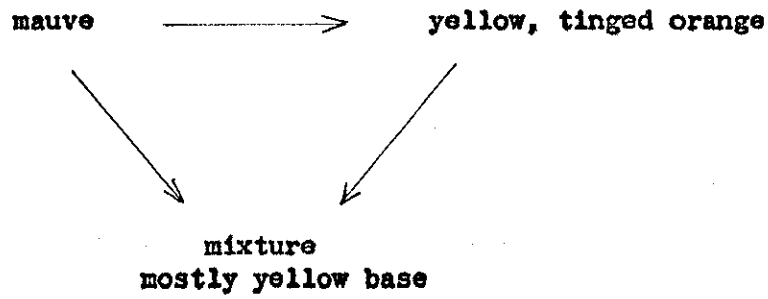

e.g.

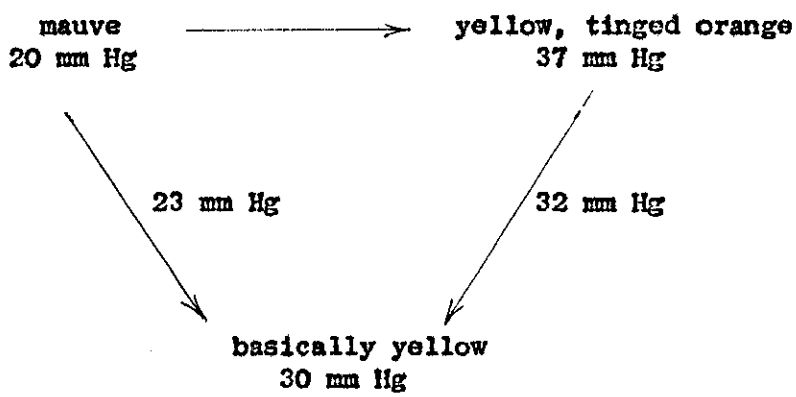

ammonia flow rate = 0.1 moles/min.

NH emission bands	2,800 - 3,900 Å
NH_2 emission bands α - bands	4,300 - 9,000 Å

Figure 31 Observed Colour Changes in the Ammonia Discharge

Figure 32 Temperature Profile of the Ammonia Discharge

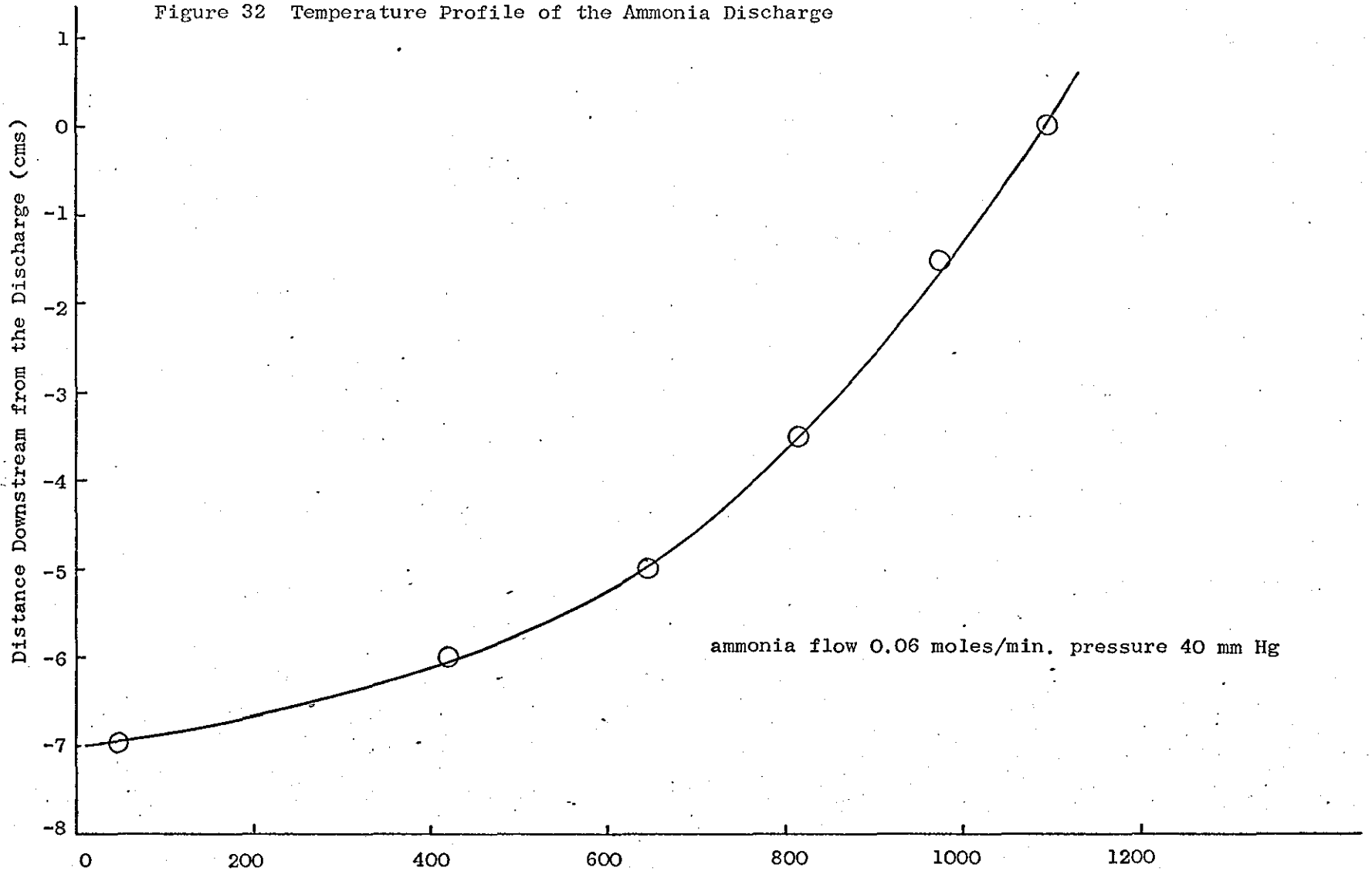

Figure 33 Power Absorption Against Ammonia Flow Rate

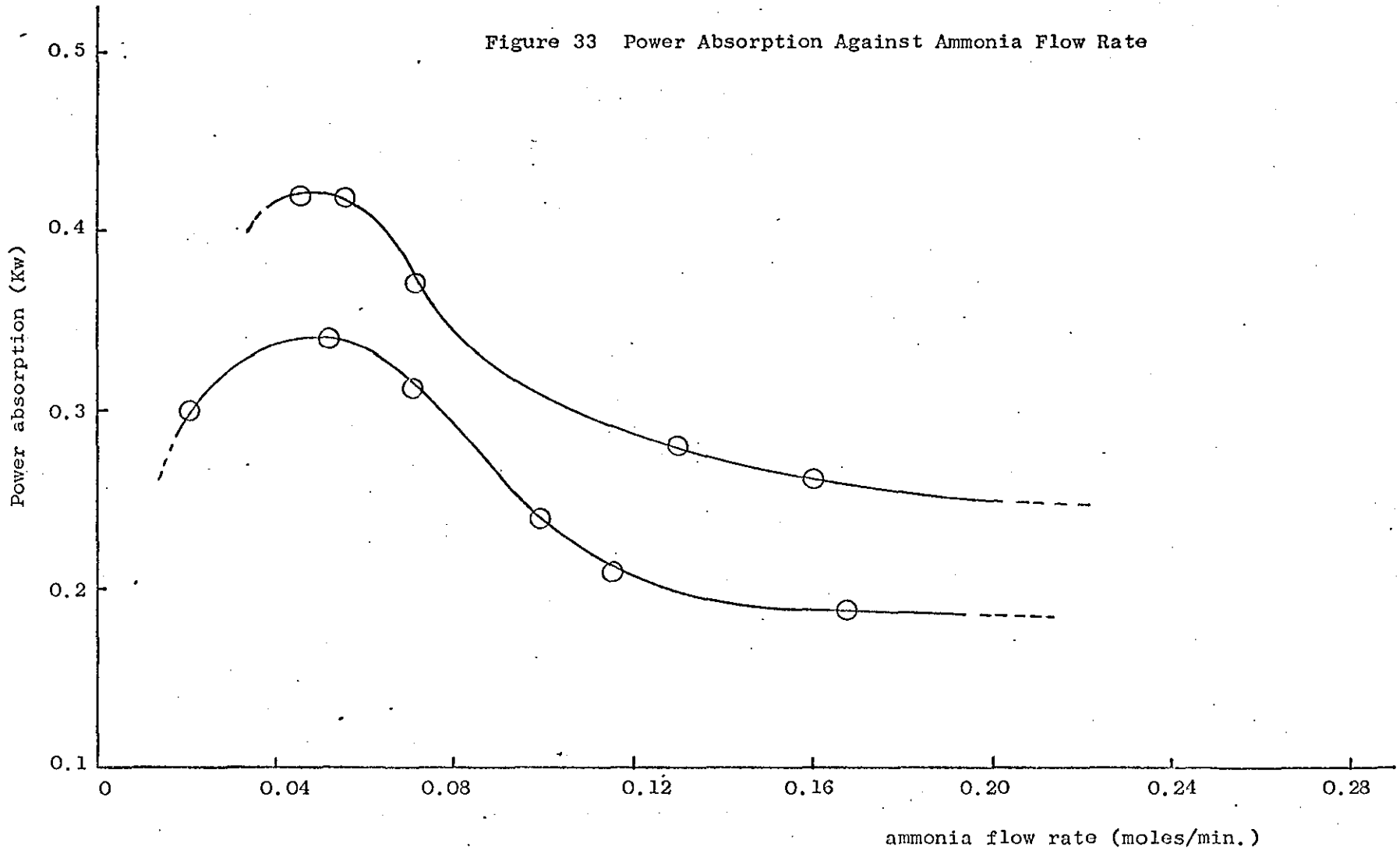

Figure 34 Power Absorption Against Reactor Pressure

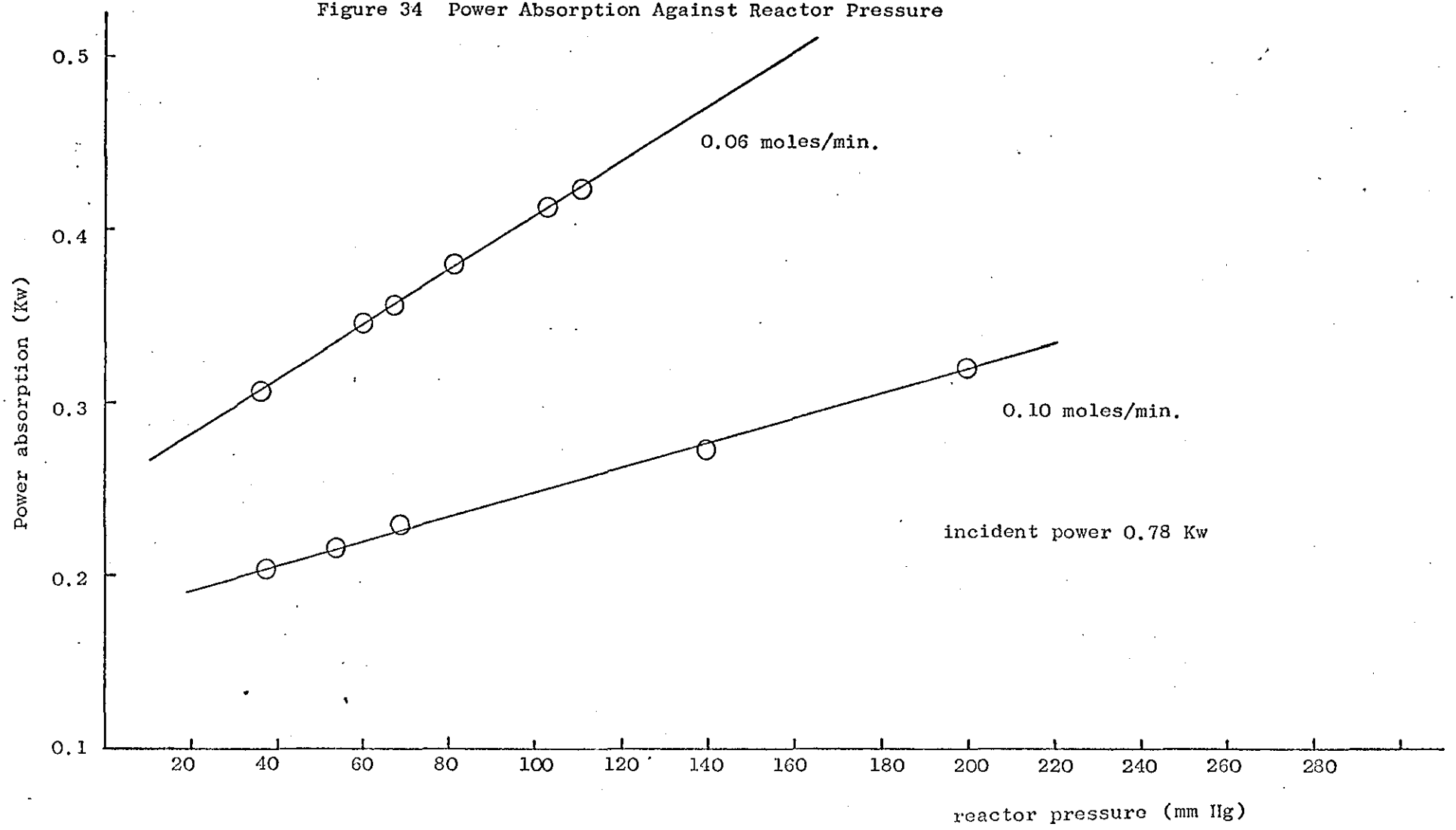

Table 3 Range of Experimental Systems and Conditions Investigated

Flow and Trapping System	Number of Runs	Range of Ammonia Flow Rates moles/min.	Range of Reactor pressures mm Hg
Absorption traps, as in Fig. 25	10	0.1 - 0.4	40 - 200
Large coil condenser trapping system, as in Fig. 27	30	0.06 - 0.4	30 - 200
Cold finger and condenser + trapping system, as in Fig. 29	30	0.05 - 0.30	30 - 190
G.L.C. sampling for detection of hydrazine	45	0.02 - 0.30	20 - 150
G.L.C. sampling for permanent gases + trapping system, as in Fig. 26	35	0.03 - 0.25	10 - 130

Table 4 Percentage Decomposition of Ammonia

Ammonia flow rate moles/min.	H_2 : N_2 ratio	Mole % ammonia decomposed
0.015	3.05:1	6.70
0.030	3.02:1	2.88
0.060	3.00:1	1.28
0.090	3.08:1	0.68
0.155	2.97:1	0.34
0.200	3.00:1	0.20
0.250	2.98:1	0.15
0.302	3.01:1	0.08

reactor pressure 25 mm Hg. ± 2

Table 5a : Mole Ratios of the Permanent Gases

Constant flow rate, 0.062 moles NH_3/min.

reactor pressure	mole ratio H_2 : N_2
36	3.09:1
61	3.00:1
68	3.02:1
81	3.04:1
98	3.08:1
113	3.04:1

Table 5b

Constant reactor pressure, 42 mm Hg.

ammonia flow rate moles/min.	mole ratio H_2 : N_2
0.042	2.97:1
0.067	2.98:1
0.092	2.99:1
0.124	3.09:1
0.141	3.00:1

Table 5c

ammonia flow rate moles/min.	reactor pressure mm Hg	mole ratio H_2 : N_2
0.40	79	2.95:1
0.485	146	3.00:1
0.249	161	2.95:1
0.163	187	2.96:1

Figure 35 Percentage Decomposition of Ammonia Against Ammonia Flow Rate

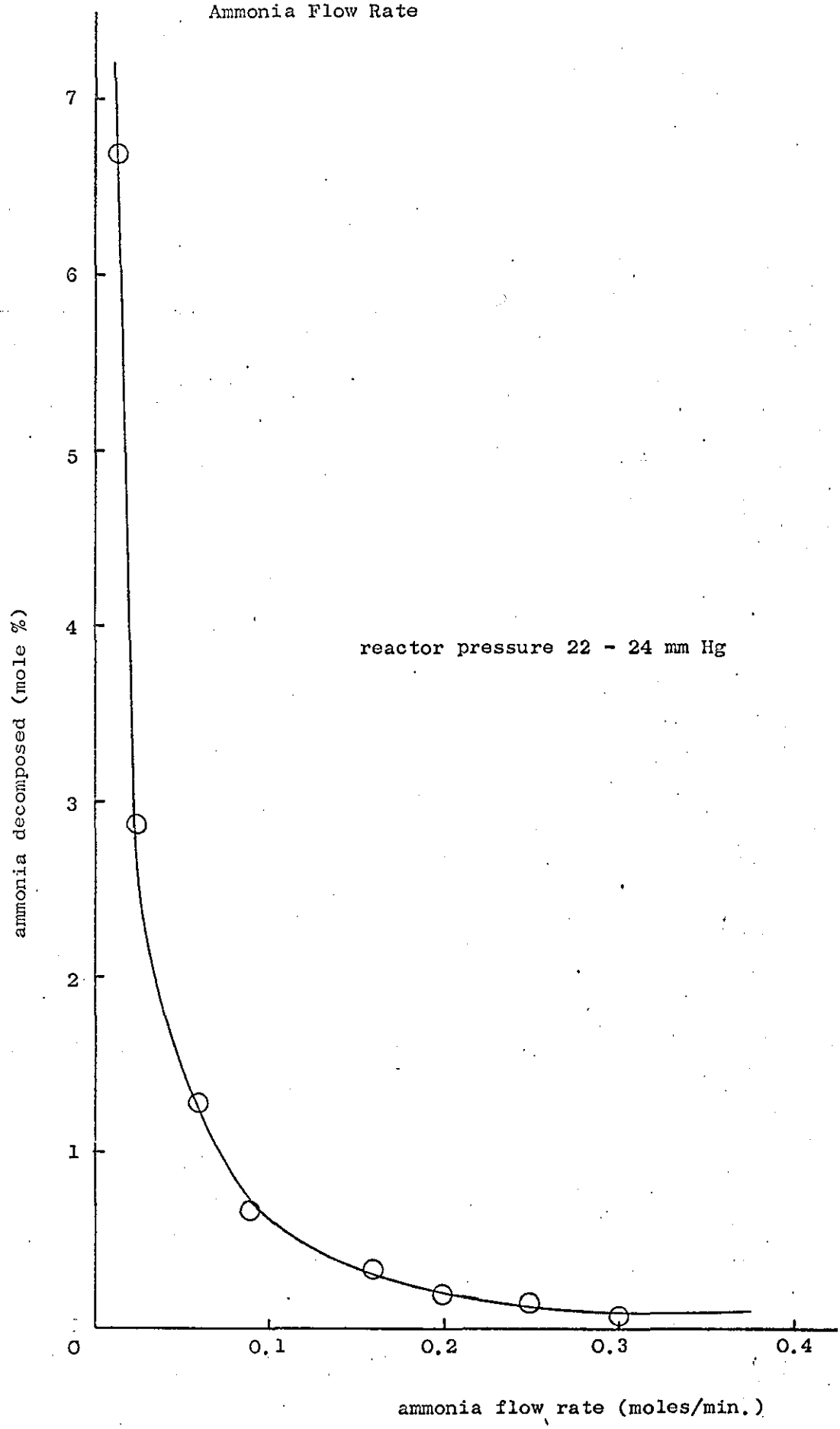

SOME REACTIONS OF BENZENE

IN THE MICROWAVE DISCHARGE

10. Some Reactions of Benzene in the Microwave Discharge

The scouting experiments previously conducted on the dissociation of benzene in the microwave discharge indicated the areas of interest, see section 8.1.3. A series of experiments were proposed involving the systems listed below,

1) discharge in benzene alone.

2) discharge in benzene in the presence of nickel.

3) discharge in benzene admixed with carbon dioxide.

4) discharge in benzene admixed with ammonia.

10.1. Experimental Details : Benzene Studies

The benzene used in the experiments was of Analar grade obtained from Fisons Limited. The carbon dioxide was a standard bottled gas from Distillers Limited and the ammonia of greater than 99.5% purity from I.C.I. Limited. All the chemicals were used without further purification.

A flow system was designed and set up, see Fig. 36. The Platon flostat provided a constant volumetric flow rate of benzene through the reactor against varying downstream pressure. A "split-diameter" silica tube was used as the reactor, see Fig. 21b. Provision was made for on-line sampling of the gas stream and/or condensing the products in a liquid nitrogen trap. Analysis of the products was made on a Pye 104 series, Model 34 gas chromatography unit. The results were recorded on a Telsec 700 flat-bed chart recorder. Nitrogen was used as the carrier gas.

The sample loop was heated to approximately 180°C to prevent condensation of high boiling compounds in the loop. The flostat was also heated to about 70°C and calibrated at that temperature with a flowmeter.

The analysis of the gaseous products proved difficult because of their wide boiling range. These difficulties were exaggerated by the lack of temperature programming facilities. However after extensive investigation a short column of a polymer bead packing, Porapak Q, proved suitable. The Porapak Q was obtained from Waters Associates Limited. Separation of hydrogen, C_2, C_3 and C_4 hydrocarbons was possible commensurate with a reasonable retention time for benzene. Standard retention times for a range of low boiling hydrocarbons were used to identify the products of the discharge. The retention times were obtained by injecting samples of the known gases. For this purpose the following gases were obtained from B.D.H. Limited:- methane, ethylene, acetylene, propane, propylene, butane, butene-1, cis butene-2, trans butene-2, isobutane, isobutylene, 1,3-butadiene.

The high boilers, recovered from the cold trap, were analyzed on a short Apiezon L column, at a higher temperature. Retention times of likely high boilers such as naphthalene and diphenyl were determined. Calibration curves of molar concentration against peak area were obtained by injection of standard 0.01 M solutions in benzene for naphthalene and diphenyl.

During an actual run, the flostat was set at a predetermined value after the discharge had struck. Samples of the reactor gases from G.L.C. analysis were taken after about five minutes. Liquid samples were collected in the cold trap. Any carbonaceous deposits in the reactor tube were burnt off after each run. Each run took approximately two hours.

Several series of experiments were conducted on the four systems involving benzene vapour. Discharges were obtained in pure benzene, benzene in the presence of nickel wire, and benzene with admixtures of carbon dioxide or ammonia. In all four systems the benzene flow rate was varied between 0.008 to 0.15 moles/min., corrected to N.T.P., over pressures ranging from 10 to 80 mm Hg.

Scouting experiments had shown the nickel wire to have a marked effect on the yield and distribution of products. The nickel was in the form of fifteen strands of 16 gauge wire, length 7", bound together and placed in the discharge zone. At least 70% of the nickel wire was downstream of the discharge. Experiments were conducted over the range of conditions mentioned above.

Benzene and ammonia in the mole ratios from 1:2 to 1:10 were passed through the microwave discharge. It was hoped that from the wide range of mole ratios investigated the optimum conditions for the production of the purple solid found in the scouting experiments would be established.

The preliminary investigations had also shown that at mole ratios of greater than 1.5:1, carbon dioxide to benzene, the decomposition of benzene was negligible. Mole ratios of less than 1.5:1 were therefore investigated.

10.2. Experimental Results : Benzene Studies

The conditions for analysis on the G.L.C. were as follows, analysis for low boilers,

nitrogen carrier gas, 120 mls/min.

oven temperature, 70°C

bridge current, 140 mA

Porapak Q column, 2' long ¼" i.d., 80 - 100 mesh

analysis for high boilers,

nitrogen carrier gas,	120 mls/min.
oven temperature,	180°C
bridge current,	110 mA
5% Apiezon L column,	2' long, ¼" i.d.

The maximum error in the analysis of each low boiling component was ±10%. The error in measuring the high boilers was greater but within ±20% for each component. The calculations of the product conversions were based on the component peak areas obtained from the chromatograph. The product conversions were expressed as the equivalent moles of benzene converted to one product per moles of benzene passed, as a percentage, and were tabulated in that form.

The retention time analysis of the low boilers showed definitely the major products were acetylene, 1,3-butadiene and a C_3 hydrocarbon. The C_3 hydrocarbon was concluded to be allene after elimination of propane and propylene by further retention time analysis. Allene could not be confirmed absolutely as samples of the gas were not available for testing.

Of the high boilers diphenyl and naphthalene were definitely identified. Other peaks were ascribed to a substituted diphenyl, phenylbutadiene and phenylacetylene.

The benzene flow rates were estimated as being accurate to within ±5%. The pressure in the reactor was measured on a mercury manometer to within ±2%. The microwave power monitors worked to an overall accuracy of ±15% but with a reproducibility of greater than 95%.

10.3. Discussion of Results : Benzene Studies

10.3.1. Benzene Alone : the Low Boilers

A large fraction of the benzene in the discharge decomposed to low boiling gaseous products such as acetylene, allene and 1,3-butadiene. Traces of ethylene and butene-1 were also found. The conversion to acetylene was independent of pressure over the range 10 - 50 mm Hg at benzene flow rates of 0.01 to 0.12 moles/min. At higher pressures experiments indicated the conversion to acetylene became pressure dependent. The plot of mole percentage against benzene flow rate is shown in Fig. 38a. Conversions to acetylene of up to 60% of the benzene were found.

The conversion to 1,3-butadiene was independent of pressure in the range studied, i.e. 10 - 50 mm Hg. The plot of conversion to 1,3-butadiene against flow rate passed through a maximum of 30% of the benzene input. The shape of the curve indicated the possibility of the 1,3-butadiene being derived from the intermediate in an unimolecular reaction, see appendix A.

Small yields of allene were produced in the discharge. The percentage conversion of benzene to allene was constant over the range of experimental conditions used, at about 2% of the benzene input. It should be noted therefore that the yield increased with flow rate.

10.3.2. Benzene Alone : the High Boilers

In the present work, evidence of the survival of the phenyl ring has been obtained in the form of the following products:- diphenyl, naphthalene, phenyl-butadiene and possibly

phenylacetylene. The formation of an amber solid, shown to be of a polybenzene structure by mass spectrometry was also noted, see Fig. 50. The polymer absorbed in the ultra-violet from 290 mμ with decreasing intensity to $\sim$ 320 mμ, see Fig. 51.

In the discharge in pure benzene vapour, the conversion to diphenyl was dependent on the reactor pressure. At a constant volumetric flow rate, increasing the pressure drastically reduced the conversion to diphenyl, see Fig. 41a. At constant pressure, a plot of conversion against benzene flow rate showed a maximum, see Fig. 42a. It was concluded that the yield of diphenyl was dependent on the residence time of the excited species from which it was derived and of the diphenyl itself in the discharge zone. The maximum conversion to diphenyl found, under the conditions of the experiments, was 2.3% of the benzene input.

Naphthalene, phenylbutadiene and phenylacetylene were produced in considerably lower yields than diphenyl. A plot of percentage conversion to the above products against flow rate showed a maximum, see Fig. 43a. The conversion decreased rapidly at higher pressures. The total maximum conversion to all three products was 0.8% of the benzene input, under the experimental conditions. Naphthalene was the major component.

Gravimetric estimates of polybenzene formation indicated that this was probably no more than 1% of the benzene input and was reasonably constant over the range of conditions used. Difficulties arose in assessing the conversion to polybenzenes in that the product was spread over a considerably area of glass-ware. Carbon formation was heavy, equivalent to the

total decomposition of about 5% of the benzene input in the 0.02 to 0.08 moles/min flow range. The carbon formation increased markedly with increasing pressure.

10.3.3. Benzene and Nickel Wire : the Low Boilers

In the presence of nickel wire in the discharge the conversion to acetylene was reduced by up to one quarter that found in benzene alone, see Fig. 38b. The percentage conversion to acetylene was independent of pressure over the range of conditions studied.

The conversion to 1,3-butadiene was reduced by up to one third of that from the pure benzene discharge. The conversion was again independent of pressure and the plot of conversion to 1,3-butadiene against flow rate showed a maximum, see Fig. 39b.

The yield of allene was virtually the same as that for the discharge in benzene alone, i.e. independent of pressure and flow rate, at about 2% benzene converted.

10.3.4. Benzene and Nickel Wire : the High Boilers

The conversion to diphenyl was doubled in the presence of nickel wire, over the range of pressures and flow rates used, see Fig. 42b. A maximum conversion of 4.6% of the benzene passed was noted. Increasing the reactor pressure drastically reduced the yield of diphenyl, see Fig. 41b.

The yields of naphthalene, phenyl-butadiene and phenylacetylene were also doubled with nickel wire in the discharge zone. Gravimetric estimates of polybenzene formation showed a slight decrease in yield. Carbon formation was also reduced.

10.4. Visual Observation of the Discharge

On first striking the discharge in benzene vapour, a pale blue colour in the discharge zone was noted. However the blue colour of the discharge was rapidly hidden consequent on the formation of carbon and polybenzene. However at flow rates $>$ 0.10 moles/min and low pressures, carbon formation was slight and the blue colour of the discharge became visible.

A similar phenomena occurred in the presence of nickel wire. The blue colour was visible over a greater range of flow rates due to the tendency for carbon to form on the nickel surface rather than on the walls of the reactor.

The blue colour observed is perhaps indicative of the presence of phenyl radicals in the discharge[103] The transition $\tilde{X}\ ^2A_1 \quad \tilde{A}\ ^2B_1$ gives rise to sharp bands in the spectral region 4320 - 5,290 A, i.e. the blue region. The excited state transitions of benzene itself are far in the ultra-violet region of the spectrum.

10.5. Interpretation of Results : the Low Boilers

Momigny and Brakier[133] compared the appearance potentials of species from the benzene mass spectrum with those of the open-chain isomers (the four hexadiynes and butadienylacetylene). They found that the mass spectrum of benzene was similar to butadienylacetylene and concluded that the formation of an open chain ion was a step in the decomposition of the benzene molecule by electron impact. Isomerization of the benzene radical ion, $C_6H_6^{+\cdot}$, into an open chain isomer was postulated. In fact they concluded

that not only $C_6H_6^{+\cdot}$ in any excited state but also $C_6H_5^{+}$ and $C_6H_4^{+\cdot}$ in their ground-states derived from benzene, were not cyclic but linear, i.e.

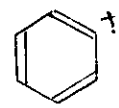

$$\rightleftharpoons \left[CH_2 = CH - CH = CH - C \equiv CH\right]^{+\cdot} \quad (1)$$

Ottinger[134] has shown, by analysis of the mass spectrum of benzene, that the following dissociation reactions can occur.

$$C_6H_6^{+\cdot} \longrightarrow C_4H_4^{+\cdot} + C_2H_2 \quad (2)$$

$$C_6H_6^{+\cdot} \longrightarrow C_6H_5^{+} + H^{\cdot} \quad (3)$$

$$C_6H_5^{+} \longrightarrow C_4H_3^{+\cdot} + C_2H_2 \quad (4)$$

It is proposed that in the present work that acetylene and 1,3-butadiene are formed by the dissociation of this linear $C_6H_6^{+\cdot}$ ion. Reaction (2), being a one step dissociation, is more likely to occur in the discharge. The C_4 fragments could conceivably react as follows,

$$C_4H_4^{+\cdot} + H_2 + e \longrightarrow C_4H_6 \quad (5)$$

to give 1,3-butadiene. From the experimental results, at low flow rates the conversion to acetylene was much greater than possible from reaction (2). Therefore further dissociation of the $C_4H_4^{+\cdot}$ must take place,

$$C_4H_4^{+\cdot} + e \longrightarrow C_2H_2 + C_2H_2 \quad (6)$$

to give two further molecules of acetylene.

With nickel wire present in the discharge the yield of acetylene was reduced. It is suggested that this is partly

explained by the catalysis of reaction (5) which prevents further dissociation of the $C_4H_4^+$ ion. Nickel also catalyzes the reaction,

$$H^{\cdot} + H^{\cdot} \longrightarrow H_2$$

which ensures the supply of hydrogen necessary for reaction (5). However the total yield of 1,3-butadiene and the C_4 components of phenylbutadiene and naphthalene was also reduced. This indicated stabilization of the primary ion of the discharge, i.e. the $C_6H_6^+$. Hence the nickel has increased the possible selectivity of reactions in the benzene discharge.

Allene was produced in constant conversion, over the range of conditions used, with or without nickel wire in the discharge. It was proposed that the production of allene or its precursor was derived from a different excited state of the benzene than that leading to the reactions discussed above. This excited state was possibly produced by the impact of an electron of energy above the mean, i.e. the excited state was only found for a narrow band of electron energies. The yield of allene was thus controlled by the number of electrons of the right energy in the discharge rather than by any chemical parameter. Ottinger[134] has found evidence for the dissociation,

$$C_6H_6^+ \longrightarrow C_3H_3^+ + C_3H_3^{\cdot} \qquad (7)$$

both of which fragments could proceed to allene.

10.5.1. Interpretation of Results : the High Boilers

The precursors of diphenyl may be excited molecules of benzene which dissociate to give phenyl radicals. The excited benzene molecules could be formed directly or through the benzene ion $C_6H_6^{\ddagger}$ by electron capture. The latter is unlikely as the $C_6H_6^{\ddagger}$ ring structure isomerizes to an open-chain, see reaction (1). Thus, diphenyl and higher polybenzenes would seem to be almost exclusively produced by the dissociation of the excited benzene molecules to phenyl radicals which then undergo subsequent reactions with other benzene molecules. This would also explain the pressure dependence of the diphenyl yield. As the reactor pressure is increased, collisional deactivation of the excited benzene molecules becomes important resulting in a decrease in the concentration of phenyl radicals.

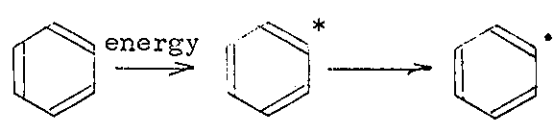

(8)

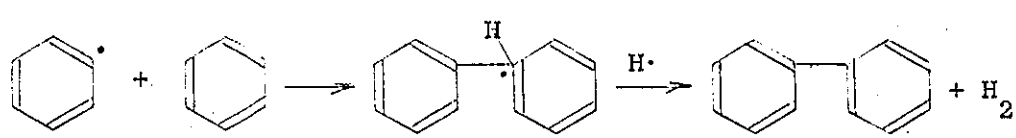

(9)

The diphenyl may then undergo further attack by phenyl radicals to give polybenzenes.

The benzene molecule could also be attacked by other highly active species in the discharge. The attack on benzene of the $C_4H_4^{\ddagger}$ fragment may explain the formation of phenylbutadiene and naphthalene, e.g.

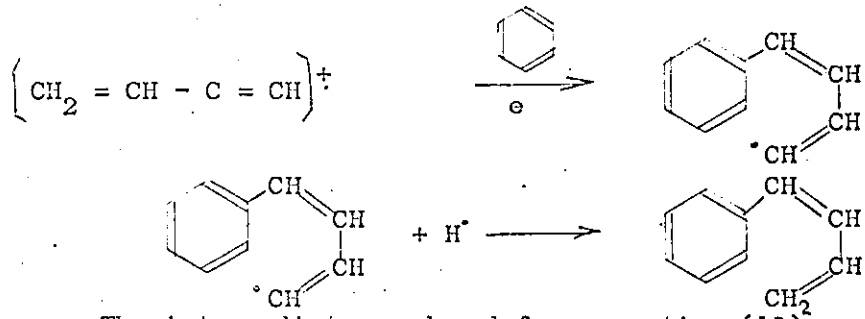

(10)

(11)

The intermediate produced from reaction (10) could undergo an internal rearrangement to give naphthalene.

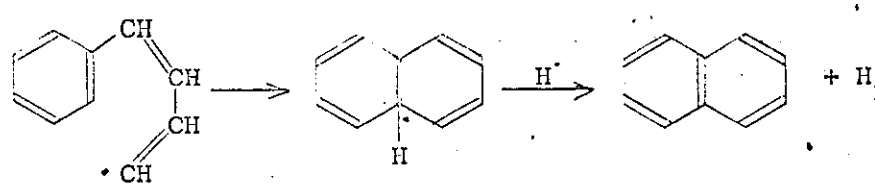

(12)

In the presence of nickel wire in the discharge the conversions to diphenyl, naphthalene and phenylbutadiene were doubled. It is suggested that the nickel catalyzed the reactions involving phenyl radicals, such as reaction (9) and also promoted the attack of $C_4H_4^{+\cdot}$ on benzene molecules, see reaction (10). The rapid removal of phenyl radicals from the discharge would decrease the amount of long-chain polybenzenes formed but increase the amount of short chain compounds, i.e. diphenyl. This was borne out by the experimental results. The catalysis of reaction (10) should increase the yield of naphthalene and phenylbutadiene; again confirmed by the experimental results.

A comparison of the curves for total benzene decomposition against flow rate of the benzene and benzene/nickel discharges indicates the nickel only slightly reduced the overall decomposition. The major effect of the nickel, therefore, was to alter the distribution of the products thus indicating a degree of selectivity.

A reaction scheme can be built up to show the formation of the products obtained from the microwave discharge in benzene vapour, with or without nickel present:-

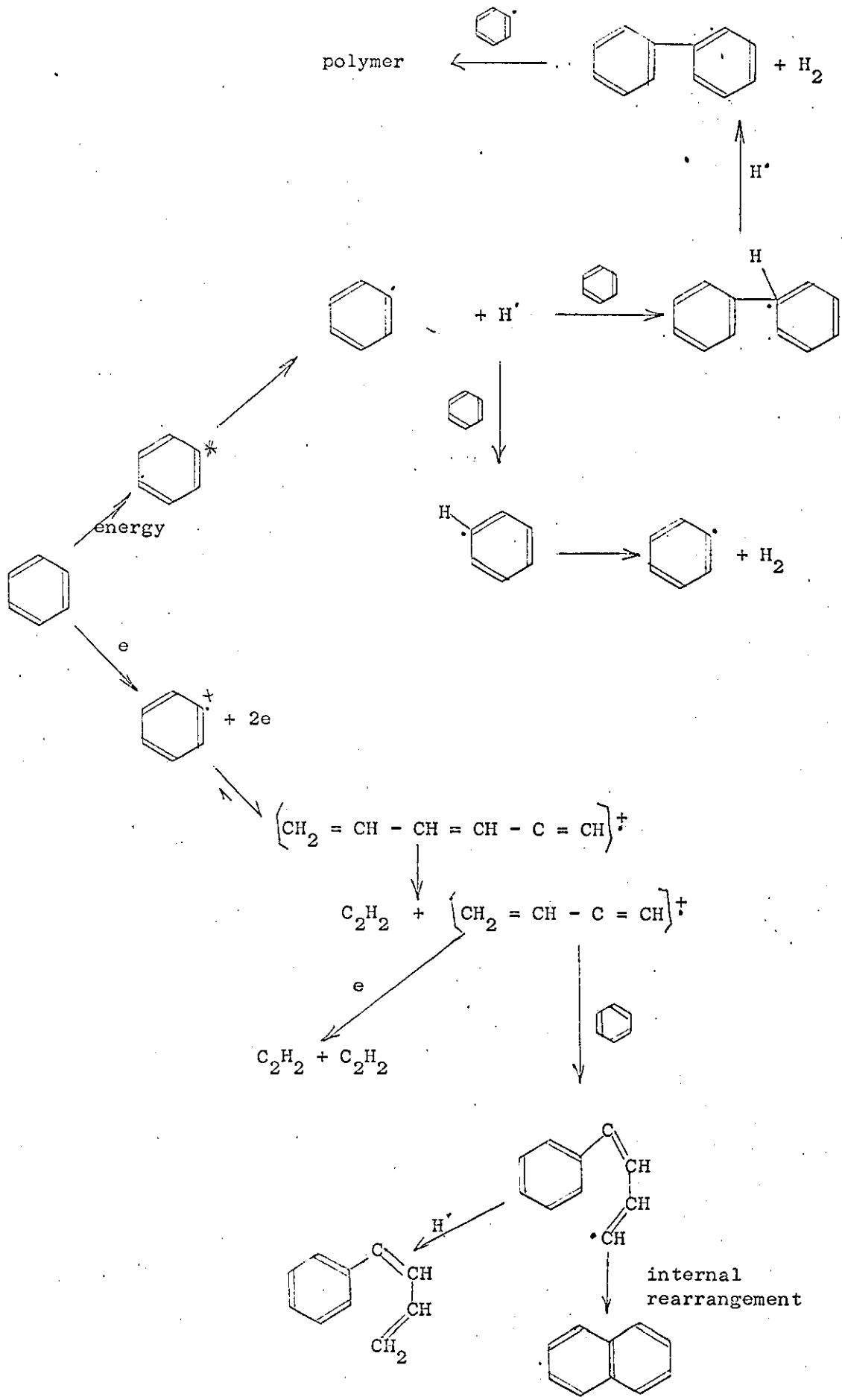
polymer
+ H_2
H·
H
+ H·
energy
*
H
+ H_2
e
+ 2e
$\{CH_2 = CH - CH = CH - C = CH\}^{+\cdot}$
C_2H_2 + $\{CH_2 = CH - C = CH\}^{+\cdot}$
e
C_2H_2 + C_2H_2
H·
internal
rearrangement

10.6. Reaction Profiles of the Volatile Products

From Figs.38a and 38b the reaction profiles indicate acetylene was the end-product of a series reaction,

$$A \longrightarrow R \longrightarrow S$$

see appendix A. This is in agreement with the proposed reaction mechanism for the production of acetylene from benzene, i.e.,

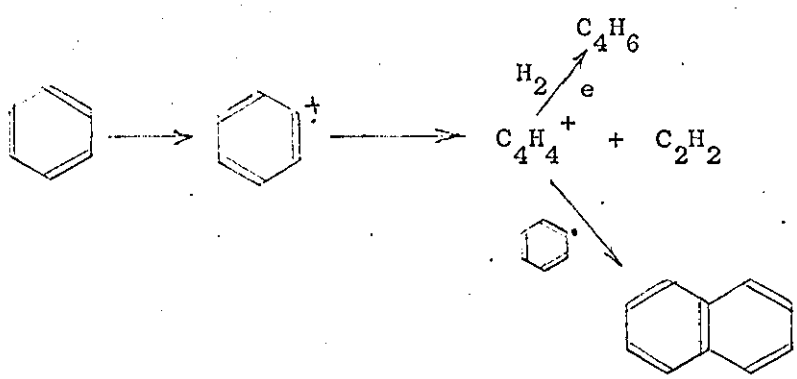

The mechanism also suggests that the conversion to 1,3-butadiene and naphthalene should pass through a maximum, i.e. they act as tracers for the disappearance of the intermediate $C_4H_4^+$. Again this is in agreement with the experimental results, see Figs. 39a and 39b.

10.7. Hydrogen Balance

A hydrogen balance between the amount of benzene decomposed and the products formed proved to be difficult. This was mainly due to the difficulties of estimating the carbon and polybenzene formation both of which produce hydrogen. Estimates of the combined carbon and polymer formation were made, gravimetrically. Difficulties arose in that at a constant benzene flow, increasing the pressure increased the carbon formation. Therefore exact estimates

of the proportion of carbon to polymer were not possible.

Free hydrogen was found in all cases, with or without nickel wire in the discharge, see Fig. 44ab.

At high flow rates $>$ 0.10 moles/min and low pressure the carbon formation was negligible though polybenzenes were still formed. Calculations based on the hydrogen demand of the identifiable products such as naphthalene, 1,3-butadiene etc. allowed estimates to be made of the amount of polybenzene formed; approximately constant at 0.5%. This agreed well with the gravimetric estimates.

From a knowledge of the hydrogen content of the volatile products and the amount of free hydrogen compared with the hydrogen content of the decomposed benzene estimates were made of the carbon and polybenzene yields over the flow range 0.01 to 0.03 moles/min at a constant pressure. Maximum conversions of the benzene input to carbon and polymer of about 7% were found, see Fig.45a. These results were again in good agreement with previous gravimetric estimates.

In the presence of nickel wire in the discharge, the yields of carbon and polymer were reduced, see Fig. 45b. The conversions to carbon and polymer were calculated from the hydrogen balance between the benzene decomposed and the volatile products.

10.8. Benzene and Carbon Dioxide

10.8.1. Discussion of Results

Scouting experiments with benzene and carbon dioxide had shown that if the mole ratio of carbon dioxide to

benzene was greater than 1.5:1, the decomposition of benzene was negligible.

In discharges of carbon dioxide and benzene, 0.5:1 mole ratio the conversion of benzene to the low boiling gaseous products was reduced by about one quarter compared with that from pure benzene, see Figs. 52 and 53. However the conversion to the low boiling hydrocarbons was dependent on pressure in contrast with the results obtained for pure benzene and benzene with nickel discharges.

The yields of diphenyl, naphthalene and phenylbutadiene were also slightly reduced compared with those from the pure benzene system, see Figs. 55 and 56.

At a mole ratio of carbon dioxide to benzene of 1.2:1 the conversion to the low boilers was reduced further. The conversion, as for the other mole ratios tried, was dependent on pressure; increasing pressure reduced the conversion to low boilers to negligible proportions. The conversion to diphenyl, naphthalene, phenylbutadiene was negligible. Carbon and polybenzene formation was also negligible.

A hydrogen balance could not be calculated as the carbon dioxide interfered with the free hydrogen in the G.L.C. analysis.

10.8.2. Interpretation of Results

At the various mole ratios of carbon dioxide to benzene tried, the decomposition of the benzene was always less than in a pure benzene discharge, see Figs. 54 and 57. The reduction in decomposition was regarded as being far in

excess of that to be expected from dilution of the benzene in the discharge. This indicated that in some way the carbon dioxide was protecting the benzene molecules.

Analysis of the products of the discharges had not shown the presence of any oxygen-containing ~~compounds~~ products. The dissociation of the carbon dioxide must therefore be a minor process.

The first ionization potential of benzene is 9.6 eV and that of carbon dioxide is 13.8 eV. However carbon dioxide has several broad bands of excitation levels ranging over 6.5 - 12 eV, peaking at 10 eV. A carbon dioxide molecule could therefore deactivate excited benzene molecules without an ionizing event occurring. If the carbon dioxide molecules were acting as an energy sink, the decomposition of benzene should decrease with increasing dilution of the benzene. Secondly, an increase in collision frequency, by increasing the pressure, should also decrease the benzene decomposition. These requirements were confirmed by the experimental results obtained, see Fig.54. Therefore deactivation of the benzene molecules by collision with carbon dioxide molecules is possibly the mechanism by which the benzene is preserved.

A likely alternative process is the scavenging of electron energy by the excitation of the carbon dioxide molecule in the region 6.5 - 10 eV. This would effectively prevent the build up of electrons of sufficient energy to ionize the benzene molecule. This scavenging process would be even more effective as the pressure was increased, or if the mole ratio of carbon dioxide to benzene was increased.

The experimental results confirm the above hypothesis, i.e. the pressure dependence of the benzene conversion to the low boilers and a decrease in the benzene decomposition as the mole ratio of carbon dioxide to benzene was increased.

10.9. Benzene and Ammonia

10.9.1. Discussion of Results

In the microwave discharge of mixtures of benzene and ammonia, scouting experiments had shown evidence of the formation of a purple coloured solid in the cold trap. Further investigation was directed towards obtaining the maximum yield of this solid.

A benzene to ammonia mole ratio of 1:2 was used, viz scouting experiments. The conversion of benzene to this solid was plotted against flow rate. The plot showed a sharp maximum, see Fig.59.The conversion was dependent on pressure. A maximum conversion of about 5% of the benzene passed was obtained. The conversions of benzene to acetylene and 1,3-butadiene were low. A quantitative estimate of the acetylene yield was not possible owing to interference of the ammonia in the G.L.C. analysis. The conversion to 1,3-butadiene was $\leq$ 0.5% of the benzene passed. Yields of the high boilers such as diphenyl, naphthalene etc. were negligible.

Experiments were also carried out with discharges in varying mole ratios of ammonia to benzene. At a constant benzene flow rate, the conversion of benzene to the solid plotted against the mole ratio of ammonia to benzene showed a flattened maximum at the ratio 8:1 respectively.

Elemental analysis of solids obtained at different mole ratios indicated that a range of products was present. The nitrogen content of the solid ranged from 9.5% to 26% by weight depending on the mole ratio of ammonia to benzene supplied to the reactor, see Table 13. At room temperature the solid was a very dark orange-brown colour. All the samples were slightly soluble in benzene, completely soluble in acetone and also partially soluble in water. This indicated a degree of polarity in the molecule(s). The solids melted with decomposition at 180°C ± 20°C. A molecular weight of about 250 was obtained by a vapour pressure determination.

Spectroscopic analysis of the solid samples was undertaken. Infra-red analysis showed the normal aromatic absorption and also absorption at ~ 1620 cm^{-1} and ~ 3,300 cm^{-1} indicative of the presence of $-NH_2$. Ultra-violet spectroscopy showed maximum absorption at ~ 300 mμ decreasing steadily to 360 mμ indicating a great deal of conjugation. Some vibrational fine structure was apparent. Absorption peaks at ~ 540 mμ and ~570 mμ were noted in the visible region, see Fig. 63.

A mass spectrum of the solid showed a range of products was present and confirmed the presence of nitrogen in the molecular structure. An azo linkage was also indicated.

10.9.2. Interpretation of Results : Benzene and Ammonia

The conversion of benzene to acetylene and 1,3-butadiene was estimated at less than 5% of benzene converted, over the range of conditions used, at a mole ratio of ammonia to benzene of 2:1. Yields of diphenyl, naphthalene etc. were negligible. This indicated a similarity to the

benzene and carbon dioxide system. However the dissociation energy for ammonia to give $-NH_2$ radicals is only 3.8 eV and to -NH radicals 8.0 eV, less than that for ionization of benzene. It was concluded therefore that the primary dissociation reactions occurring in the discharge were those of ammonia alone. The radicals produced from the dissociation of ammonia then attacked the benzene molecules. This would explain the absence of the usual products of the benzene discharge.

From the spectroscopic data and the molecular weight determination, it was proposed that the coloured solids were derivatives of azobenzene. The infra-red spectra showed the presence of $-NH_2$ groups. Using the data from the elemental analyses, the coloured solids were suggested as being amino-substituted azobenzenes, with the number of amino groups varying between two and six, e.g.

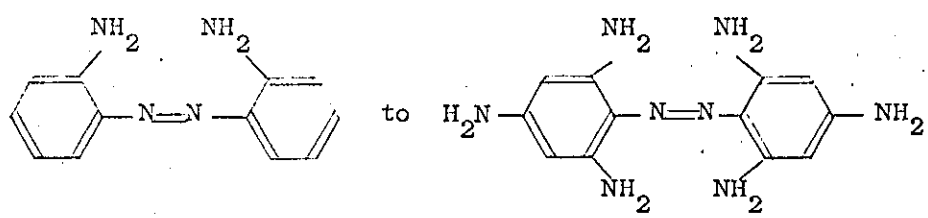

The above compounds are similar to various dyes obtained by conventional chemical techniques. For instance Aniline Yellow which is aminoazobenzene and Bismarck Brown G, which is a trisubstituted amino-azobenzene. Chrysoidine G,

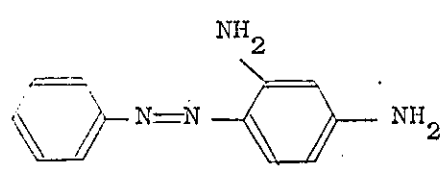

is an orange dye and is still in use today[135].

The previous investigation of the microwave discharge in pure ammonia indicated that the predominant radical species was NH, see section

$$NH_3 + \text{energy} \longrightarrow (NH_3)^* \longrightarrow \dot{N}H_2 + \dot{H}$$

$$\dot{N}H_2 + \text{energy} \longrightarrow (\dot{N}H_2) \longrightarrow \ddot{N}H + \dot{H}$$

A combination of the two radicals,

$$\ddot{N}H + \dot{N}H_2 \longrightarrow N_2H_3^{\cdot}$$

would give the hydrazo radical, a possible precursor to the azo-linkage. However evidence for this reaction has not been reported in the literature. Another possibility is the combination of NH radicals[117] to give a highly excited species $(N_2H_2)^*$ capable of attacking the benzene ring. A mechanism for the formation of azo-benzene can now be proposed,

$$NH_3 + \text{energy} \longrightarrow (NH_3)^* \longrightarrow \ddot{N}H$$

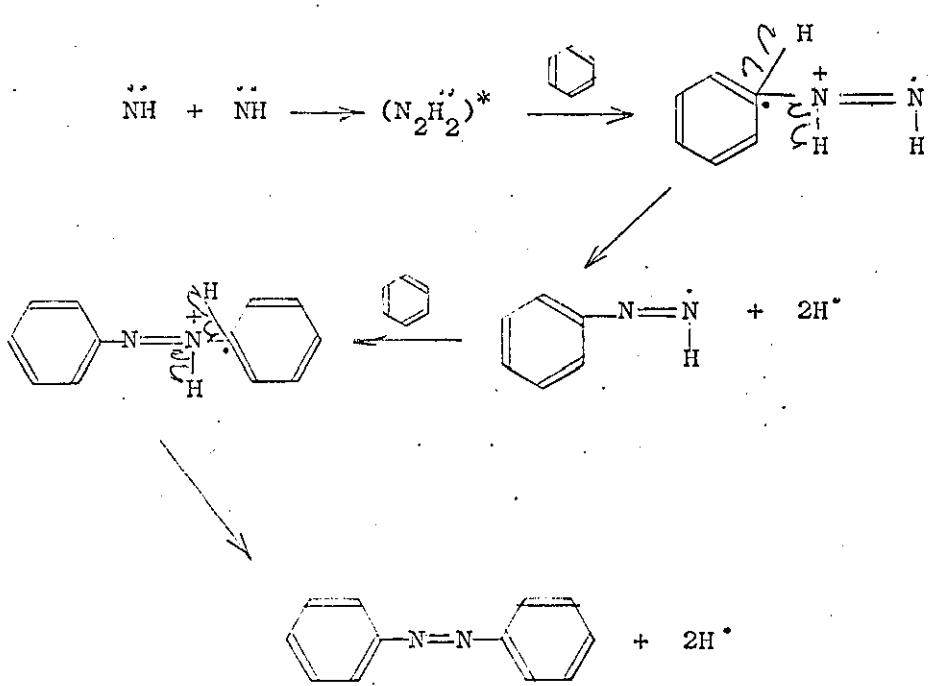

NH_2 groups are indicated by the infra-red spectra of the solids. These could conceivably arise from the attack of NH_2 radicals.

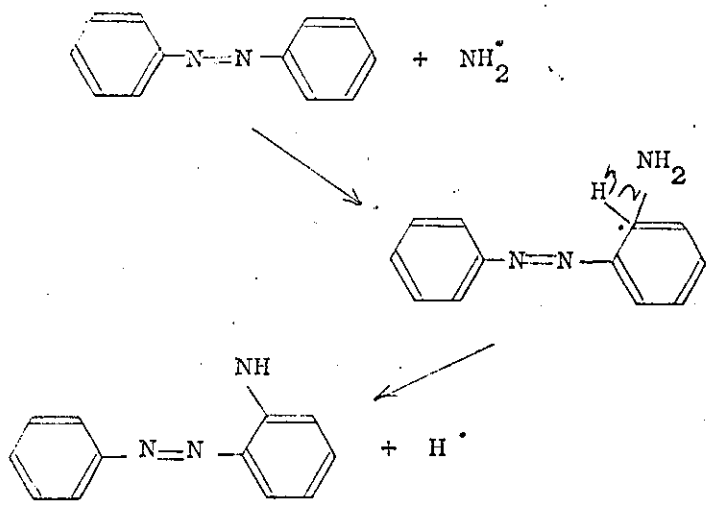

or more probably by the attack of NH radicals and subsequent hydrogenation of the NH group.

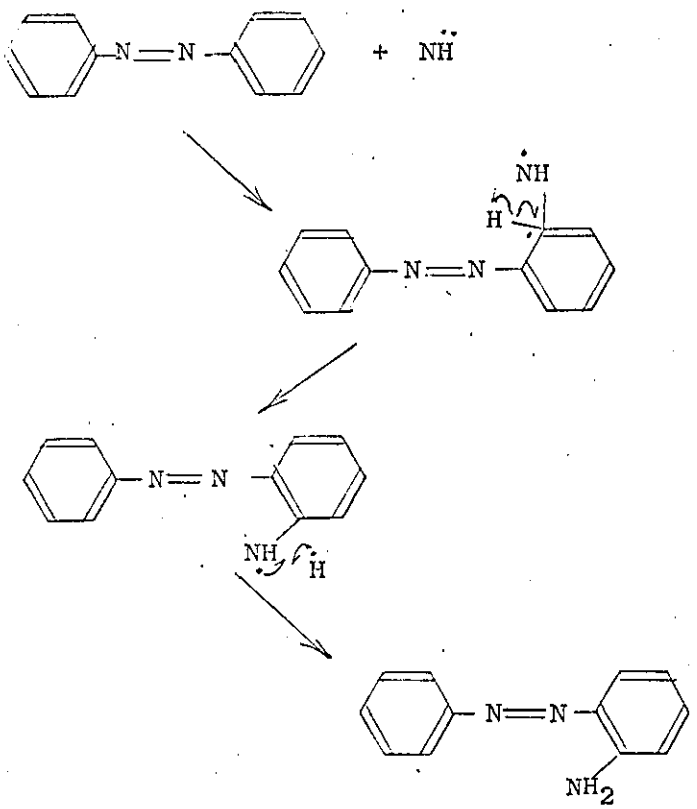

It should be noted that the solid was only found in the cold trap. This indicated the final reaction sequence must have occurred in the cold trap. Some long-lived

species, i.e. lifetime 0.1 sec. must therefore have been present in the discharge product stream. The azo-substituted benzene intermediate may possibly exist for that length of time. These species could then react with benzene in the cold trap to give the azobenzene derivatives.

10.10. General Observations : Benzene Studies

The mechanisms presented for the reactions of benzene in the microwave discharge are in good agreement with the experimental results. For instance, in the discharge in benzene with nickel present, the conversion of benzene to the low boilers was reduced. The effect was postulated as being due to the stabilisation of the benzene ion. Thus the percentage distribution of the low boilers should not alter. This is confirmed by the experimental results, see Fig. 47a,b.

10.10.1. Energy Yields

The energy yield of a product is the parameter most widely quoted when considering the economics of a process. Energy yields for the production of acetylene, diphenyl and the azobenzene derivatives are shown in Figs. 48, 49 and 64. In this case the energy yield is calculated on the basis of a kilowatt-hour supplied to the microwave generator. The efficiency of a magnetron is about 50% and this is not likely to be improved in the near future. The absorption of the microwaves is only about 25% in the present system. This is due mainly to the high minimum power output of the magnetron. However the absorption may be increased up to 80% under optimum conditions of flow rate power input and pressure. Thus the energy yields quoted may be quite easily trebled. The energy yield of the derivatives of azobenzene would then be commercially very attractive.

10.10.2. Conclusions

The experimental results from discharges in pure benzene agree fairly well with the results of other workers[83-86], in several respects. Diphenyl and naphthalene were found and the conversion to these was pressure dependent. Acetylene and allene were also found; in agreement with Stille et al[83] who used an r.f. discharge. However there is no precedent in the literature for the formation and identification of 1,3-butadiene; a necessary precursor for the production of naphthalene reported by several workers[86,91].

Several investigations[83,86,91] into the reactions of benzene in various types of discharges have reported the presence of methyl substituted molecules such as toluene, methylacetylene, methylnaphthalene etc. Jennings[136] suggested that CH_3^+ could be formed from the dissociation of doubly charged benzene ions. He found evidence for the process,

$$C_6H_6^{2+} \longrightarrow CH_3^+ + C_5H_3^+$$

Methyl-substituted molecules were not found in the present work. Therefore it was concluded that the doubly-charged benzene ion did not occur in the microwave discharge, under the experimental conditions used. This would seem to indicate a difference in electron energy distribution attained in the microwave discharge as opposed to other forms of discharges.

The present author found that in the presence of nickel wire the yield of diphenyl doubled. This indicated the preservation of the phenyl radical. It suggests a

degree of selectivity is obtainable in the microwave discharge. The benzene molecule was also protected by the presence of carbon dioxide in the discharge.

It is perhaps the microwave discharge in benzene and ammonia mixtures that aroused the most interest. The possible formation of a single basic product suggested a selectivity unparalleled in other discharge work. The production of the NH radical proposed as necessary for the formation of the product is indicative of electrons of a higher mean energy than that found in other discharges. However the absence of doubly-charged ions in the microwave suggests that although the mean electron energy may be higher, the distribution of energies is narrower than say a d.c. glow discharge.

It is concluded therefore that the microwave discharge has a narrower and higher band of electron energies than normally found in electric discharges. It is this narrow distribution of electron energies that enhances the selectivity of reactions in the microwave discharge.

EXPERIMENTAL DATA :

BENZENE STUDIES

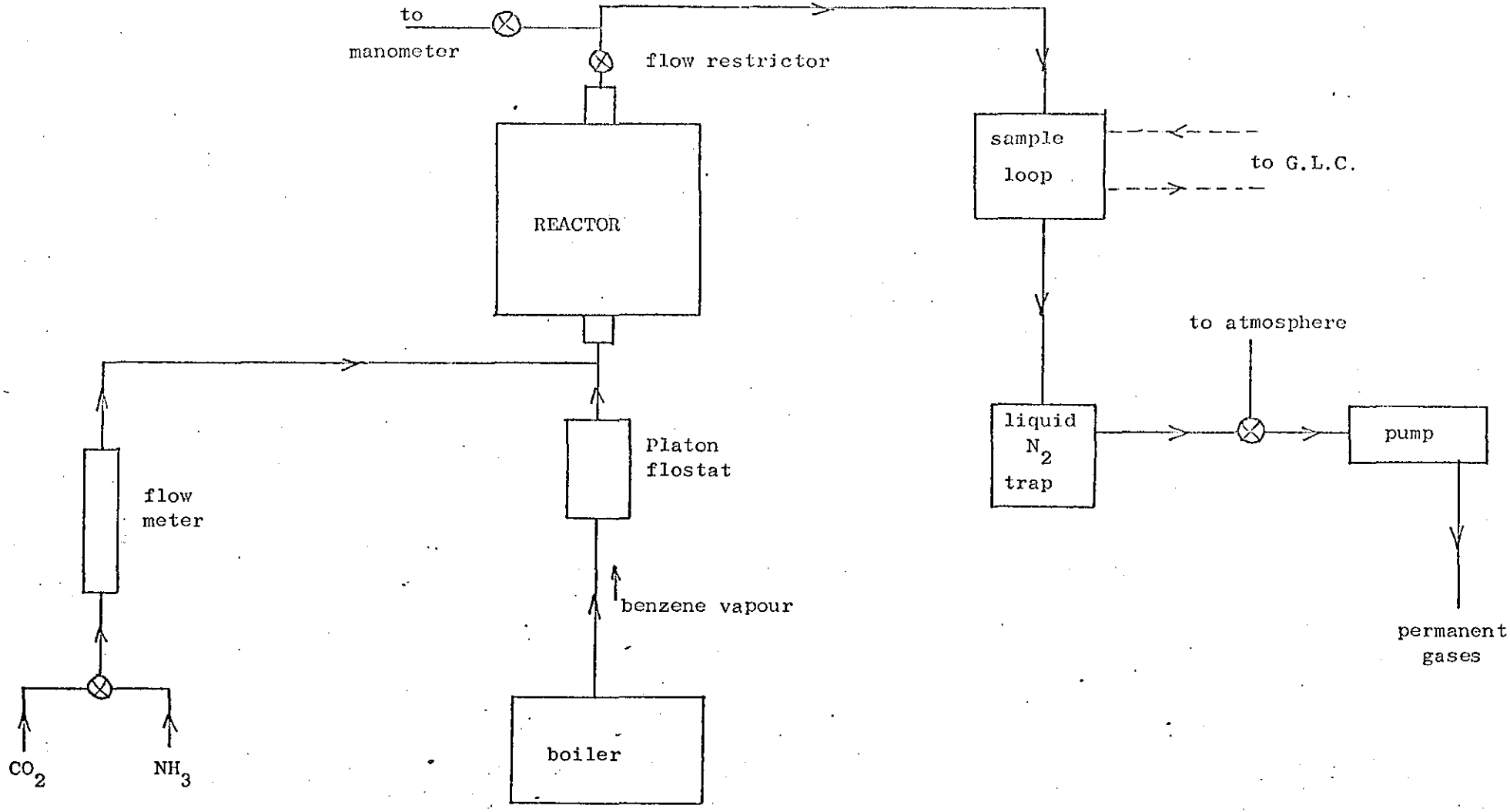

Figure 36 Flow System for the Study of the Reactions of Benzene in the Microwave Discharge.

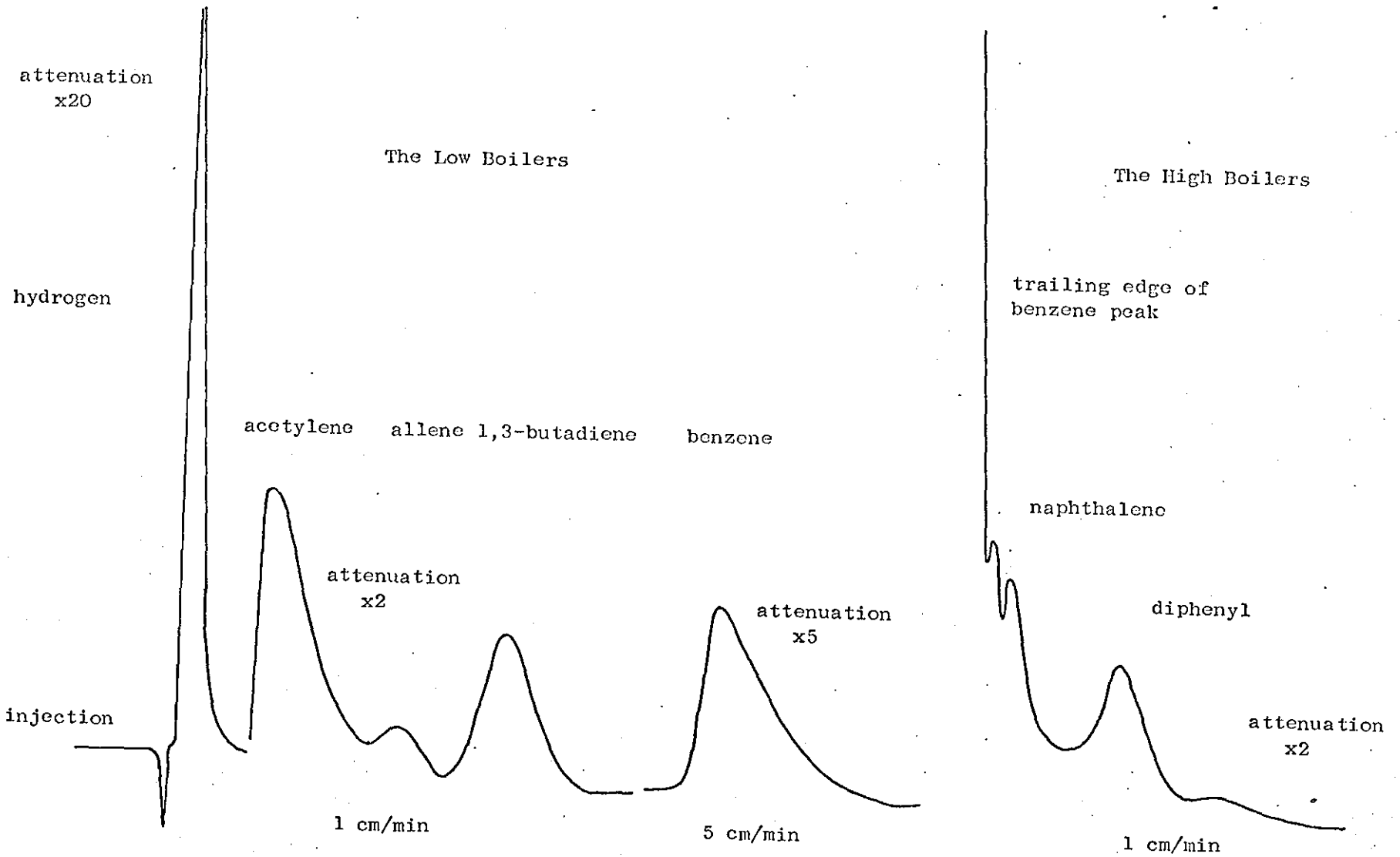

Figure 37 Typical Example of the G.L.C. Analysis of the Discharge Products.

Table Ca Benzene Alone : the Low Boilers

power input 0.78 Kw reactor pressure 10 - 20 mm Hg

benzene flow rate, moles/min.	reactor pressure mm Hg	power absorption Kw	% conversion to acetylene	% conversion to allene	% conversion to 1,3-butadiene
0.0095	15	0.23	47.50	2.30	9.60
0.0146	10	0.23	31.70	1.60	18.48
0.0198	12	0.24	17.50	2.90	29.46
0.0252	10	0.24	10.52	1.30	19.85
0.0288	12	0.24	14.70	1.00	24.80
0.0289	14	0.24	10.35	2.10	23.60
0.0328	11	0.22	6.44	1.10	12.48
0.0402	19	0.22	7.60	1.55	8.35
0.0499	12	0.22	4.90	0.90	5.20
0.0725	14	0.21	2.10	0.70	1.00
0.0880	15	0.20	1.80	0.50	0.55
0.102	16	0.19	2.48	0.78	0.43

Key

In the Figures representing the conversions of benzene to the discharge products, different symbols are used to denote a pressure range from which the experimental points were obtained, i.e.

10 - 20 mm Hg

20 - 30 mm Hg

30 - 50 mm Hg

unless the pressure range is stated on the figure.

Table 6b Benzene Alone : the Low Boilers

power input 0.78 Kw reactor pressure 20 - 30 mm Hg

benzene flow rate, moles/min.	reactor pressure mm Hg	power absorption Kw	% conversion to acetylene	% conversion to allene	% conversion to 1,3-butadiene
0.0113	25	0.24	39.50	2.10	11.40
0.0271	27	0.24	18.10	1.77	21.80
0.0415	23	0.25	7.63	2.15	7.98
0.0513	23	0.23	4.40	1.65	7.20
0.0753	25	0.23	2.30	0.84	0.50
		reactor pressure 30 - 50 mm Hg			
0.0091	49	0.25	57.80	2.30	12.10
0.0129	45	0.25	23.50	1.00	25.60
0.0226	38	0.25	15.30	1.80	25.10
0.0795	40	0.24	2.51	1.53	0.40

Table 7 Benzene Alone : the High Boilers

power input 0.78 Kw reactor pressure 10 - 20 mm Hg

benzene flow rate, moles/min.	reactor pressure, mm Hg	power absorption Kw	% conversion to naphthalene	% conversion to diphenyl
0.0144	12	0.25	0.49	2.04
0.0158	11	0.25	0.60	1.92
0.0178	11	0.25	0.79	2.45
0.0190	12	0.25	0.48	2.22
0.0378	12	0.21	0.68	2.28
0.0486	12	0.25	0.73	2.02
0.0572	13	0.22	0.98	1.93
0.0621	13	0.21	0.45	2.05
0.0658	12	0.20	0.35	1.95
0.0701	13	0.21	0.35	1.67
0.0930	13	0.20	0.04	1.25
		reactor pressure 20 - 30 mm Hg		
0.0615	21	0.23	0.24	1.20
0.0632	21	0.22	0.15	1.18
0.0776	28	0.24	0	0.34
0.0879	20	0.20	0.24	0.77

Table 8 Benzene and Nickel : the Low Boilers

power input 0.78 Kw reactor pressure 10 - 20 mm Hg

benzene flow rate, moles/min.	reactor pressure mm Hg	power absorption Kw	% conversion to acetylene	% conversion to allene	% conversion to 1,3-butadiene
0.0149	14	0.24	32.80	2.80	18.90
0.0207	10	0.24	14.50	2.55	18.60
0.0313	10	0.23	6.40	1.90	12.70
0.0368	11	0.23	4.66	1.00	9.37
0.0552	11	0.22	4.80	1.30	7.32
0.0998	13	0.21	2.90	0.67	2.30
		reactor pressure 20 - 30 mm Hg			
0.0257	25	0.25	11.40	1.82	13.80
0.0474	28	0.24	6.30	1.15	2.30
0.120	24	0.22	1.74	0	trace
0.159	25	0.22	0.83	0	trace
		reactor pressure 30 - 50 mm Hg			
0.0127	37	0.25	46.80	3.60	17.00
0.0195	42	0.26	26.50	2.80	21.00
0.0372	37	0.24	6.30	2.00	7.10
0.189	35	0.23	1.65	0	trace

Table 9 Benzene + Nickel : the High Boilers

power input 0.78 Kw reactor pressure 10 - 20 mm Hg

benzene flow rate, moles/min.	reactor pressure, mm Hg	power absorption Kw	% conversion to naphthalene	% conversion to diphenyl
0.0098	15	0.25	0.89	1.72
0.0146	15	0.23	1.23	3.30
0.0270	15	0.21	1.82	4.77
0.0395	16	0.22	1.61	3.75
0.0442	16	0.21	1.32	3.90
0.0537	16	0.22	1.25	3.43
0.0592	18	0.22	0.83	2.93
0.0640	16	0.20	0.78	3.03
0.0644	18	0.25	0.98	2.62
0.0647	12	0.20	0.49	2.66
0.0654	17	0.24	0.53	2.68
0.0735	19	0.23	0.35	2.13
		reactor pressure 20 - 30 mm Hg		
0.0550	28	0.25	0.13	0.97
0.0622	22	0.22	0.23	1.87
0.0624	22	0.23	0.30	1.93
		reactor pressure 30 - 50 mm Hg		
0.0572	32	0.23	0	0.19
0.0667	35	0.23	0	0.28

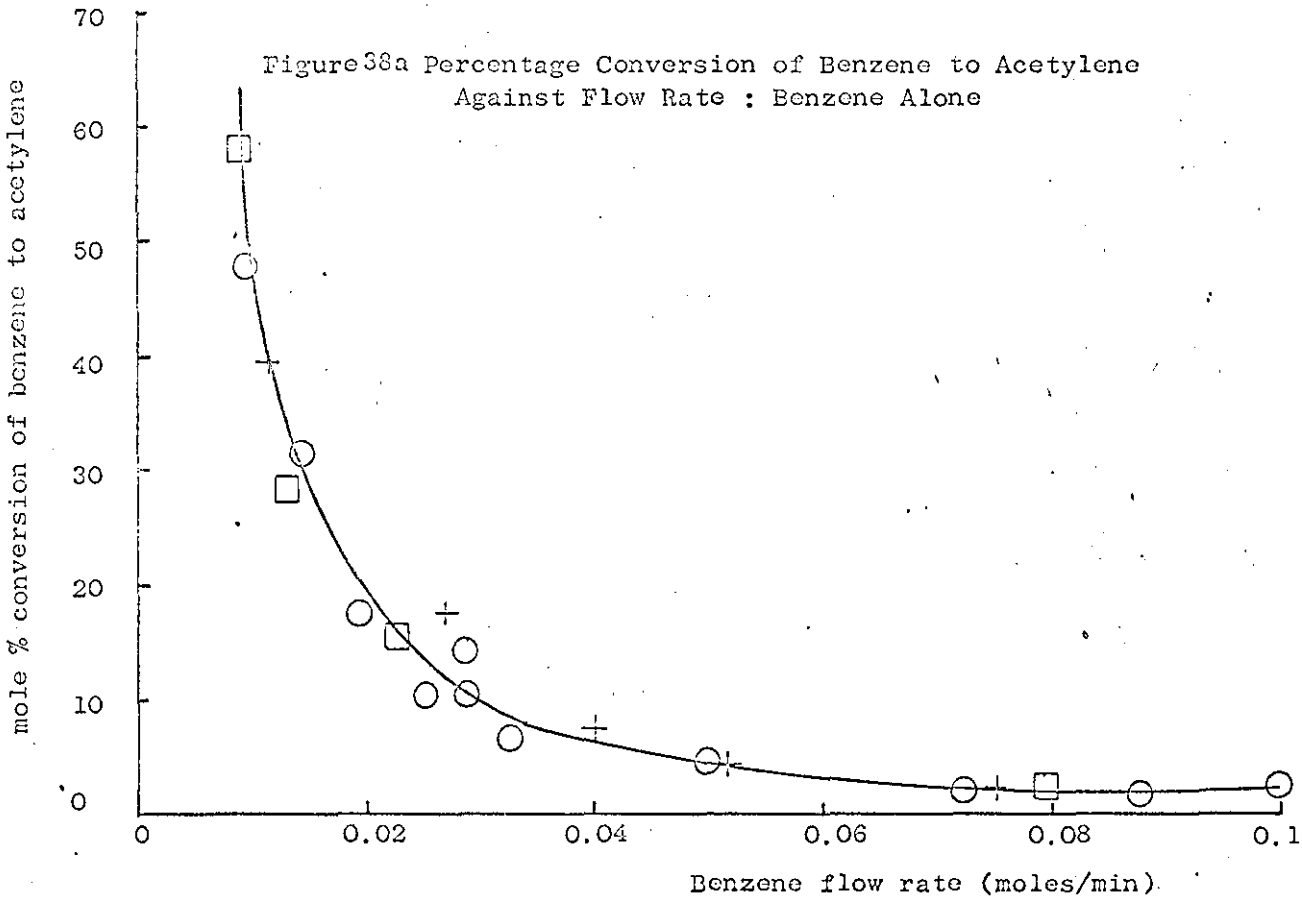

Figure 38a Percentage Conversion of Benzene to Acetylene Against Flow Rate : Benzene Alone

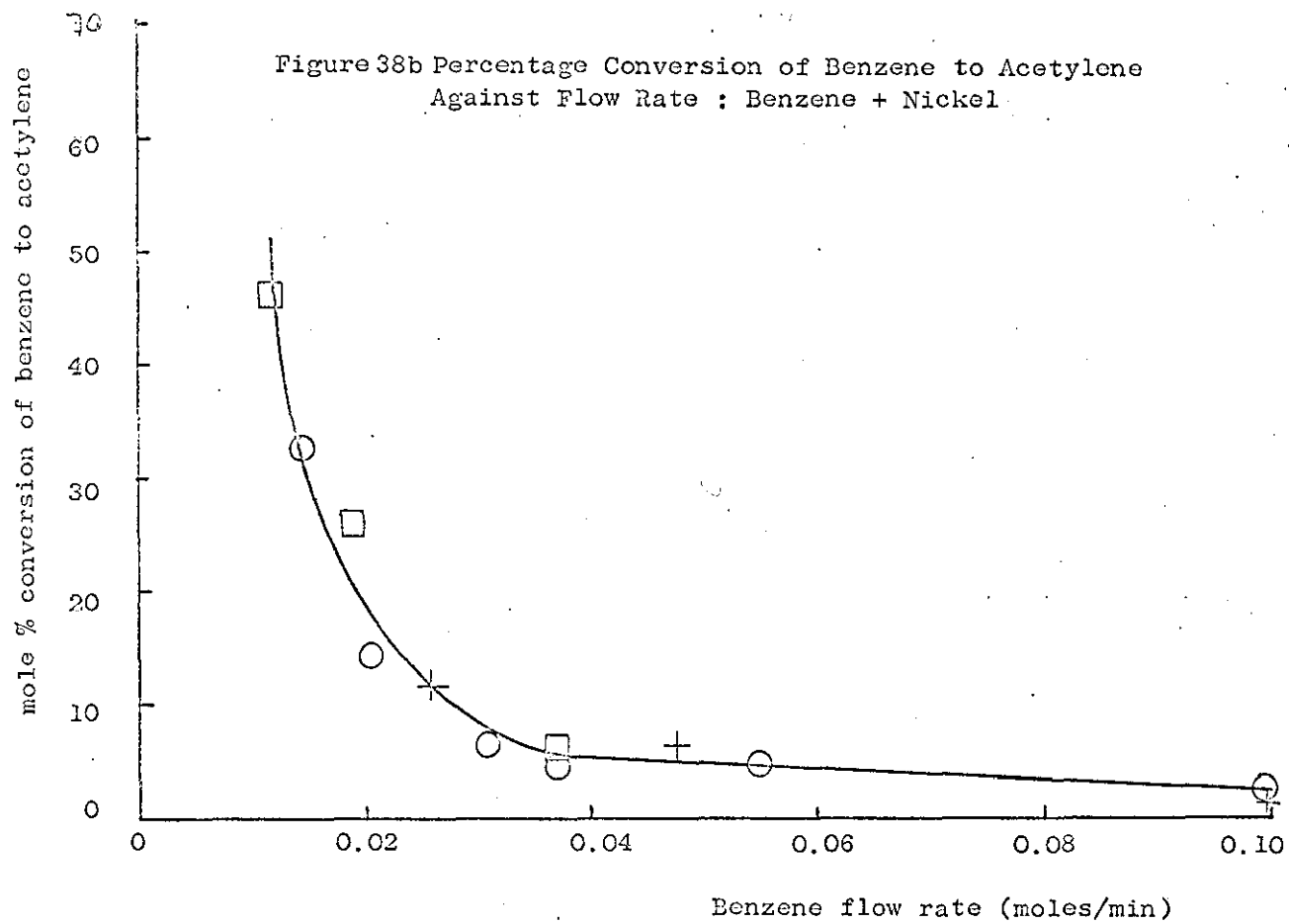

Figure 38b Percentage Conversion of Benzene to Acetylene Against Flow Rate : Benzene + Nickel

Figure 39a Percentage Conversion of Benzene to 1,3-butadiene Against Flow Rate : Benzene Alone

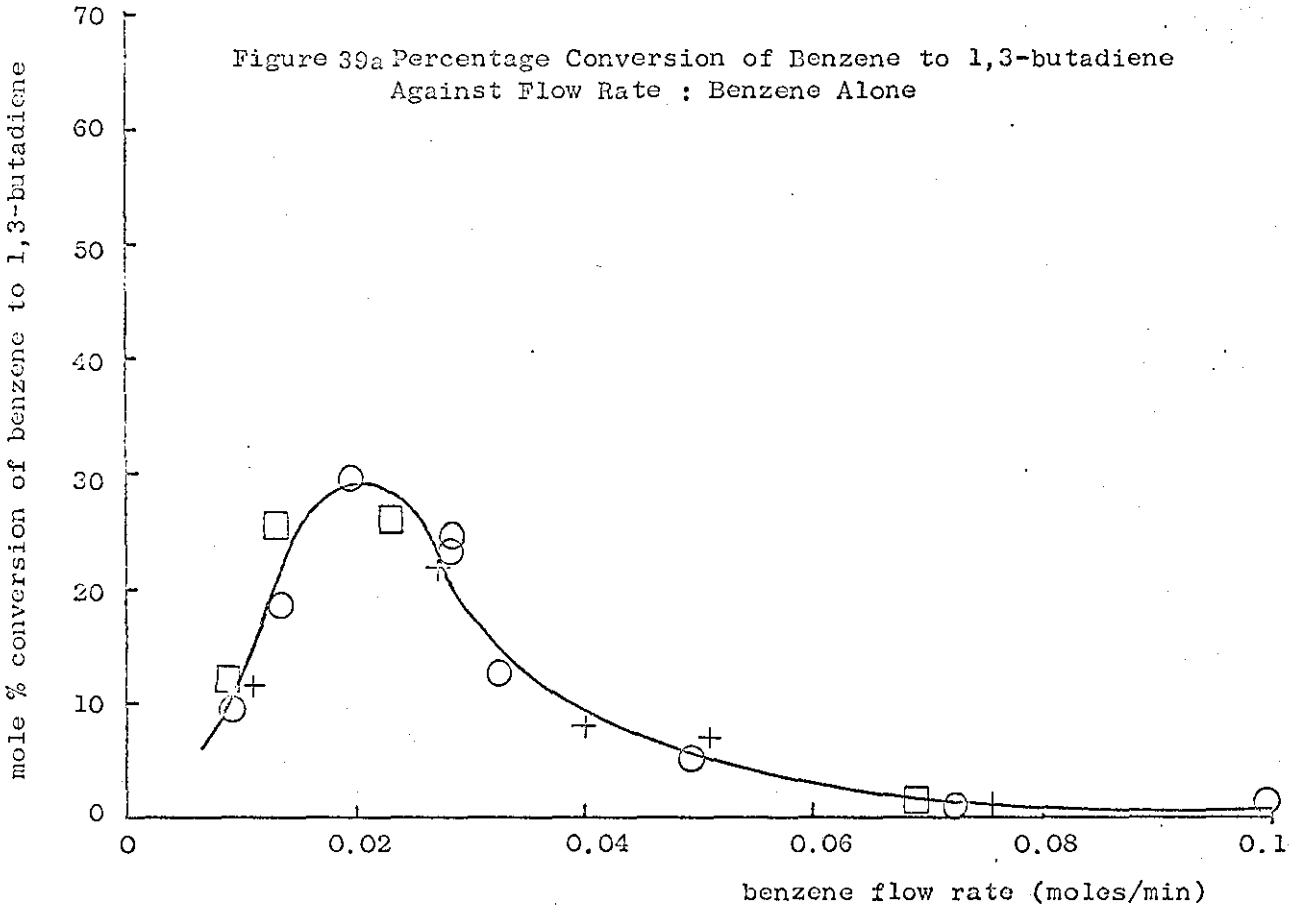

Figure 39b Percentage Conversion of Benzene to 1,3-butadiene Against Flow Rate : Benzene + Nickel

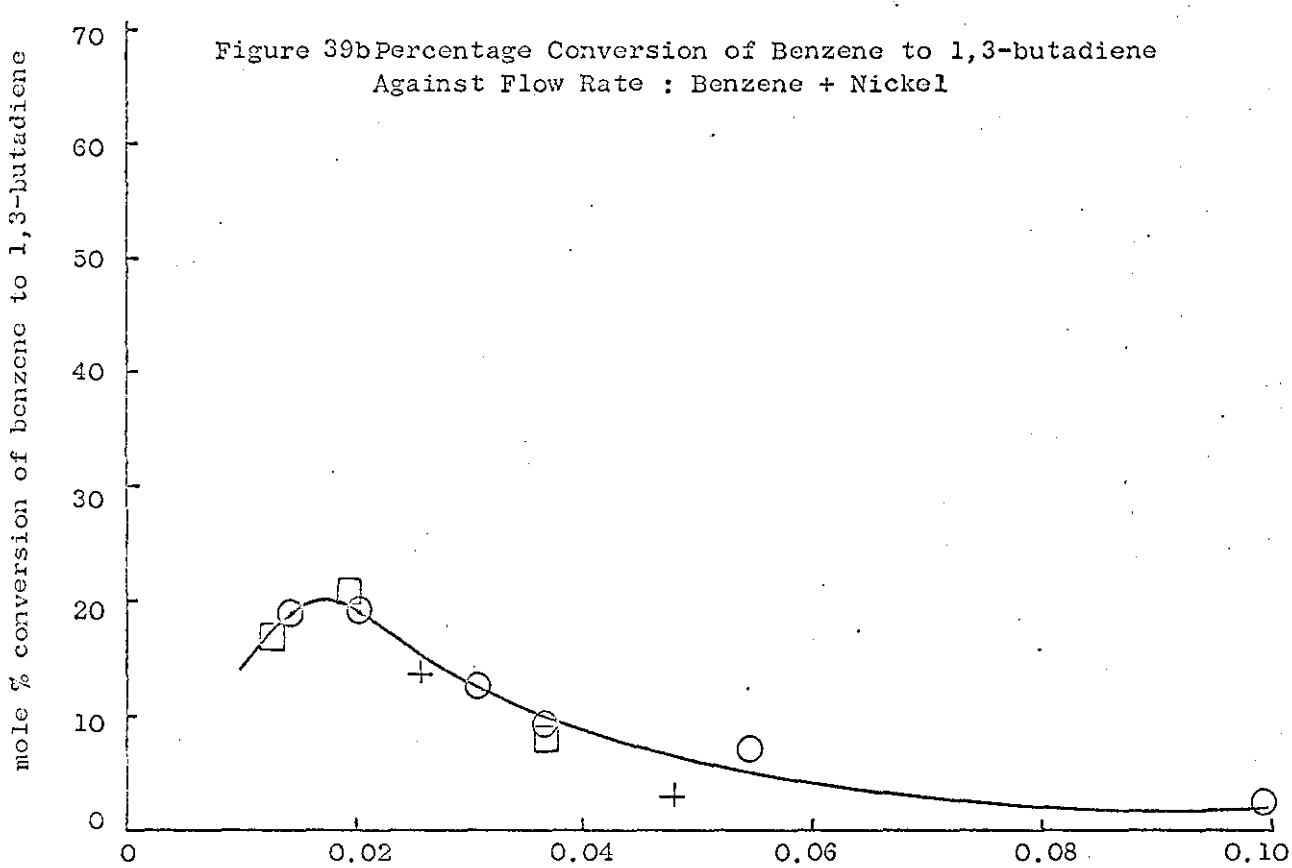

Figure 40a Percentage Conversion of Benzene to Allene Against Flow Rate : Benzene Alone

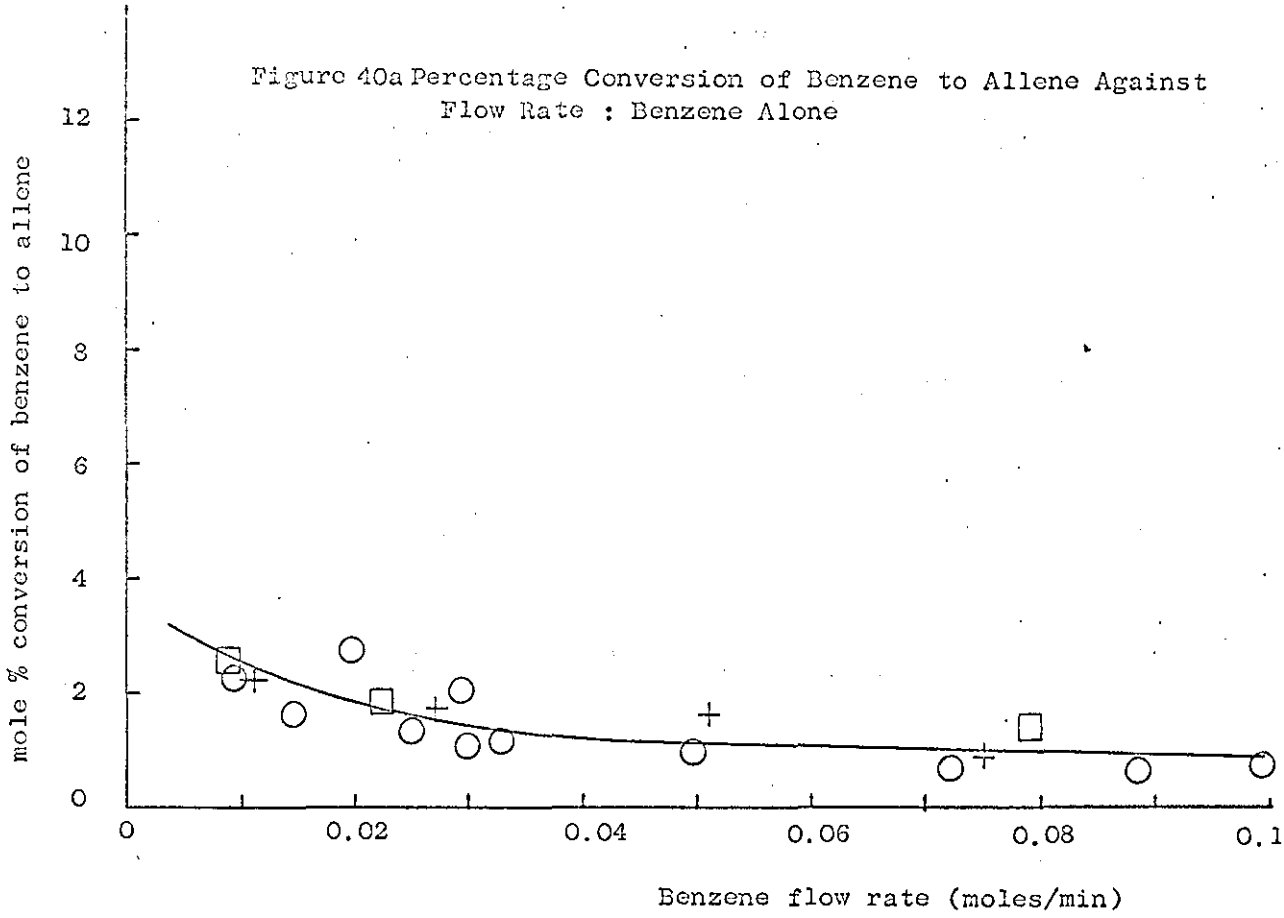

Figure 40b Percentage Conversion of Benzene to Allene Against Flow Rate : Benzene + Nickel

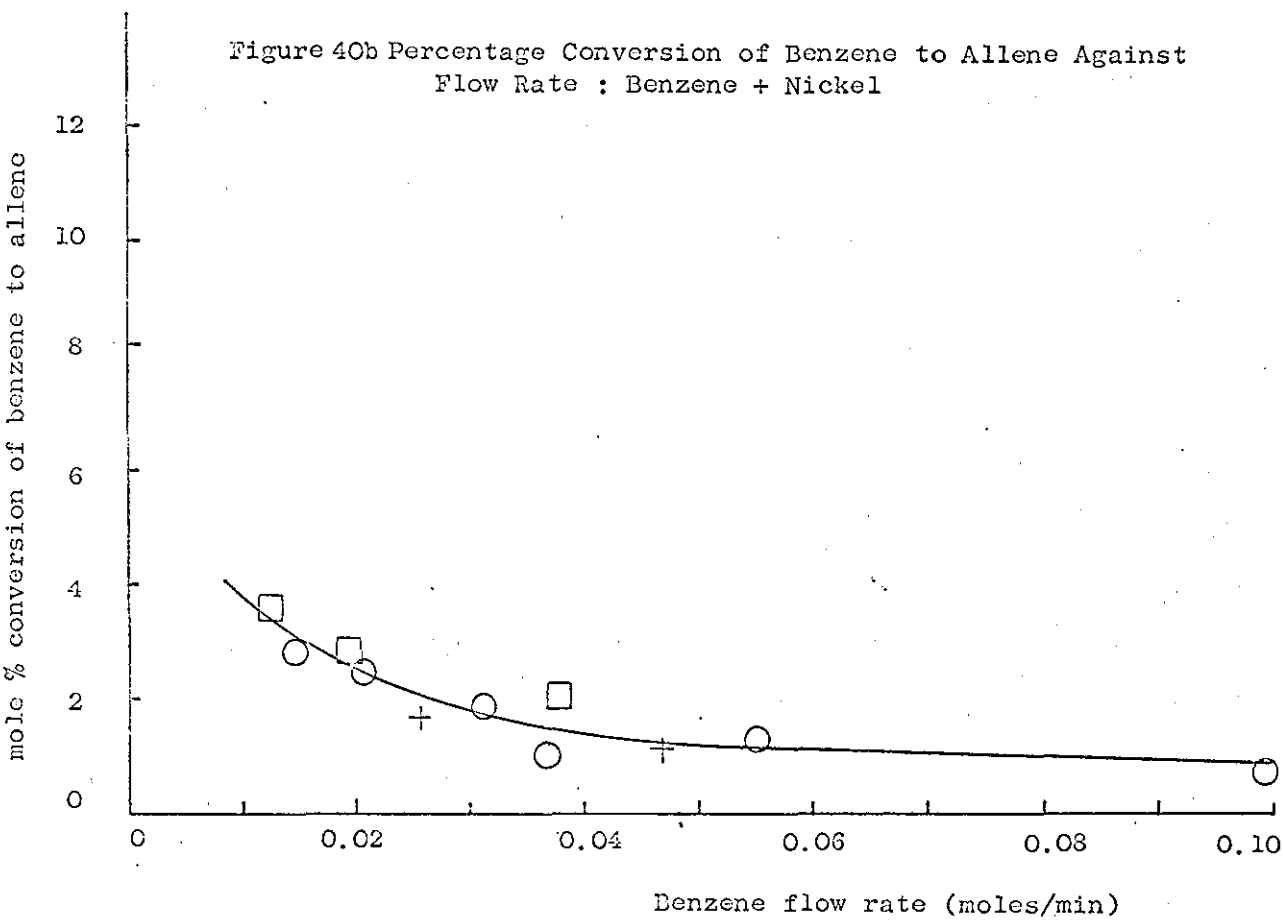

Figure 41a Percentage Conversion of Benzene to Diphenyl Against Reactor Pressure : Benzene Alone

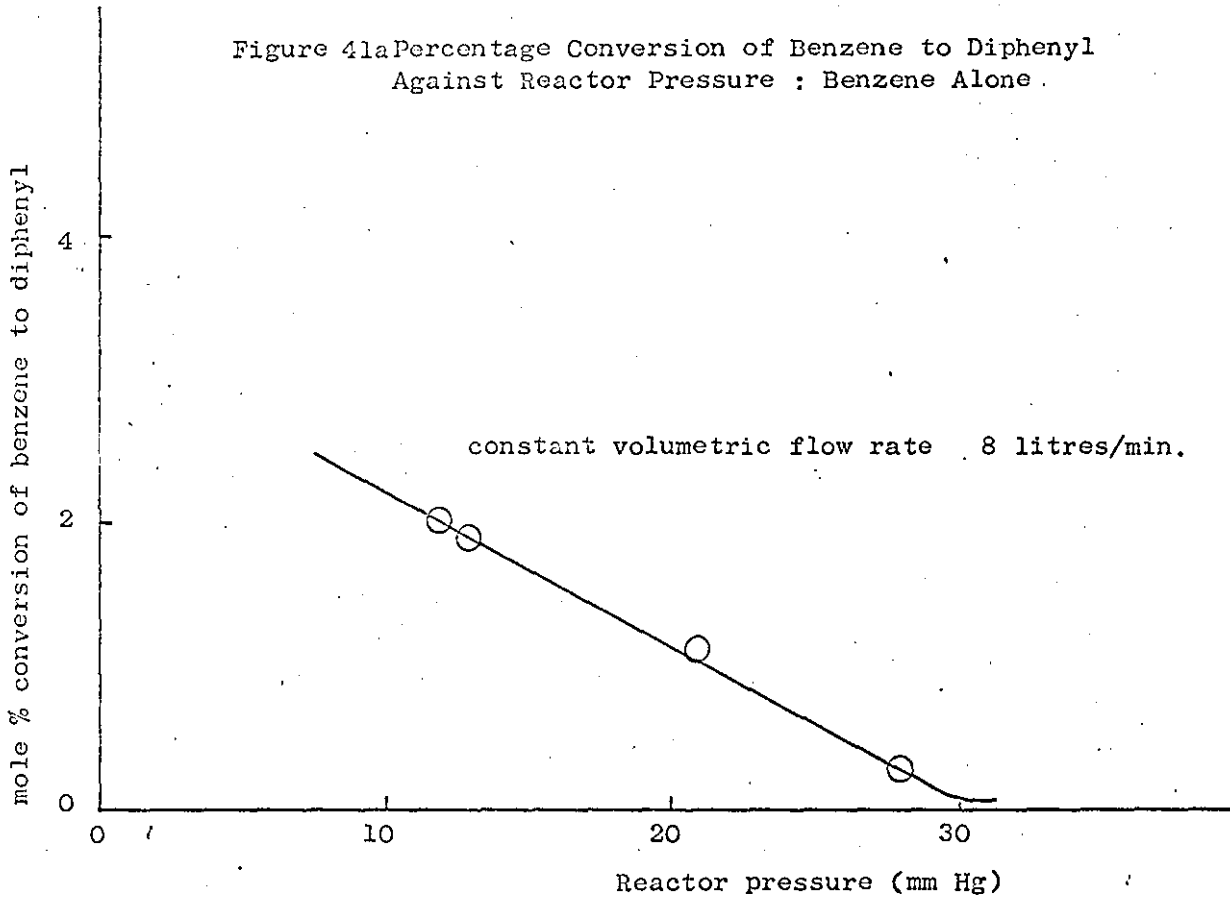

Figure 41b Percentage Conversion of Benzene to Diphenyl Against Reactor Pressure : Benzene + Nickel

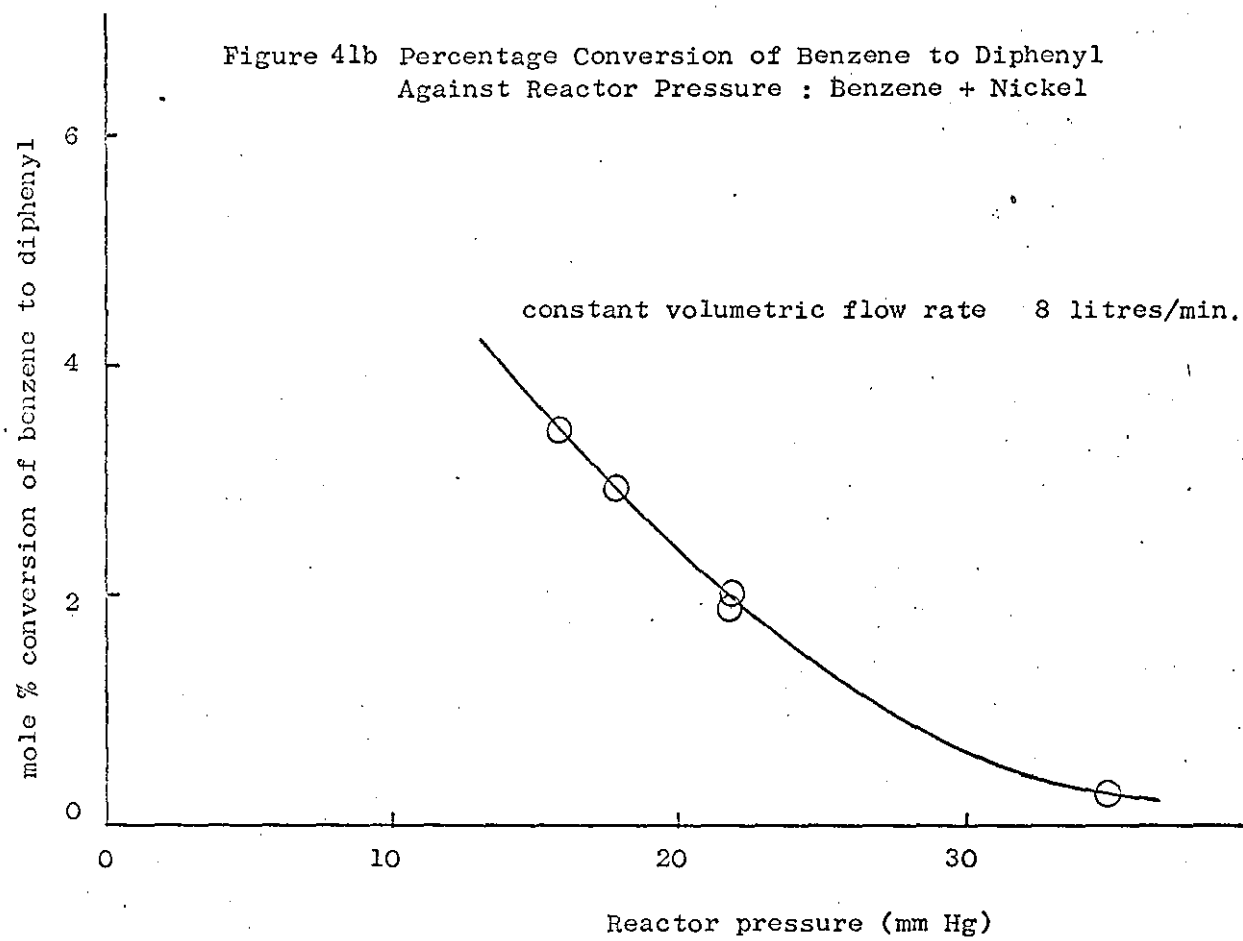

Figure 42a Percentage Conversion of Benzene to Diphenyl Against Flow Rate : Benzene Alone

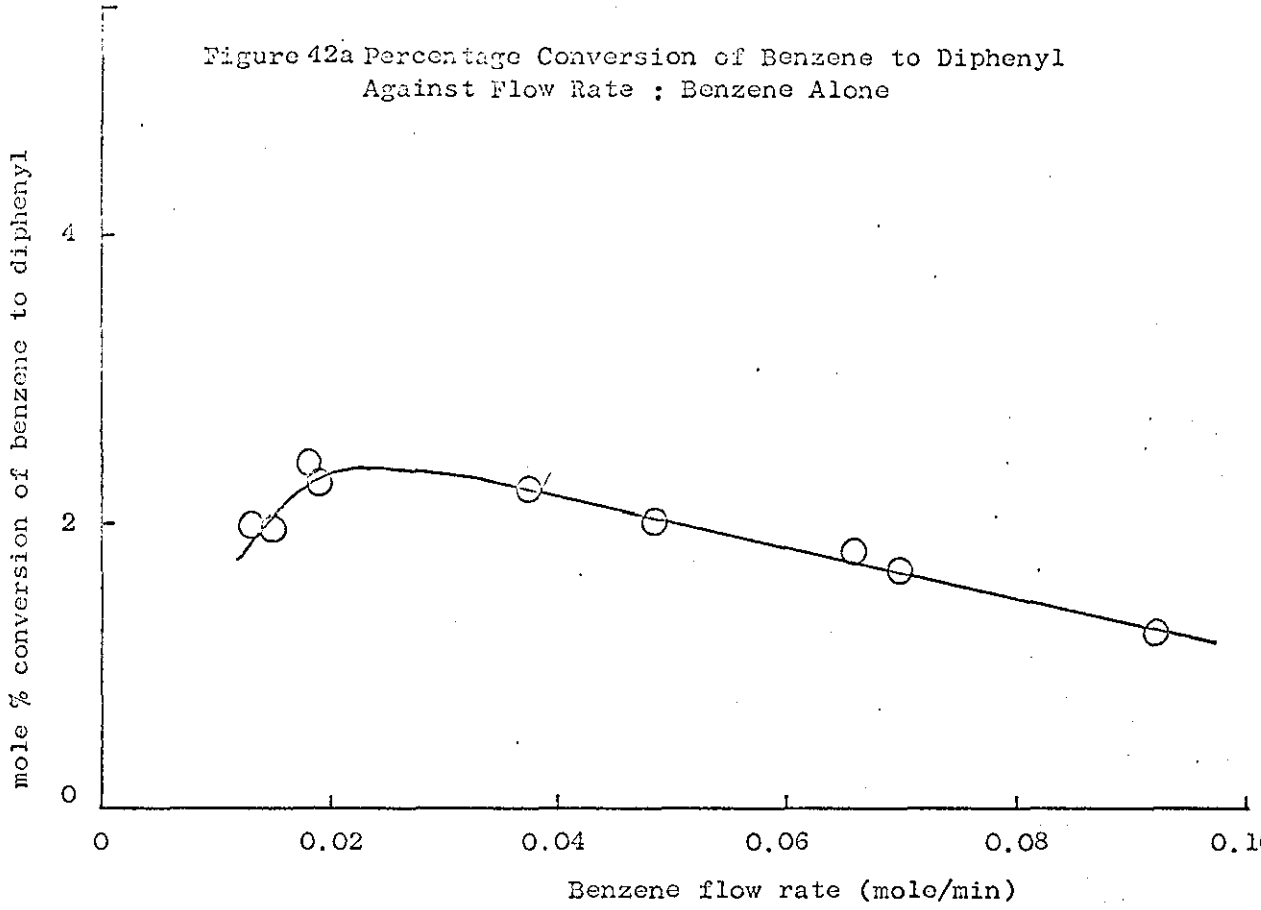

Figure 42b Percentage Conversion of Benzene to Diphenyl Against Flow Rate : Benzene + Nickel

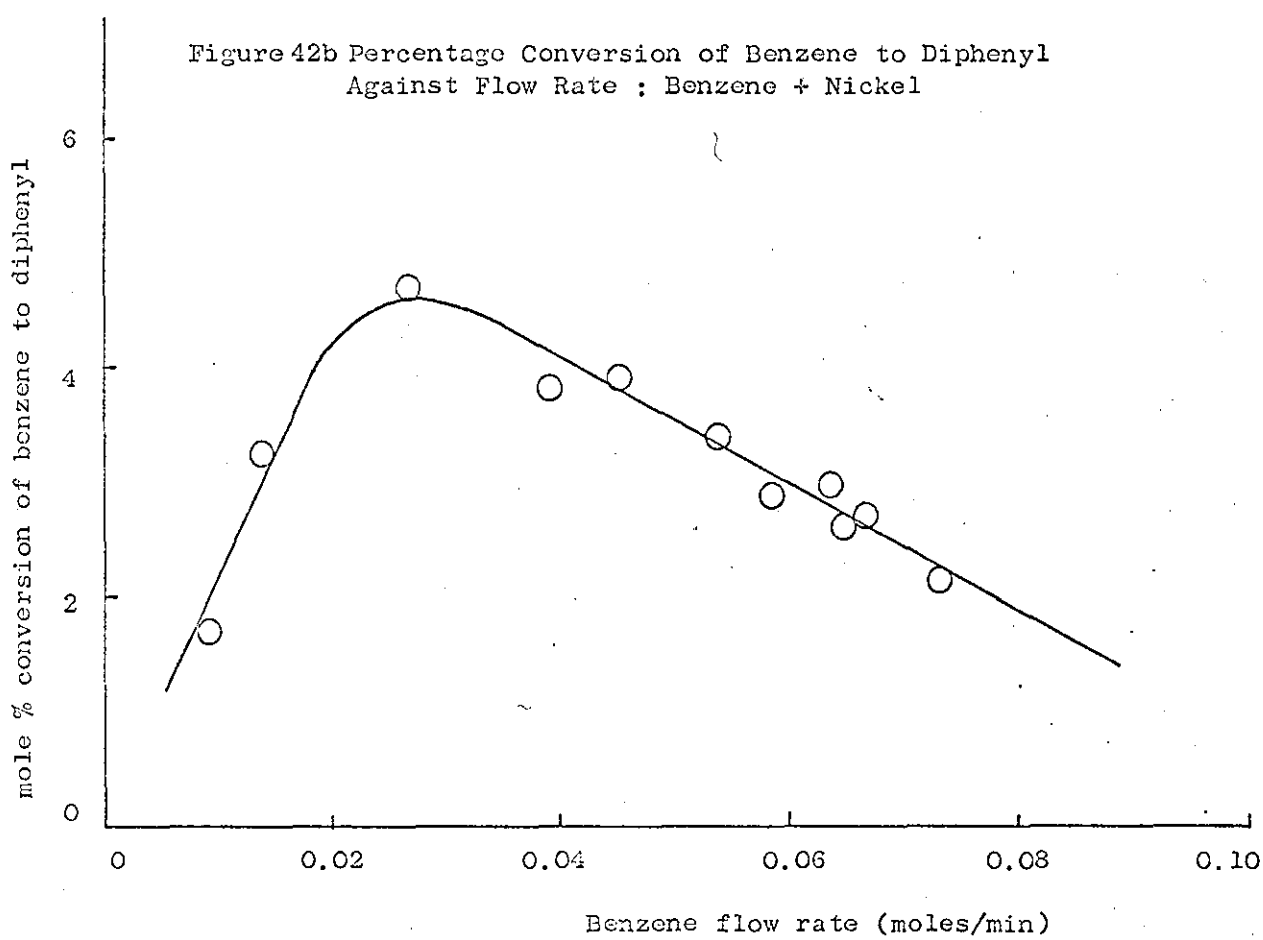

Figure 43a Percentage Conversion of Benzene to Naphthalene Against Flow Rate : Benzene Alone

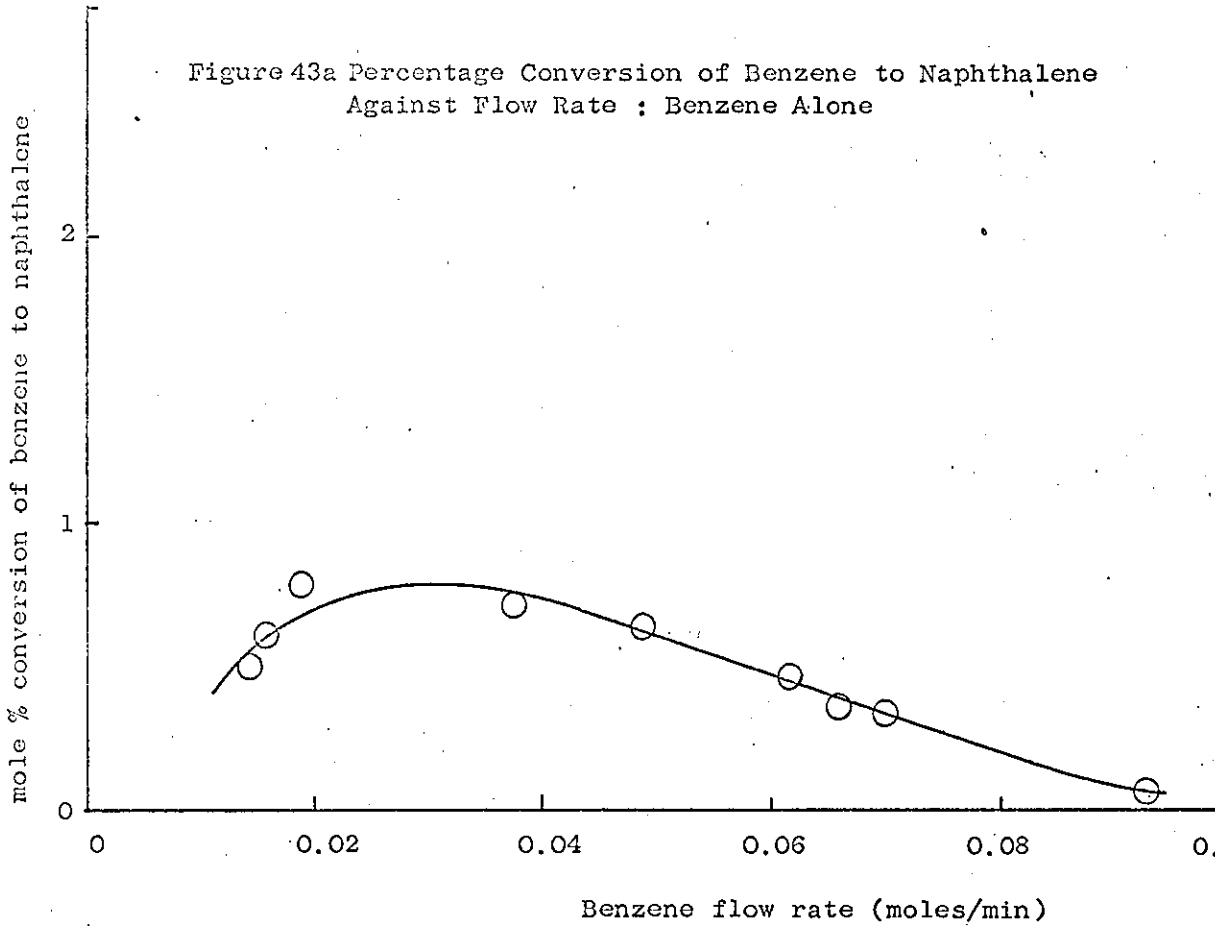

Figure 43b Percentage Conversion of Benzene to Naphthalene Against Flow Rate : Benzene + Nickel

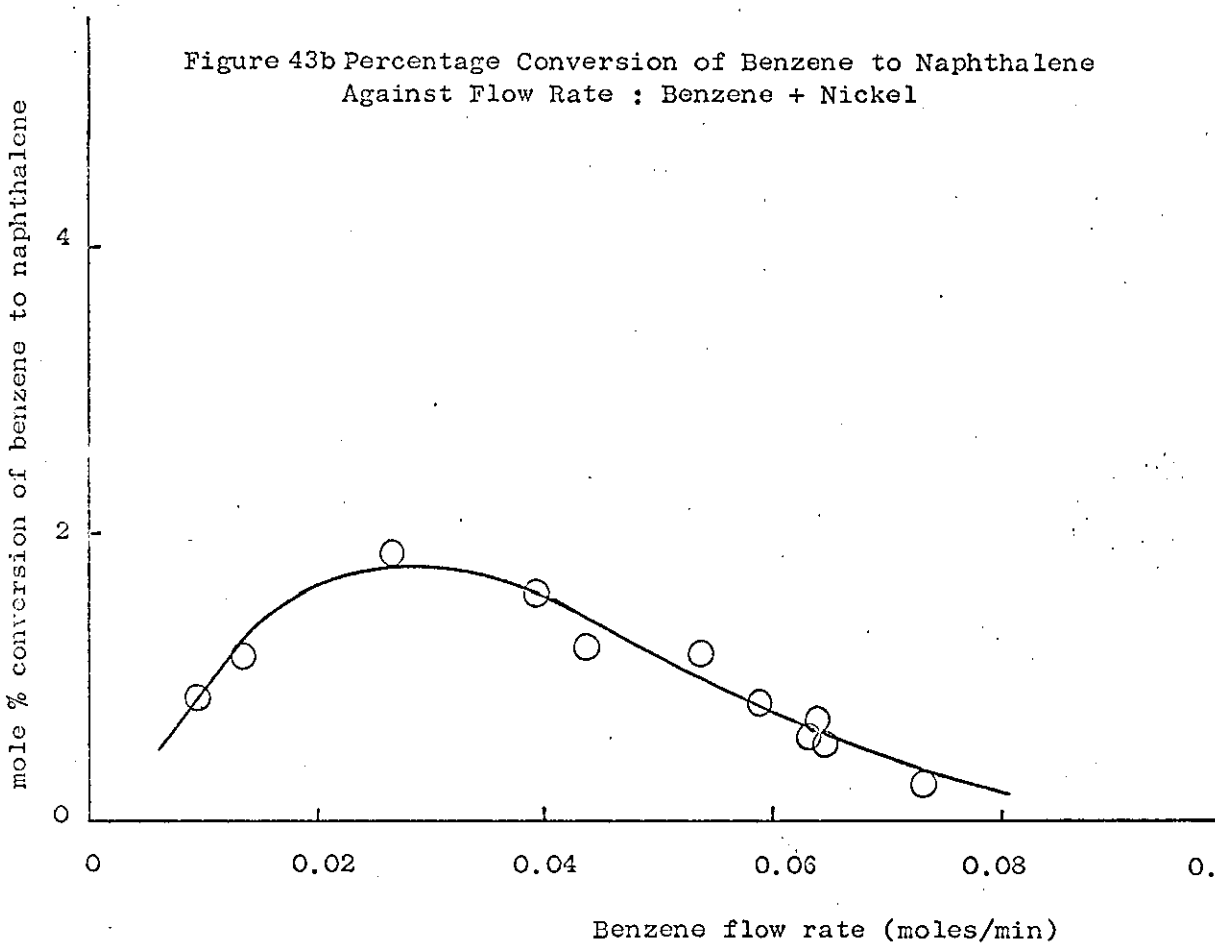

Figure 44a Percentage Free Hydrogen of Hydrogen Content of Benzene Passed Against Benzene Flow Rate : Benzene Alone

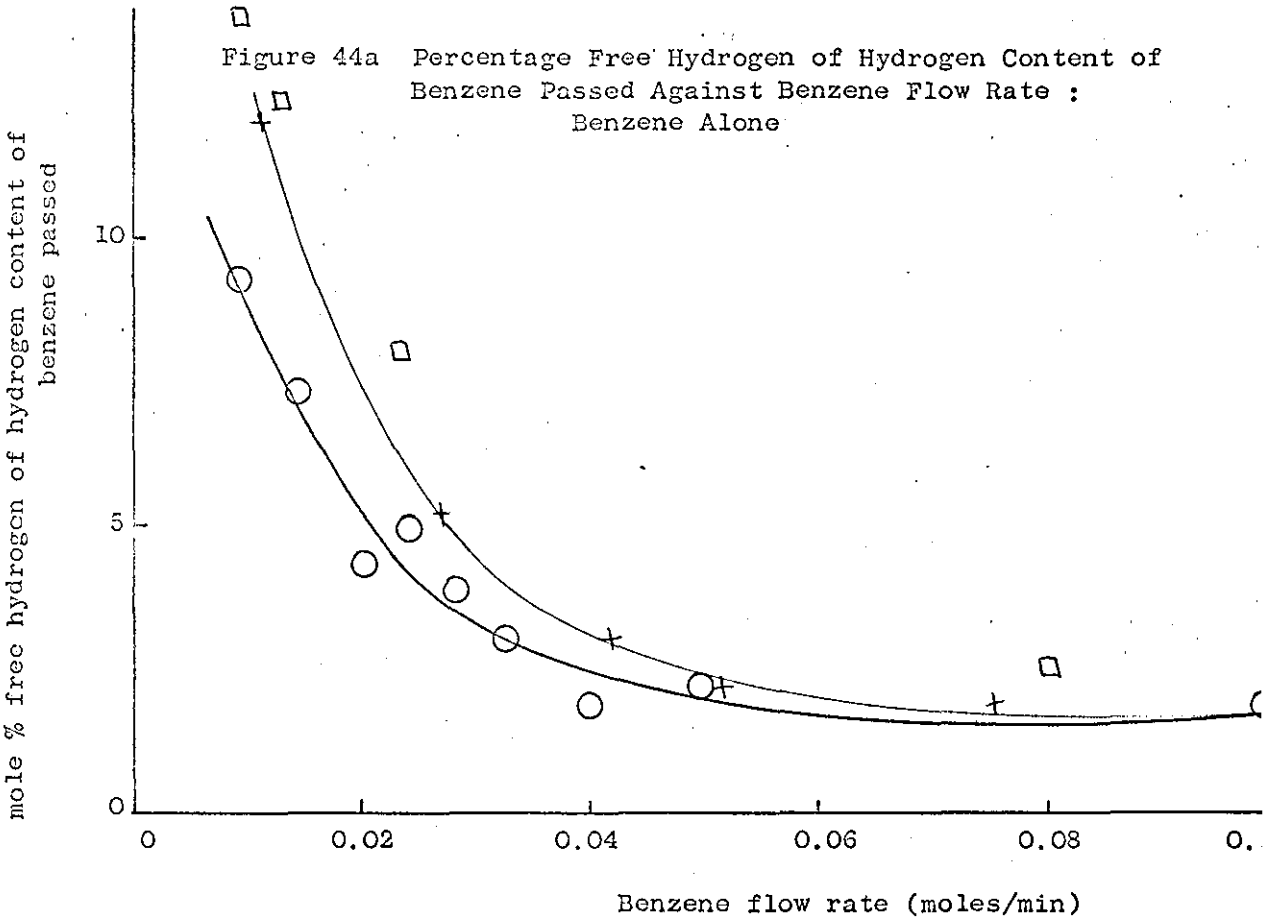

Figure 44b Percentage Free Hydrogen of Hydrogen Content of Benzene Passed Against Benzene Flow Rate : Benzene and Nickel

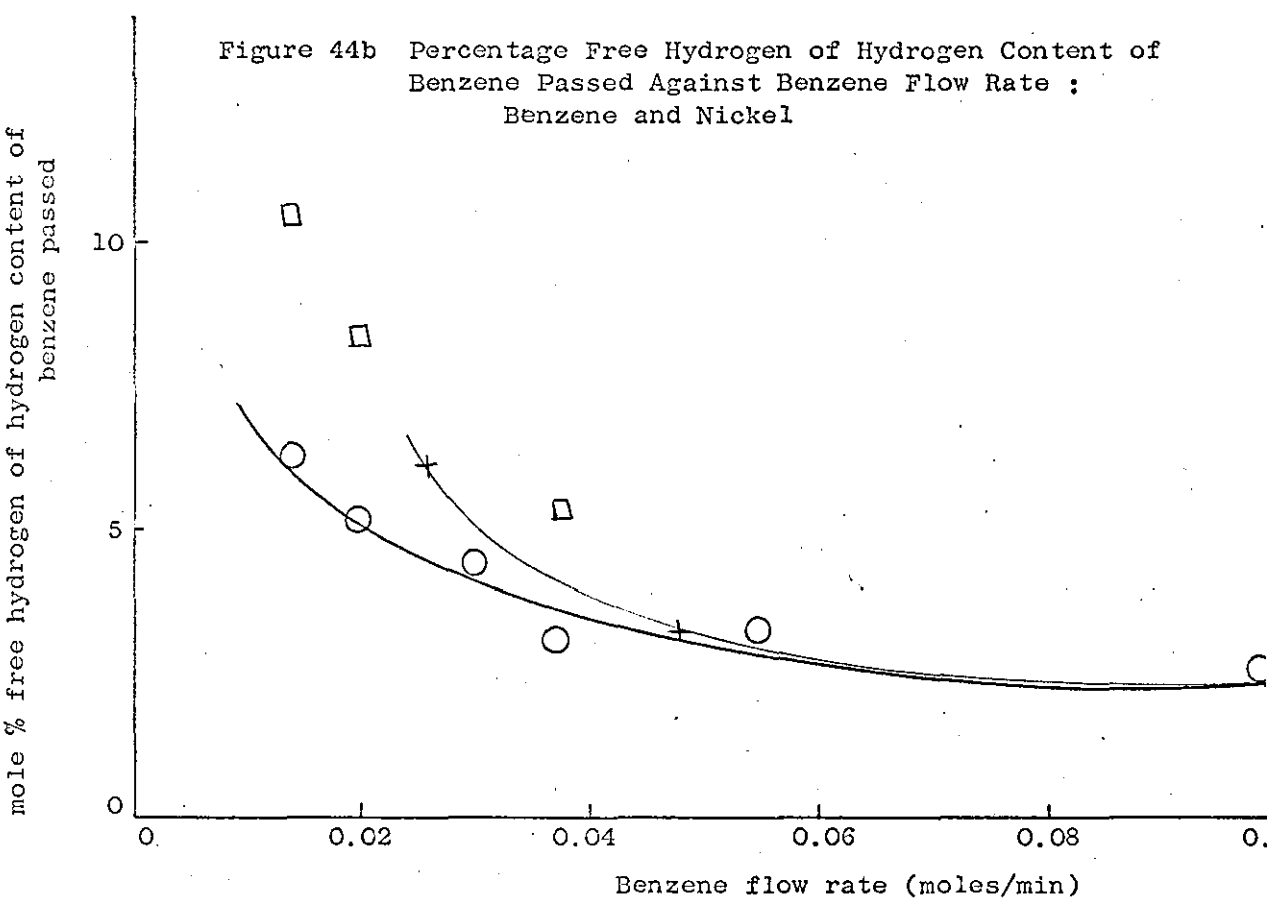

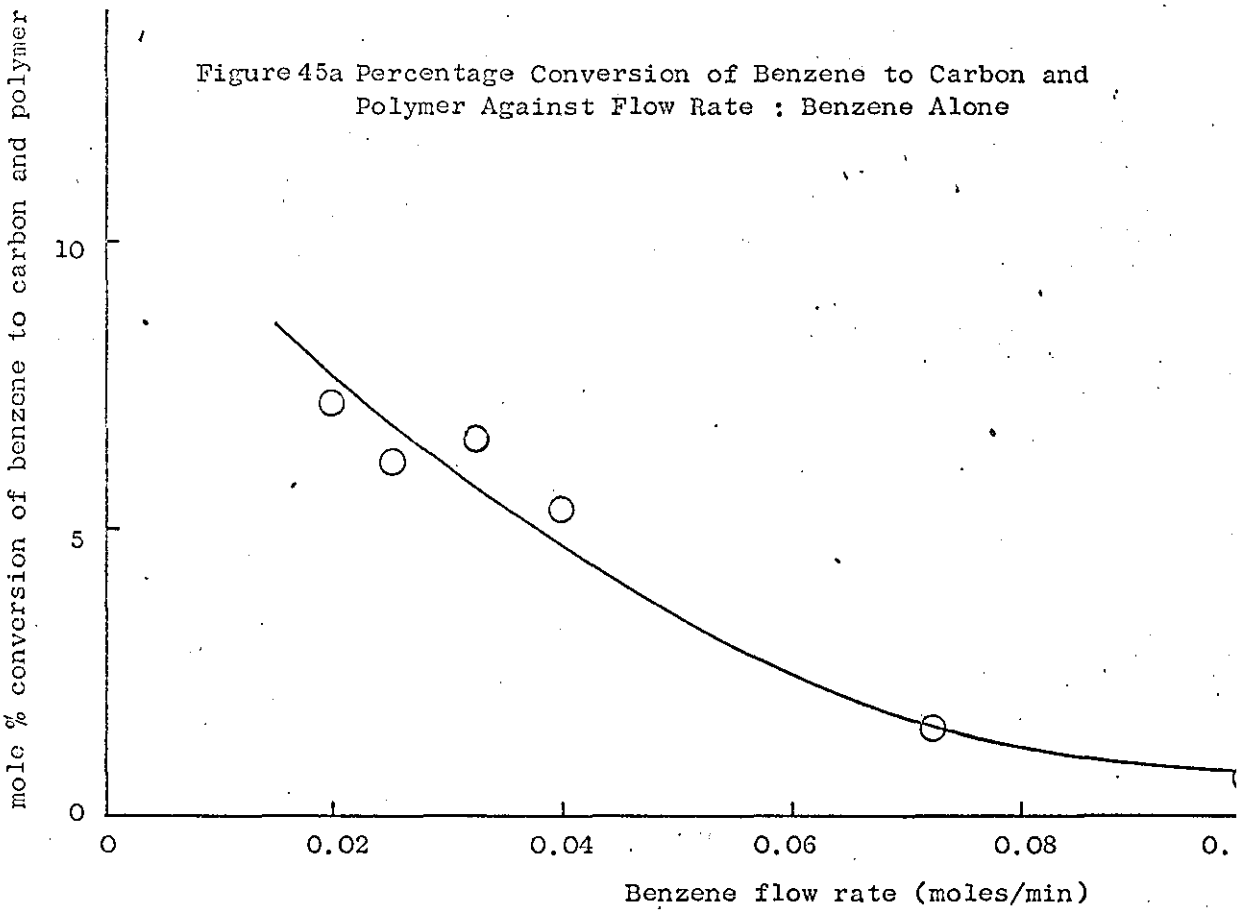

Figure 45a Percentage Conversion of Benzene to Carbon and Polymer Against Flow Rate : Benzene Alone

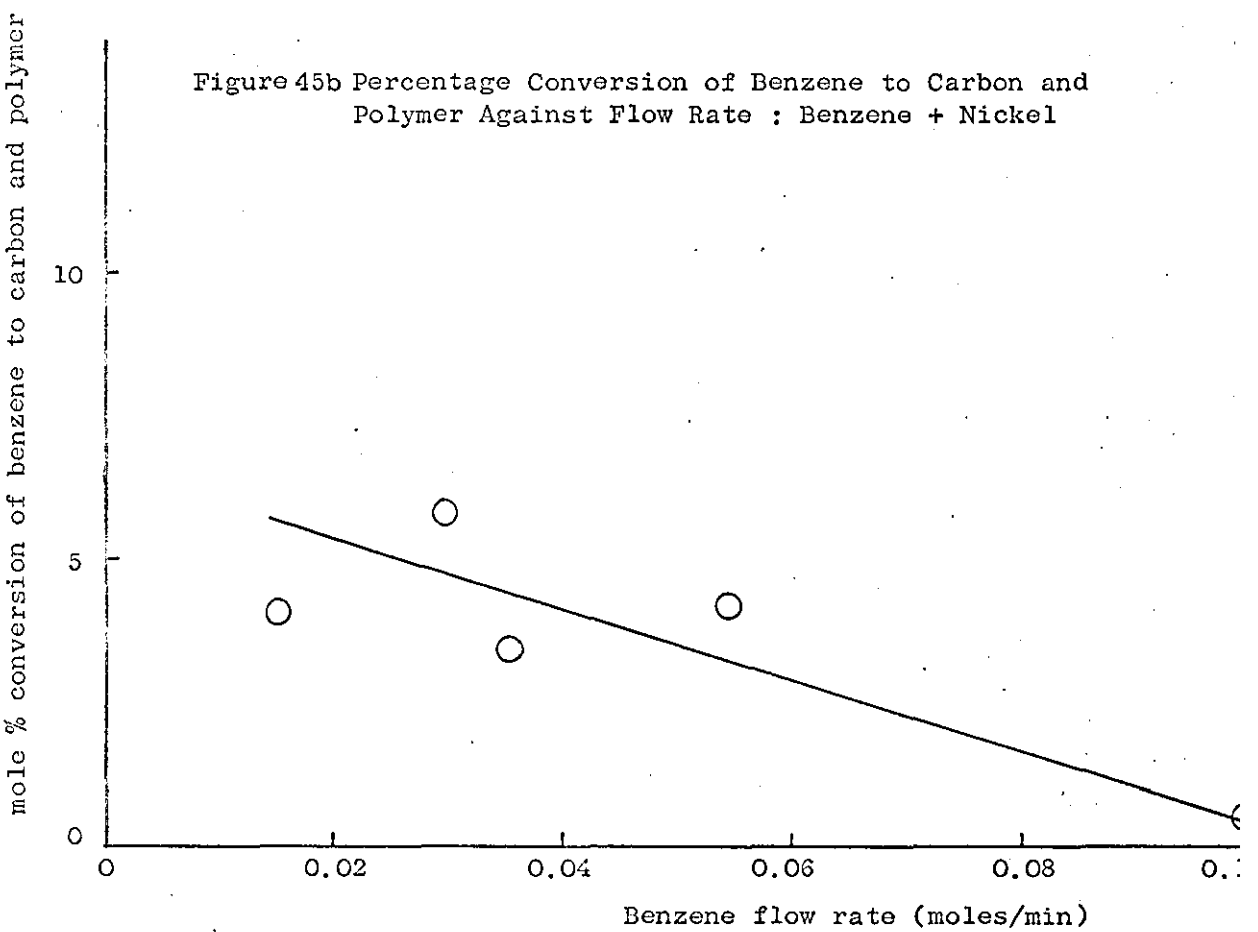

Figure 45b Percentage Conversion of Benzene to Carbon and Polymer Against Flow Rate : Benzene + Nickel

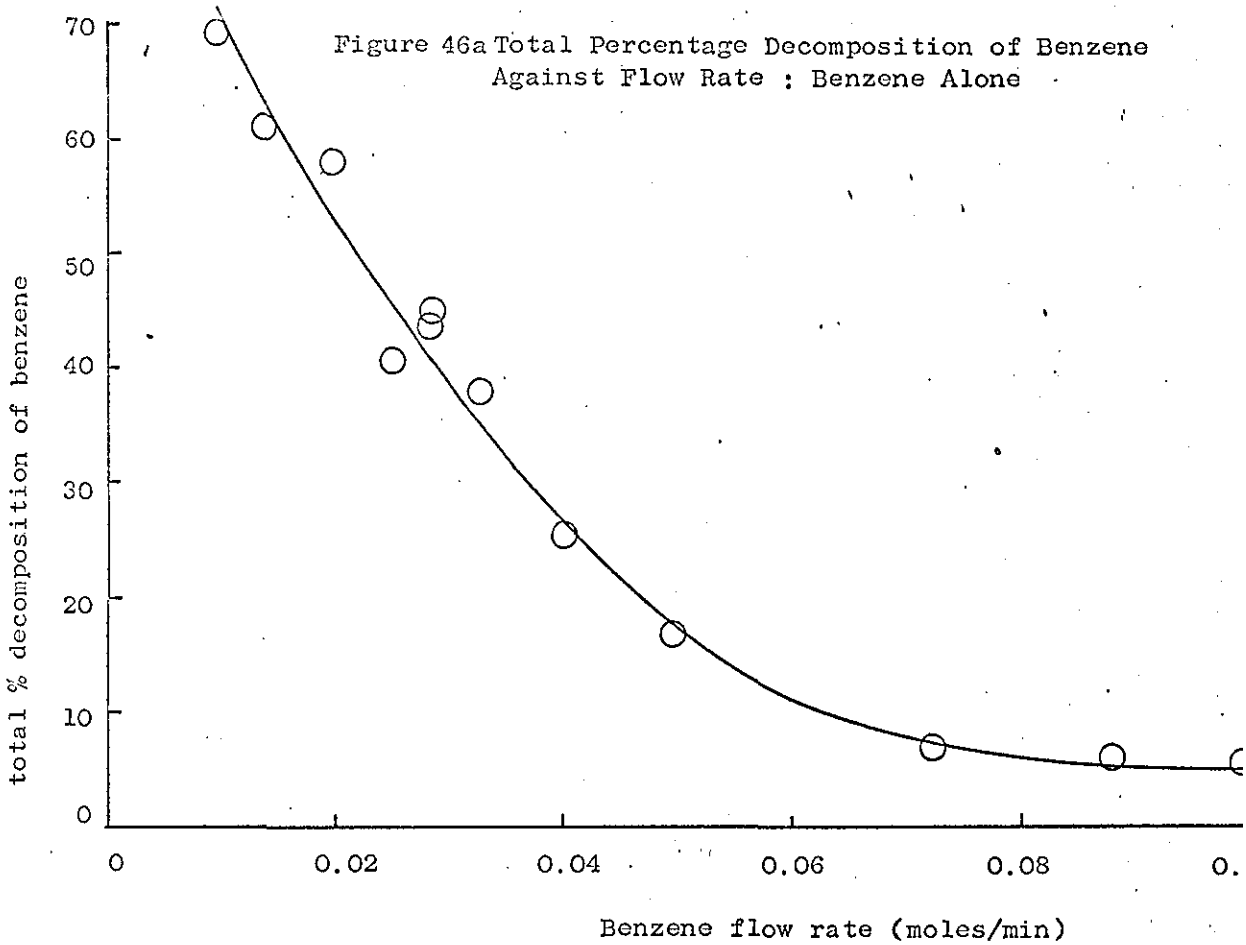

Figure 46a Total Percentage Decomposition of Benzene Against Flow Rate : Benzene Alone

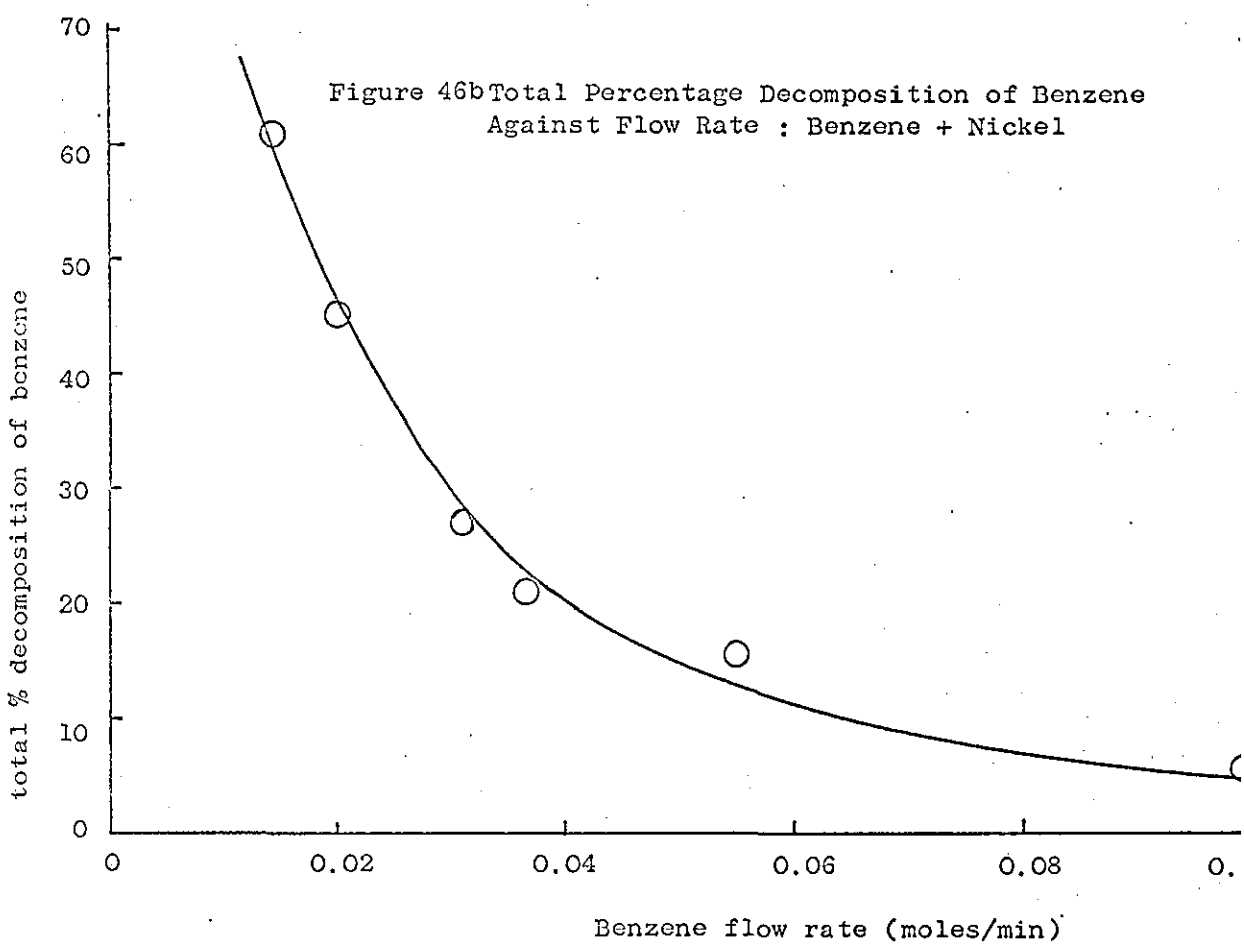

Figure 46b Total Percentage Decomposition of Benzene Against Flow Rate : Benzene + Nickel

Figure 47a Mole Ratio of Acetylene : 1,3-butadiene Against Flow Rate : Benzene Alone.

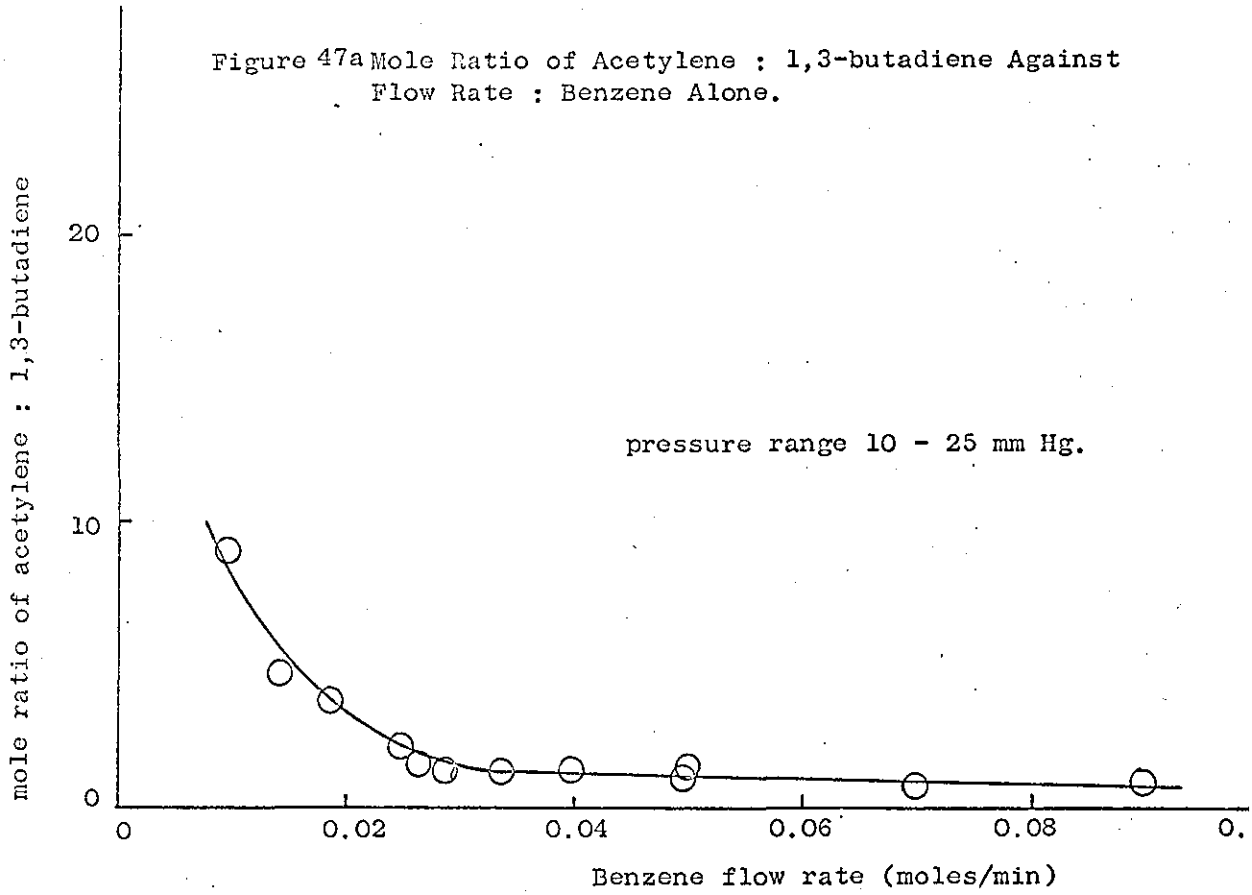

Figure 47b Mole Ratio of Acetylene : 1,3-butadiene Against Flow Rate : Benzene and Nickel.

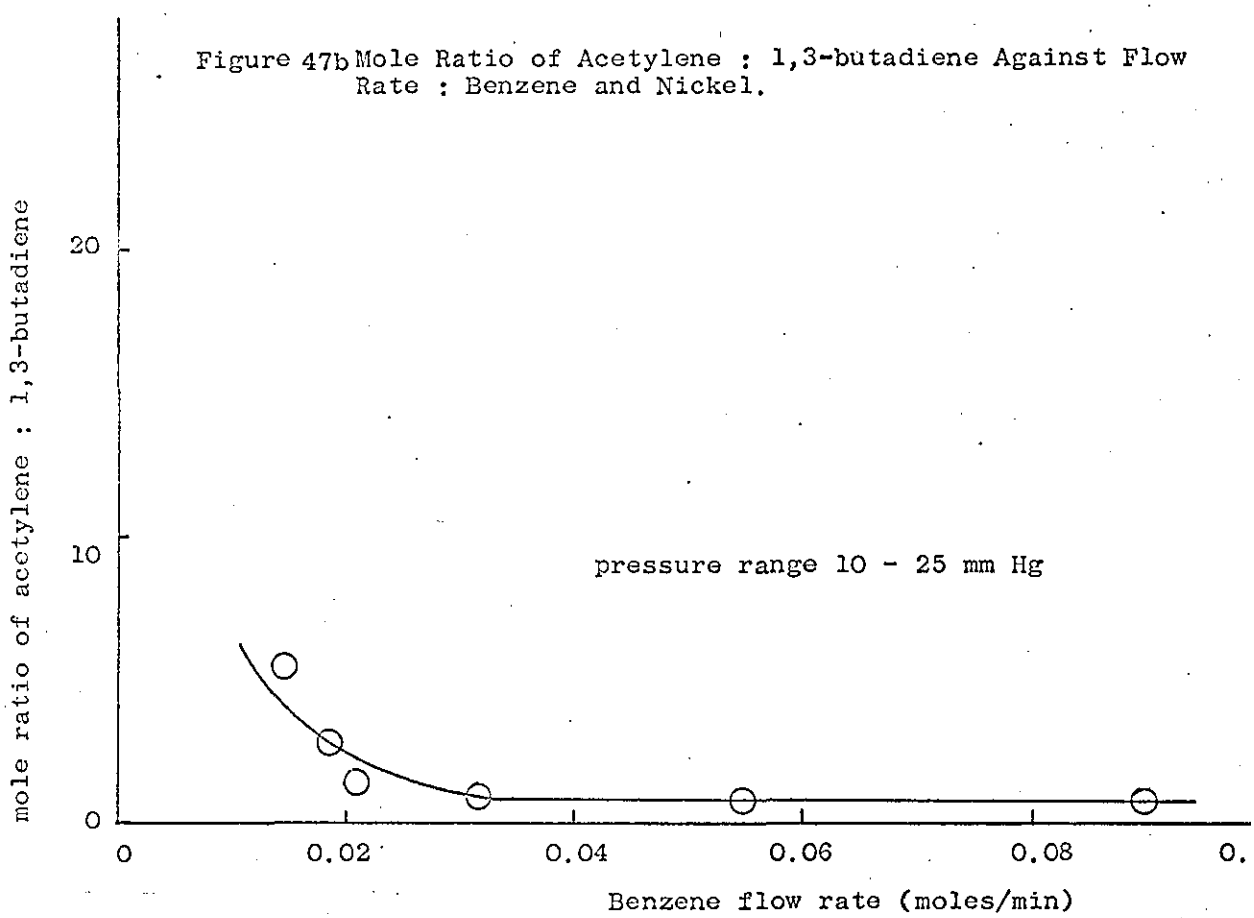

Figure 48 Energy Yield of Acetylene Against Flow Rate

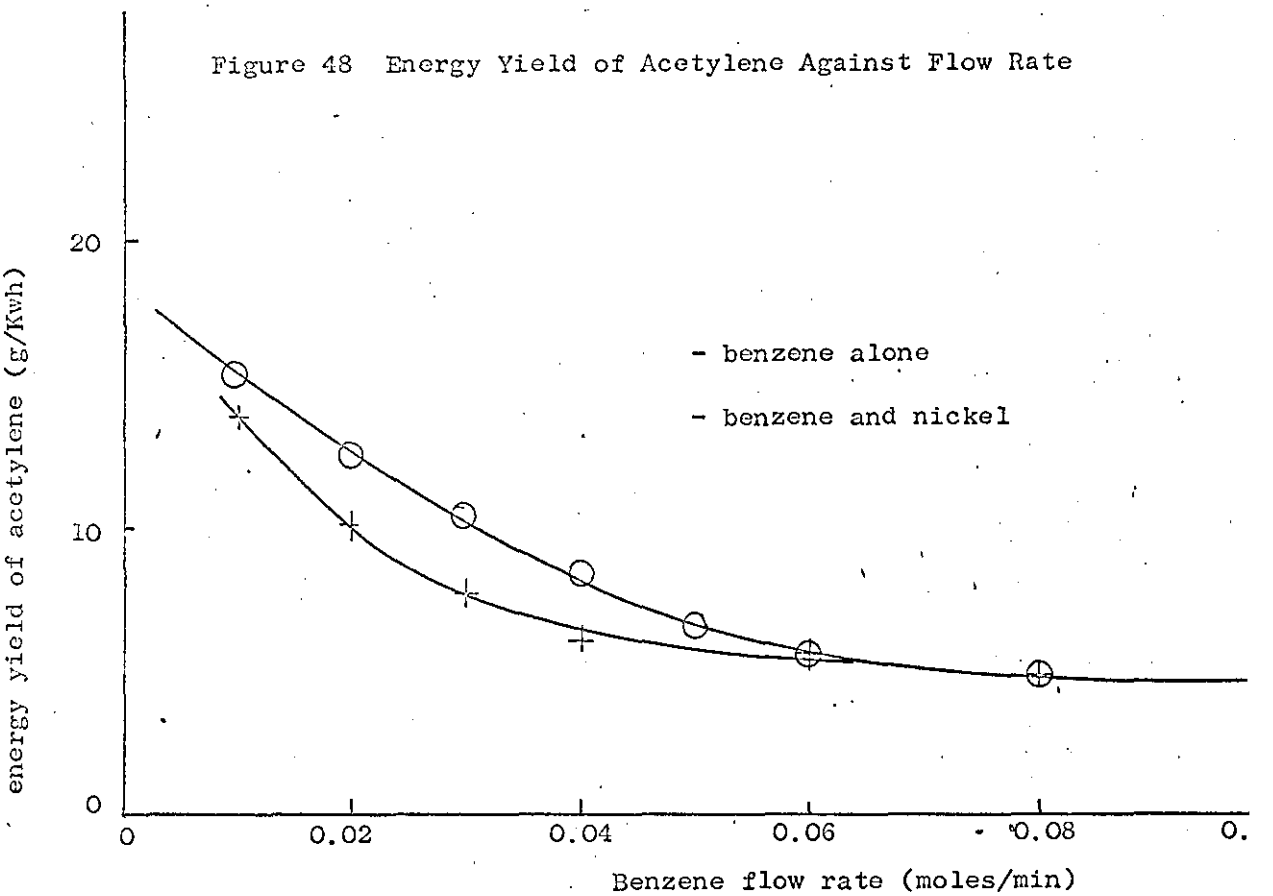

Figure 49 Energy Yield of Diphenyl Against Flow Rate

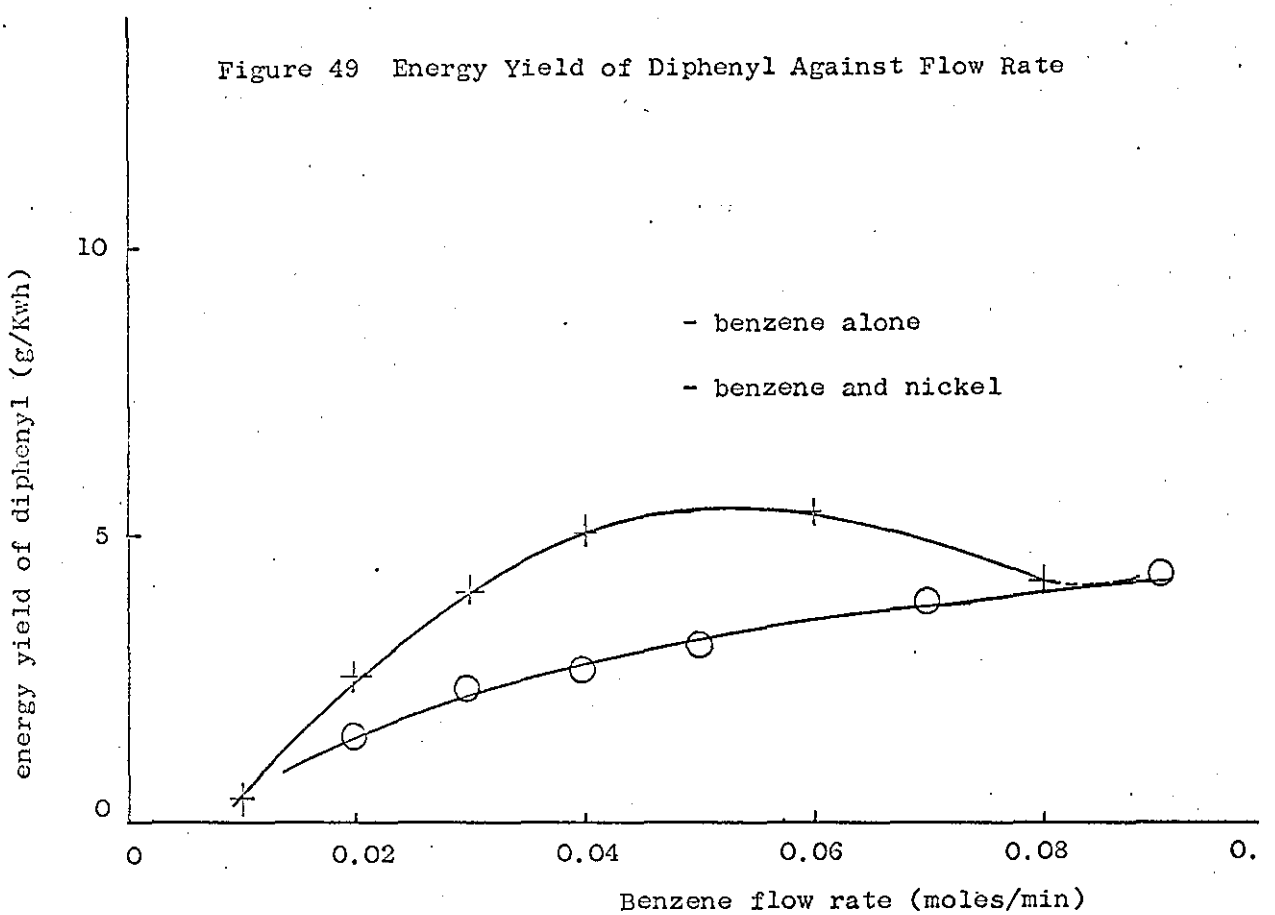

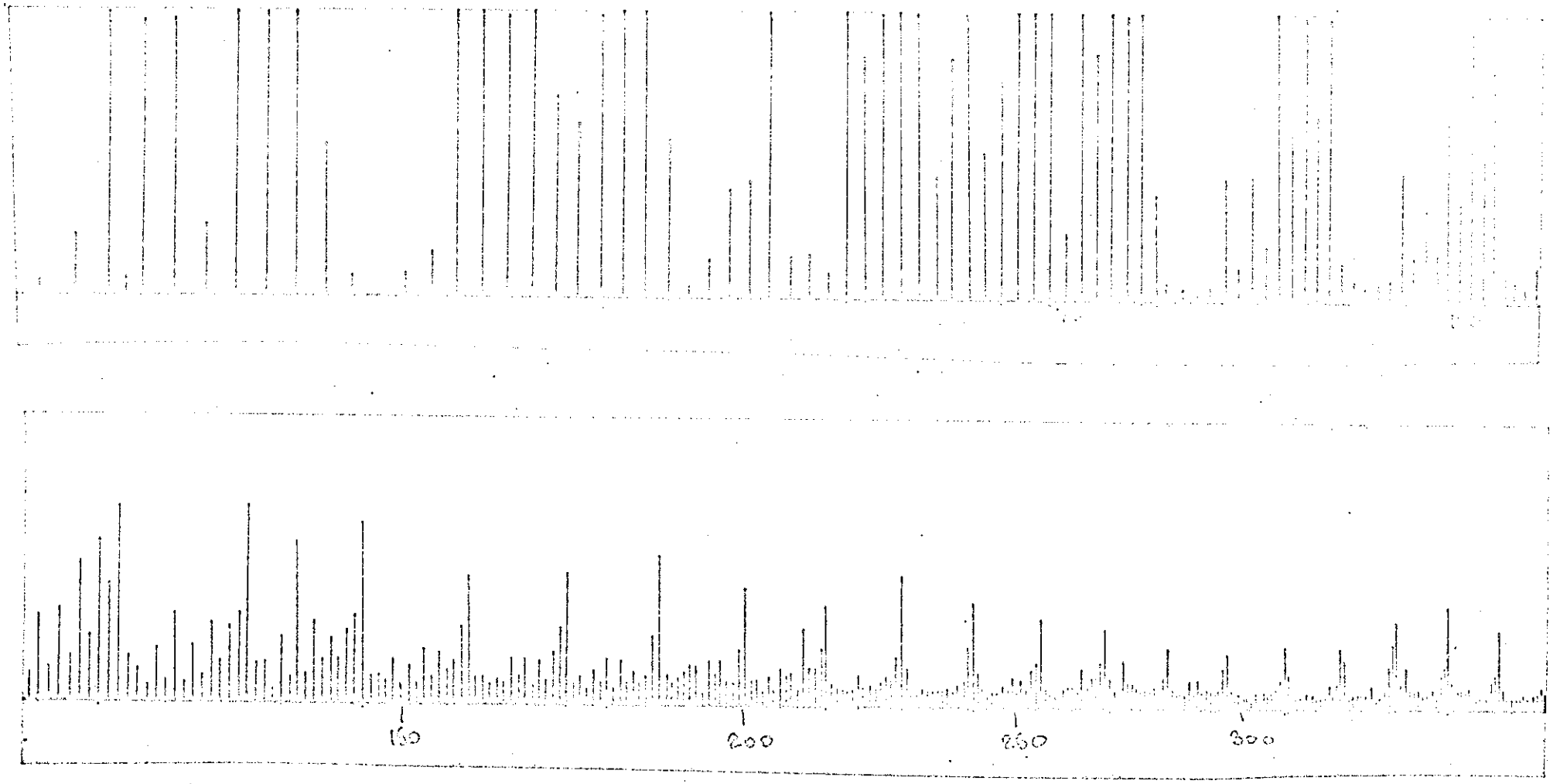

Figure 50 Typical Mass Spectrum of Polybenzenes found from the Benzene Discharge.

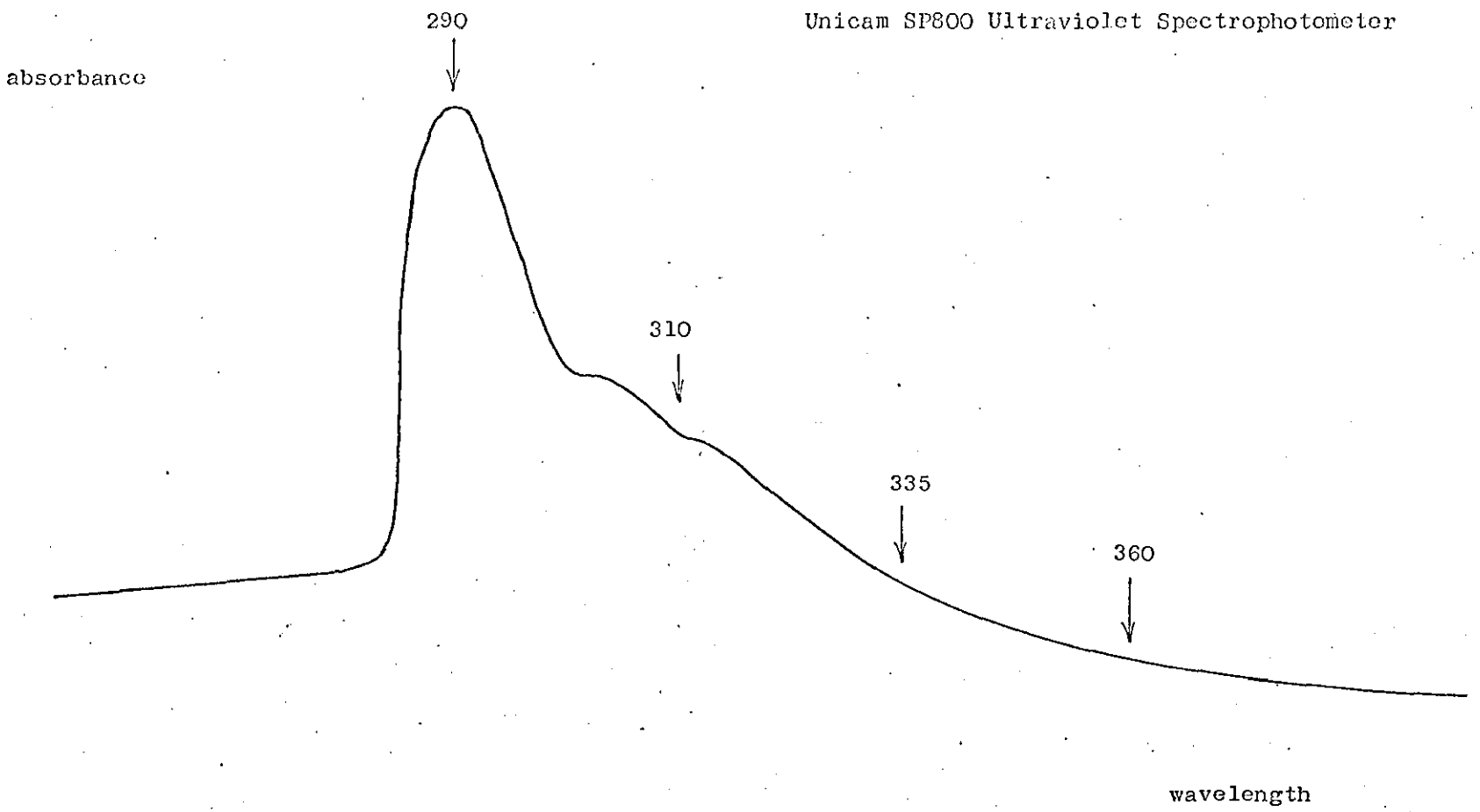

Figure 51 Typical Ultraviolet Spectra of the Polybenzenes from the Benzene Discharge.

Table 10 Benzene and Carbon Dioxide, 2:1 ; the Low Boilers

power input 0.78 Kw

benzene flow rate, moles/min.	reactor pressure mm Hg	power absorption Kw	% conversion to acetylene	% conversion to 1,3-butadiene
0.0105	46	0.24	14.76	4.47
0.0151	61	0.25	9.12	6.40
0.0209	25	0.25	41.50	2.14
0.0292	20	0.24	22.90	4.15
0.0457	25	0.24	15.20	3.80
0.0533	41	0.24	6.86	7.06
0.0578	26	0.24	7.63	4.20
0.0630	28	0.23	5.30	5.25
0.0952	46	0.24	2.07	0.39
0.0979	33	0.24	4.38	4.82
0.101	39	0.23	4.00	4.92

Table 11 Benzene and Carbon Dioxide, 2:1 : the High Boilers

power input 0.78 Kw

benzene flow rate, moles/min.	reactor pressure mm Hg	power absorption Kw	% conversion to naphthalene	% conversion to diphenyl
0.0095	22	0.23	0.08	0.26
0.0184	18	0.22	0.23	0.72
0.0376	18	0.23	0.55	1.78
0.0466	19	0.24	0.55	1.94
0.0627	20	0.22	0.17	0.88
0.0737	22	0.22	0.12	0.43

Figure 52a Percentage Conversion of Benzene to Acetylene Against Flow Rate : Benzene and Carbon Dioxide, 2:1

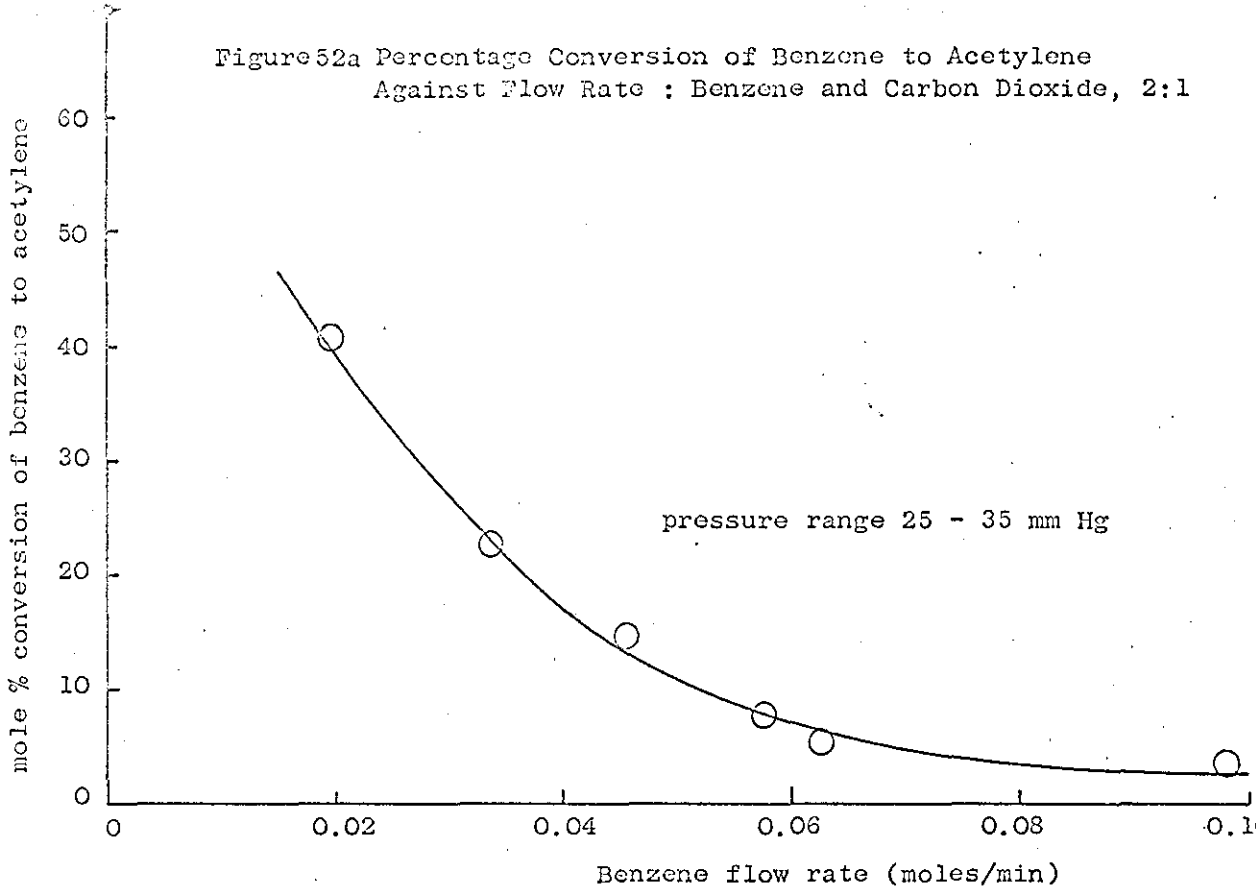

Figure 52b Percentage Conversion of Benzene to Acetylene Against Reactor Pressure : Benzene and Carbon Dioxide, 2:1

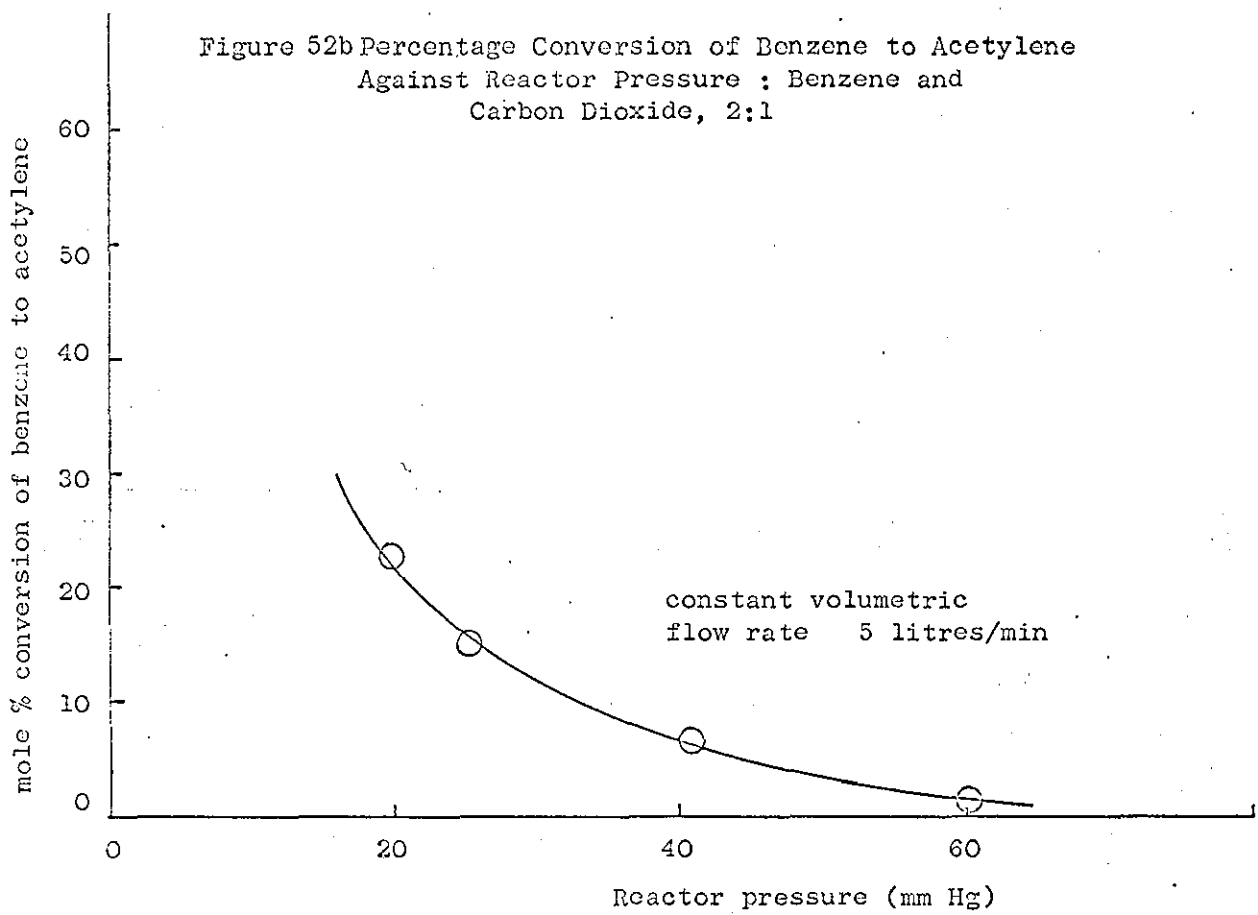

Figure 53 Percentage Conversion of Benzene to 1,3-butadiene Against Flow Rate : Benzene and Carbon Dioxide, 2:1

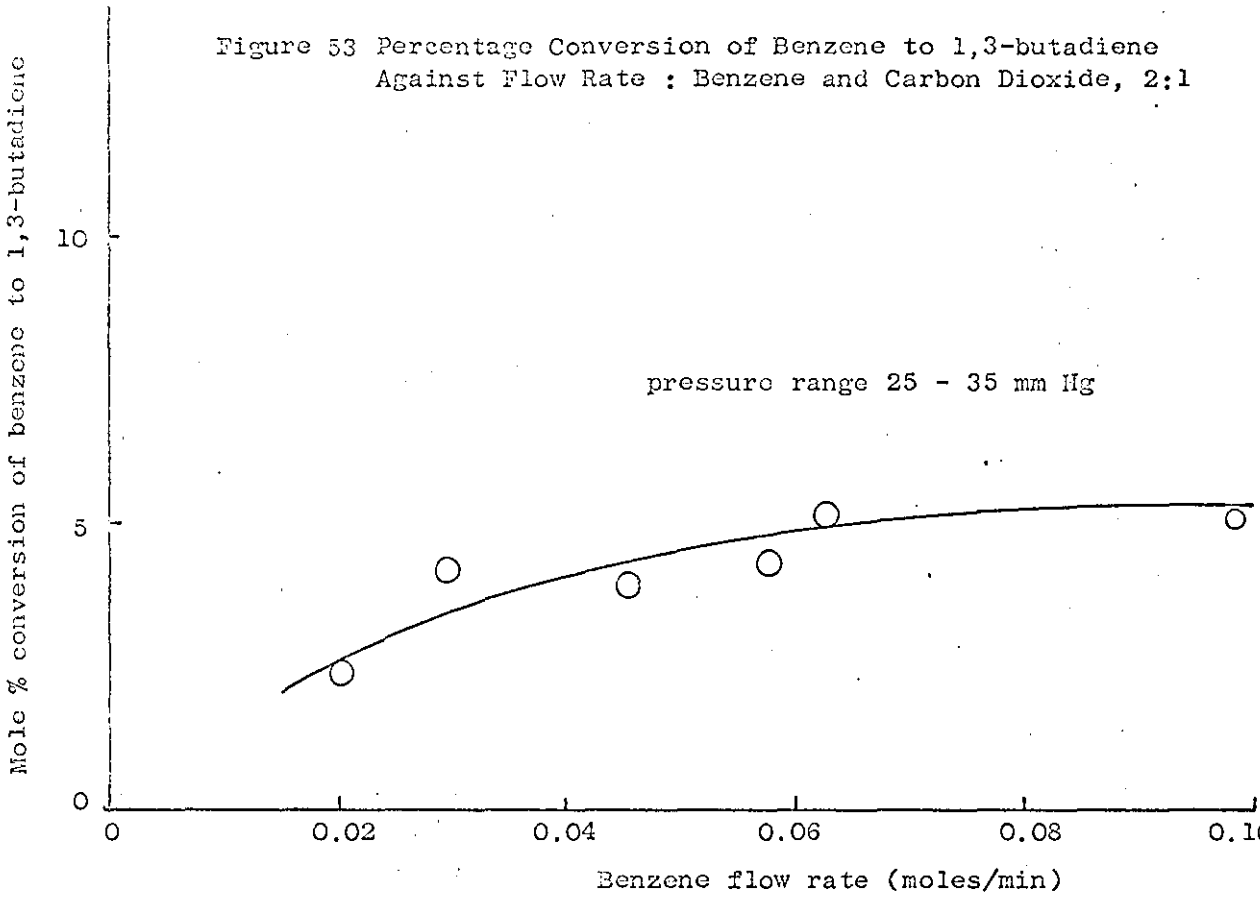

Figure 54 Total Percentage Decomposition of Benzene Against Flow Rate : Benzene and Carbon Dioxide, 2:1

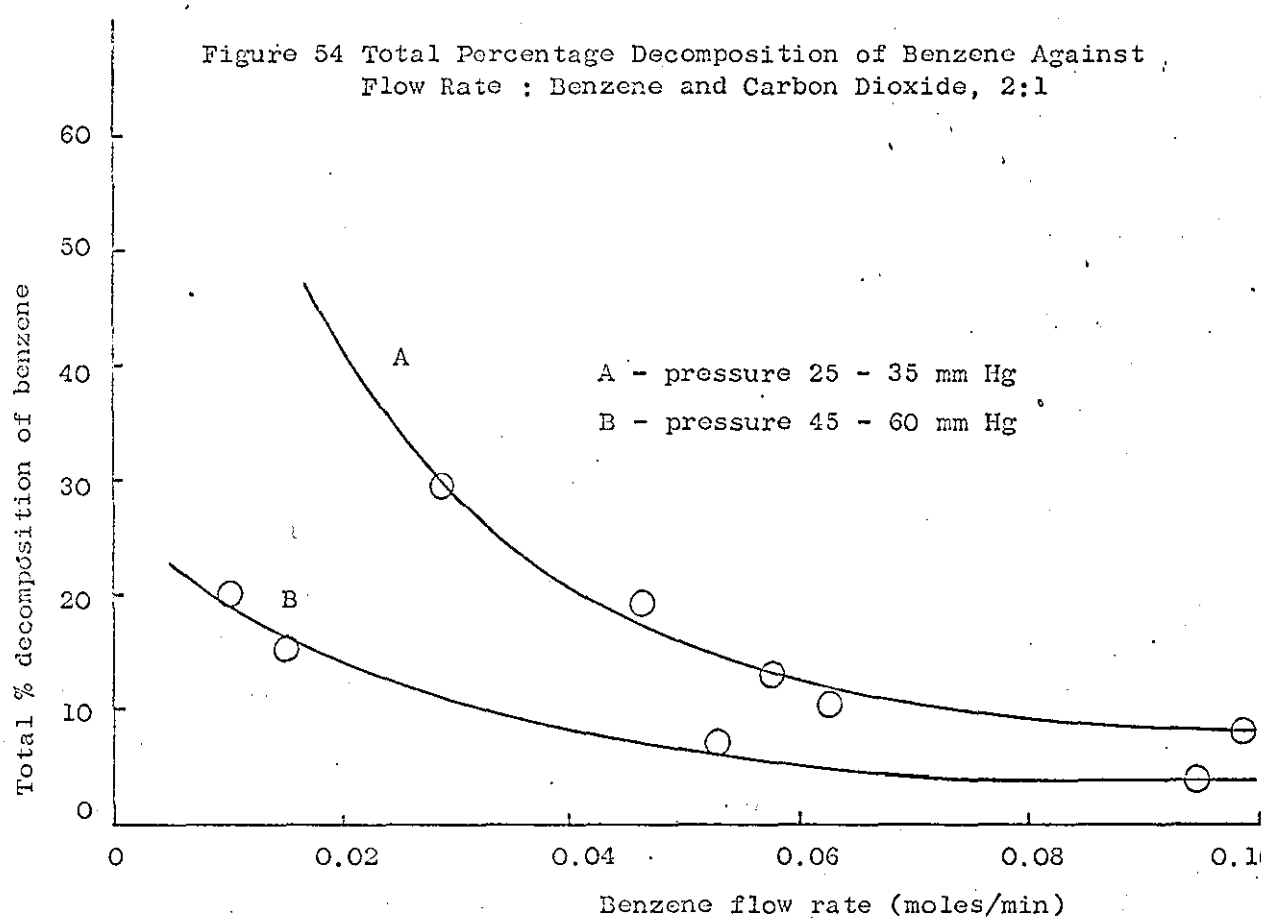

Figure 55 Percentage Conversion of Benzene to Diphenyl Against Flow Rate : Benzene and Carbon Dioxide, 2:1

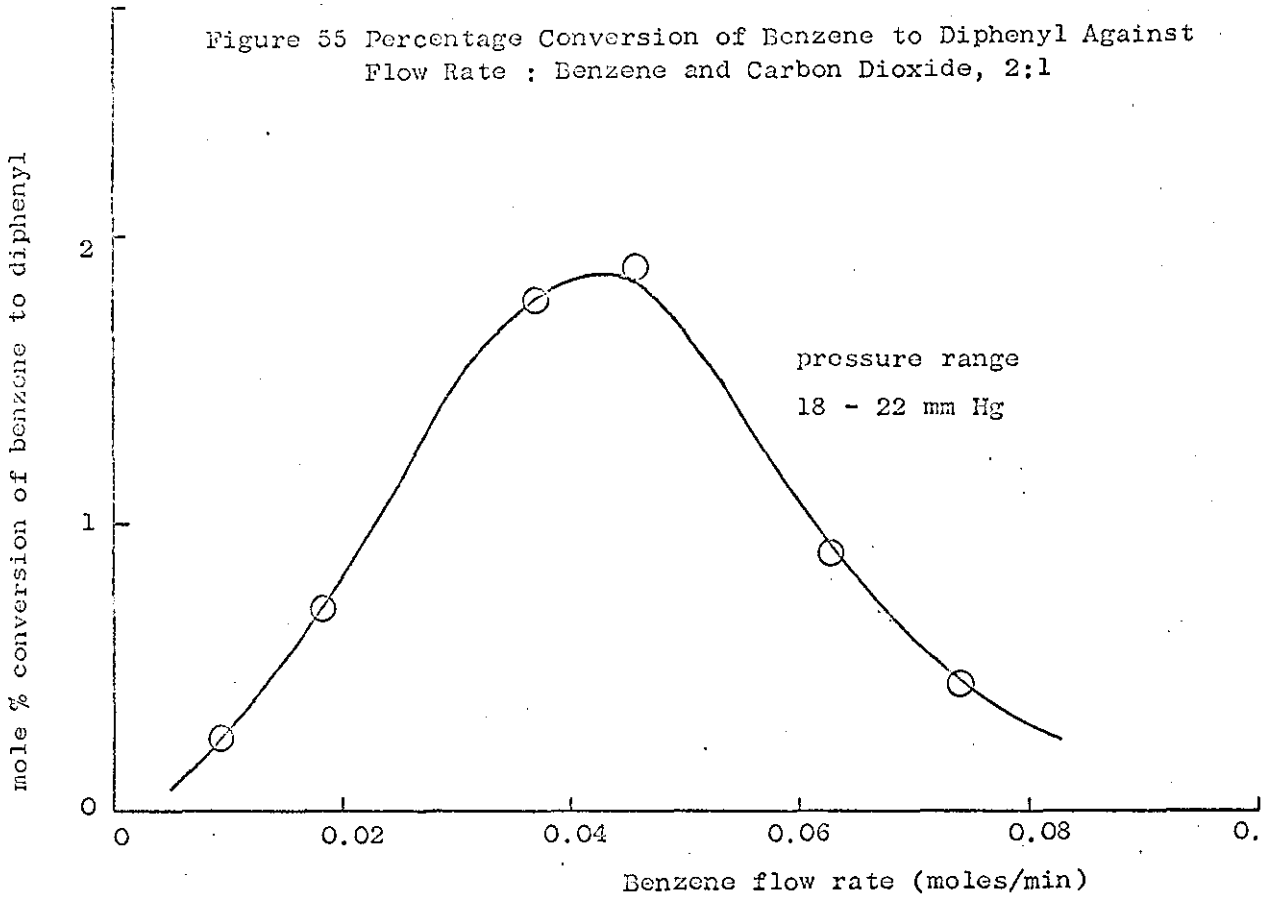

Figure 56 Percentage Conversion of Benzene to Naphthalene Against Flow Rate : Benzene and Carbon Dioxide, 2:1

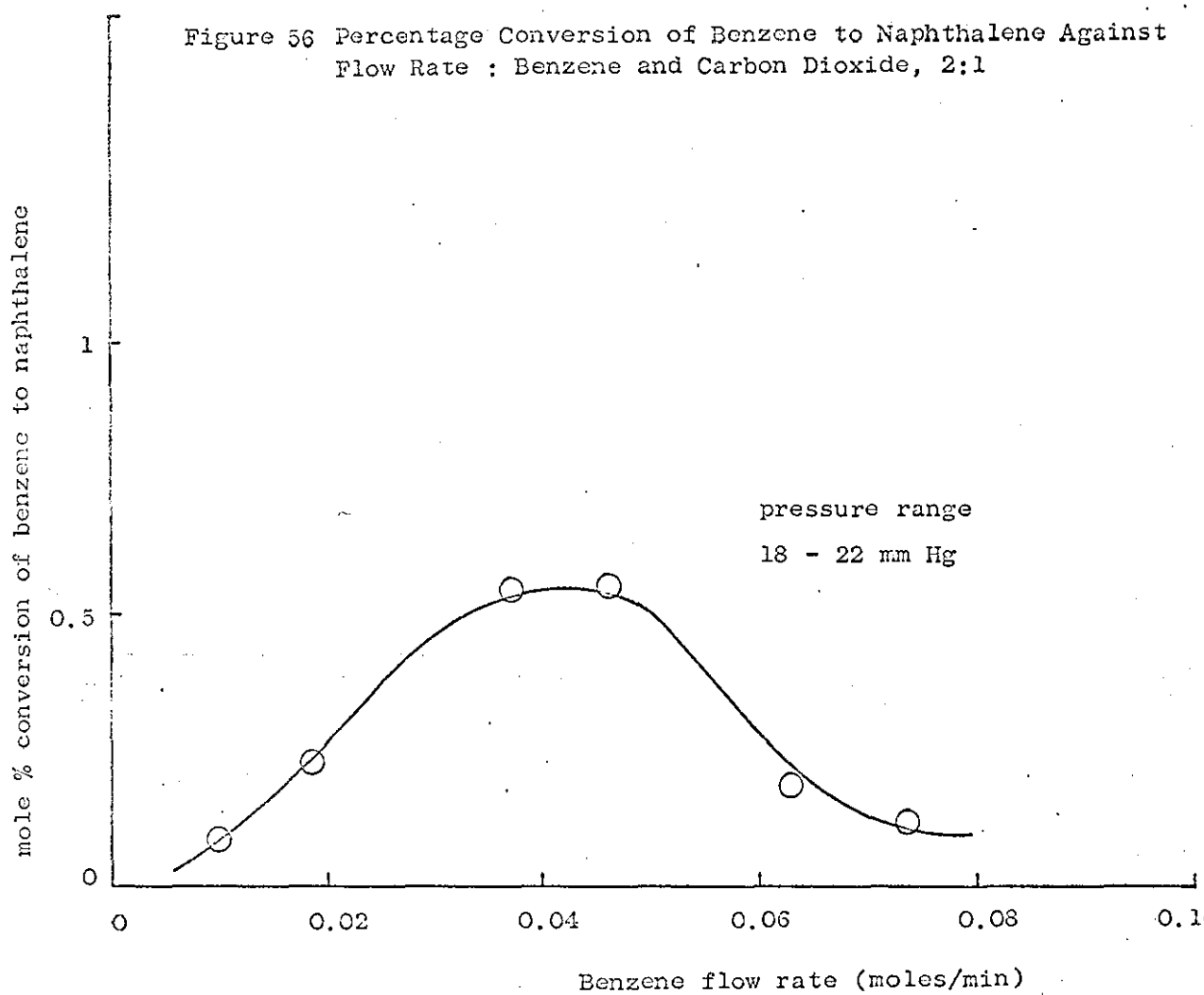

Figure 57 Total Percentage Decomposition of the Benzene Against Flow Rate : Benzene and Carbon Dioxide, 1:1.2

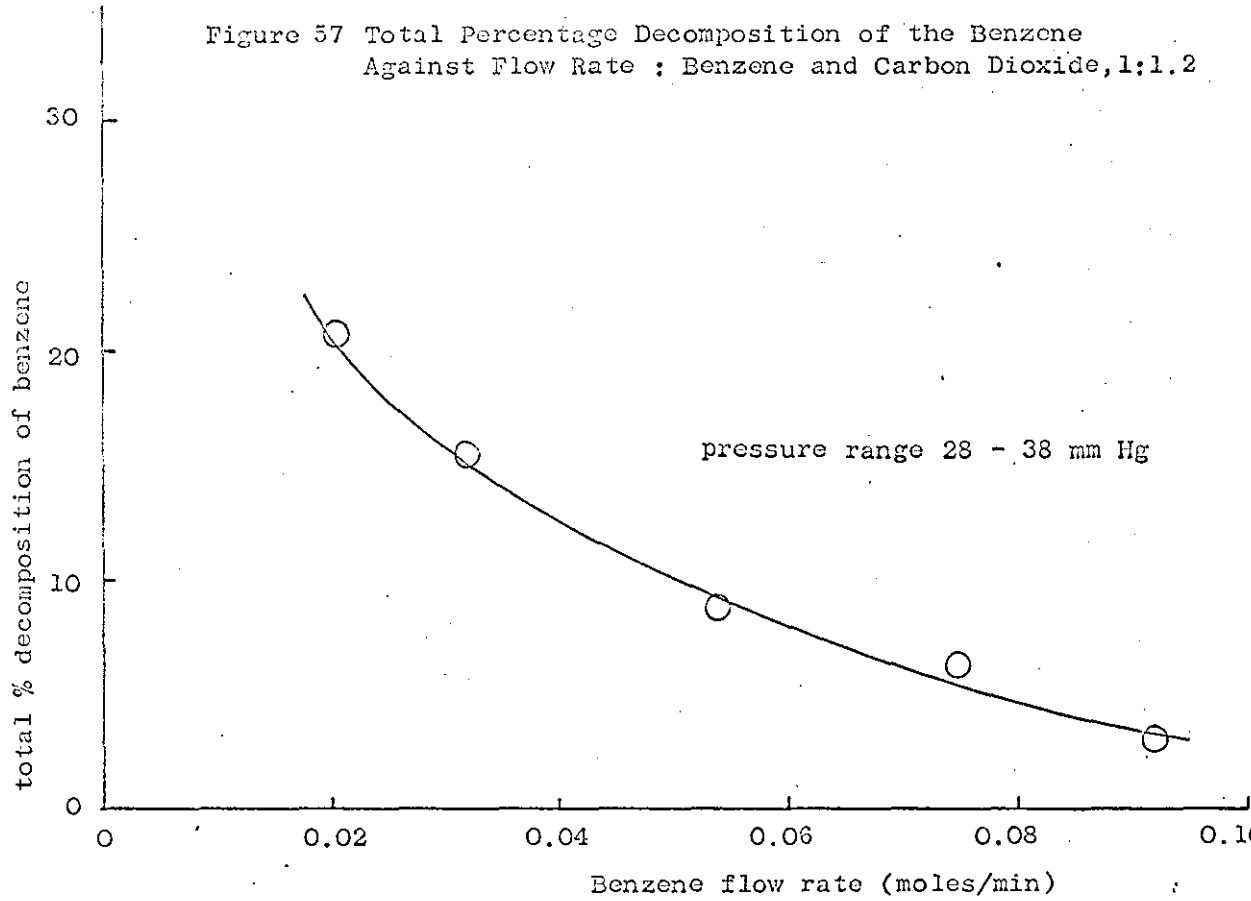

Figure 58 Percentage Conversion of Benzene to Acetylene, Against Flow Rate : Benzene and Carbon Dioxide, 1:1.2

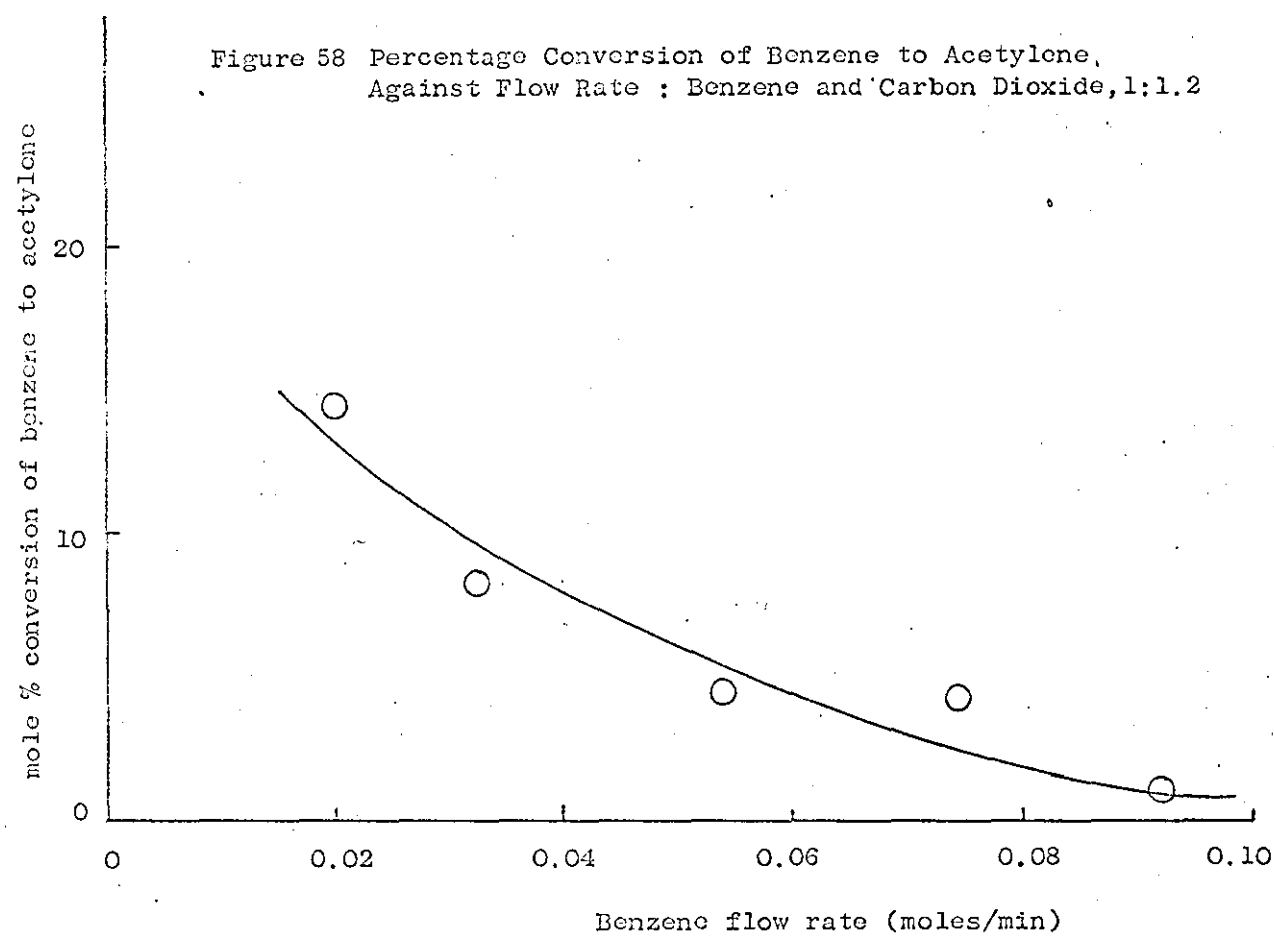

Table 12 Benzene and Ammonia : the Low Boilers

power input 0. 78 Kw reactor pressure 10 - 20 mm Hg

benzene flow rate moles/min.	reactor pressure mm Hg	power absorption Kw	% conversion to 1,3-butadiene
0.0086	15	0.22	trace
0.0106	15	0.22	0.04
0.0152	14	0.21	0.06
0.0263	15	0.22	0.28
0.0349	15	0.22	0.59
0.0486	18	0.21	0.61
0.0518	16	0.21	0.54
0.0525	20	0.22	0.51
0.0804	13	0.20	0.15
	reactor pressure 20 - 30 mm Hg		
0.0235	29	0.24	trace
0.0508	23	0.22	0.34
0.0529	22	0.23	0.23
	reactor pressure 30 - 50 mm Hg		
0.0349	35	0.24	0.38
0.0445	31	0.23	0.34
0.102	31	0.22	0.16

Figure 59 Percentage Conversion of Benzene to Derivatives of Azobenzene Against Flow Rate : Benzene and Ammonia, 1:2

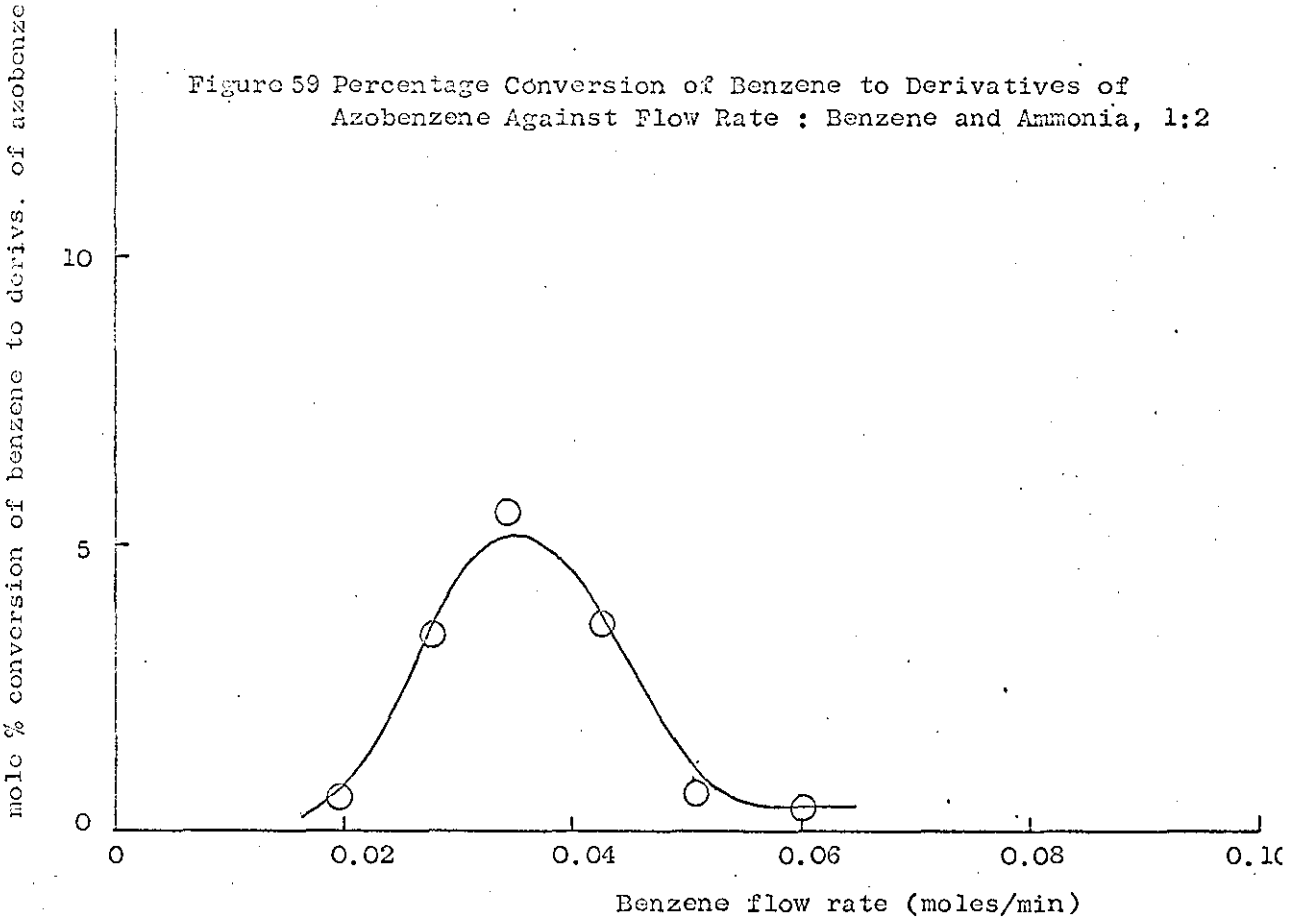

Figure 60 Percentage Conversion of Benzene to 1,3-butadiene Against Flow Rate : Benzene and Ammonia, 1:2

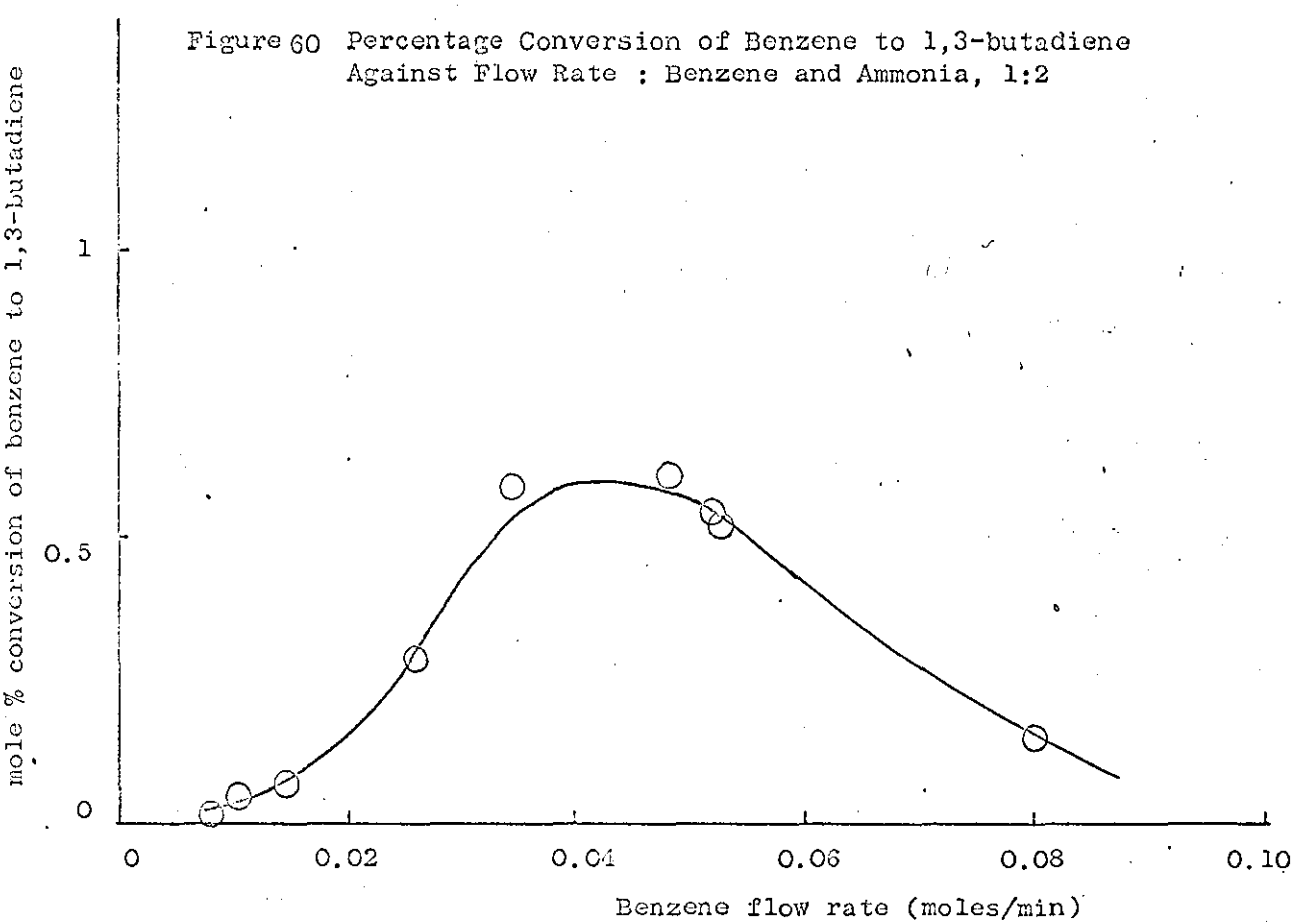

Figure 61 Percentage Conversion of Benzene to Derivatives of Azobenzene as a Function of the Mole Ratio of Ammonia to Benzene

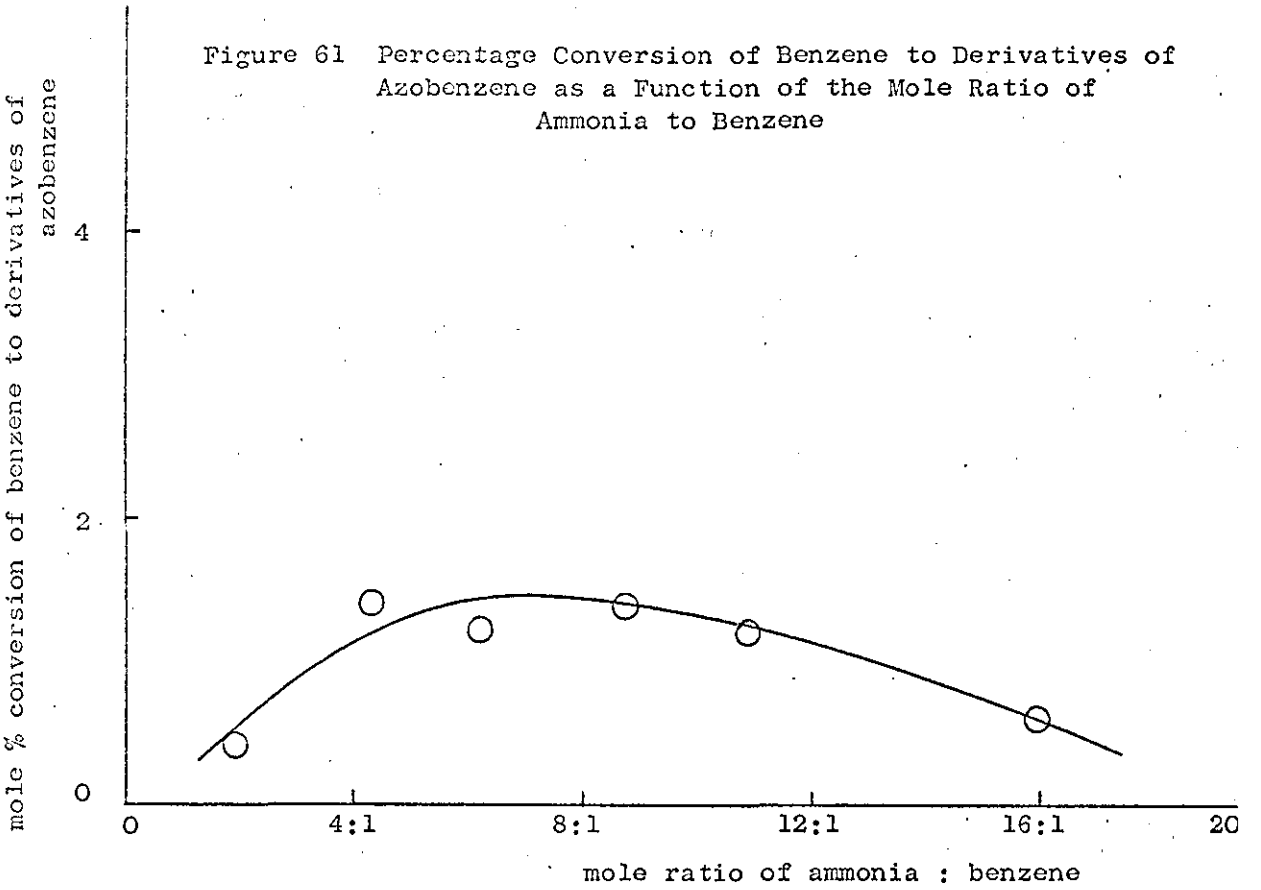

Table 13 Percentage of Nitrogen in the Derivatives of Azobenzene benzene flow rate 0.049 moles/min, pressure range 18 - 58 mm Hg, power input 0.78 Kw.

mole ratio ammonia : benzene	weight % nitrogen
2:1	9.50
3.1:1	15.35
4.4:1	18.42
6.6:1	19.44
7.4:1	22.76
8.8:1	23.64
11:1	24.24
16:1	27.39

The accuracy of the elemental analysis must be regarded with some suspicion; the total percentage of the components C, H, N always being less than 95%. Therefore an error of $\pm$ 15% in the values for the nitrogen percentages above may be present.

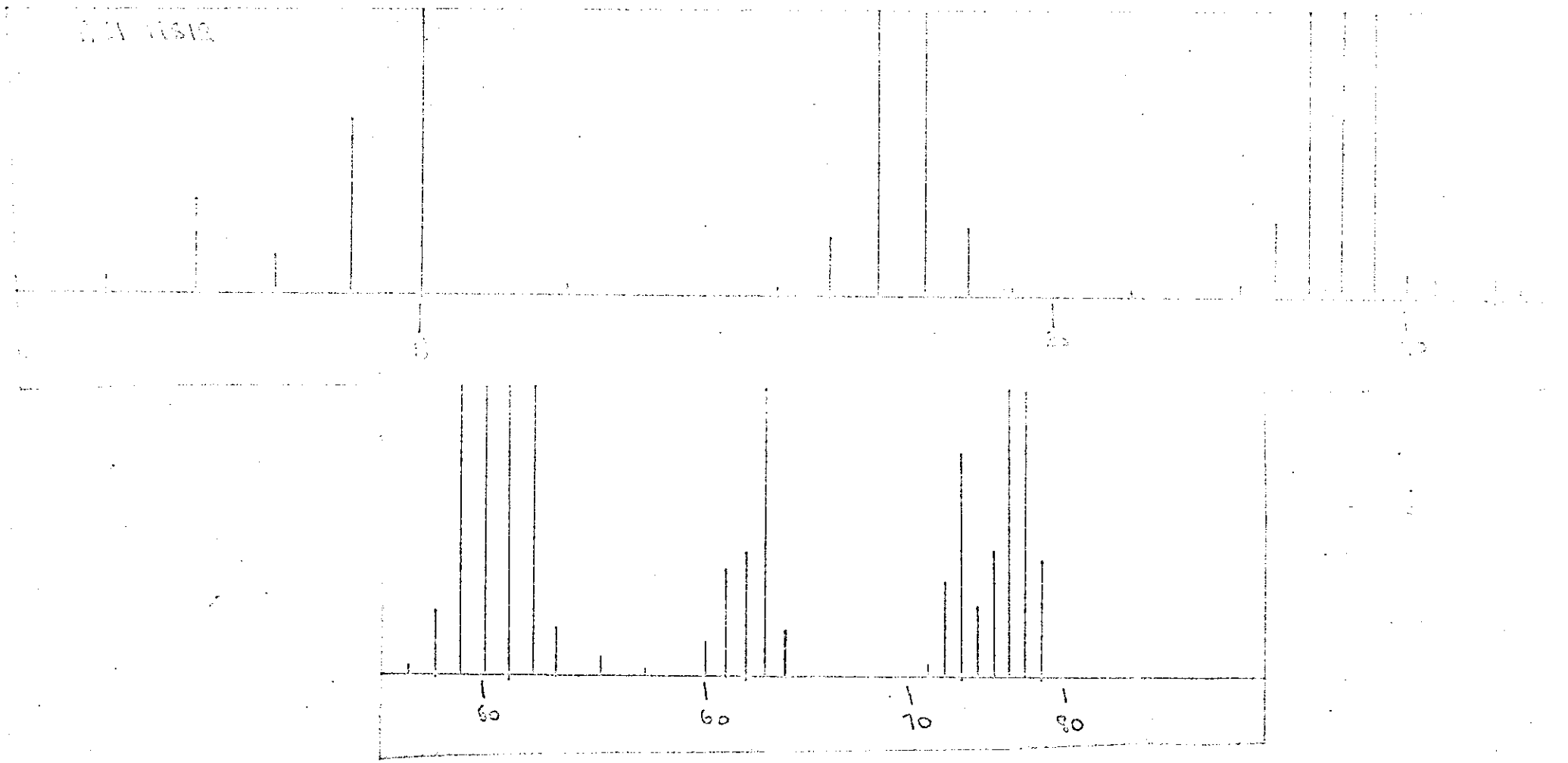

Figure 62 Typical Mass Spectrum, up to m/e 80, of the Azobenzene Derivatives

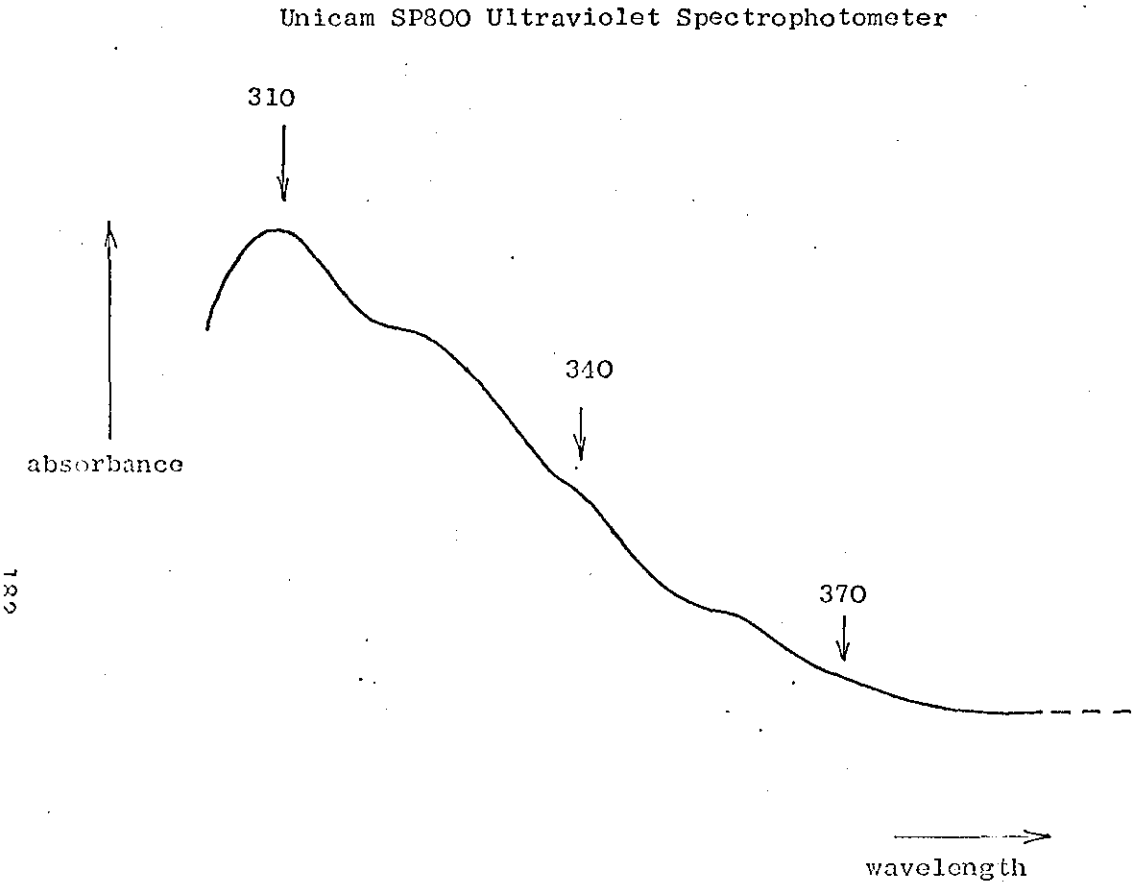

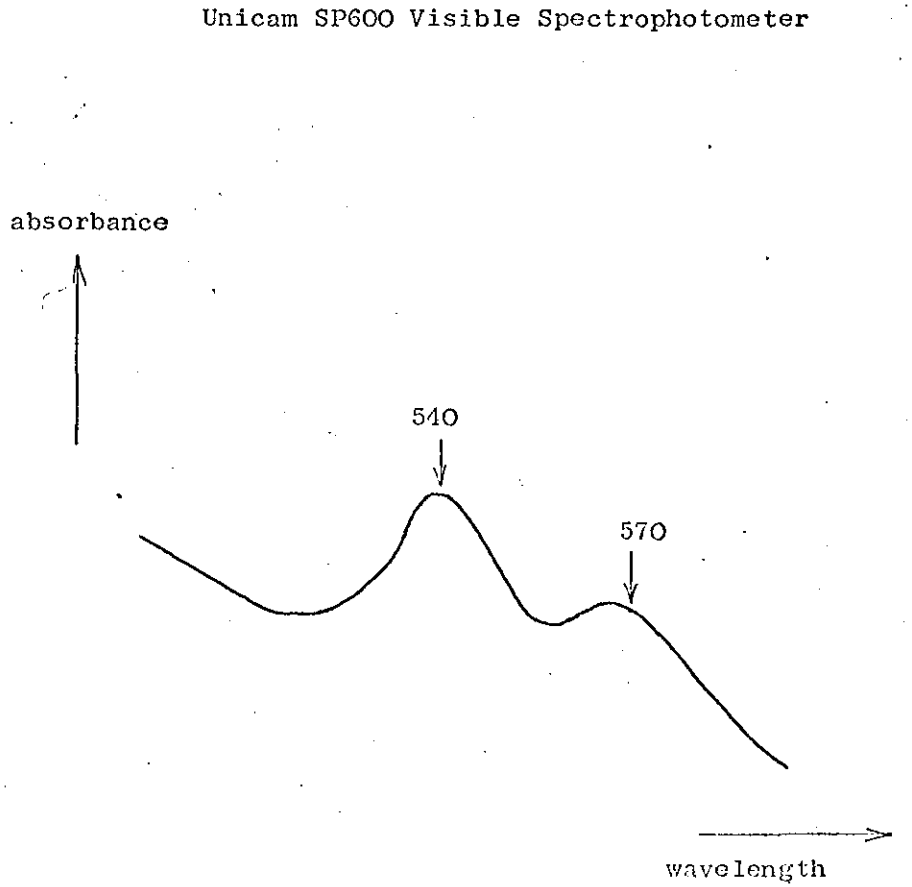

Figure 63 Qualitative Ultraviolet and Visible Spectra of the Derivatives of Azobenzene : Benzene and Ammonia, 1:2

Figure 64 Energy Yield of Azobenzene Derivatives Against Flow Rate

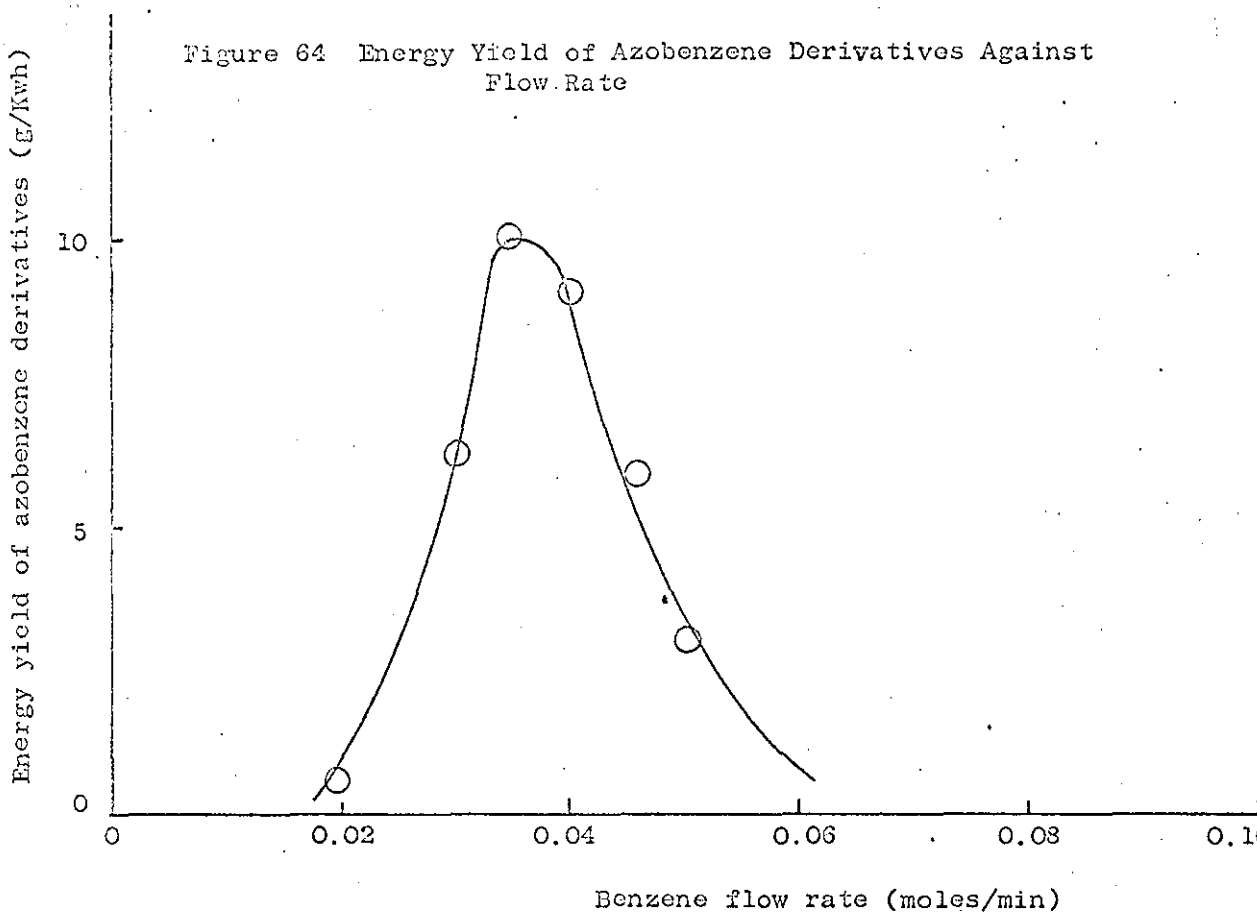

SOME REACTIONS OF CYCLOHEXANE IN THE MICROWAVE DISCHARGE

11. Some Reactions of Cyclohexane in the Microwave Discharge

Scouting experiments had shown the cyclohexane discharge to be influenced by the presence of nickel and admixtures of carbon dioxide in a similar way to the benzene discharge, see section 8.1.2.. It was to investigate this apparent similarity of breakdown in the discharge that experiments were proposed for the following three systems,

(1) discharges in cyclohexane alone.

(2) discharges in cyclohexane in the presence of nickel.

(3) discharges in cyclohexane admixed with carbon dioxide.

Further evidence was also sought to confirm the influence of nickel in the discharge in promoting selective reactions.

11.1. Experimental Details : Cyclohexane Studies

The discharge flow system and analytical procedures were similar to those used in the benzene investigation, see section 10.1. The cyclohexane was of Analar quality from Fisons Chemicals Limited. The carbon dioxide was obtained from Distillers Co. Limited and used without further purification.

In all the experiments conducted on the three systems mentioned above the cyclohexane flow rates varied between 0.007 and 0.18 moles/min., corrected to N.T.P.; the pressures ranged from 10 - 50 mm Hg. The experiments followed those conducted in the benzene discharge. For example, in discharges of mixtures of cyclohexane and carbon dioxide the mole ratios used were 2:1 and 1:1.2.

11.2. Experimental Results

The conditions for G.L.C. analysis of the volatile products were the same as for the benzene investigation.

The volatile products from the discharge were identified by G.L.C. retention time analysis. The range of gaseous products was greater than that found in the benzene discharge. This was mainly because of the greater amount of available hydrogen in the discharge. In the cyclohexane discharge, with or without nickel, the major products were propylene and butene-1. Hydrogen, ethane, ethylene, propane and butane were detected as minor products, i.e. $\lesssim$ 10% conversion of the cyclohexane input. Traces of allene and possibly dicylohexyl were indicated.

The major product of the discharges in cyclohexane and carbon dioxide mixtures was found to be acetylene. Propylene and butene-1 were present as minor products. A quantitative estimation of the free hydrogen was not possible due to interference of the carbon dioxide in the G.L.C. analysis.

The maximum error in the analysis of each low boiling component was $\pm$ 10% except for ethylene and ethane which were subject to an error of $\pm$ 20%. The increased error for the C_2 hydrocarbons arose from an incomplete separation of the component peaks from the tail of the free hydrogen peak in the G.L.C. analysis. Also the on-line G.L.C. analysis only allowed the estimation of total C_3 hydrocarbons, i.e. propane, propylene and allene, and total C_4 hydrocarbons, i.e. butane, butene-1 and 1,3-butadiene. However analysis of the condensed products showed propylene and butene-1 to be the major components of the C_3 and C_4 hydrocarbons respectively.

The cyclohexane flow rates were estimated as being accurate to within $\pm$ 5%. The reactor pressure was measured on a mercury manometer to within $\pm$ 2%. The microwave power

monitors worked to an overall accuracy of ± 15% but with a reproducibility of greater than 95%.

11.3. Discussion of Results

11.3.1. Cyclohexane Alone

The plot of the percentage conversion of the cyclohexane input to the C_2 hydrocarbons, i.e. ethylene and ethane, against flow rate is a shallow curve, see Fig.66a ; the conversion decreasing with flow rate. It should be noted however that the yield of C_2 hydrocarbons increased with flow rate, see Fig. 66a. The conversion of the cyclohexane to ethylene and ethane was pressure dependent over the range investigated, 10 - 50 mm Hg. Semi-quantitative estimations indicated a fairly constant ratio of ethylene to ethane of 2:1. The highest conversion to C_2 hydrocarbons was found to be less than 10% of the cyclohexane input, under the experimental conditions used. In several cases traces of acetylene were found at very low cyclohexane flow rates, <0.008 moles/min.

The plot of conversion to C_3 hydrocarbons of the cyclohexane passed against flow rate showed a sharp maximum reminiscent of the profiles obtained for 1,3-butadiene production in the benzene discharge, see Fig. 67a. A maximum conversion to C_3 hydrocarbons, mostly propylene, of about 18% was noted. Increasing the reactor pressure markedly decreased the conversion to C_3 hydrocarbons.

Fig. 68a shows the conversion of cyclohexane to C_4 hydrocarbons, mostly butene-1, decreased markedly with increasing flow at a constant pressure. The yield of the C_4 hydrocarbons also decreased drastically with increasing

pressure. An interesting feature of the results was that the yield of the C_4 hydrocarbons was always greater than the yield of C_2 hydrocarbons. This suggested a secondary production of C_4 hydrocarbons from the reactions of some C_2 intermediates.

Traces of a compound, possibly dicyclohexyl were found, $<0.1\%$ conversion of the cyclohexane input. Alkyl-substituted cyclohexanes were not found. Slight deposits of an amber coloured solid were formed on the walls of the reactor tube under all the experimental conditions used. Elemental analysis of the solid showed a carbon to hydrogen ratio of 1:1, i.e. unsaturated. Carbon formation was always slight though increasing with pressure. The conversion of cyclohexane to carbon and polymer was $<2\%$ of the cyclohexane input.

11.3.2. Cyclohexane with Nickel Present

In the presence of nickel the conversion to C_2 hydrocarbons was greater by up to one half, at low flow rates 0.02 to 0.04 moles/min, compared with the discharge in cyclohexane alone, see Fig. 66b. Semi-quantitative estimates of the yields of ethylene and ethane indicated a ratio of 2:1. As the flow rate was increased the conversion to C_2 hydrocarbons approximated to that obtained in the discharge in cyclohexane alone. The conversion was independent of pressure over a fairly wide range, 10 - 40 mm Hg.

The percentage conversion of cyclohexane to C_3 hydrocarbons was increased by up to one half, at low flow rates 0.02 to 0.05 moles/min, of that from cyclohexane alone, see Fig. 67b. A maximum conversion to C_3 hydrocarbons

of 28% was found. The conversion of the cyclohexane was also independent of pressure over the pressure range 10 - 40 mm Hg.

At low flow rates, the conversion to C_4 hydrocarbons was noticeably reduced compared with the discharges in cyclohexane alone, see Fig.68b. As before, the yield of C_4 hydrocarbons decreased rapidly with increasing pressure, see Fig.68b.

Traces of a compound, probably dicyclohexyl, were found; $<$ 0.1% conversion of the cyclohexane input. Alkyl-substituted cyclohexanes were not detected. Carbon and polymer formation was slight; $<$ 1% conversion of the cyclohexane input. Acetylene was not detected though this could be attributed to a higher minimum flow rate than that at which acetylene was detected in the discharge in cyclohexane alone.

It should be noted that as the cyclohexane flow rate was increased the yields to C_2, C_3 and C_4 hydrocarbons approximated to those from discharges in cyclohexane alone.

11.4. Hydrogen Balance

The on-line G.L.C. gas analysis separated C_2, C_3 and C_4 hydrocarbons. Unfortunately separation of the individual components such as propylene and propane in the parent C_3 peak was not possible with the on-line gas sampling technique. Analysis of the condensed products had shown propylene and butene-1 to be the major products but exact ratios of the major to minor products such as propane and butane were not possible. The uncertainty as to the ratios of ethylene : ethane, propylene : propane and butene-1 : butane, under all the experimental conditions used, meant that an accurate hydrogen balance was not possible. This

difficulty in calculating a hydrogen balance applied to both the discharges in cyclohexane alone and those in cyclohexane with nickel present.

A hydrogen balance on the discharge products from mixtures of cyclohexane and carbon dioxide was not possible owing to interference of the carbon dioxide in the G.L.C. analysis.

11.5. Visual Observations

Carbon and polymer formation in all cases, with or without nickel, was slight; equivalent to less than 2% of the cyclohexane input. Increasing the cyclohexane flow rate decreased the carbon formation. With nickel present the carbon tended to form on the nickel surface (cf. benzene discharge).

In discharges of mixtures of cyclohexane and carbon dioxide the carbon and polymer formation was negligible, under the experimental conditions investigated.

11.6. Interpretation of Results : Cyclohexane Studies

11.6.1. Mass Spectrometry and Radiolysis Data from the Literature

Abramson and Futrell[137] have investigated, by mass spectrometry, the various ion-molecule reactions of fragment ions produced from cyclohexane. The only secondary species detected were $C_6H_{11}^+$, $C_6H_{10}^+$ and a small amount of $C_4H_9^+$. No ions longer than C_6 were found. They also found that the fragment ions $C_4H_8^+$ and $C_3H_6^+$ from cyclohexane reacted in a similar way to the butene-1 and propylene parent ions, respectively. All fragment ions reacted via the hydride transfer reaction,,

$$R^{+} + C_6H_{12} \longrightarrow RH + C_6H_{11}^{+} \qquad (1)$$

and $C_3H_6^{+}$, $C_4H_8^{+}$ also abstracted H_2 to give $C_6H_{10}^{+}$.

Abramson and Futrell[137] detected an extremely reactive species, $C_2H_4^{+}$. The results indicated the major reaction pathway for $C_2H_4^{+}$ ions from cyclohexane was charge exchange,

$$C_2H_4^{+} + C_6H_{12} \longrightarrow \left(C_6H_{12}^{+}\right)^{*} + C_2H_4$$

The $C_3H_6^{+}$ ion was also shown to undergo this charge exchange reaction.

Dissociation reactions of metastable species such as,

$$\left(C_6H_{12}^{+}\right)^{*} \longrightarrow C_4H_8^{+} + C_2H_4$$
$$\longrightarrow C_5H_9^{+} + CH_3^{\cdot}$$

have been recorded[138]. However these reactions were quenched with increasing pressure and the following competing reaction was thought more likely to occur,

$$\left(C_6H_{12}^{+}\right)^{*} + C_6H_{12} \longrightarrow \left(C_6H_{12}^{+}\right) + \left(C_6H_{12}\right)^{*} \qquad (2)$$

Evidence has been reported of the $C_2H_4^{+}$ reacting with other species from the fragmentation of cyclohexane to give larger ions[139].

Radiolysis experiments on liquid cyclohexane have resulted in the formation of free hydrogen, cyclohexene and bicyclohexyl [140-142]. Mixtures of cyclohexane and cyclohexene have also been subjected to radiolysis[143]. It was found the presence of cyclohexene greatly increased the number of alkyl-substituted cyclohexanes whilst decreasing the yield of short chain C_1 - C_4 products. Comparable gas-phase radiolysis experiments gave a much wider range of products, mainly C_1 - C_4 hydrocarbons, with only slight amounts of cyclohexene and

polycyclohexyls[144,145].

Experiments on the photolysis of cyclohexane at 1236 A and 1048-67 A,[146] showed that an increase in the photon energy resulted in an increase in the relative importance of process producing H atoms or alkyl radicals, while the yields of products attributed to "molecular abstraction" processes, such as the formation of molecular hydrogen, diminished.

From the various investigations reported in the literature several general trends of the possible fragmentation of cyclohexane are indicated. For instance in the gas phase, yields of cyclohexane, dicyclohexyls are small. The higher the energy input the greater the trend away from hydrogen abstraction reactions. Bearing in mind these general points the following list of reactions, postulated from mass spectrometry work, indicates the likely dissociation reactions of cyclohexane in the present work:-

$$C_6H_{12} \xrightarrow{e} C_6H_{12}^{+\cdot} + 2e \qquad (3)$$

$$C_6H_{12}^{+\cdot} \longrightarrow C_5H_9^{+} + CH_3^{\cdot} \qquad (4)$$

$$\longrightarrow C_4H_8^{+\cdot} + C_2H_4 \qquad (5)$$

$$\longrightarrow C_4H_8 + C_2H_4^{+\cdot} \qquad (6)$$

$$\longrightarrow C_2H_5^{+} + 2CH_2 + H^{\cdot} \qquad (7)$$

$$C_6H_{12}^{+} + e \longrightarrow C_3H_6 + C_3H_6 \qquad (8)$$

and the hydrogen abstraction reactions discussed previously.

11.6.2. Interpretation of the Microwave Discharge Results

In the present work the major products of the discharge

in cyclohexane alone were propylene and butene-1. Minor products such as ethylene, ethane, propane, butane and hydrogen were also found. Traces of acetylene, 1,3-butadiene and possibly allene and dicyclohexyl were indicated. The reaction (6),

$$C_6H_{12}^{+\cdot} \longrightarrow C_4H_8 + C_2H_4^{+\cdot}$$

results in the direct formation of butene-1 from the series reaction,

$$\text{cyclohexane} \longrightarrow \text{cyclohexane ion} \longrightarrow \text{butene-1}$$

as indicated by the reaction profile obtained from experimental data, see Fig. 68. Reaction (6) is more likely than reaction (5),

$$C_6H_{12}^{+\cdot} \longrightarrow C_4H_8^{+\cdot} + C_2H_4$$

as the charge usually remains on the smaller fragment. The relatively small yield of ethylene found from experiments tends to confirm that reaction (5) is a minor process.

The yield of butene-1 was always in great excess of the C_2 hydrocarbons under the experimental conditions investigated. Therefore reaction (6) cannot be the only source of C_4 species. Reactions between C_2 fragments to give a C_4 hydrocarbon are unlikely because of the low concentration of excited C_2 fragments in the discharge. The more likely alternative is the attack of the $C_2H_4^{+\cdot}$ fragment on cyclohexane to give a C_8 intermediate which then breaks down to give two molecules of butene-1

$$C_2H_4^{+\cdot} + C_6H_{12} \longrightarrow \left[C_8H_{16}^{+\cdot}\right]^* \xrightarrow{e} C_4H_8 + C_4H_8 \qquad (7)$$

This reaction is possible because of the very active nature of the $C_2H_4^{+\cdot}$ fragment. However no analogue of this reaction is indicated in reported investigations of the radiolysis or mass spectra of cyclohexane.

The $C_2H_4^{+\cdot}$ species could conceivably undergo the hydrogen abstraction reaction found in the radiolysis of cyclohexane,

$$C_2H_4^{+} + C_6H_{12} \longrightarrow C_6H_{10}^{+} + C_2H_6 \qquad (10)$$

$$\downarrow$$

$$C_4H_6 \xleftarrow{e} C_4H_6 + C_2H_4$$

However the importance of these hydrogen abstraction reactions has been found to diminish with increasing pressure, i.e. 5 mm Hg. Therefore in the present work the attack of $C_2H_4^{+\cdot}$ on the cyclohexane, indicated in reaction (7), is more likely to occur.

Evidence has been reported in the literature of the reaction

$$C_6H_{12}^{+\cdot} + e \longrightarrow C_3H_6 + C_3H_6$$

which results in the formation of two molecules of propylene. The reaction profile obtained from the experimental results suggests that the propylene is derived from an intermediate of a series reaction, see section 10.6. Therefore the production of propylene should trace the disappearance of the intermediate $C_6H_{12}^{+\cdot}$. With further experimental data reaction constants could possibly be obtained for the reactions involving $C_6H_{12}^{+\cdot}$.

Traces of acetylene found at very low flow rates in discharges of cyclohexane alone may be formed by reaction (7),

$$C_6H_{12}^{+\cdot} \longrightarrow C_2H_5^{+} + 2C_2H_2 + H^{\cdot}$$

though the energy demand for this reaction is high. Another possibility is the progressive dehydrogenation of cyclohexane to give benzene which then dissociates to give acetylene, see section 10.3.1.

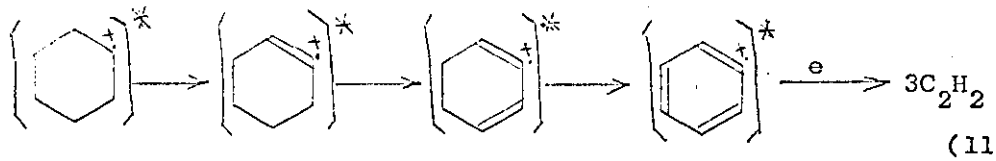

(11)

The mass spectra of samples of the condensed discharge products of cyclohexane showed traces of benzene were present, see Fig. 65. Hence reaction (11) is probably the mechanism for the production of acetylene.

The yields of the C_2, C_3 and C_4 hydrocarbons decreased markedly with increasing pressure. As the total conversion of cyclohexane is reduced this indicates the production of the $C_6H_{12}^{\dagger\cdot}$ species must have been curtailed. The increased collisional deactivation at higher pressures has therefore reduced the ionization of the cyclohexane. The reduction of the cyclohexane decomposition with increasing flow rate can be attributed to the lower residence time of the gas molecules in the discharge zone.

The possible formation of dicyclohexyl in the discharge is probably by a free radical mechanism similar to the production of diphenyl from benzene, see section 10.3.2.

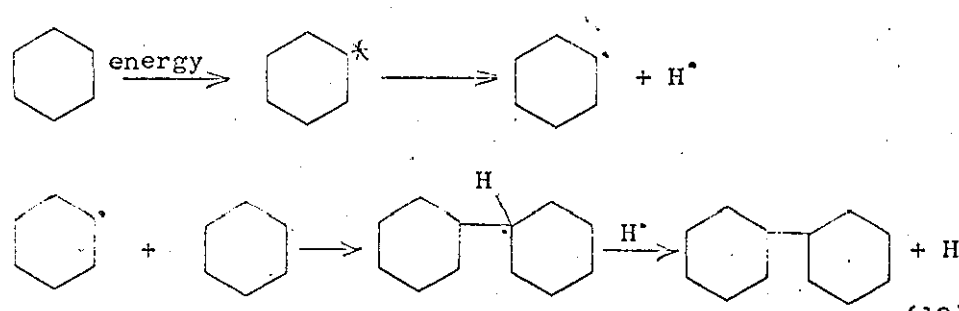

(12)

A reaction scheme can thus be built up to indicate the

possibly mechanisms by which the products of the discharges in cyclohexane are formed:-

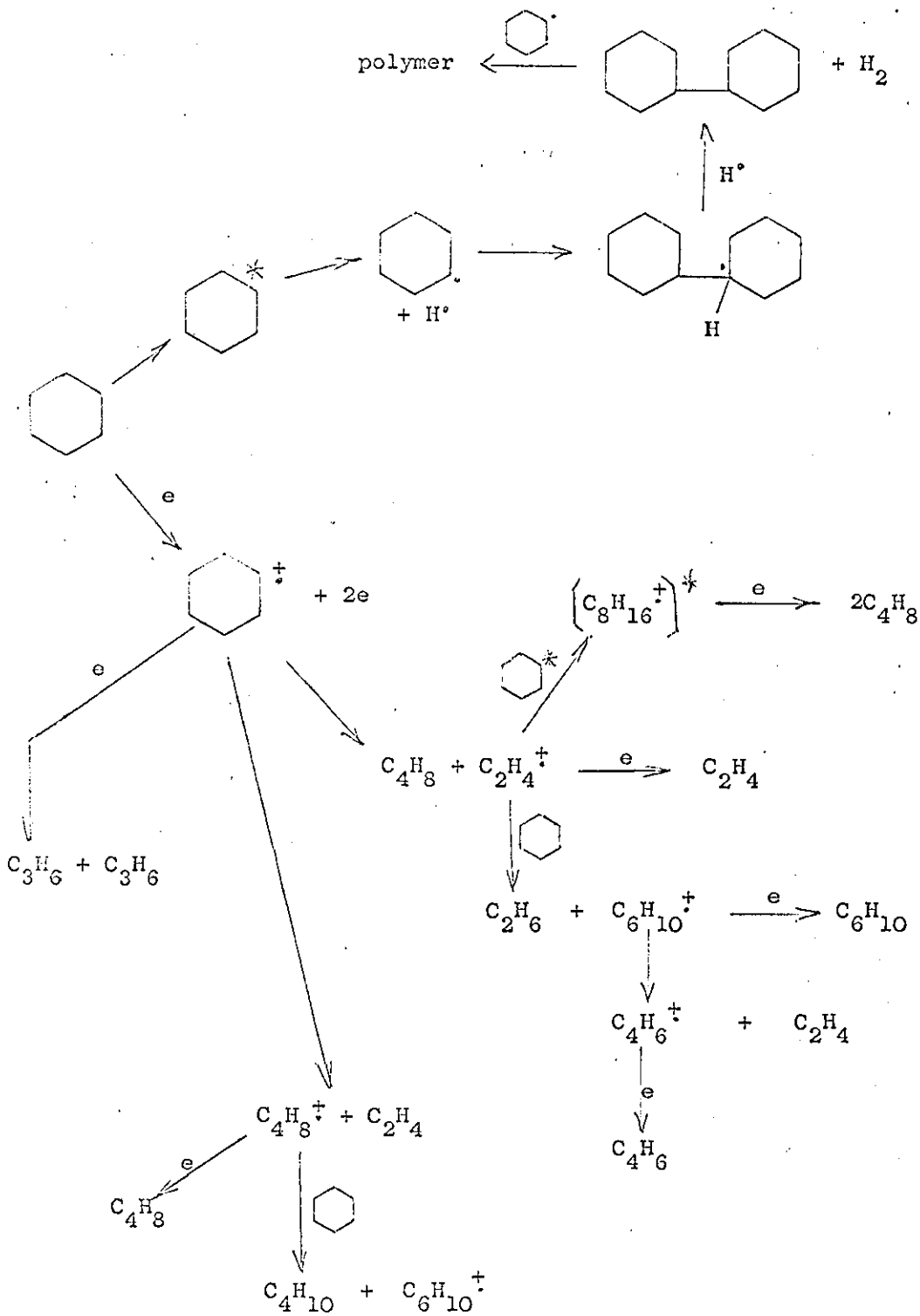

The formation of cyclohexene and benzene postulated in the reaction scheme could not be, unfortunately, determined quantitatively because of interference of the cyclohexane in the G.L.C. analysis.

In the presence of nickel in the cyclohexane discharge the yields of the C_3 hydrocarbons and of the C_2 hydrocarbons were increased at low flow rates, see Fig. 66, 67. The yield of C_4 hydrocarbons was decreased. However the overall percentage decomposition of the cyclohexane was about the same as for the discharges in cyclohexane alone. This suggests the nickel selectively promoted such reactions as,

$$C_6H_{12}^{+\cdot} \xrightarrow{e} C_3H_6 + C_3H_6 \qquad (8)$$

The increase in the C_2 yield with a consequent decrease in the C_4 hydrocarbon yield suggests either:

(a) the promotion of the reaction (5)

$$C_6H_{12}^{+\cdot} \longrightarrow C_4H_8^{+\cdot} + C_2H_4$$

rather than reaction (6) which leads to the $C_2H_4^{+\cdot}$ species. This would explain the increase in the conversion to C_2 hydrocarbons consequent with a decrease in the C_4 hydrocarbon yield as reaction (9) would be prevented. This would also explain why reaction (8) is only promoted at low flow rates. At high flow rates less $C_6H_{12}^{+\cdot}$ species would reach the nickel surface and thus the effect of catalysing reaction (8) would be greatly decreased.

or

(b) the deactivation of the excited $C_8H_{16}^{+\cdot}$ intermediate of reaction (9) which then proceeds via the hydrogen abstraction reaction of reaction (10)

$$C_2H_4^{+\cdot} + C_6H_{12} \longrightarrow \left(C_8H_{12}^{+\cdot}\right)^* \xrightarrow{M} C_2H_6 + C_6H_{10}^{+\cdot} \longleftarrow C_8H_{12}^{+\cdot} \qquad (10)$$

The decrease in yield of the C_4 hydrocarbons occurs only at low flow rates. This seems to indicate that the nickel acts via (b). As the flow rate was increased, the $\left(C_8H_{12}^{+\cdot}\right)^*$ could not diffuse to the nickel surface before fragmentation via reaction (9) occurred.

11.7. Cyclohexane and Carbon Dioxide

11.7.1. Discussion of Results : Cyclohexane to Carbon Dioxide 2:1

At a mole ratio of cyclohexane to carbon dioxide of 2:1 the conversion to both C_3 and C_4 hydrocarbons was approximately constant over a wide range of flow rates, at a constant pressure. The yields of C_3 and C_4 hydrocarbons decreased with increasing pressure. The maximum conversion to C_3 hydrocarbons was about 5% and to C_4 hydrocarbons about 7% at pressures between 20 - 30 mm Hg, and flow rates of 0.01 to 0.12 moles/min. These are widely differing values to those obtained in the cyclohexane discharge, with or without nickel.

Accurate estimates of the conversion to ethylene and ethane and also free hydrogen were not possible owing to interference of the carbon dioxide in the G.L.C. analysis. Semi-quantitatively the yields of ethylene and ethane appeared low, $\angle$ 2% conversion of the cyclohexane input. A feature of great interest was the high conversion to acetylene at low flow rates 0.01 to 0.04 moles/min. of up to 50% of the cyclohexane input. The conversion to acetylene was also pressure independent. It should be noted however that the

overall percentage decomposition was still much less than for the discharge in cyclohexane alone.

Polymer and carbon formation was negligible. Oxygen-containing products were not detected.

11.7.2. Cyclohexane and Carbon Dioxide : 1:1 and Carbon Dioxide in Excess

At mole ratios cyclohexane to carbon dioxide of 1:1 and with carbon dioxide in excess the overall percentage decomposition of cyclohexane was $\angle$ 10% under all the experimental conditions investigated. Only traces of acetylene were found at very low flow rates. The conversion to other C_2 hydrocarbons was less than 1% and to the C_4 hydrocarbons less than 4% The conversion to C_3 hydrocarbons was approximately the same as found when the cyclohexane was in excess.

Polymer and carbon formation was negligible. Oxygen-containing products were not detected.

11.8. Interpretation of Results

At a mole ratio of cyclohexane to carbon dioxide of 0.5:1 the drastic change in the product distribution and the overall reduction in product yields indicated that the carbon dioxide was interfering in the dissociation of the cyclohexane ion. The drastic reduction in the formation of the usual products, mainly propylene and butene-1, suggests that the carbon dioxide prevented the ionization of the cyclohexane. This is reminiscent of the effect of carbon dioxide in the benzene discharge, see section 10.8.2. The ionization potential of cyclohexane is $\sim$ 10.30 eV, less than that of the excited levels found in carbon dioxide. It is postulated therefore that the carbon dioxide, either deactivated the excited molecules by collision or, by a scavenging process,

removed the high energy electrons necessary for the ionization of cyclohexane. With increasing pressure the effect of the carbon dioxide would be even greater and the decomposition of the cyclohexane by ionization process should decrease. This is confirmed by the experimental results.

If the ionization of the cyclohexane was blocked, the production of acetylene must have proceeded via another mechanism. A reaction mechanism has already been postulated, see section 11.6.2. the acetylene being produced from the dissociation of benzene molecules derived from the dehydrogenation of excited cyclohexane molecules.

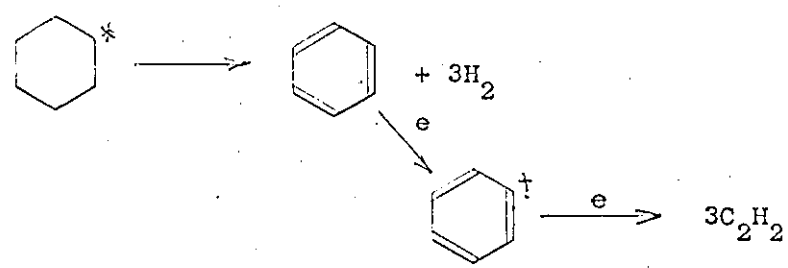

Acetylene was only found at low pressures $\lesssim$ 30 mm Hg. At higher pressures the successive dehydrogenation of a cyclohexane molecule would be unlikely in view of the greater collision frequency.

At higher mole ratios of carbon dioxide to cyclohexane the overall decomposition of the cyclohexane was reduced further and was dependent on pressure. This can be explained by the higher concentration of carbon dioxide in the discharge amplifying the deactivating and/or electron-scavenging processes discussed above. Acetylene was not detected but this may be due to the higher reactor pressures, $\gtrsim$ 40 mm Hg, enforced on the flow system by the higher mole ratios of carbon dioxide to benzene.

The conversion to C_3 hydrocarbons was favoured as evidenced by the experimental data. This indicates the energetics of the reaction to C_3 hydrocarbons must be more favourable than a C_2 : C_4 fragmentation; the twisting vibration of the chair and boat forms of cyclohexane may lower the activation energy required for the C_3 : C_3 fragmentation. Carbon and polymer formation was negligible.

11.9. Conclusions : Cyclohexane Studies

The cyclohexane studies though not particularly interesting from a commercial viewpoint have confirmed that the presence of nickel in the discharge zone improves the selectivity of certain reactions. The decomposition of the cyclohexane could be varied by varying flow rate or pressure. Carbon dioxide blocked the ionization of the cyclohexane and this led to the production of the new product, i.e. acetylene indicating a possible new technique in discharge chemistry.

EXPERIMENTAL DATA :

CYCLOHEXANE STUDIES

Table 14a Cyclohexane Alone : the Low Boilers

power input 0.78 Kw reactor pressure 10 - 20 mm Hg

cyclohexane flow rate, moles/min.	reactor pressure mm Hg	power absorption Kw	% conversion to C_2 hydrocarbons	% conversion to C_3 hydrocarbons	% conversion to C_4 hydrocarbons
0.0115	10	0.23	8.45	12.50	52.20
0.0169	19	0.23	7.99	13.80	39.50
0.0198	15	0.23	7.30	17.24	38.20
0.0260	19	0.23	6.92	17.26	30.96
0.0335	16	0.23	5.82	14.5	23.45
0.0446	13	0.24	5.41	9.30	15.28
0.0518	16	0.24	3.89	9.78	13.40
0.0567	15	0.23	4.61	7.32	13.98
0.0583	15	0.23	3.94	6.20	12.54
0.0647	17	0.23	4.20	6.50	11.08
0.0648	12	0.22	3.84	6.39	11.94
0.0723	16	0.22	3.45	6.94	10.04
0.109	19	0.22	1.05	5.44	7.99

Table 14b Cyclohexane Alone : the Low Boilers

reactor pressure 20 - 30 mm Hg

cyclohexane flow rate, moles/min.	reactor pressure mm Hg	power absorption Kw	% conversion to C_2 hydrocarbons	% conversion to C_3 hydrocarbons	% conversion to C_4 hydrocarbons
0.0232	27	0.23	6.21	13.97	20.16
0.0309	21	0.23	5.17	11.41	17.40
0.0378	26	0.23	4.63	9.86	11.23
0.0463	21	0.23	3.73	8.70	5.62
0.0571	24	0.23	2.58	6.35	4.15
0.0975	23	0.22	2.52	4.50	2.96
	reactor pressure 30 - 50 mm Hg				
0.0156	34	0.23	4.41	6.05	18.85
0.0278	36	0.24	3.05	8.10	10.54
0.0325	32	0.23	2.58	7.35	8.65
0.0506	37	0.23	2.00	3.95	5.10
0.0718	41	0.23	1.95	3.13	3.25
0.0873	42	0.23	1.89	2.05	2.78

Table 15a Cyclohexane and Nickel : the Low Boilers

power input 0.78 Kw reactor pressure 10 - 20 mm Hg

cyclohexane flow rate, moles/min.	reactor pressure mm Hg	power absorption Kw	% conversion to C_2 hydrocarbons	% conversion to C_3 hydrocarbons	% conversion to C_4 hydrocarbons
0.0142	16	0.24	17.59	18.92	41.22
0.0155	19	0.24	14.95	25.40	17.27
0.0238	17	0.24	13.99	27.54	21.71
0.0249	17	0.24	13.69	25.12	16.78
0.0310	19	0.24	11.95	25.40	17.27
0.0336	17	0.23	11.17	26.32	13.70
0.0368	17	0.24	9.69	22.12	16.08
0.0478	15	0.24	9.95	15.8	9.95
0.0595	17	0.23	6.54	13.2	9.54
0.0836	19	0.23	4.27	6.95	8.23

Table 15b Cyclohexane and Nickel : the Low Boilers

power input 0.78 Kw reactor pressure 20 - 30 mm Hg

cyclohexane flow rate, moles/min.	reactor pressure mm Hg	power absorption Kw	% conversion to C_2 hydrocarbons	% conversion to C_3 hydrocarbons	% conversion to C_4 hydrocarbons
0.0210	23	0.23	14.56	25.32	13.56
0.0432	25	0.24	8.46	16.03	6.25
0.0643	28	0.23	5.75	9.95	4.53
0.0730	24	0.23	4.70	9.42	4.20
0.0990	24	0.24	3.54	6.09	3.54
		reactor pressure 30 - 50 mm Hg			
0.0156	35	0.24	18.95	22.15	9.97
0.0315	42	0.24	10.80	21.83	5.63
0.0440	44	0.24	8.75	15.05	3.55
0.0513	32	0.24	7.20	14.46	3.00
0.0650	33	0.24	5.84	9.85	2.85

Figure 66a Percentage Conversion of Cyclohexane to C_2 Hydrocarbons Against Flow Rate : Cyclohexane Alone

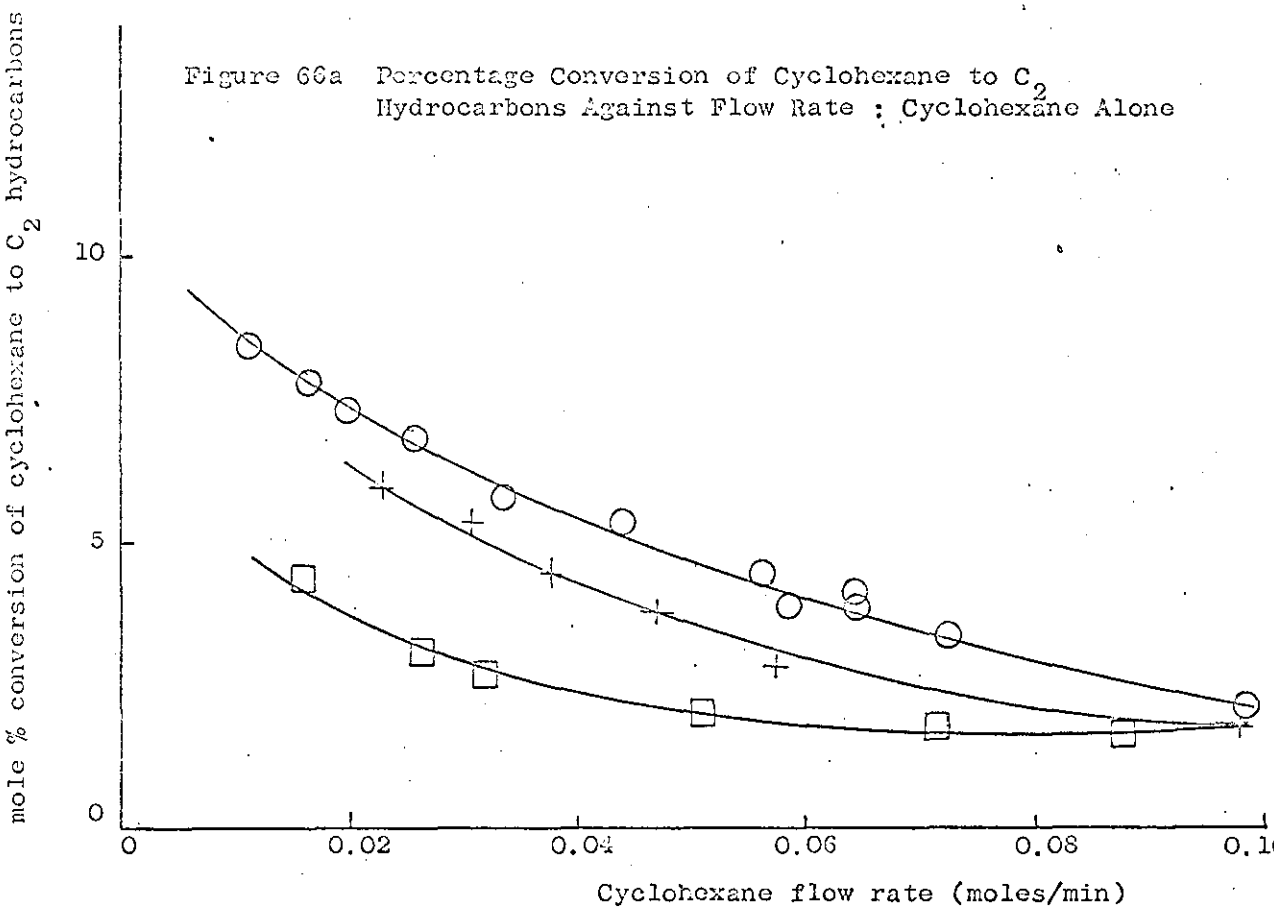

Figure 66b Percentage Conversion of Cyclohexane to C_2 Hydrocarbons Against Flow Rate : Cyclohexane and Nickel

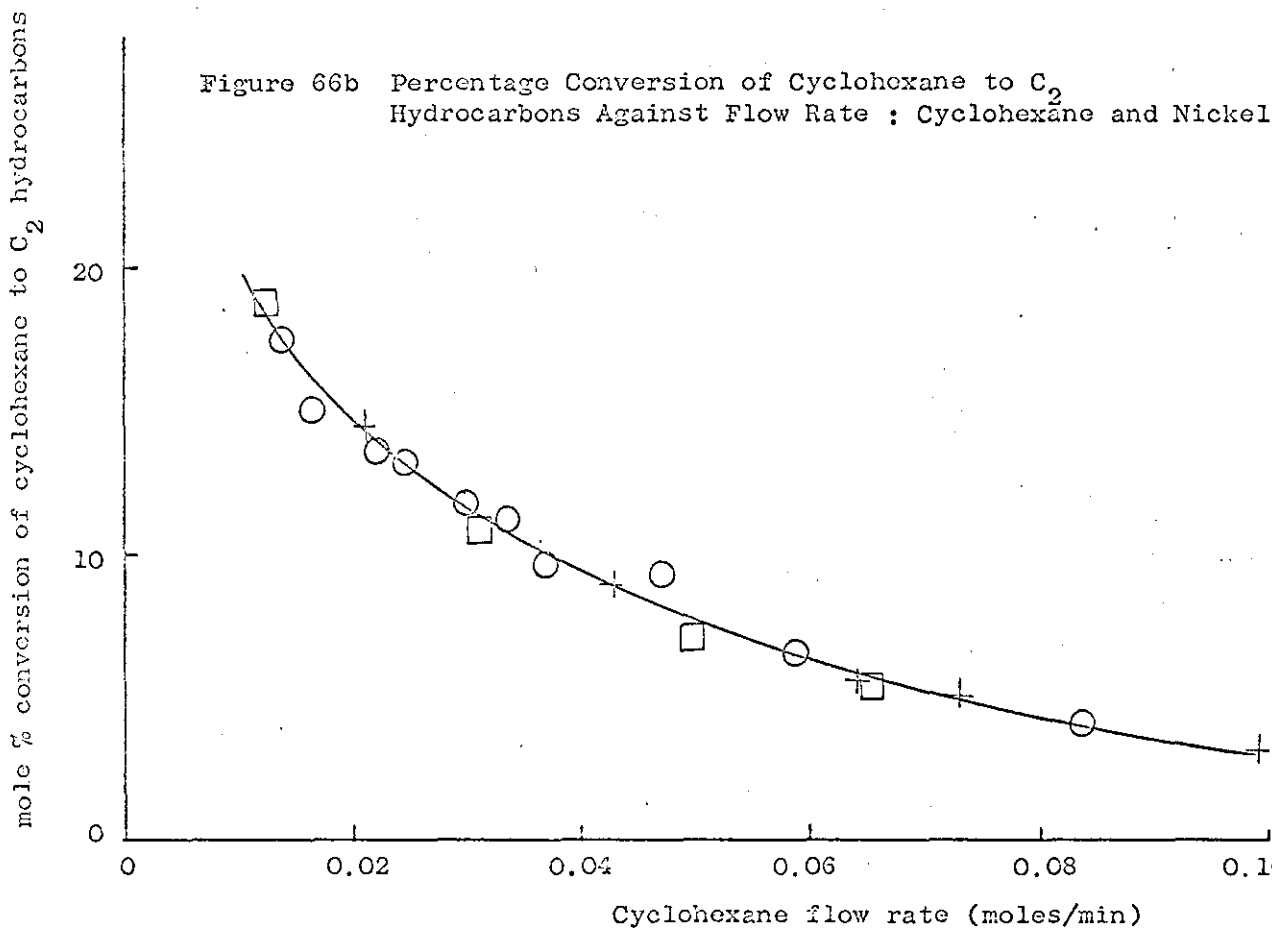

Figure 67a Percentage Conversion of Cyclohexane to C_3 Hydrocarbons Against Flow Rate : Cyclohexane Alone

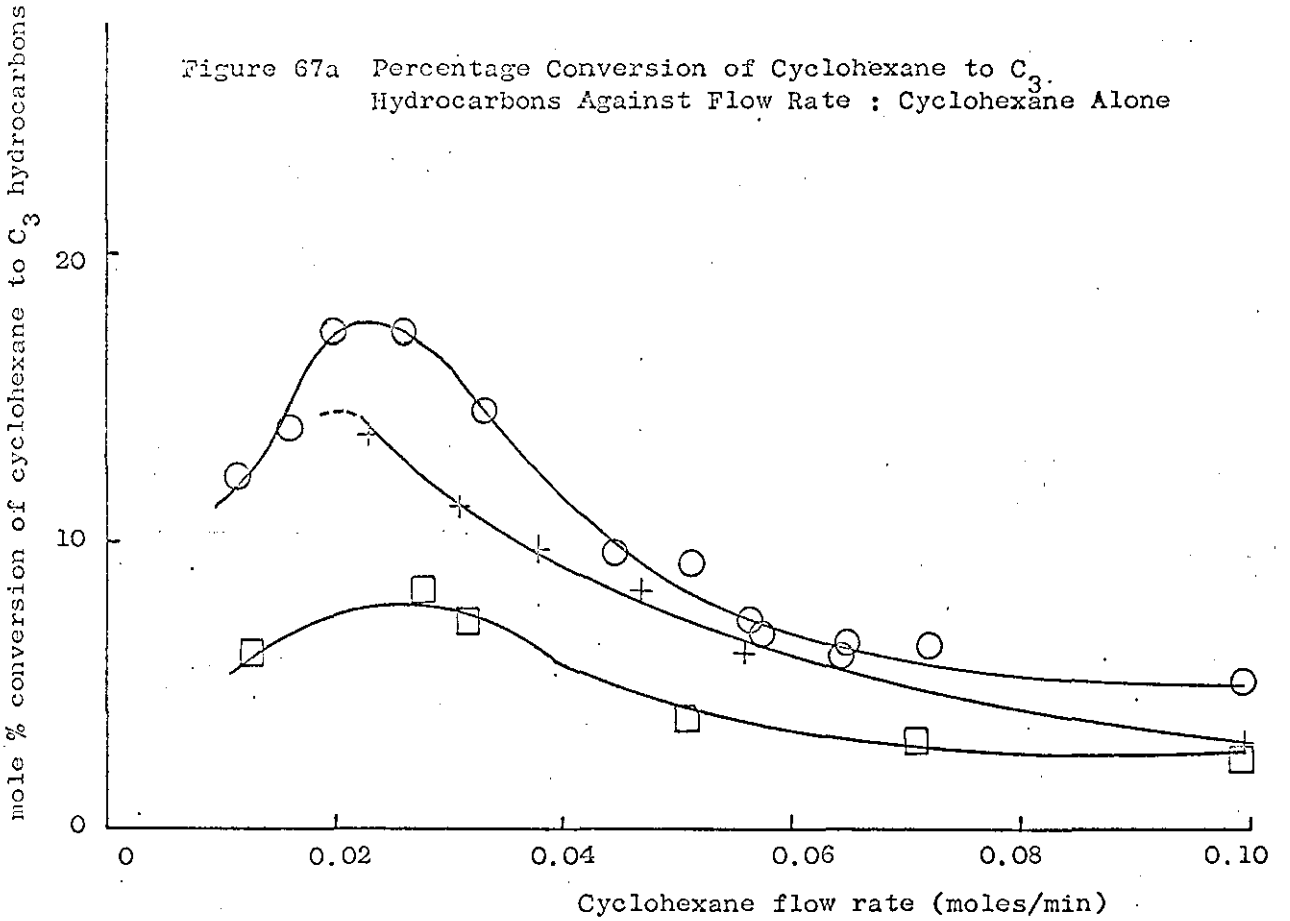

Figure 67b Percentage Conversion of Cyclohexane to C_3 Hydrocarbons Against Flow Rate : Cyclohexane and Nickel

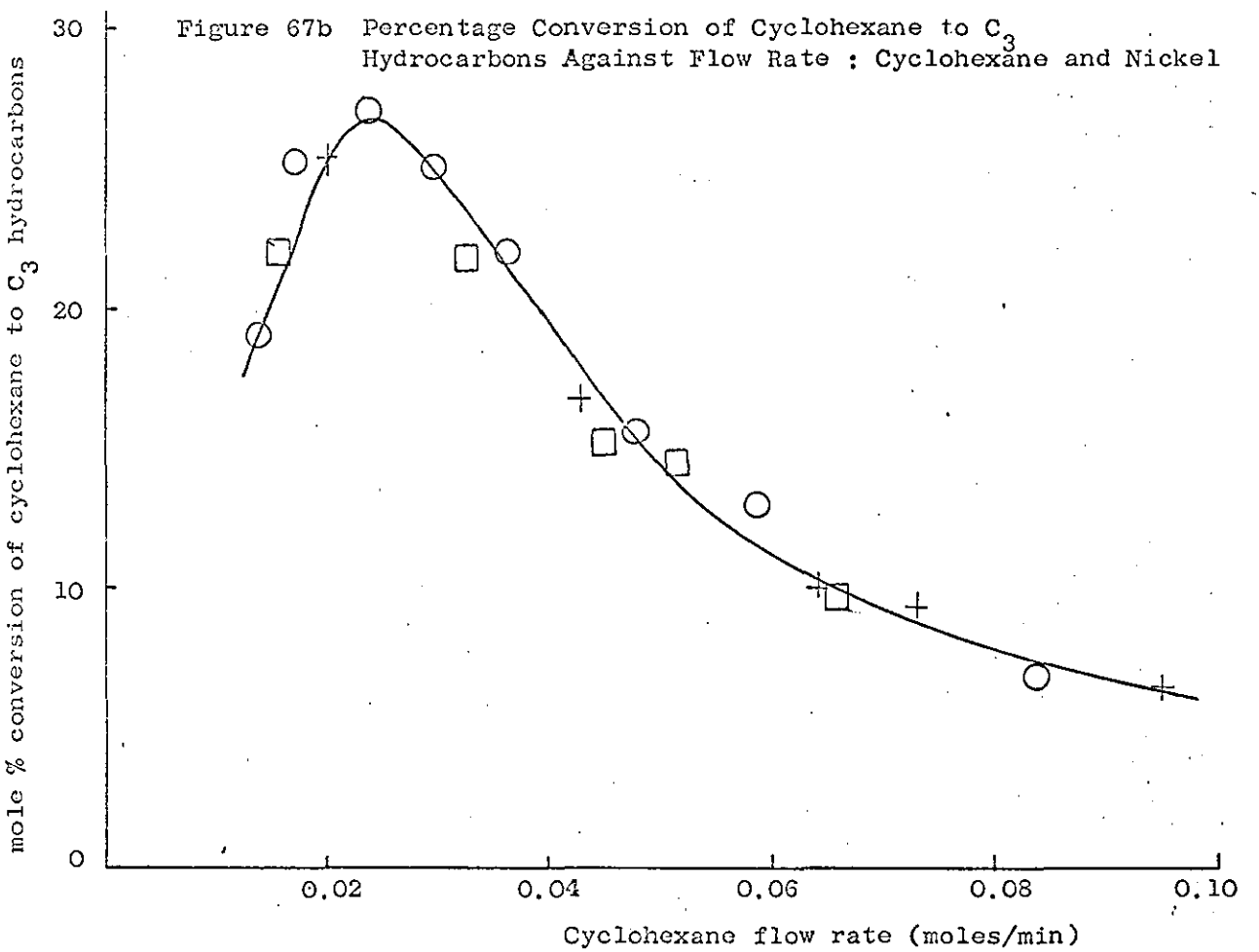

Figure 68a Percentage Conversion of Cyclohexane to C_4 Hydrocarbons Against Flow Rate : Cyclohexane Alone

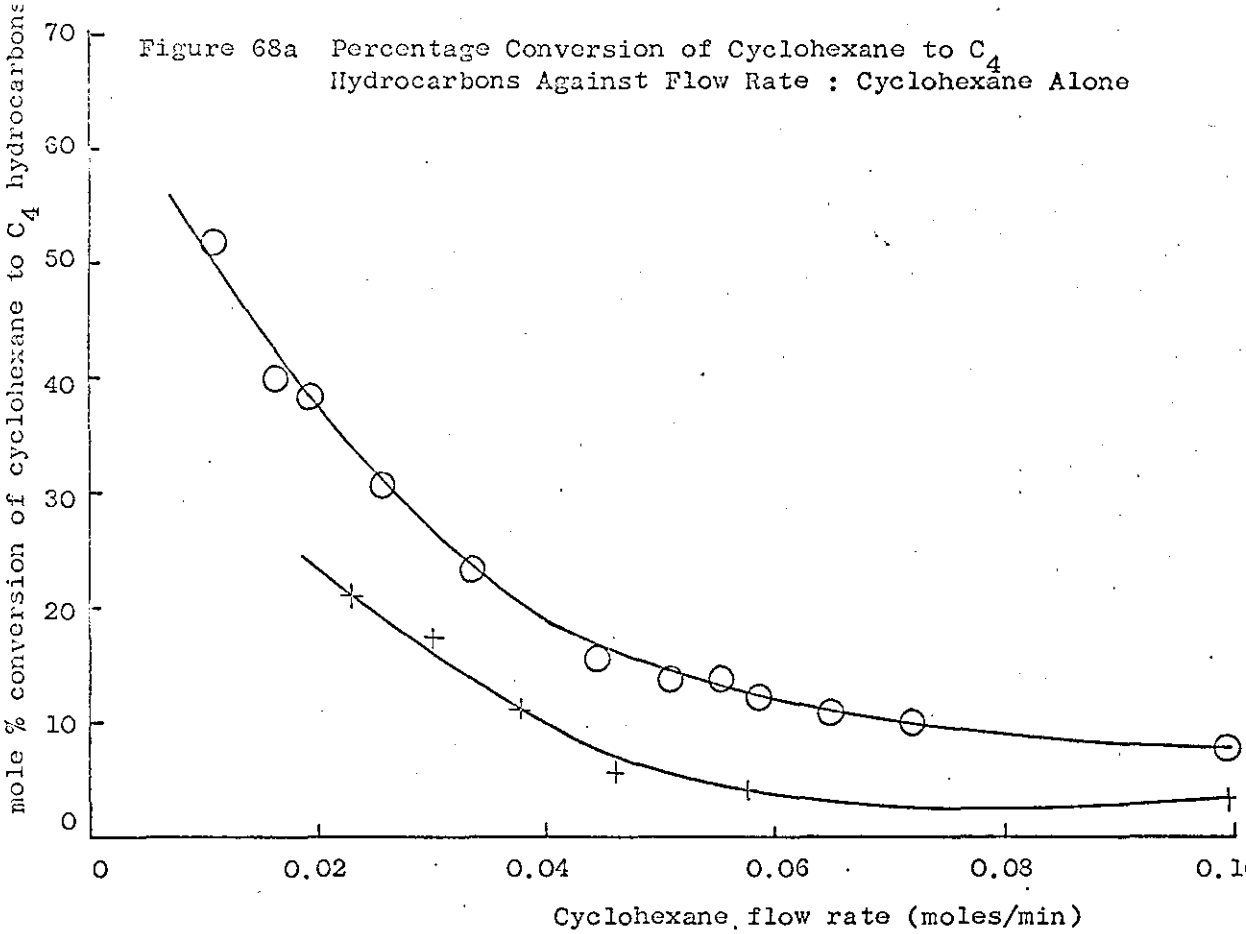

Figure 68b Percentage Conversion of Cyclohexane to C_4 Hydrocarbons Against Flow Rate : Cyclohexane and Nickel

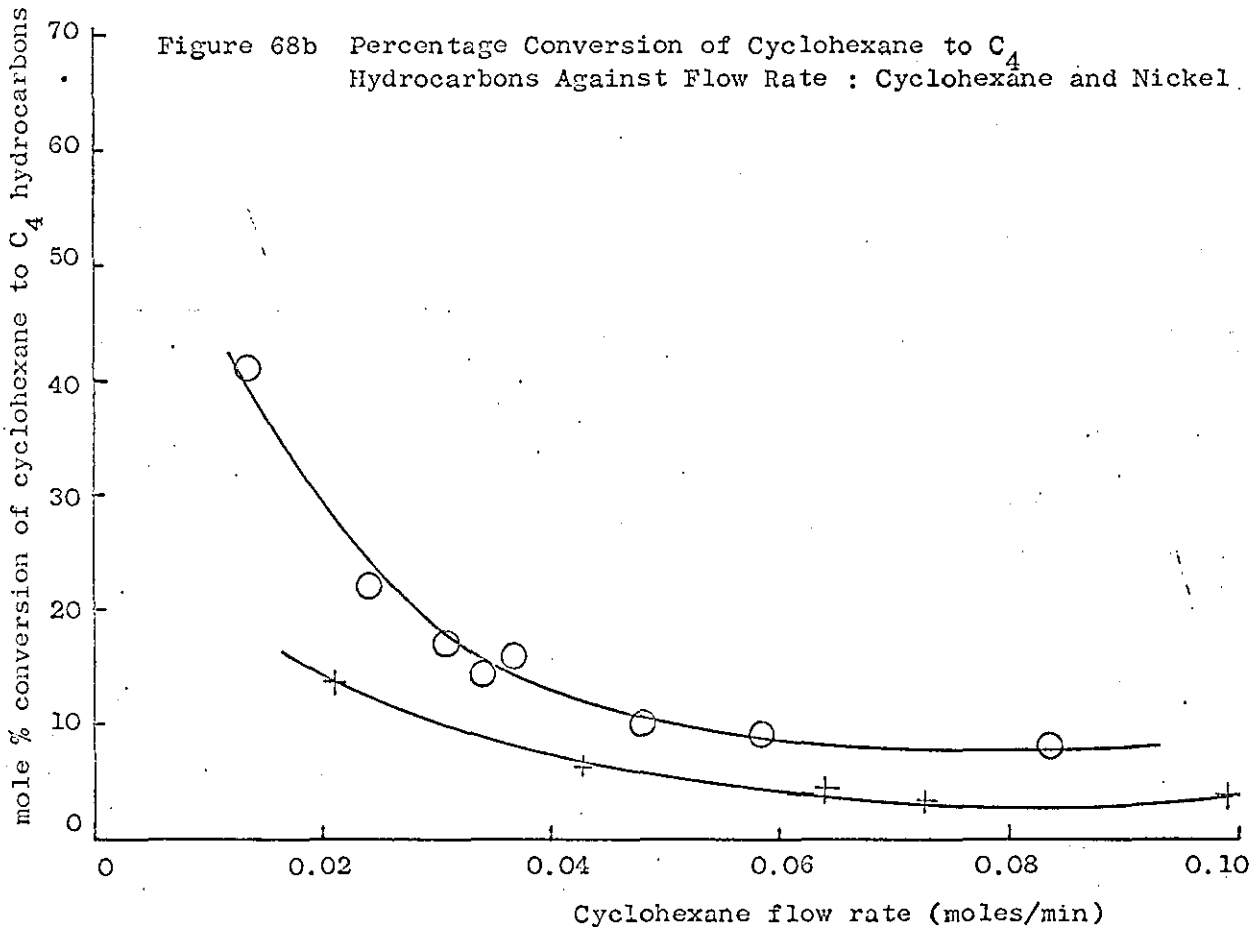

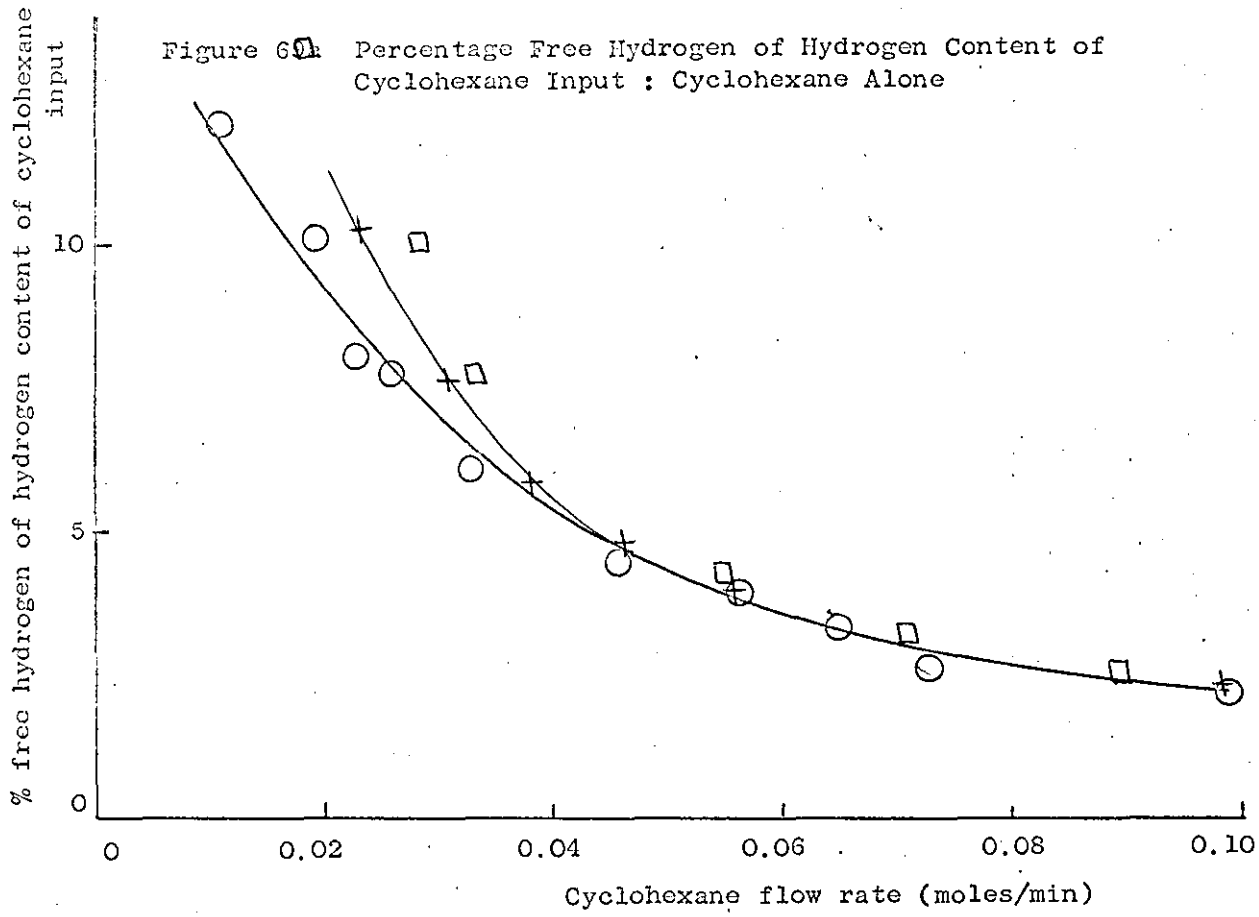

Figure 69a Percentage Free Hydrogen of Hydrogen Content of Cyclohexane Input : Cyclohexane Alone

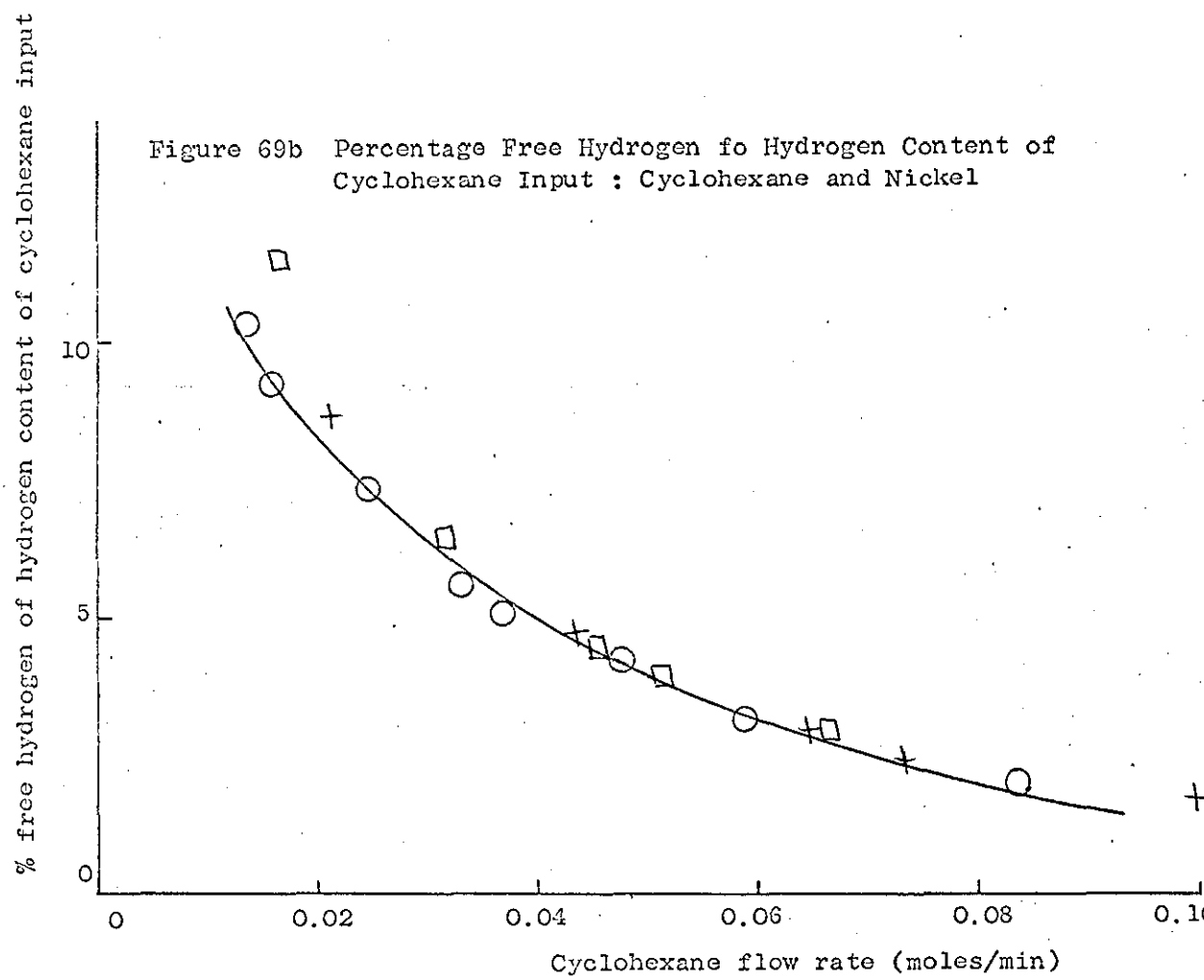

Figure 69b Percentage Free Hydrogen fo Hydrogen Content of Cyclohexane Input : Cyclohexane and Nickel

Figure 70a Percentage Decomposition of Cyclohexane to Gaseous Products Against Flow Rate : Cyclohexane Alone

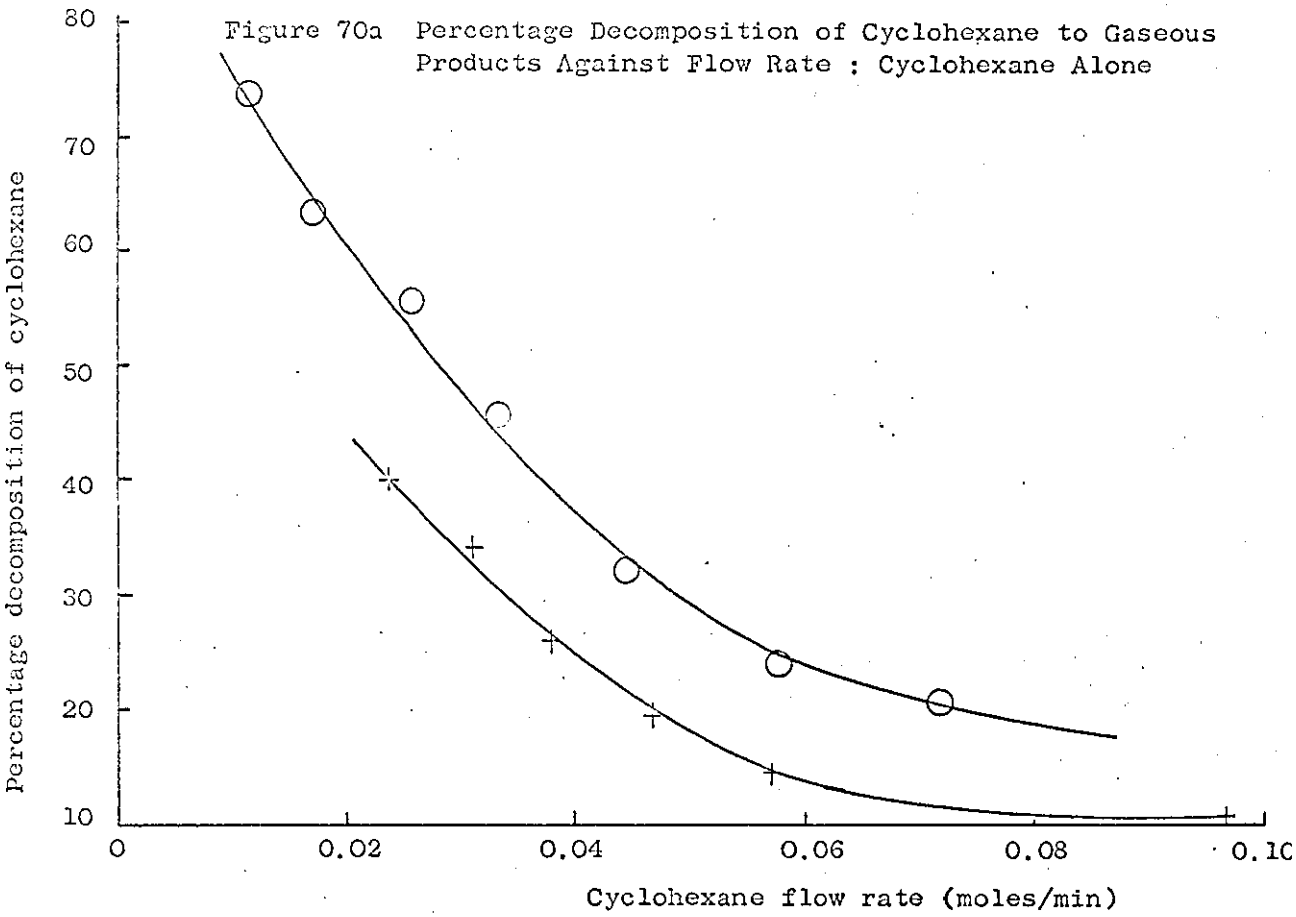

Figure 70b Percentage Decomposition of Cyclohexane to Gaseous Products Against Flow Rate : Cyclohexane and Nickel

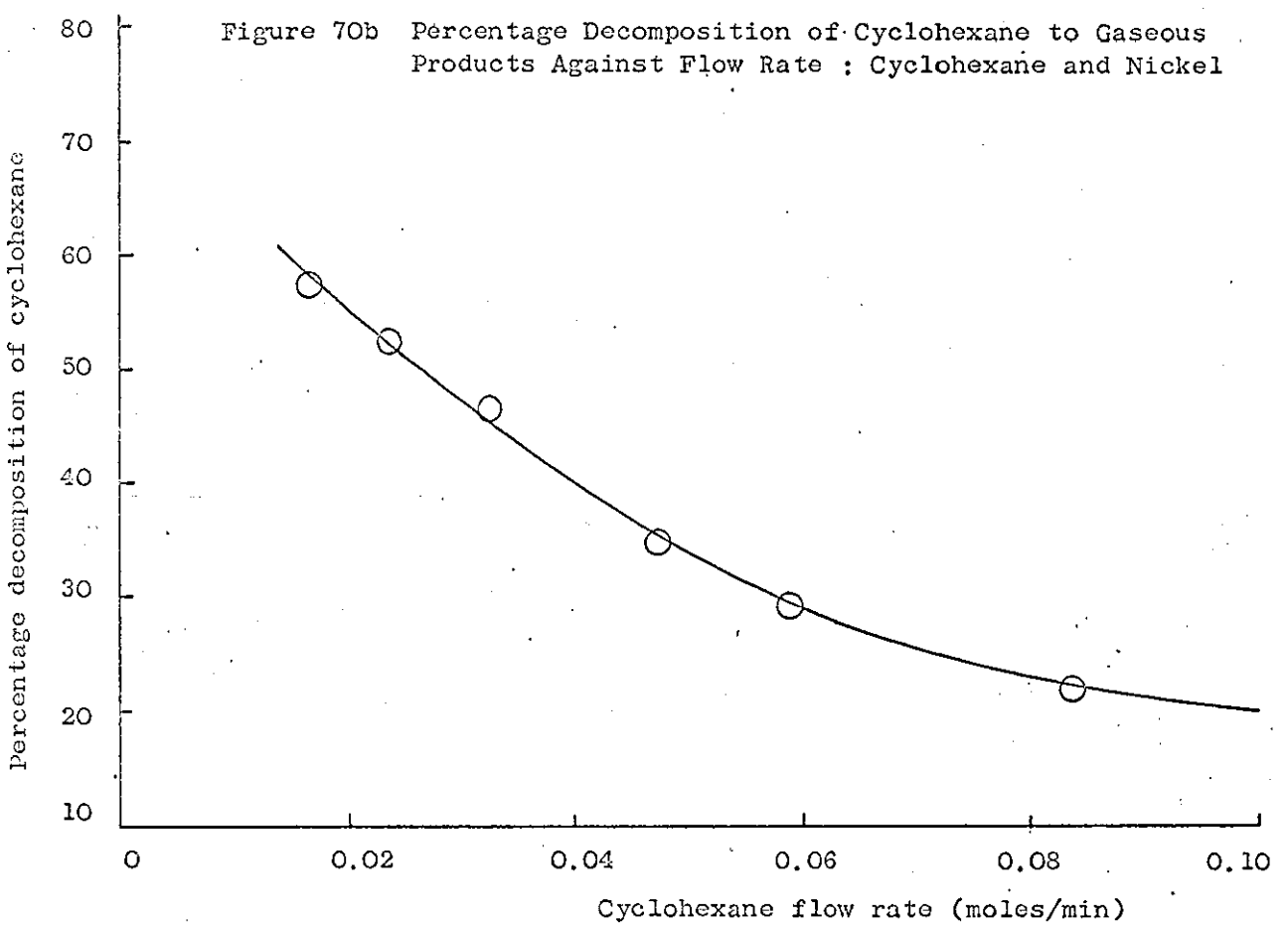

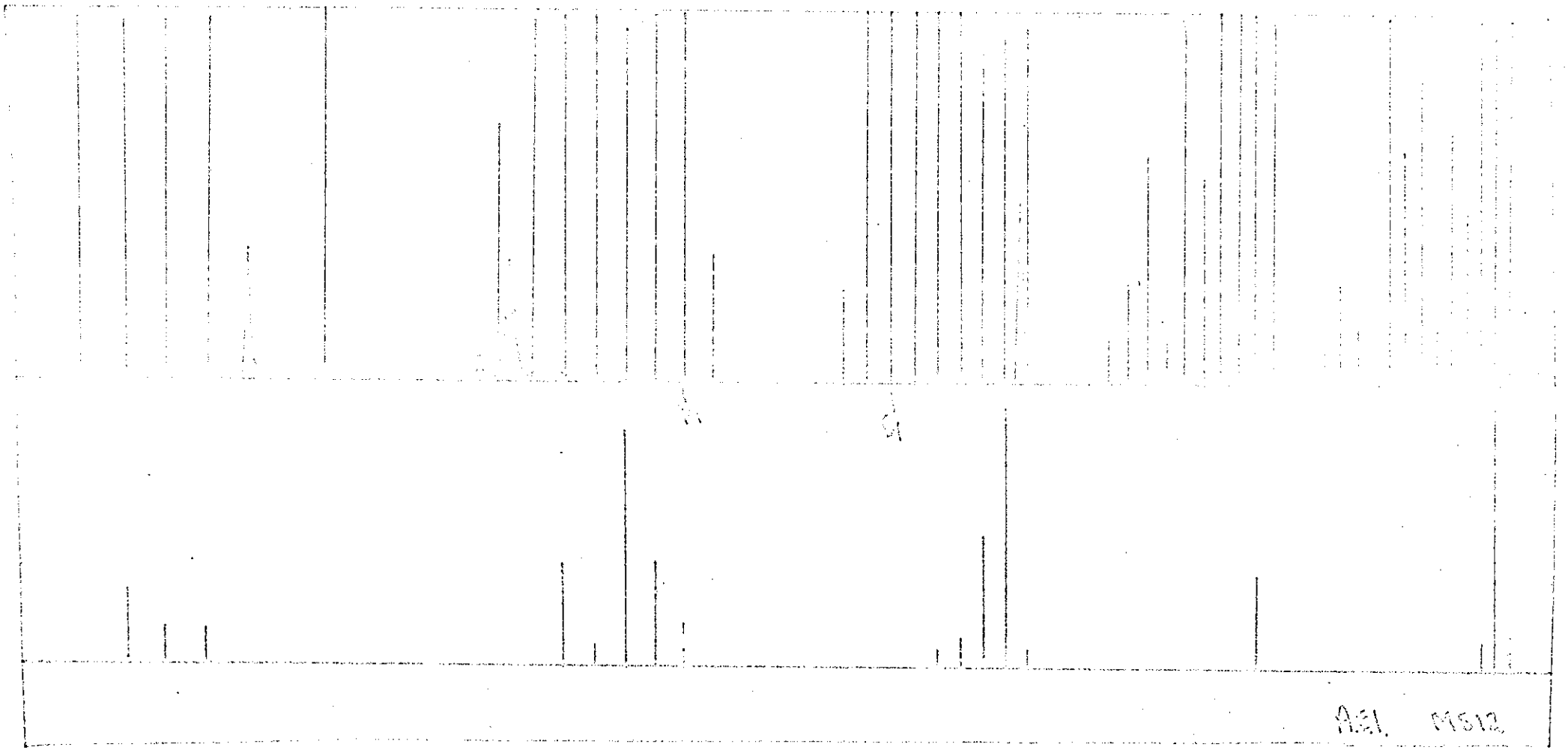

Figure 65 Typical Mass Spectrum of the Condensed Products of Cyclohexane Showing Traces of Benzene

Table 16 Cyclohexane and Carbon Dioxide : the Low Boilers

power input 0.78 Kw mole ratio 2:1

cyclohexane flow rate, moles/min.	reactor pressure mm Hg	power absorption Kw	% conversion to acetylene	% conversion to C_3 hydrocarbons	% conversion to C_4 hydrocarbons
0.0126	26	0.22	57.94	0	0
0.0209	26	0.22	33.2	3.38	2.94
0.0270	25	0.23	22.7	3.76	3.54
0.0338	26	0.22	21.57	3.80	3.64
0.0408	25	0.24	11.23	3.54	3.86
0.0478	27	0.23	5.41	3.93	4.01
0.0711	29	0.22	2.08	5.06	4.83
0.109	32	0.21	1.54	4.75	5.84

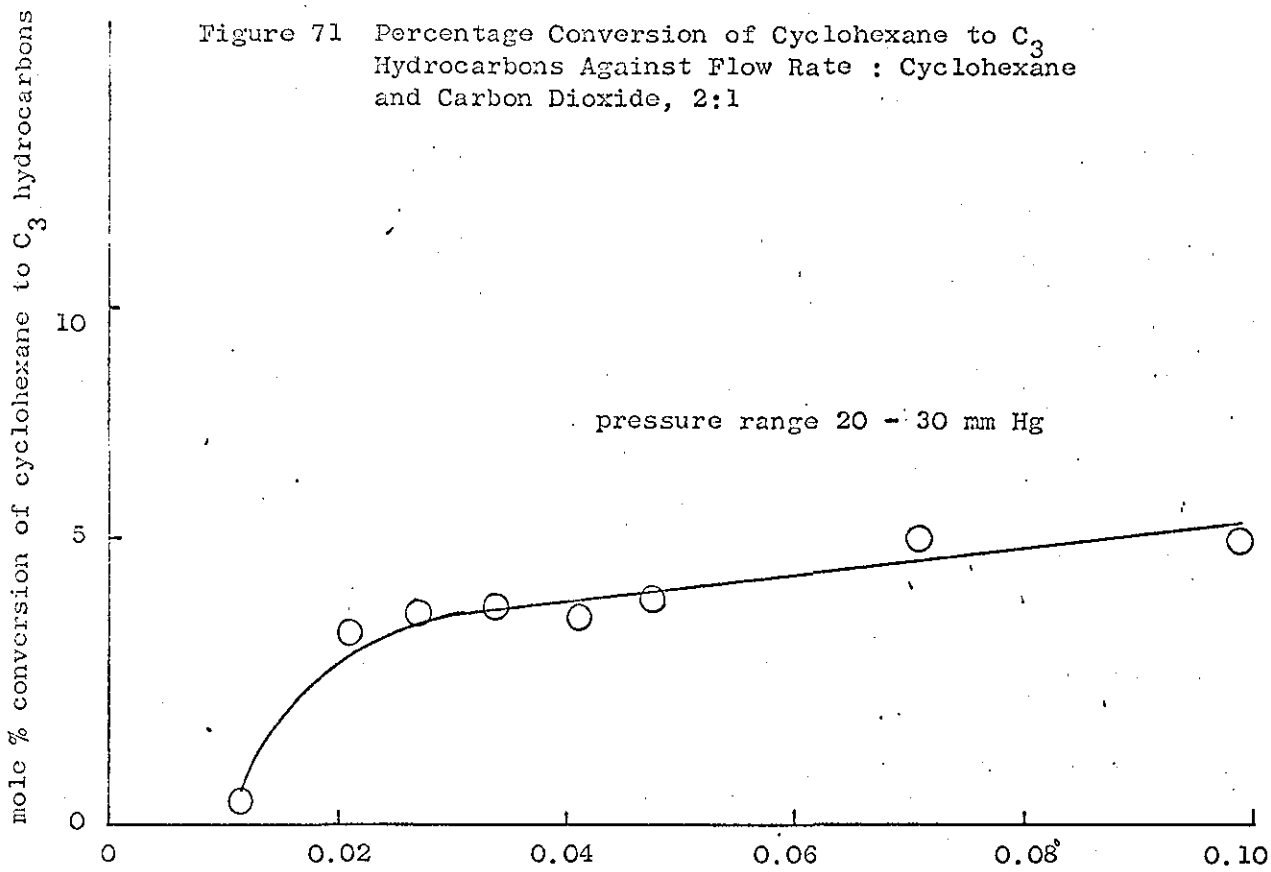

Figure 71 Percentage Conversion of Cyclohexane to C_3 Hydrocarbons Against Flow Rate : Cyclohexane and Carbon Dioxide, 2:1

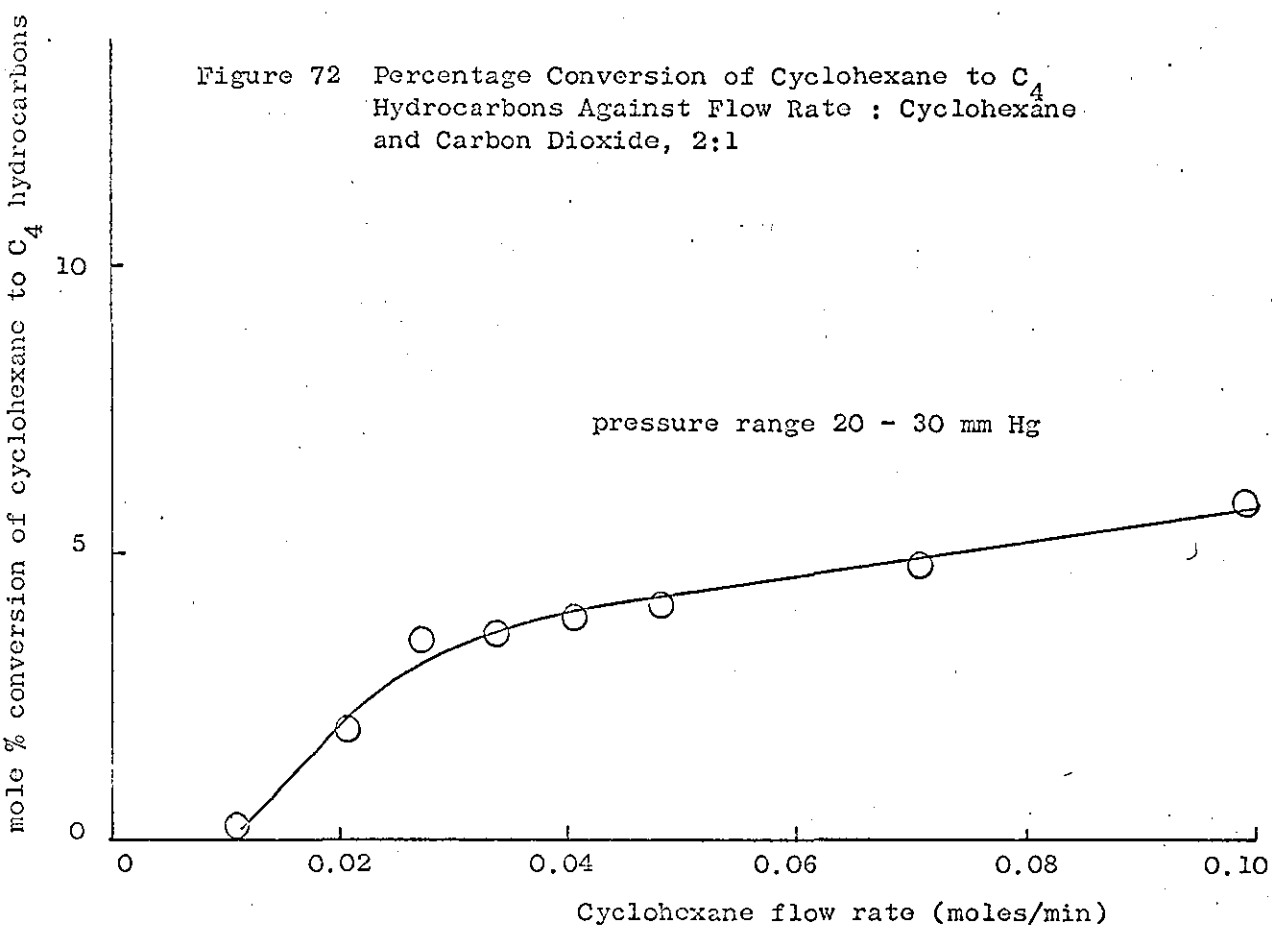

Figure 72 Percentage Conversion of Cyclohexane to C_4 Hydrocarbons Against Flow Rate : Cyclohexane and Carbon Dioxide, 2:1

Figure 73 Percentage Conversion of Cyclohexane to Acetylene Against Flow Rate : Cyclohexane and Carbon Dioxide, 2:1

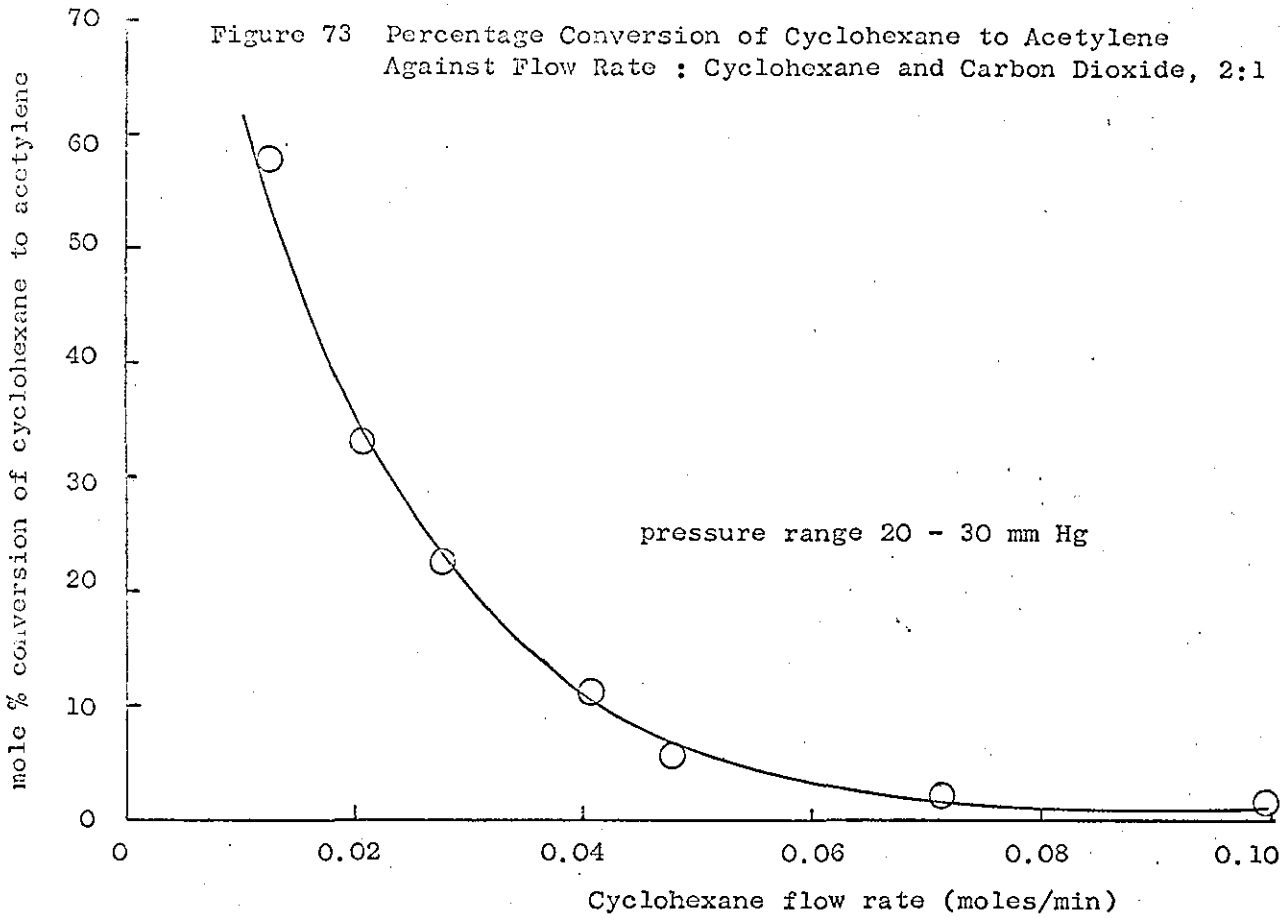

Figure 74 Percentage Decomposition of Cyclohexane to Gaseous Products Against Flow Rate : Cyclohexane and Carbon Dioxide, 2:1

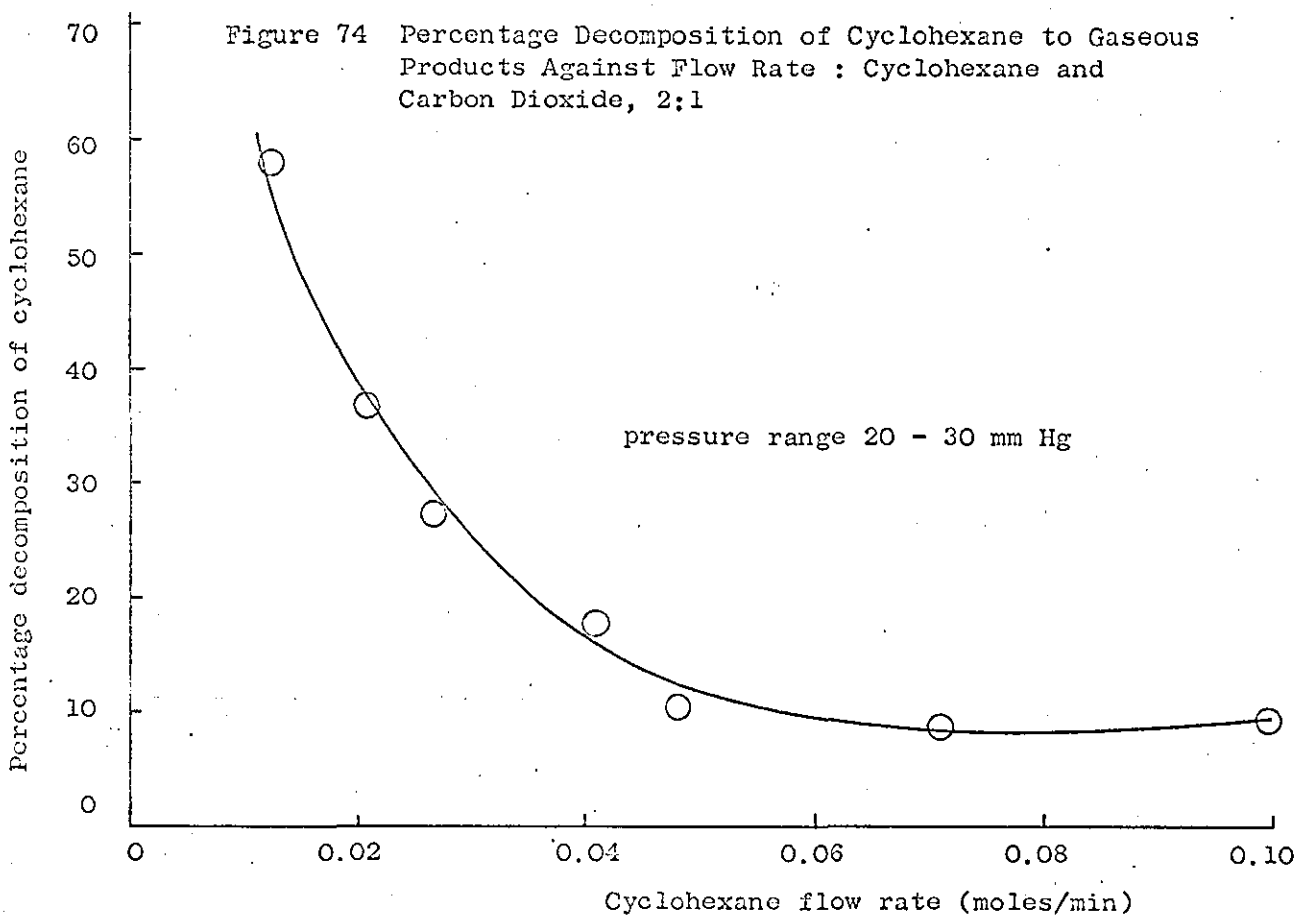

GENERAL CONCLUSIONS

12. Comparison of the Benzene and Cyclohexane Discharges

The first ionization potentials of benzene and cyclohexane are 9.3 eV and 10.3 eV respectively. The degree of decomposition of the two compounds, by ionization processes, in the discharge would thus be expected to be similar. This is essentially borne out by the experimental results.

In both systems C_2 and C_4 hydrocarbons were found in good yield. The major difference was the high conversion of cyclohexane to C_3 hydrocarbons compared with that of benzene which gave mainly acetylene and 1,3-butadiene. This is probably due to the lower energy needed to disrupt the appropriate bonds in the chair and boat configuration of cyclohexane.

The effect of nickel in the benzene and cyclohexane discharges was similar in that the overall decomposition was not reduced but the distribution of products was changed.

The presence of carbon dioxide in the cyclohexane discharge resulted in less decomposition than in the corresponding benzene discharge. This is consistent with the views postulated on the protecting influence of the carbon dioxide, see section 10.8.2. and was expected with the higher ionization potential of cyclohexane.

A consequence of the comparative stability of the phenyl radical was the production of diphenyl and polybenzenes in fairly good yield. Only traces of dicyclohexyl were found, possibly suggesting the cyclohexyl radical is less stable than the phenyl radical.

12.1. General Conclusion

The investigation of the microwave discharge in ammonia

indicated that the microwaves induced higher levels of excitation in the gas molecules than the corresponding d.c. discharge. Further evidence of an apparently different distribution of electron energies in the microwave discharge was provided by the benzene discharge. The absence of doubly-charged benzene ions, indicated by the absence of methyl groups in the products, suggested a narrower distribution of energies than that normally found in a d.c. discharge.

The presence of nickel in the microwave discharge has been shown to be effective in promoting selective reactions. Excess carbon dioxide was effective in protecting the ring structures of benzene and cyclohexane.

Discharges in mixtures of ammonia and benzene produced an unparalled selectivity in reaction to give amino-substituted azobenzenes. This is a potentially important economic process.

12.2. Proposals for Further Work

The influence of reactor design should be investigated fully with the view to:

(a) improving the selectivity of the reactions, e.g. a bias towards either the production of R or S in the series reaction, $A \longrightarrow R \longrightarrow S$.

(b) improving the utilisation of the available microwave power. This may involve a change in the resonant cavity or the power inputs to the cavity.

The above studies should be applied fully to the reactions in benzene vapour. Particularly the discharges in benzene and ammonia to improve the yield of the amino-substituted

azobenzene. The effect of nickel in the discharges of mixtures of benzene and ammonia should also be investigated.

The pulsing of the microwave power could prove to be very important in increasing yields and should be investigated fully. If possibly a spectroscopic examination of the microwave discharges in the vapour under investigation should be undertaken. This would prove valuable in clarifying the reaction mechanisms and also give direct evidence of the radicals and ions involved in the chemical reactions.

Investigations into the possible production of phenol or benzaldehyde from discharges in benzene and steam or benzene and carbon monoxide respectively are proposed.

APPENDIX A

Appendix A

Reaction Profiles : Complex Reactions

Consider the general first-order reactions

$$A \longrightarrow R \longrightarrow S$$

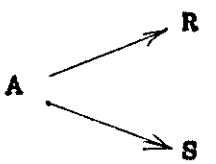

For parallel reactions as soon as any reactant is converted, both R and S can form in principle; the selectivity depending on the individual rate constants of the reactions involved. Examples are shown in Fig. 75.

In consecutive reactions, R is formed first and is subsequently converted to S. Initially the selectivity of R is unity where the selectivity is defined as the ratio between the amount of a product and the amount of reactant converted. However in principle the selectivity of the reaction to R decreases to zero as the reaction proceeds. Therefore the conversion of A $\longrightarrow$ R will pass through a maximum, see Fig. 76.

It can be seen therefore that the shape obtained by plotting concentration-time or concentration-conversion curves for a reaction sequence can indicate the reaction path. If sufficient data is available, the rate constants of individual reactions can be obtained. However it should be noted that the reaction profile is influenced by the reactor type.

The yield of R is always greater in the plug flow.reactor than in the backmix reactor. Hence if R is the desired product, and the raw material cost is low, the plug flow or batch reactor is favoured.

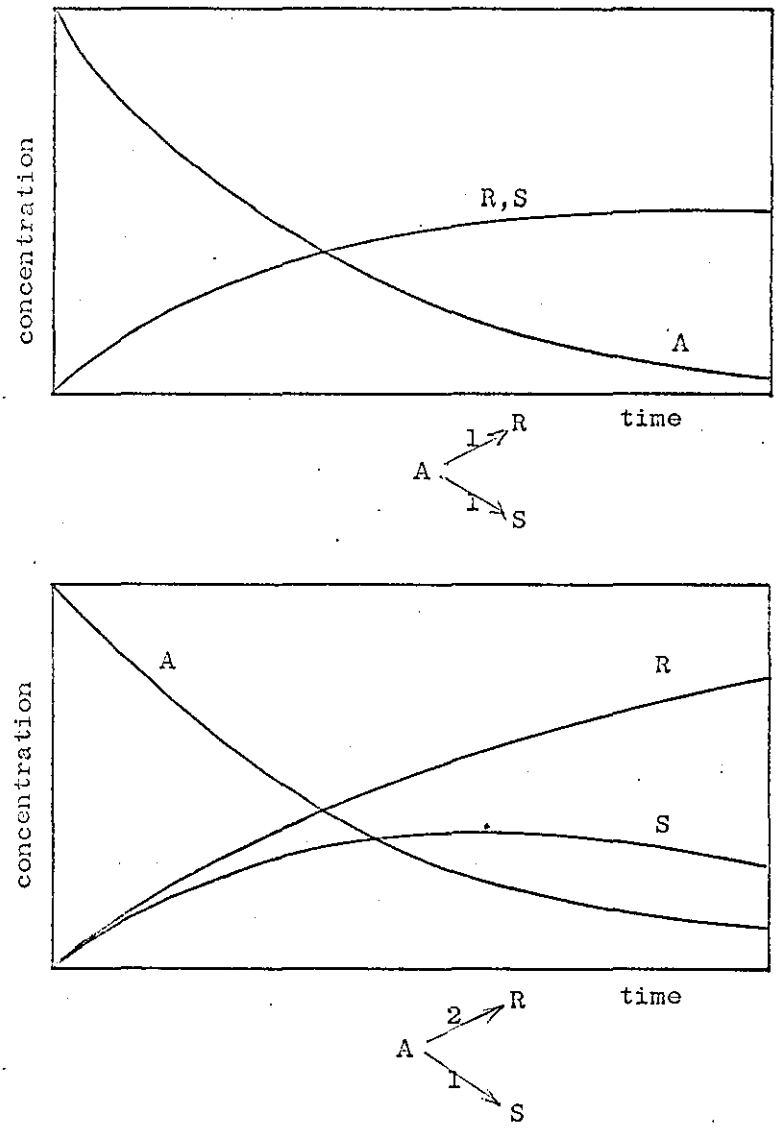

Figure 75 Typical Concentration-Time Curves for Parallel Reactions

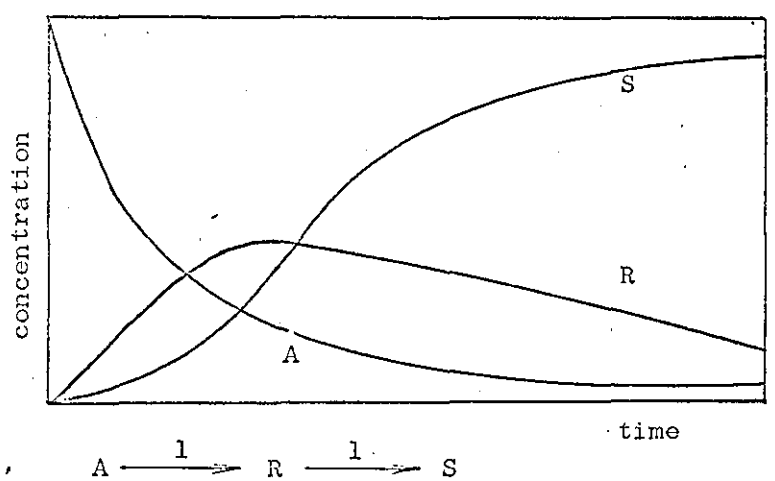

Figure 76 A Typical Concentration-Time Curve for a Series Reaction.

APPENDIX B

Appendix B

Temperature Profiles of the Benzene and Cyclohexane Discharges

A Ni-Cr/Al-Ni thermocouple connected to a bridge circuit was used for the temperature measurement. The thermocouple was moved through the discharge zone and thus a temperature gradient with distance was obtained.

It should be noted that the thermocouple was open to bombardment by excited species and recombination of atoms on the surface of the thermocouple. The temperatures recorded were therefore higher than the actual temperature in the discharge.

The maximum temperatures observed for both the benzene and cyclohexane discharges were below 950^{o}C under the experimental conditions stated. The relatively low gas temperatures show that the reactions observed in the benzene and cyclohexane systems were not due to pyrolysis.

Figure 77 Temperature Profile in the Benzene Discharge

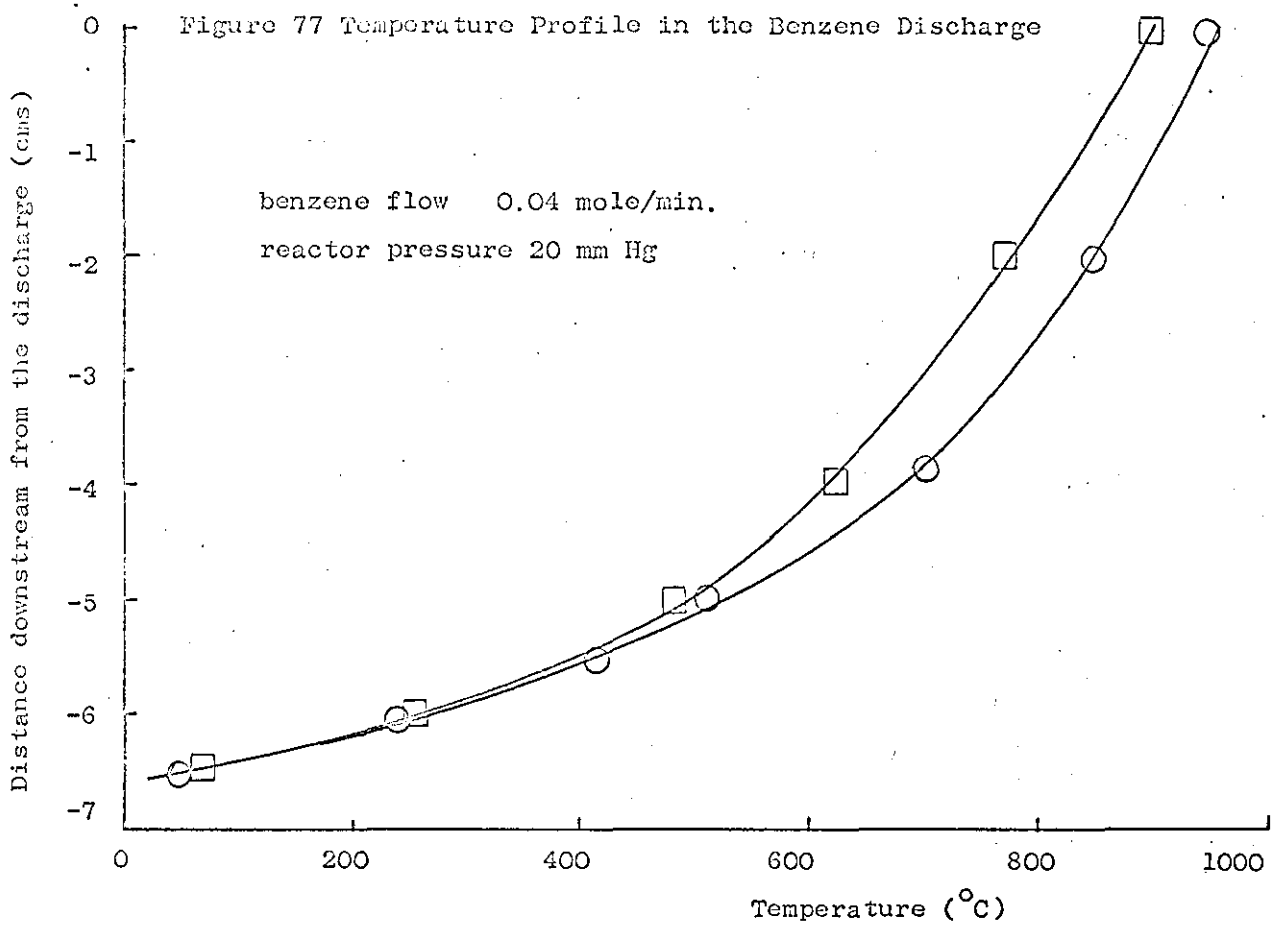

Figure 78 Temperature Profile in the Cyclohexane Discharge

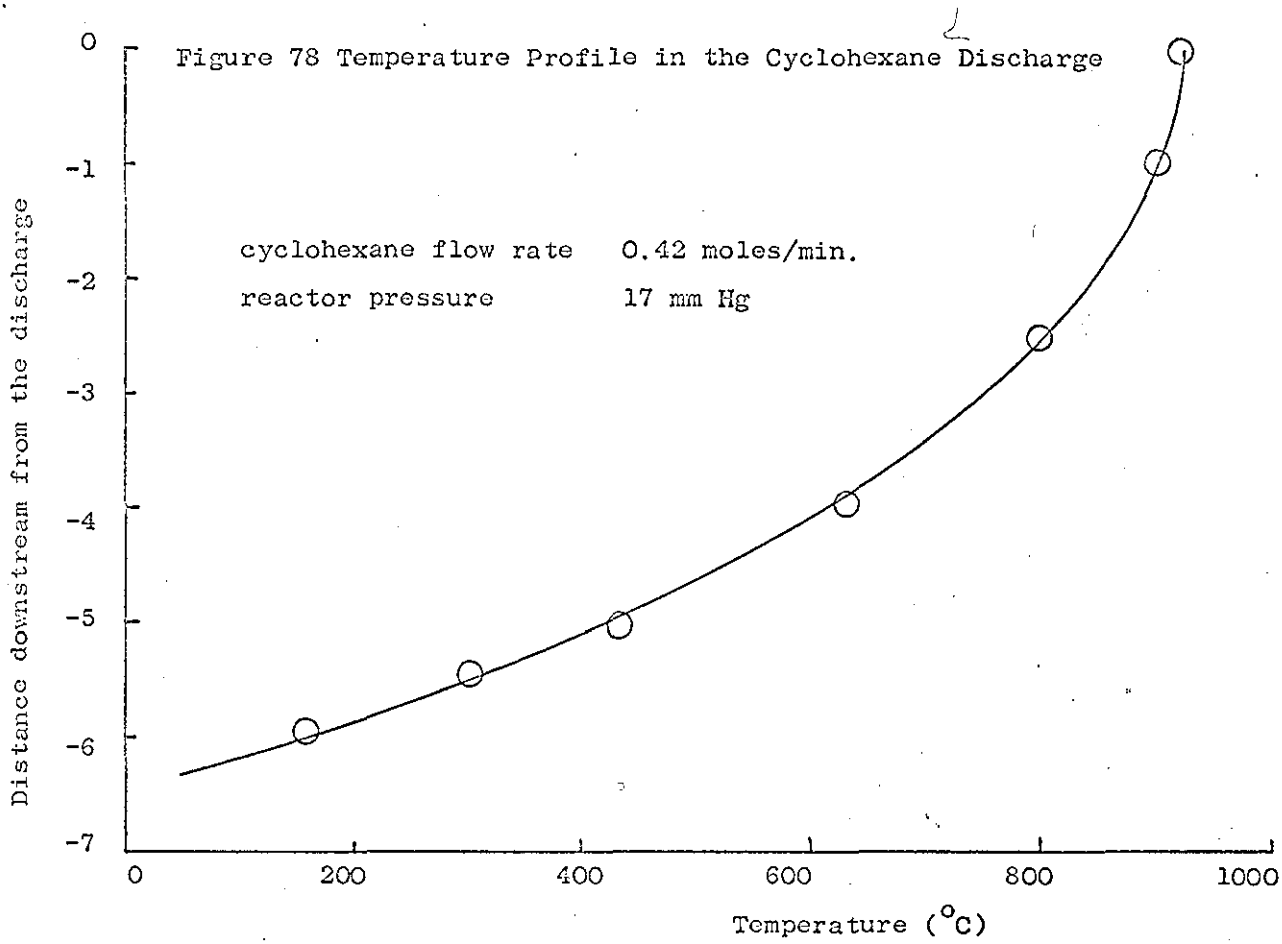

BIBLIOGRAPHY

Bibliography

1. Llewellyn-Jones, F., The Glow Discharge, Methuen & Co., 1966. Brown, S.C., Introduction to Electrical Discharges in Gases, Wiley & Sons Ltd., 1966.
2. Francis, G., Ionization Phenomena in Gases, Butterworths, 1960.
3. Meek, J.M. and Craggs, J.D., Electrical Breakdown of Gases, O.U.P., 1953.
4. Baddour, R.F. and Timmins, R.S., The Application of Plasmas to Chemical Processing, Pergamon Press, 1967.
5. Romig, M.F., Phys.Fluids, 3, 129 (1960).
6. Herlin, M.A. and Brown S.C., Phys.Rev., 74, 291, 910, 1650 (1948).
7. Macdonald, A.D. and Brown S.C., Phys.Rev., 75, 411 (1949); ibid., 76, 1634 (1949).
8. Posin, D.Q., Phys.Rev., 73, 496 (1948).
9. Gould, L. and Roberts, L.W., J.Appl.Phys., 27, 1162 (1956)
10. Corrigan, S.J.B. and Von Engel, A., Proc.Roy.Soc., A245, 335 (1958).
11. Prowse, W.A. and Jasinski, W., Proc.Instn.Elec.Engrs., 98(IV), 101 (1951); ibid., 99(IV), 194 (1952).
12. Prowse, W.A. and Lane, P.E., Nature, 172, 116 (1953).
13. Stevenson, D.P., J.Phys.Chem., 61, 1453 (1957).
14. Frankevich, E.L. and Tal'roze, V.L., C.A. 52:5139h, 53:877d.
15. Fehsenfeld, F.C. et al, J.Chem.Phys., 44, 3022 (1966).
16. Lampe, F.W. and Field, F.H., Tetrahedron, 7, 189 (1959).
17. Lampe, F W. et al, J.Am.Chem.Soc., 79, 6132 (1957).
18. Field, F.H. et al, J.Am.Chem.Soc., 79, 2665 (1957).
19. Franklin, J.L., C.A.62:15448e.
20. Field, F. and Franklin, J., Electron Impact Phenomena, Academic Press Inc., 1957.
21. Munson, M.S., Franklin, J.L. and Field, F.H., J.Phys.Chem., 68, 3098 (1964).
22. Kaufmann, F., C.A.57:8035f.
23. Field, F.H., J.Am.Chem.Soc., 83, 1523 (1961).

24. Golden, P.D., et al, J.Chem.Phys., 44, 4095 (1966).

25. Trotman-Dickenson, A.F., Free Radicals, Methuen, 1959.

26. Purnell, J.H. and Quin, C.P., J.Chem.Soc., 4128 (1961).

27. Prilezhaeva, N. and Naether, H., C.A.32:7823[7].

28. Broida, H.P. and Lutes, O.S., J.Chem.Phys., 28, 725 (1958).

29. Filippov, Yu.V., C.A.54:16234f.

30. Samoilovich, V.G., Filippov, Yu.V., C.A.58:12172f, 5264e.

31. Lunt, T., Advances Chem. Series, 21, 280 (1959).

32. Cromwell, W.E. and Manley, C.A.54:3008c.

33. Shaw, T.M., J.Chem.Phys., 30, 1366-7 (1959).

34. Bak, B. and Rastrup-Anderson, J., Acta.Chem.Scand., 16, 111 (1962).

35. Bejsovec, V., C.A.61:6500d.

36. Corrigan, S.J.B., J. Chem.Phys., 43, 4381 (1966).

37. Shaw, T.M., J.Chem.Phys., 31, 1142 (1959).

38. Rony, P.R. and Hanson, D.N., J.Chem.Phys., 44, 2536 (1966).

39. Jackson, D.S. and Schiff, H.I., J.Chem.Phys., 23, 2333 (1955).

40. Kistiakowsky, G.B. and Volpi, G.G., J.Chem.Phys., 27, 1141 (1957).

41. Fontana, B.J., J.Appl.Phys., 29, 1668 (1958).

42. Barylett, F.D.A., C.A.:61, 5045a.

43. Armstrong, D.A. and Winkler, C.A., J.Phys.Chem., 60, 1100 (1956).

44. Kaufman, F., Proc.Roy.Soc., A245, 123 (1958).

45. Linnett, J.W. and Marsden, D.G.H., Proc.Roy.Soc., A234, 489 (1956).

46. Young, R.A. et al, J.Phys.Chem., 69, 1763 (1965).

47. Young, R.A. et al, J.Chem.Phys., 40, 117 (1964).

48. Ultee, C.J., J.Chem.Phys., 41, 281 (1964).

49. Semiokhin, I.A. et al, C.A.61:12759e, C.A.61:15399c, C.A.62:9901e.

50. Semiokhin, I.A. et al, C.A.62:2322h.

51 Wilde, K.A. et al, C.A.47:11049e.

52. Clyne, M.A.A. and Thrush, B.A., Nature, 189, 56 (1961).

53. McCarthy, R.L., J.Chem.Phys., 22, 1360 (1954).

54. Strutt, R.J., Proc.Roy.Soc., A85, 219 (1911).

55. Cooper, W.W. et al, Ind.Eng.Chem.Fundam,, 7, 400 (1968).

56. Gokhale, S.D. and Jolly, W.L., Inorg.Chem., 4, 596 (1965).

57. Lindahl, C.B. and Jolly, W.L., Inorg.Chem,, 1, 958 (1962).

58. Holmes, W.C. & Co. Ltd., Brit. 1,009, 331.

59. Frazer, J.W. and Holzmann, R.T., J.Am.Chem.Soc., 80, 2907 (1958).

60. Emeleus, H.J. and Tittle, B., J.Chem.Soc. (London), 1644 (1963).

61. H'in, D.T. and Eremin, E.N., C.A.61:15899d.

62. Popovici, C., C.A.64:18592b.

63. Badareu, E. et al, C.A.54:3010d.

64. Tsentsiper, A.B., et al, C.A.59:4626g.

65. Badareu, E., Albu, C. and Popovici, C., C.A.58:6201c.

66. Thornton, J.D. and Sergio, R., Nature, 213, 590 (1967).

67. Kulcsar, J. and Vodnar, I., C.A.56:2012b.

68. Norrish, R.G.W., C.A.44:6803i.

69. Luk'yanov, V.B., C.A.68:90857r.

70. Miyazaki, S., C.A.57:4467h; 52:14345d; 53:4668a.

71. Gupta, P.C., C A.53:17728a, 54:15027d.

72. Anand, V.D., C.A.58:12410p.

73. Jolly, W., Tech.Inorg.Chem., 1, 179-203 (1963).

74. Heyns, K., Walter, W. and Meyer, E., C.A.52:5140d.

75. Czuchajowski, L., Franck, H. and Goreska, W., C.A.69:9718e.

76. Hay, P.M. and Stevens, J.P., Am.Chem.Soc.Div.Fuel Chem.Preprints, 82 (1967).

77. Takahishi, S., C.A.55:11144h.

78. Kokurin, A.D. and Gruzdera, V.V., C.A.55:25227g.

79. Kolyubin, A.A., C.A.53:854a; C.A.54:20483d.

80. Coates, A.D., C.A.61:205b.

81. Arnold, G., C.A.62:15542d.

82. Inoue, E., C.A.51:14567h; 52:2763g; 53:4974a.

83. Stille, J.K., et al, J.Org.Chem., 30, 3116 (1965).

84. Kraajveld, H.J. and Waterman, H.I., C.A.57:10627f.

85. Nishi, M., C.A.50:12660h.

86. Schuler, H. et al, C.A.54:22012a.

87. Agirbiceam, et al, C.A.53:2781f.

88. Vastola, F.J. and Wightman, J.P., J.Appl.Chem., 14, 69 (1964).

89. Streitweiser, A. and Ward, H.R., J.Am.Chem.Soc., 84, 1065 (1962).

90. Ranley, M.W. and O'Connor, W.F., Am.Chem.Soc.Div.Fuel Chem. Preprints, 63 (1967).

91. Kawahata, M., Am.Chem.Soc.Div.Fuel Chem. Preprints, 64 (1967).

92. Hollahan, J.R. and McKeever, R.P., Am.Chem.Soc.Div.Fuel Chem. Preprints, 78 (1967).

93. Sugino, K. and Inoue, E., C.A.45:9499; 47:7918f; 47:12048h.

94. Thomas, C.L., (Sun Oil Co.) U.S. 2,749, 297-8.

95. Sugino, K and Inoue, E., C.A.45:5536a.

96. Andersen, W.H. et al, Ind.Eng.Chem., 51, 527 (1959).

97. Carbough, D.C. et al, J.Chem.Phys., 47, 5211 (1967).

98. Devins, J.C. and Burton, M., J.Am.Chem.Soc., 76, 2618 (1954).

99. Thornton, J.D. and Spedding, P.L., Nature, 213,1118 (1967).

100. Miyazaki, S. and Takahishi, S., C.A.51:9335d.

101. Ouchi, K. et al, C.A.47:421c, 1496b, 67961, 12048f.

102. Cooper, W.W., S.B. Thesis, Dept.Chem.Eng., M.I.T., 1963.

103. Herzberg, G., Electronic Spectra of Polyatomic Molecules, Van Nostrand, 1966.

104. Herzberg, G. and Ramsay, D., J.Chem.Phys., 20, 347 (1952).

105. Dressler, K. and Ramsay, D., Phil.Trans.Roy.Soc., A251, 553 (1959).

106. Okabe, H. and Lenzi, M., J.Chem.Phys., 47, 5241 (1967).

107. Stuken and Wedge, Z. Naturforsch, 18a, 900 (1963).

108. Robinson, G.W. and McCarty, M., J.Chem.Phys., 30, 999 (1959). 28, 349 (1958).

109. Schnell, O. and Dressler, K., J.Chem.Phys.

110. Hanes, M.H. and Bair, E.J., J.Chem.Phys., 38, 672 (1963).

111. Dyne, P., Can.J.Phys., 31, 453 (1953).

112. Salzman, P. and Bair, E.J., J.Chem.Phys., 41, 3654 (1964).

113. Wiig, E.D. and Kistiakowsky, G.B., J.Am.Chem.Soc., 54, 1806 (1932).

114. Dixon, J.K., J.Am.Chem.Soc., 54, 4262 (1932).

115. Ghosh, P.K. and Bair, E.J., J.Chem.Phys., 45, 4738 (1966).

116. Schiavello and Volpi, G.G., J.Chem.Phys., 37, 1510 (1962).

117. Diesen, R.W., J.Chem.Phys., 39, 2121 (1963).

118. Devins, J.C. and Burton, M., J.Am.Chem.Soc., 76, 2618 (1954).

119. Rothsack, H.A., C.A.55:22997i.

120. Westhaver, J.W., J.Phys.Chem., 37, 897 (1933).

121. Miyazaki, S. and Takahishi, S., C.A.52:14345d, 53:4668a.

122. Ouchi, K., C.A.47:2612g, 4201, 421b.

123. MacDonald, C.C. and Gunning, J.Chem.Phys., 23, 532 (1955).

124. MacDonald, C.C., Kahn and Gunning, J.Chem.Phys., 22, 908 (1954).

125. Manion, J.P. and Davies, D.J., U.S. 3,396,098, (1965).

126. Devins, J.C. and Burton, M., U.S. 2,849, 357 (1958).

127. Penneman and Audrieth, Anal.Chem., 20, 1058 (1948).

128. Vogel, A.I., Quantitative Inorganic Chemistry, Longmans (1961).

129. Audrieth, L. and Ogg, B., The Chemistry of Hydrazine, Wiley & Sons, (1951).

130. Pesez, and Petit,, Bull.soc.Chim., France, 122 (1947).

131. Pearse, R. and Gaydon, A., Identification of Molecular Spectra, Chapman & Hall (1963).

132. Hanratty, T.J. et al, Ind. & Eng.Chem., 43, 1113 (1951).

133. Momigny, J., Brakier, L. and D'or, L., C.A.59:7065g.

134. Ottinger, Ch., Z. Naturforsch, 20a, 1229, (1965).

135. Finar, I.L., Organic Chemistry, Longmans, (1963).

136. Jennings, M., J.Chem.Phys., 43, 4176 (1965).

137. Abramson, F.P. and Futrell, J.H., J.Phys.Chem., 71, 3791 (1967).

138. Brown and Benz, J.Chem.Phys., 48, 4303, (1968).

139. Munson, M.S., Franklin, J.L. and Field, F., J.Phys.Chem., 68, 3098 (1964).

140. Dyne, P.J. and Stone, J.A., Can.J.Chem., 39, 2381 (1961).

141. Toma, S.Z. and Hamill, W.H., J.Am.Chem.Soc., 86, 1478 (1964).

142. Schuler, R.H., J.Phys.Chem., 61, 1472 (1957).

143. Theard, L.M., J.Phys.Chem., 69, 3292 (1965).

144. Manion, J.S. and Burton, M., J.Phys.Chem. 56, 560 (1952).

145. Ausloos, P. and Lias, S.G., J.Chem.Phys., 43, 127 (1965).

146. Ausloos, P., Rebbert, R.E. and Lias, S.G., Conference Radiation Chemistry, II, 1968.